THE
PHYSICAL REVIEW
A Journal of Experimental and Theoretical Physics Established by E. L. Nichols in 1893
VOL. 50, No. 12 DECEMBER 15, 1936 SECOND SERIES

A Numerically Consistent Corpuscular Theory of Cosmic Rays*

W. F. G. SWANN, *Bartol Research Foundation of the Franklin Institute, Swarthmore, Pennsylvania*
(Received October 2, 1936)

Theories for consideration divide themselves into two categories, those in which the primaries function as the measured entities, and those in which secondaries or higher order radiations play a significant or even a dominant role.

Primaries as measured entities. There exists a curve relating altitude and latitude, such that the rays which can just penetrate the earth's magnetic field at an assigned latitude can penetrate the atmosphere down to the altitude given by the curve. The curve cuts the sea-level axis at a latitude customarily associated with that at which the increase of intensity with latitude ceases for further increase of latitude. For all altitudes above the curve in question, and in particular for all altitudes above sea level, with latitude less than the sea-level critical latitude, there can be no variation of primary intensity with altitude; and, appeal must be made to secondaries for variation of intensity with altitude in these regions. In regions where the primary intensity varies with altitude, that variation must depend upon the energy spectrum of the incoming rays. The type of energy distribution necessary to secure an exponential law is determined. Its form depends upon the law of energy absorption in the atmosphere. Two cases are considered. They correspond to

$$-dE_x/dx=\alpha \quad (1); \qquad -dE_x/dx=\alpha+\lambda E_x \quad (2)$$

where E_x is the energy at the distance x from the top of the homogeneous water equivalent atmosphere, α corresponds to loss by ionization, and λE_x to loss by secondary production. Case (1) leads to an energy distribution which predicts at high altitudes a latitude variation which is enormous and out of all possible harmony with the facts. Case (2) leads to a reasonable high altitude latitude variation. However, the other difficulties concerned with a predicted absence of variation of intensity with altitude in equatorial regions remain.

Combination of primaries and secondaries as measured entities. The writer generalizes his former theory according to which the primaries produce secondaries in numbers which increase with increase of primary energy. The theory of the soft component is first considered, with (2) as a basis. The energy distribution function, $F(E)$ necessary to give an exponential law for the primaries is of the form $F(E)=B_p/(E+\alpha/\lambda)^p$; and, with this form the absorption coefficient μ_s is $\mu_s=(p-1)\lambda$. For mathematical convenience the quantity $W=(E+\alpha/\lambda)$, which is nearly the same as E is used throughout for purposes of discussion instead of the true energy E. It is shown that if the number of secondaries n_s accompanying a primary is given by $n_s=\gamma W_x^s$, then below the critical latitude $\mu_s=\lambda s$, and above the critical latitude $\mu_s=(p-1)\lambda$. If, in accordance with R. A. Millikan's observations we are to have μ_s the same above and below the critical latitude we must have $s=(p-1)$. If, moreover, μ_s has to have the value 0.5 per meter of water equivalent we must have $s=1.5$, and so $p=2.5$ when λ is assigned the value 0.33, which value is determined from the energy for penetration of the earth's magnetic field, 6×10^9 ev, at the critical latitude. The equality of μ_s above and below the critical latitude leads inevitably to an expression for the secondary intensity whose evaluation involves the integration of dW/W between a lower limit which is finite and an upper limit which is infinite unless we assign a finite upper limit E_M, beyond which $F(E)$ is zero. The concept of an upper limit E_M, and so an upper limit of W_M of W is consequently admitted; and, for purposes of illustration the limit taken is $E_M=5\times10^{10}$ ev. The intensity of the secondaries is proportional to $e^{-\mu_0 x}\log_e W_M/W_\varphi$ below the critical latitude, where W_φ is the value of W for penetration of the earth's field at latitude φ. It thus shows a latitude variation. There is also a stronger latitude variation of the primary intensity which, however, does not vary with altitude below the critical latitude. The combined sea-level latitude variation is too great to correspond to the observations and it is necessary to look for the hard component to iron it out.

The hard component. A hard component showing no latitude effect when combined with the foregoing contri-

* A paper delivered at the Tercentenary Conference of Arts and Sciences at Harvard University, September, 1936.

butions to the intensity can be made to provide a satisfactory sea-level latitude variation, a satisfactory ratio of the intensities of the hard and soft components, and a satisfactory increase of latitude effect with altitude through the logarithmic term referred to above. A photon component can therefore fulfill the requirements; but, it is also shown that a charged particle component, operating mainly through its secondaries, will do equally well. Were it not for requirements of variation of latitude effect with altitude, it would be possible to tell the story of both the hard and the soft components as the outcome of the suitably chosen energy distribution in the incoming rays, which rays could then be all of one type. The increase of latitude effect with altitude demands, for the two types of primaries, properties which are different as regards production of secondaries.

Miscellaneous phenomena. It appears that the average energy of the hard component primaries is determined mainly by the upper limit of their energies while that of the soft component primaries is determined mainly by the lower limit for penetration of the earth's magnetic field. The conditions provided for the hard component secondaries are such that those secondaries completely outweigh the primaries in number; and, this explains why but few very high energy primaries are found in cloud chambers. The higher energy members of the soft component primaries are outweighed by their secondaries but this is not so for the lower energy members. The maximum in the intensity altitude curves shown by Regener's results and by those of the Bartol Research Foundation of the Franklin Institute is attributed to a range phenomena of the secondaries and results from the limitations of the atmosphere. The so-called secondary hump in the said curves represents the transition which occurs on crossing the critical-altitude critical-latitude curve. The theory provides for the fact that the east-west asymmetry increases with altitude more rapidly than does the total radiation. It provides for such apparently paradoxical conclusions as those resulting from the fact that there is very little asymmetry in shower production in lead, suggesting that showers are produced by hard rays, while shower production increases with altitude more rapidly than the cosmic radiation, suggesting that it is produced by soft rays. The theory in fact makes shower production in lead increase with the energy of the primaries, but provides nevertheless for its rapid increase with altitude in such a manner as to give, at first sight, the impression that it is produced by a soft radiation.

An alternative choice of constants. If one permits a value of λ as large as 0.5, it is possible to provide for $\mu_z=0.5$ by the assumption that the number of secondaries accompanying a soft component primary is proportional to W_z, or approximately to E_z as assumed in the writer's theory published earlier. This is attended with several advantages; but, necessitates relinquishment of the association between the sea-level critical latitude at 41 degrees and the critical latitude for the soft component. It becomes necessary to assume a second critical latitude phenomenon for the soft component primary, which critical latitude phenomenon does not show itself at all until an altitude of 0.6 meter above sea level is reached. It now becomes necessary to look to the hard component for the sea-level latitude effect. The soft component, however, provides the variation of latitude effect with altitude.

1. Introduction

THE evidence drawn from the variation of cosmic-ray intensity, with latitude at high altitudes, has created a school strongly in favor of the view that the entities which enter our atmosphere from outer space and are directly or indirectly responsible for cosmic-ray phenomena are charged particles.[1] It is true that the facts are unable to deny that an appreciable portion of the cosmic rays observed at sea level may result from uncharged entities entering the atmosphere, but they do not require this; and, according to A. H. Compton, practically a hundred percent of the rays observed at high altitudes owe their origin to charged particles. It is true that some of the high altitude data upon which Compton's conclusions were based have become subject to question as the result of observations secured since the time when he expressed the foregoing opinion. However, the likelihood of a purely corpuscular origin seems sufficiently great to make worth while an attempt to account for all of the phenomena in terms of charged particles.

There are three possibilities as to the relationship between the primary rays and the phenomena observed. The first visions the observed rays as the primary particles themselves; the second regards them for the most part as long range secondaries, initiated directly or indirectly by the primaries, and perpetuating in large measure the directional characteristics of the primaries. The third possibility represents a combination of the first and second. Presumably nobody would deny that even if the first possibility represented the main story, there would be, in the observed phenomena, many secondaries, since such are actually observed in cloud chamber and other experiments. In the second or third type of hypothesis cited above, however, I do not imply a condition in which the role of the secondaries is

[1] A. H. Compton, Rev. Sci. Inst. **7**, 71 (1936).

limited to a mere complicating function which tends to obscure the story, but rather one in which the law of their production, as a function of the energies of the primaries, etc., plays a definite part in determining the main features characteristic of cosmic-ray phenomena and, in particular, the law of apparent absorption. Neither is it implied that the secondaries are necessarily produced from the primaries in single acts. Photons, for example, may function as intermediaries.

2. Nature of Primary Rays in Relation to the Hypothesis That They Constitute the Observed Entities

Electrons (positive and negative), alpha-particles, protons and other heavy particles have been suggested as primaries.[1] The investigations performed by the Bartol Foundation of the Franklin Institute both in the laboratory[2] and in the stratosphere,[3] have not given any evidence for the occurrence of protons, or other heavy particles functioning as the measured entities, with observable absorption,[4] however much such particles may participate in "silento" through the action of the secondaries which they may produce. Thus, in considering the case of primaries as *measured entities*, it would seem that we must confine our attention to positive and negative electrons, although much of the analysis which follows is applicable to other entities as well.

We shall confine attention throughout to the vertical intensity. The energy for vertical entry through the earth's magnetic field is 17×10^9 ev at the equator, 6×10^9 ev at 41 degrees magnetic latitude, and about 3×10^9 ev at 50° magnetic latitude for example.

At the equator, the rays which can penetrate the earth's magnetic field can also penetrate the atmosphere. There is, however, a magnetic latitude φ_{c0} sufficiently great that the energy of penetration of the field is only just sufficient to provide for penetration of the atmosphere. This latitude is customarily taken as the latitude at which the sea-level intensity fails to increase further with increase of latitude. It is 41° and corresponds, as has been stated, to an energy of penetration of 6×10^9 ev.

For each altitude there is a critical magnetic latitude φ_{cx}, such that the rays which can penetrate the magnetic field can also penetrate down to the altitude concerned. The form of the curve giving the relation between critical latitude and critical altitude is a function of the law governing the absorption of energy in the atmosphere. Two laws present themselves for our consideration in view of what will follow. They are

$$-dE_x/dx=\alpha, \tag{1}$$

$$-dE_x/dx=\lambda E_x+\alpha, \tag{2}$$

where E_x is the energy of a primary ray at a depth x below the top of the homogeneous water equivalent atmosphere, α is the loss per unit of path in ionization, and λ is a constant.[5]

On the basis of the first law we cannot account for an energy of atmospheric penetration anything like as high as 6×10^9 ev. The second form of law with $\lambda=0.333$ and $\alpha=0.77\times10^6$ per meter of water equivalent[6] provides a satisfactory solution, giving a range equal to that of the vertical atmosphere for an energy of 6×10^9 ev. The solution of (2) is

$$E_x+\alpha/\lambda=(E+\alpha/\lambda)e^{-\lambda x}, \tag{3}$$

where E is the energy of the ray at vertical entry

[1] W. F. G. Swann, Phys. Rev. **49**, 478 (1936); also C. G. and D. D. Montgomery, W. E. Ramsey and W. F. G. Swann, Phys. Rev. **50**, 403 (1936).

[2] L. H. Rumbaugh and G. L. Locher, Phys. Rev. **49**, 855 (1936).

[3] The hypothesis that the primaries are the observed entities implies that a measurable fraction of them terminate their paths in the region of observation. The experiments cited in reference 2, were based upon an attempt to detect the protons near the ends of their ranges. High energy protons which passed right through the atmosphere without being stopped therein in measurable amount would be permissible in the light of reference 2. Such protons might be the basis of initiating secondary radiation which functioned as a large part of the observed radiation.

[5] The second of these laws has already been introduced by the writer in a former publication, Phys. Rev. **48**, 641 (1935). See also W. F. G. Swann, Phys. Rev. **46**, 828 (1934).

[6] This value of α is based upon A. Eisl's value 32.2 ev as the energy necessary to produce a pair of ions (see Ann. d. Physik **3**, 277 (1929)), and upon an assumption of 38 ion pairs per centimeter of path at N.T.P., as found by W. E. Ramsey and the writer, in an investigation as yet unpublished. C. D. Anderson and S. H. Neddermeyer (Int. Conf. Phys. **1**, 171 (1935)) quote data corresponding to values of α ranging between 10^8 ev and 1.5×10^8 ev, but it would seem that their values require division by the density of air at N.T.P. in relation to the density of water $\times10^{-3}$.

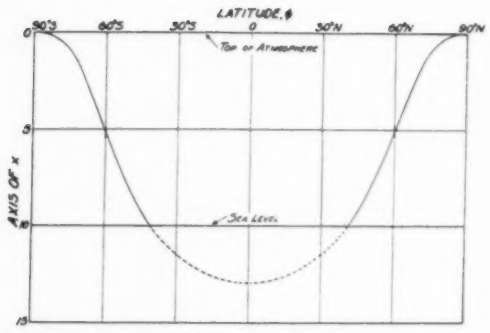

FIG. 1. The curve gives for any magnetic latitude the depth to which primary electrons, which can just penetrate the earth's magnetic field at that latitude, can reach in the homogeneous water equivalent atmosphere. The curve is calculated on the law of absorption specified in Eq. (2) with $\lambda=0.33$ and $\alpha=0.77\times10^{3}$ per meter of water equivalent.

into the atmosphere. The range R of the rays is given by putting $E_x=0$, so that

$$e^{\lambda R}=1+\lambda E_i/\alpha. \tag{4}$$

Fig. 1 shows the relation between the critical latitude and critical altitude as drawn from (4), with the foregoing quoted values of λ and α.

Now it is manifest that if we regard the primary rays as the measured entities there should be absolutely no variation of intensity with altitude in the regions lying above the curve in Fig. 1; and, in particular, there should be no variation with altitude for all latitudes below the sea-level critical latitude. Such a conclusion is contrary to the facts. In order therefore to secure an increase of intensity with altitude below the critical latitude *it is necessary to suppose that the primaries are accompanied by secondaries whose number increases with the altitude and so with the energy of the primary.*[7]

Quite apart from the foregoing consideration, however, other difficulties arise as a result of the law of distribution of incoming primary energies which it is necessary to assume in order to account for the variation of intensity with altitude in the regions where such variation of intensity is to be expected. For the elucidation of this matter, and also to provide the material for subsequent developments we shall proceed to determine the energy distribution necessary to provide for an exponential law or a combination of contributions obeying exponential laws.

[7] I exclude here considerations founded upon "straggling," as such lines of escape do not seem to have been developed in sufficient detail to result in the correlation with all of the facts concerned.

3. Spectral Energy Distribution Necessary to Provide Exponential Law of Absorption of Primaries

In the remainder of this paper, whenever we speak of the "intensity of the rays," we shall refer to the coefficient of $dsd\omega$ in the expression for the number of rays passing per second through the horizontal element of area ds within the limits specified by the vertical solid angle $d\omega$.

Let us suppose that the range R in the homogeneous atmosphere is given as a function of its initial energy E by the relation

$$E=\psi(R). \tag{5}$$

Let N be the intensity at a depth x below the top of the homogeneous atmosphere. If dN is the change of N in a distance dx, then $-dN$ is the contribution to the intensity by those rays which, at the top of the atmosphere have energies between E and $E+dE$, where

$$E=\psi(x);\quad dE=(d/dx)[\psi(x)]dx. \tag{6}$$

Thus, if the energy distribution of the vertical rays at the top of the atmosphere is given by

$$dN_0=F(E)dE \tag{7}$$

at the poles, for example, where all of the rays can enter the atmosphere, we have

$$-dN=F[\psi(x)](d\psi/dx)dx. \tag{8}$$

If N is to be exponential in x, with an absorption coefficient μ, then

$$N=N_0e^{-\mu x} \tag{9}$$

and

$$-dN=\mu N_0e^{-\mu x}dx. \tag{10}$$

It is to be observed that N_0 is given by

$$N_0=\int_0^\infty F(E)dE. \tag{11}$$

It is further to be observed that, in accordance with the conclusions reached in Section 2, relation (9) holds only for depths x greater than x_φ, where

$$\psi(x_\varphi)=E_\varphi. \tag{12}$$

In other words, it holds for $\varphi > \varphi_{cz}$. By comparison of (8) and (10), we thus have

$$F[\psi(x)](d\psi/dx) = \mu N_0 e^{-\mu x}.$$

The solution of this equation for F is

$$F(\xi) = \mu N_0 e^{-\mu\chi(\xi)}((d\chi(\xi))/d\xi), \tag{13}$$

where ξ is any variable, and $\chi(\xi)$ is the function which expresses R as a function of E through (5) in the form

$$R = \chi(E). \tag{14}$$

Thus
$$F(E) = \mu N_0 e^{-\mu R}(dR/dE), \tag{15}$$

where R is given as a function of E by (14), or if we prefer by (5). The energy spectrum thus becomes determined explicitly, directly we have assigned the range as a function of the energy through (5). It is to be observed, however, that the experimental existence of an exponential law of intensity up to any altitude h only determines the energy distribution for energies greater than a minimum value determined by $E = \psi(h)$, so that at any latitude φ, the energy distribution is only determined for values of E greater than the minimum energy of entry E_φ, as indeed might be concluded from fundamental considerations.

Case of constant energy loss per unit of path. This corresponds to Eq. (1) and yields

$$F(E) = (\mu/\alpha)N_0 e^{-\mu E/\alpha}, \tag{16}$$

or, starting with $F(E)$ as fundamentally assigned we see that if

$$F(E) = Ae^{-\beta E} \tag{17}$$

an exponential law will result for the intensity for $\varphi > \varphi_{cz}$ with

$$\mu = \alpha\beta; \quad N_0 = (\alpha/\mu)A = A/\beta. \tag{18}$$

With $\alpha = 0.77 \times 10^8$; and, $\mu = 0.5$ for the soft component of the radiation, both expressed in terms of 1-meter water equivalent, we have $\beta = 0.65 \times 10^{-8}$. The vertical intensity at the top of the atmosphere at magnetic latitude φ is given by integrating (17) from the entrance energy E_φ to infinity, and is proportional to exp $(-0.65 \times 10^{-8} E)$. The ratio of the corresponding intensities at latitudes 41° and the equator, for example, is therefore exp $[0.65 \times 10^{-8}(17-6) \times 10^9] = \exp(71.5)$, an enormous quantity out of all harmony with any possibility in relation to the facts.

Case where the energy loss per unit of path is composed of a constant part α, plus a part λE_x proportional to the energy of the primary. Using (15) in combination with (4), which was derived from (2) we find

$$F(E) = \frac{\mu\alpha^{\mu/\lambda}N_0}{\lambda^{(1+\mu/\lambda)}}\left[E + \frac{\alpha}{\lambda}\right]^{-(1+\mu/\lambda)}. \tag{19}$$

In terms of $F(E)$ regarded as fundamentally assigned, we conclude that provided that

$$F(E) = B_p/(E+a)^p, \tag{20}$$

where B_p and p are constants, an exponential law of the type (9) will result for the intensity, for $\varphi > \varphi_{cz}$, with

$$\mu = (p-1)\lambda, \tag{21}$$

$$(p-1)N_0 = (\lambda/\alpha)^{p-1}B_p, \tag{22}$$

provided that $a = \alpha/\lambda$.

It is of significance to note that both for this case and for that founded upon constant energy loss per unit of path, μ is not determined uniquely by the energy loss per centimeter of path, but depends also upon the law of energy distribution in the spectrum of the entering rays. In principle, the condition $a = \alpha/\lambda$ is illogical since it makes $F(E)$ depend upon processes of energy loss in the atmosphere. The condition $a = 0$ would remove the logical difficulty, but would destroy to some extent the exponential form for the intensity inherent in (20). However, since α/λ is of the order 4×10^8, and so is much smaller than even the energy necessary for penetration of the earth's magnetic field in all but the highest latitudes, the neglect of α/λ is not of fundamental importance. In other words, the α/λ contribution is not of fundamental importance one way or another. For these reasons we shall retain it, since its presence adds to the mathematical simplicity of our operations. In fact, in all that follows, we shall make our discussions in terms of $E + \alpha/\lambda$ instead of E, and shall use, in fact, a new quantity W, defined by

$$W = E + \alpha/\lambda. \tag{23}$$

Again, the vertical intensity at latitude φ is obtained by integrating $F(E)$ from E_φ, to infinity, and by use of (20) and (21) is seen to be proportional to $(E+\alpha/\lambda)^{(1-p)}$, where $(p-1) = \mu/\lambda$. Thus, in terms of the values already quoted, we

find that the ratio of the intensities at 41° and at the equator is $(173/63)^{1.5}=4.3$. This value is quite reasonable in relation to the possibilities suggested by such experimental data as exist.

However, as already pointed out, such variation in the vertical intensity as is found at the top of the atmosphere should, on the present form of theory, be found also at all altitudes, including sea level, for $\varphi<\varphi_{c0}$. Moreover, no variation of any kind with altitude is provided for the regions $\varphi<\varphi_{cx}$ and no explanation is provided for the so-called hard component. We shall attack these matters in the next section.

4. Development of the View That the Observed Entities are Combinations of Primaries and Secondaries

Following the first analysis made by R. A. Millikan, various analyses of intensity-altitude cosmic-ray data have been made from time to time. W. Kramer[8] specified four components for the radiation with separate absorption coefficients, and with corresponding intensity coefficients J which correspond to the relative intensities for the different components when $x=0$. Kramer's values are as follows:

μ	0.52	0.16	0.075	0.021
J	92	4.3	3.3	0.4

We shall omit the small component with $\mu=0.021$. We shall assign $\mu=0.5$ for the soft component, and we shall lump the second and third components into one hard component with $\mu=0.12$. We shall assign the intensities of the hard and soft components so as to result in the same ratio for the sea-level values as is given by Kramer's soft component, and the combined value of his second and third components. Thus we have

μ	0.12	;	0.50
J	9.6	;	90.4

In former publications, the writer has emphasized the role played by secondaries and even rays from cosmic-ray bursts in contributing to the *observed* cosmic radiation;[9] and in particular he has developed a theory[10] in which it was supposed that the primaries passed, for the most part, right through the atmosphere and produced along their paths secondaries which perpetuated the directions of flight of the primaries. It was supposed, to a first approximation, that the product of the number of secondaries produced, per unit of path, and the range of the secondaries was proportional to the energy of the primary. These assumptions led to an exponential law for the measured intensity of the secondaries. It was not supposed that the primaries of necessity produced their secondaries in single acts. Photons, for example, might intervene as intermediaries. In the more detailed development of the theory, the law of loss of energy was generalized to the type (2), and it was shown that, in this form the theory possessed the power to correlate a large number of experimental phenomena. The primaries paid to the measured radiation a direct contribution whose story was not developed in any great detail. In the present section we propose to amplify the story in greater detail, particularly with regard to the mutual relationship of the primaries and higher order radiations, and we shall develop the theory to the point of harmonizing its numerical predictions with experiment.

The primary background. It will turn out that we shall have to use a primary background composed of contributions which, in the case of the background of the soft component, at any rate, obeys an exponential law. For this purpose, therefore, we have the form of $F(E)$ already developed in Eq. (20), which, as will readily be seen, is not limited to a single component but, in the form

$$F(E)=B_p/(E+\alpha/\lambda_p)^p+B_q/(E+\alpha/\lambda_q)^q, \quad (24)$$

for example, is capable of giving rise to two primary absorption coefficients of the form $(p-1)\lambda_p$ and $(q-1)\lambda_q$ as the result of a single type of primary entity. Unfortunately the desirable consummation inherent in such a hope will have to be modified for reasons which will develop later; but, in the meantime, it is of importance to realize that the different contributions to $F(E)$ pay independent contributions to the primary intensity, and therefore to the intensities of the

[8] W. Kramer, Zeits. f. Physik **85**, 411 (1933).

[9] W. F. G. Swann, Phys. Rev. **43**, 945 (1933); Phys. Rev. **44**, 1025 (1933); Phys. Rev. **46**, 432 (1934); also J. Frank. Inst. **220**, 373 (1935), in which the property of high degree of conservation of direction by secondaries is demonstrated.

[10] W. F. G. Swann, Phys. Rev. **46**, 828 (1934); Phys. Rev. **48**, 641 (1935).

secondaries arising from those primary contributions.

In what follows, it will become necessary to introduce an upper limit E_M to the energy of the primaries. This will destroy the rigorous realization of the exponential form for the component concerned, but it will turn out that no serious consequences result therefrom.

We confine our attention to a single component. We utilize the quantity W defined in (23), which quantity is approximately the energy of a ray; and, bearing in mind (4), we obtain the vertical intensity N_p of the primaries for $\varphi > \varphi_{cz}$ by integrating $F(E)$ up to $W_M = E_M + \alpha/\lambda$, from a lower limit $\alpha e^{\lambda x}/\lambda$, corresponding to $E_x = 0$. For $\varphi < \varphi_{cz}$, the lower limit of W is $W_\varphi = E_\varphi + \alpha/\lambda$, where E_φ is the energy for vertical entry at the latitude φ. Thus

$$N_p = \frac{B_p}{(p-1)}\left(\frac{\lambda}{\alpha}\right)^{p-1}\left[e^{-(p-1)\lambda x} - \left(\frac{\lambda W_M}{\alpha}\right)^{-(p-1)}\right] \quad \text{for } \varphi > \varphi_{cz}, \quad (25)$$

$$N_p = \frac{B_p}{(p-1)}\left[W_\varphi{}^{-(p-1)} - W_M{}^{-(p-1)}\right] \quad \text{for } \varphi < \varphi_{cz}, \quad (26)$$

where p is related to the absorption coefficient μ, by

$$(p-1)\lambda = \mu. \quad (27)$$

For latitudes below the sea-level critical latitude, there is no variation with altitude; and for greater latitudes N_p changes from the form specified by (25) to that specified by (26) at the altitude given by Fig. 1. When W_M is infinite, (25) is purely exponential.

For the case where p is equal to or less than unity, an upper limit to E_M is necessary for the realization of a finite value for N_p. The case where $p = 1$ is of interest; and, in that case

$$N_p = B_p \log_e [\lambda W_M/\alpha e^{\lambda x}] \text{ for } \varphi > \varphi_{cz}, \quad (28)$$

$$N_p = B_p \log_e [W_M/W_\varphi] \quad \text{for } \varphi < \varphi_{cz}. \quad (29)$$

When N_p does not obey a true exponential law, it is convenient to define a variable coefficient of absorption μ_x as

$$\mu_x = -(1/N_p)dN_p/dx.$$

We then have

$$\mu_x = (p-1)\lambda/[1-(\alpha e^{\lambda x}/\lambda W_M)^{p-1}], \quad (30)$$

and, for $p = 1$

$$\mu_x = \lambda/\log_e [\lambda W_M/\alpha e^{\lambda x}]. \quad (31)$$

Both (30) and (31) approach their ideal values $\mu = (p-1)\lambda$, when $W_M = \infty$.

Theory of soft component

Certain guiding considerations control us in our choice of a theory at this stage. The first concerns the striking fact, which has been carefully established by R. A. Millikan and his collaborators,[11] that the coefficient of absorption for the soft component is 0.5 everywhere, i.e., for regions above and below the critical latitude.

Suppose now that the number n_s of secondaries accompanying a primary at the place where it has an energy E_x is a function of E_x, or rather of W_x of the form $n_s = f(W_x)$. Then, in view of (3) we have

$$n_s = f(We^{-\lambda x}), \quad (32)$$

where W is the value of W_x at $x = 0$. The number of primaries lying within the range W_x to $W_x + dW_x$ is equal to the number which at $x = 0$ lie within the range W to $W + dW$, where W is related to W_x by (3). Thus, at places for which $\varphi < \varphi_{cz}$, and in particular for φ less than the sea-level critical latitude, we must have, for the intensity of the secondaries

$$N_s = \int_{W_\varphi}^{W_M} F(W) f(We^{-\lambda x}) dW. \quad (33)$$

In order that N_s shall be exponential in x, with a coefficient μ_s, it is necessary and sufficient that $f(We^{-\lambda x})$, that is n_s shall be of the form

$$n_s = \gamma(We^{-\lambda x})^s,$$

where $s\lambda = \mu_s$, and γ is a constant.

In this case, with $F(W) = B_p/W^p$ (33) becomes

$$N_s = \gamma B_p e^{-\mu_s x} \int_{W_\varphi}^{W_M} W^{(s-p)} dW. \quad (34)$$

Incidentally, with the value $\lambda = 0.33$ and $\mu_s = 0.5$ already assigned, the condition $s\lambda = \mu_s$ gives $s = 1.5$.

[11] I. S. Bowen, R. A. Millikan and H. V. Neher, Phys. Rev. **44**, 246 (1933); also R. A. Millikan, H. V. Neher and S. Korff, Phys. Rev. **49**, 871 (1936).

For $\varphi > \varphi_{cz}$, i.e., for latitudes greater than the critical latitude, the primaries also suffer absorption. Now it has been shown elsewhere by the writer[12] that if the primaries obey a true exponential law, then over the range in which they obey that law there is a constancy of "quality" with altitude in the sense that, at all altitudes, the energy spectrum must be the same. All energies change in the same proportion with altitude. Under these conditions, regardless of the law of production of secondaries as a function of the primary energy, the factor of proportionality between intensities of secondaries and of primaries must be the same at all altitudes. *Under such conditions the secondary intensity must obey an exponential law with the same absorption coefficient as that of the primaries.* Thus if E_M is sufficiently large to guarantee a true exponential relation for N_p, in order to obtain a coefficient $s\lambda$ for the secondaries we must have, in accordance with (27) for E_M infinite,

$$(p-1)\lambda = s\lambda.$$

Hence $$(p-1) = s. \tag{35}$$

Thus (34) yields

$$N_s = \gamma B_p e^{-\mu_s z} \log_e (W_M/W_\varphi) \text{ for } \varphi < \varphi_{cz}. \tag{36}$$

For $\varphi > \varphi_{cz}$, the only change necessitated is the replacement of the lower limit W_φ by $\alpha e^{\lambda z}/\lambda$. Thus

$$N_s = \gamma B_p e^{-\mu_s z} \log_e (\lambda W_M/\alpha e^{\lambda z}) \text{ for } \varphi > \varphi_{cz}. \tag{37}$$

It is to be noted that regardless of the values of s and of λ the logarithmic form in (36) and (37) is inevitable.

With $s = 1.5$, necessitated by the values of μ_s and λ concerned, (35) gives $p = 2.5$, so that

$$F(E) = B_p/W^{2.5}. \tag{38}$$

For the general case

$$p = 1 + \mu/\lambda. \tag{39}$$

It will readily be seen that with the value $p = 2.5$, and with an upper limit as low even as 5×10^{10} ev the departure of (25) from the true exponential form is negligible.

It is of interest to observe that *the equality of μ_s for regions above and below the critical latitude leads inevitably to the form of dependence of secondary production upon primary energy and to the value of p for the primaries.*

Note on the significance of the relation between secondary production and primary energy. We have regarded the number n_s of secondaries accompanying a primary as a function of W_z, i.e.,

$$n_s = f(W_z). \tag{40}$$

If r is the range of a secondary, and σ is the number of secondaries produced per unit of path, we have, approximately

$$n_s = \sigma r = f(W_z). \tag{41}$$

If ϵ is the energy of a secondary, and if we regard the term λE_z in (2) as representative of the loss encountered per unit of path in producing these secondaries, then

$$\sigma\epsilon = \lambda E_z = \lambda W_z, \text{ approximately.} \tag{42}$$

Thus, from (41) and (42)

$$\epsilon/r = \lambda W_z/(f(W_z)). \tag{43}$$

For the special case to which we have been led, where $n_s = \gamma W_z^{s}$, we have

$$\epsilon/r = \lambda/\gamma W_z^{(s-1)}. \tag{44}$$

The content of our assumption is comprised in the following: Suppose that theory or experiment has given us some relation between r and ϵ. Then (43) becomes an expression of an assumption as to how ϵ depends upon E_z. Next (42) becomes a statement of how σ is to depend upon E_z in order that the energy loss per unit of path shall be proportional to E_z. With (42) and (43) holding, (40) becomes provided for. In subsequent determination of the constants concerned, the constant γ, for example, our main care must be to see that ϵ/r as given by (44) does not come out smaller than would be reasonable for the average energy per unit range of a secondary. Thus, ϵ/r should not be less than 10^8 ev per meter of water equivalent, so that if the upper limit of the energies concerned is E_M (or W_M approximately), we must have

$$\gamma < \lambda/(W_M^{0.5} \times 10^8), \tag{45}$$

for the case where $s = 1.5$.

The hard component

At this stage our theory has given us a satisfactory preliminary account of the soft compo-

[12] W. F. G. Swann, Phys. Rev. **47**, 575 (1935).

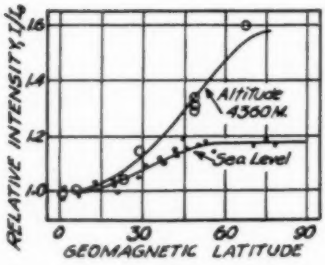

FIG. 2. Data, quoted from A. H. Compton, on the variation of cosmic-ray intensity with latitude at sea level and 4360 meters altitude.

nent. We must, however, examine it in relation to the latitude effect, and here the hard component will become involved. We shall denote by R_0 the ratio of the vertical sea-level intensity at the sea-level critical latitude to the corresponding sea-level intensity at the equator. R_x shall be the corresponding ratio for the same latitudes at the depth x below the top of the atmosphere.

For the secondaries, R is obtainable from (36). For an upper energy limit equal to 5×10^{10} ev $R_x=R_0=1.92$, and for an upper limit of 10^{11} ev it is 1.56.

The latitude ratio for the primaries is given by (26); and, for the above upper limits the ratios are approximately the same and are 5.5 and 4.9, respectively, since $p=2.5$. The resultant sea-level latitude ratio *for the soft component* cannot be less than the value given by the logarithmic term. It is then necessary to look to the hard component to iron out the sea-level ratio to the observed value, say 1.14,[13] leaving the soft component dominant at high altitudes, however.

An easy way to dispose of the hard component is to attribute it to photons, in which case it would have no latitude effect. On a preliminary survey such a procedure presents difficulties which tend to evaporate upon further scrutiny, however. The situation is worthy of discussion.

The latitude effect in the light of a hard component which itself shows no latitude effect. If we take Kramer's data, we find that the intensities of the hard and soft components at *sea level* are in the ratio 4.8 to unity. Taking these figures as applying to some place above the sea-level critical latitude, we find that if y is the ratio of the vertical intensity for the soft component at $\varphi=\varphi_{c0}$ to that at $\varphi=0$, and if 1.14 is the corresponding ratio for the total intensity, and if the hard component has no latitude effect

$$R_{c0}=(N_s+4.8N_s)/(N_s/y+4.8N_s)=1.14,$$

where N_s is the intensity of the soft component. Thus $y=3.5$. Incidentally this represents the maximum latitude effect which can be produced between φ_{c0} and $\varphi=0$ at any altitude apart from the invocation of circumstances of a type extraneous to those involved in the expression of the intensity in the form of the sum of two exponential contributions. Of course, the latitude effect extends to greater latitudes at higher altitudes. In fact, at any altitude, it extends to the latitudes given by Fig. 1, and naturally the intensity ratio goes on increasing up to this latitude. The value $y=3.5$ while theoretically attained only at the top of the atmosphere would be approached at altitudes for which the soft component dominates the hard component. Thus, for example, at an altitude corresponding to $x=6$ meters of water, we should have for the ratio of the intensity at $\varphi=42°$ to that at $\varphi=0$, a value R_6 given by

$$R_6=(4.52+4.67)/(4.58/3.5+4.8)=1.55,$$

for the case where $R_{c0}=1.14$ for sea level. The numbers 4.58 and 4.8 represent the relative vertical intensities at $x=6$ meters of water, calculated from Kramer's data cited earlier, in which the relative intensities of the soft and hard components at $x=0$ are 90.4 and 9.6, respectively, and in which the corresponding absorption coefficients are 0.5 and 0.12.

Now at an altitude of 4360 meters, which is not far from the equivalent of $x=6$ meters of water, A. H. Compton's data shown in Fig. 2 give a value of R_6 equal to 1.30. The excess of this ratio over unity, which is the thing which counts, is thus only a little more than one-half of the excess calculated on the assumption that the hard component shows no latitude effect. A latitude effect for the hard component would reduce the foregoing discrepancies, but would call for a charged corpuscular origin for the hard component, or at any rate for a portion of it.

While the foregoing considerations appear to mitigate against the claim of photons for the

[13] P. Auger and L. Leprince-Ringuet, Int. Cong. Phys. 1, 188 (1935).

position of the hard component, their force becomes annulled in the light of the conditions to which our theory of the soft component has led—conditions in which for $\varphi < \varphi_{c_0}$ there is a primary contribution to the intensity, a contribution independent of altitude but dependent on latitude, and which possesses the power to provide at sea level the necessary latitude variation which a photon component would lack. In the light of these considerations, let us therefore examine the possibilities inherent in the assumption of a "non-field sensitive," a noncharged hard component, remembering of course that if such a component is to affect Geiger counters, it must act through its secondaries. Using (25), (26), (36) and (37) and recalling that $p=2.5$ we find for the vertical cosmic-ray intensity I,

$$I = B_p\left[\frac{2}{3}\left(\frac{\lambda}{\alpha}\right)^{1.5} + \gamma \log_e\left(\frac{W_M\lambda}{\alpha e^{\lambda x}}\right)\right]e^{-\mu_s x} + Ae^{-\mu_h x} - \frac{2}{3}B_p\left(\frac{1}{W_M}\right)^{1.5} \quad \text{for } \varphi > \varphi_{cz}, \quad (46)$$

$$I = \frac{2}{3}B_p\left[\frac{1}{W_\varphi^{1.5}} - \frac{1}{W_M^{1.5}}\right] + B_p\gamma\left[\log_e\left(\frac{W_M}{W_\varphi}\right)\right]e^{-\mu_s x} + Ae^{-\mu_h x} \quad \text{for } \varphi < \varphi_{cz}, \quad (47)$$

where A is the intensity of the hard component whose absorption coefficient is μ_h.

Only for $\varphi > \varphi_{cz}$ does our theory give a primary as well as a secondary variation with altitude for the soft component; and, it must be in this region that we regard Kramer's analysis as applicable. The contribution in (46) which is proportional to γ is not truly exponential,[14] but involves a slowly varying logarithmic coefficient. For the purpose of comparison with Kramer's analysis we shall regard the comparison as made at sea level, and shall evaluate the logarithmic coefficient in question there.

We assume $\lambda=0.33$ and $\alpha=0.77\times10^8$, as before, write $\gamma_0=\gamma\times10^{12}$, $A_0=A\times10^{12}$, and assume, for purposes of trial that $E_M=5\times10^{10}$ ev, which corresponds to $W_M=502\times10^8$ ev. Then Kramer's value 9.4 for the ratio of the intensities of the soft and hard components causes (46) to yield

$$0.190B_p + 2.041\gamma_0 B_p = 9.4A_0. \quad (48)$$

Eq. (47), with $\mu_s=0.5$ and $\mu_h=0.12$ gives, for the sea-level critical-latitude ratio

$$\frac{1.27\times10^{-3}B_p + 13.76\times10^{-3}\gamma_0 B_p + 0.301A_0}{2.88\times10^{-4}B_p + 7.12\times10^{-3}\gamma_0 B_p + 0.301A_0} = R_0, \quad (49)$$

(48) and (49) yield

$$(7.35+79.1\gamma_0)/(6.37+72.4\gamma_0) = R_0. \quad (50)$$

If we assign $R_0=1.14$, we find $\gamma_0=0.043$ so that $\gamma=0.043\times10^{-12}$.

This value of γ leads to results which are not unreasonable. Thus, for the highest energy assigned, $W_M=502\times10^8$ ev (44) gives $\epsilon/r=0.3\times10^8$. This value, for the average energy per unit range of the secondary is dangerously small. However, in all places where observations are made which would have any significance in relation to our formulae, W would be much smaller than 5×10^{10} ev. Thus at $x=4$ meters, the maximum energy would be $5\times10^{10}\times\exp[-1.3] = 1.2\times10^{10}$, and the corresponding value of ϵ/r would be about 0.75×10^8 ev. This represents the worst case, and for all lower values of W, the value of ϵ/r is greater.

The foregoing value of γ means that a 10^{10} ev primary would be accompanied by about 40 secondaries.

The ratio of the *total* number of secondaries to primaries for $\varphi > \varphi_{cz}$ is given by the ratio of the two contributions to the soft component in (46). It does not vary greatly with altitude (for $\varphi > \varphi_{cz}$) and amounts at sea level and at magnetic latitude 50° to 1 to 1.9. However, as already implied, the ratio is greater for the high energy primaries, being, as we have already shown, 40 for a 10^{10} ev primary. It is thus easy to see why cloud chamber photographs would not show many high energy particles. Such particles would be represented mainly by their low energy secondaries.

[14] No apology is needed for our departing from the true exponential forms. As a matter of fact the correct forms for the intensities above and below the critical latitude must fit together on the curve represented in Fig. 1. The sum of two exponentials, with constant absorption coefficients could not possibly fit together on this curve even with the best adjustment of the intensity coefficients. Thus the form of theory leading to true exponentials would be illogical. The departure from the true exponential forms in our theory provide for just those elements necessary to secure the fit along the curve Fig. 1.

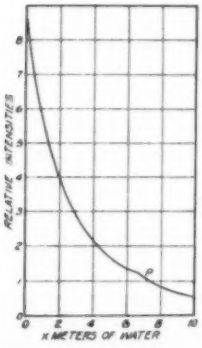

FIG. 3. Relative cosmic-ray intensities as a function of depth below the top of the homogeneous water equivalent atmosphere. The curve is drawn from the theoretical formulae given in Eqs. (46) and (47). The point P is representative of the secondary hump in the intensity altitude curves.

Variation of latitude effect with altitude. On account of the logarithmic term in (47), the latitude effect varies with altitude. With the value of γ chosen to give a sea-level latitude ratio of 1.14, the value of R_x at 6 meters of water equivalent depth comes out as 1.19; and, at $x=4$ meters it is 1.29. The maximum vertical current ratio for any altitude is the ratio of the intensity at the latitude and altitude determined by Fig. 1, to the intensity at the same altitude at the equator. The ratio in question comes out as 1.79 for $x=6$ meters and 2.66 for $x=4$ meters.

The increase of latitude effect with altitude is thus of the same order of magnitude as to correspond to Compton's data but is somewhat smaller. If the hard component possessed a sea-level latitude effect, the effect would be to weaken still further the increase of latitude effect with altitude. The increase of latitude effect with altitude is bound up with the logarithmic term in (47); and, as we have seen the logarithmic form is inevitable if μ_s is to have the same value above and below the critical latitude. The maximum latitude effect attainable at high altitudes is limited by the logarithmic form of this term. The increase of latitude ratio with altitude is very sensitive to the choice of the upper limit. Only when that upper limit approaches close to the limit necessary for vertical entry at the equator does one obtain any increase of latitude ratio with altitude at all. In fact, our theory makes the increase with altitude a symbol of the existence of an upper limit. If $E_M=1.7\times10^{10}$ ev, which is the energy for vertical entry at the equator, the latitude effect of the logarithmic term will be infinite. We are limited, however, in the degree of smallness of the value which we may assign to E_M, since we must permit rays to come in from the due east and due west; and, to secure entry in the equatorial plane this would necessitate an energy of about 6.0×10^{10} ev. Even if we should adopt as low a value as 2.5×10^{10} ev for E_M, the maximum latitude ratio for the logarithmic term for $x=4$ meters would only amount to 8.75, and the complete latitude ratio, including the hard component would be 3.0. All of the published data on variations of intensity with latitude give ratios less than 2, when the observations have been made with a single instrument at different latitudes. Such latitude ratios of the order of 2 to 1, and even 10 to 1 and more as have been quoted as applicable to the top of the atmosphere, depend upon comparison of observations taken with different instruments in different flights. Such comparisons are attended by the greatest difficulty. In the first place, the whole significance of the intensity is modified by the existence of a maximum. This maximum, on the theory developed in this paper, would simply be indicative of the fact that near the top of the atmosphere the range of the secondary electrons is greater than that corresponding to the whole of the air above the point of observation, so that the intensity suffers in relation to the value given by the theory on account of the absence of enough air to produce all of the secondaries required by theory. On this basis the observations of the Bartol Foundation lead to a secondary range of about 82 centimeters of water equivalent. However, our theory provides for a variation of the energy and so of the range of the secondaries with primary energy. There should, therefore, on this account be some variations in the altitude of the maximum with latitude. Then, matters are complicated considerably by the fact that, as the Bartol Research Foundation observations have shown,[15]

[15] See, for example, W. F. G. Swann and G. L. Locher, National Geographic Society, Contributed Technical Papers, Stratosphere Series, No. 1, 7 (1935), in which publication it appears that the horizontal intensity forms 20 percent of the vertical at 40,000 feet; see also W. F. G. Swann, J. Frank. Inst. **222**, 1–11 (1936) in which from our observations in the flight by Professor and Mrs. Jean Piccard we obtained more than 50 percent for the ratio

the horizontal intensity is comparable with the vertical intensity in the stratosphere on account of the bending of the paths of the secondary rays by the earth's magnetic field. Undoubtedly many of the secondary rays actually approach the apparatus from a direction below horizontal, so that the variation of shielding conditions in different experiments is apt to have an important bearing upon the results, particularly as it was formerly supposed that shields were only effective when placed *above* the ionization chambers.

The secondary hump in the intensity-altitude curve. Intimately bound up with the latitude effect is another having to do, possibly, with the secondary hump—the hump below the maximum —characteristic of intensity-altitude curves. At any latitude, there is a value of x determined by Fig. 1, for which the expression for the vertical intensity changes from the type characterized by (46), to that characterized by (47). Above this altitude the chief change is that resulting from the absence of the direct contribution to the soft component by its primaries. We should thus expect a hump in the ionization altitude curve at the value of x concerned. This hump should start at sea level for $\varphi=\varphi_{c0}=41°$, and should gradually climb up the curve with increasing latitude. Intensity-altitude curves obtained with ionization chambers must, of necessity, tend to obscure this hump, since there is a different critical latitude corresponding to each direction from the zenith. Fig. 3 represents the vertical intensity-altitude curve plotted from Eqs. (46) and (47), with the constants already determined and for magnetic latitude 55°. The curve does not, of course, show a maximum, since the maximum represents an added feature depending upon the limitations of the atmosphere as already stated. It does show the secondary hump at $x=6.6$ meters of water. This value of x is considerably greater than the value suggested by high altitude data. It is for this reason moreover that, in spite of our adjustment of the absorption coefficients and the relative sea-level intensities of the hard and soft components to their experimentally established values, the ratio of the total intensity even at $x=0$ to that at sea level is given by the curve as only about 17 instead of three or four times that value, as it should be. Above the secondary hump, the radiation becomes robbed not of its absorption coefficients but of part of its intensity factor; and, if the hump comes at too low an altitude, the ratios of the high altitude intensities to those at sea level became seriously affected. While the exact position of the secondary hump may be regarded at first sight as a matter of refinement which an approximate theory cannot be expected to reveal, it must be admitted that the defect inherent in a failure to make the right prediction becomes more vital on mature consideration. Fortunately, a way of overcoming the difficulty exists; but, since it involves a rather radical change in our views as to the significance of the critical latitude, and since it has been developed since this paper was presented at the Harvard Tercentenary Conference, it is here relegated to an Addendum at the end of the paper.

Possibilities inherent in a field sensitive hard component. If the hard component is of a charged particle type, and is to show an increase with altitude in equatorial regions, it also must be represented by secondaries. The coefficient of absorption is one-quarter that of the soft component, so that if the number of secondaries accompanying a hard component primary, which we shall call a q primary is to be proportional to $(E+\alpha/\lambda_q)^{s_q}$, i.e., $W_q^{s_q}$, we must again have $\mu_h=s_q\lambda_q$.

The most elegant solution of the problem would be one in which we had simply *one form of primary*, with an energy spectrum given by

$$F(W)=B_p/W^p+B_q/W^q, \tag{51}$$

and with a law of production of secondaries such that the number n_s of secondaries accompanying a primary was

$$n_s=\gamma W^{1.5}+kW^{1.5/4}. \tag{52}$$

The working out of the theory would then tell the story of *both the hard component and the soft component simply as the outcome of the form of the energy distribution in the incoming primaries.* The constants λ and α would, of course, be the same for the q primaries as for the p primaries. As a matter of fact, it is perfectly possible to fit up a

of the horizontal to the vertical intensity. In the last flight made by Captain A. W. Stevens and O. Anderson our apparatus gave practically as much horizontal as vertical intensity. It is of course to be observed that horizontal intensities as measured by Geiger counters correspond to the sum of the intensities for two diametrically opposite directions.

theory along these lines, and provide for the right ratio of the intensities of the components and for the sea-level latitude ratio. However, difficulty is encountered in the matter of the variation of latitude effect with altitude. The significant elements are these: If for the q primaries we proceed as we have done for the p primaries, we should conclude that $(q-1)=\mu_h/\lambda=0.38$; and, in line with our former demonstration, the contribution of the q secondaries to the intensity through the term $kW^{1.5/4}$ would come out proportional to $B_q \log_e (W_M/W_\varphi)$ below the critical latitude. However, there would be two additional "cross product terms" in the contribution to the secondaries, a term proportional to the integral of $(1/W^{2.5})(W^{1.5/4})kB_p$, and a term proportional to $(1/W^{1.38})(W^{1.5})\gamma B_q$. Below the critical latitude, for example, these two terms are proportional, respectively, to $B_p k(W_\varphi^{-1.88}-W_M^{-1.88})$ and $B_q\gamma(W_M^{0.12}-W_\varphi^{0.12})$. Of these two terms, the former contributes to the hard component and the latter to the soft component. There are thus two contributions to the soft component secondaries, one proportional to $B_p\gamma \log_e W_M/W_\varphi$, and one proportional to $B_q\gamma(W_M^{0.12}-W_\varphi^{0.12})$. Now when we make use of the intensity ratio of the soft and hard components, it becomes possible to show that the latter contribution to the secondaries dominates the former, and so determines in large measure the latitude effect at high altitudes since it is part of the soft component. However, the latitude effect of this term is weaker than that of the logarithmic term. It is, in fact weaker in this respect than all of the other contributions from the p primaries or secondaries or the q primaries or secondaries. Thus, its dominance at high altitudes tends to cause a decrease rather than an increase of latitude effect with altitude. *It is for this reason that it appears necessary to separate the p primaries and the q primaries into two distinct classes*, one whose law of production is given by $n_s=\gamma W_p^{1.5}$, and the other whose law of production is given by $kW_q^{1.5/4}$. As already stated, apart from the requirements of the increase of latitude effect with altitude, it would be possible to fit up a theory based upon (52), although even then it would be necessary, as indeed it is in any case, to assume for the q primaries a value of q less than 1.38, or even a negative value of q so as to avoid having too large a sea-level latitude effect for the hard component.

Let us then take for the q primaries a contribution to $F(W)$ of the form

$$F(W)=B_qW^n \tag{53}$$

and assume that the number of secondaries n_s accompanying a primary is

$$n_s=kW^{s_q},$$

where $$s_q\lambda_q=\mu_h.$$

We then have for the primary intensity

$$N_q=\frac{B_q}{(n+1)}\left[W^{n+1}-\left(\frac{\alpha e^{\lambda_q x}}{\lambda_q}\right)^{n+1}\right] \quad \text{for } \varphi>\varphi_{qcx}, \tag{54}$$

$$N_q=\frac{B_q}{(n+1)}[(W_{M_q})^{n+1}-(W_{\varphi_q})^{n+1}] \quad \text{for } \varphi<\varphi_{qcx}, \tag{55}$$

and for the secondary intensity

$$N_{sq}=\frac{kB_q}{(n+1+\mu_h/\lambda_q)}\left[(W_{M_q})^{n+1+\mu_h/\lambda_q}-(\alpha e^{\lambda_q x}/\lambda_q)^{n+1+\mu_h/\lambda_q}\right]e^{-\mu_h x} \quad \text{for } \varphi>\varphi_{qcx}, \tag{56}$$

$$N_{sq}=\frac{kB_q}{(n+1+\mu_h/\lambda_q)}\left[(W_{M_q})^{n+1+\mu_h/\lambda_q}-(W_{\varphi_q})^{n+1+\mu_h/\lambda_q}\right]e^{-\mu_h x} \quad \text{for } \varphi<\varphi_{qcx}. \tag{57}$$

Here we have recognized values of λW_M and critical latitudes which may be different for the q primaries than for the p primaries.

The essential thing to observe is that the greater n, the more does N_q approach a radiation with zero absorption coefficient, the more nearly does N_{sq} approach a true exponential with absorption coefficient μ_h, and the smaller the latitude effects of both N_q and N_{sq}, as shown by (55) and (57). Thus, for example, if $n=2$, and $W_{M_q}=5\times10^{10}$ ev, the ratio of N_{sq} at $\varphi=41$ degrees to the value at the equator is less than $[1-(6/50)^3]/[1-(17/50)^3]$, i.e., less than 4 percent. For $n=3$, it is only about 1.3 percent. Moreover, there is no limitation upon k, and so

upon the ratio of the secondaries to the primaries other than that imposed by the necessity of (44) leading to a reasonable value for ϵ/r where γ is replaced by k, λ by λ_q, and s by s_q. Remembering that n_s, the number of secondaries per primary is equal to kW^s, (44) becomes $\epsilon/r=\lambda_q W/n_s$. Hence, if ϵ/r is to be greater than 10^8 and if λ_q is comparable with λ for the p primaries, we have $W/n_s>3\times10^8$. Thus for a 5×10^{10} ev q primary, we can have n_s comparable with 200. This would correspond to $k=200/(5\times10^{10})^{0.36}$; and a 10^9 volt q primary would be accompanied by $200/(50)^{0.36}=50$ secondaries. Thus, under such conditions, the secondaries would dominate the primaries.

With a very small latitude effect provided for the hard component, there would be no marked critical latitude for it; and, its relationship to the soft component would be exactly the same as that already discussed in the case of the nonfield sensitive hard component. The net latitude effect would be calculated as before, and the variation of net latitude effect with altitude would follow as before.

Thus, it appears possible to supplement the story of the soft component equally well with a hard component which is field sensitive or with one which is not—a photon component, for example. The ratio of intensities of hard component to soft component can be provided for. The correct latitude effect can be provided for as can also the variation of latitude effect with altitude.

Relation of theory to shower production and to asymmetry

Shower production. It is a well established experimental fact that the rate of production of small showers from lead increases with altitude at a rate greater than the rate of increase of the total radiation. In fact, the shower production increases approximately with a coefficient equal to that of the soft component of the radiation. This has given rise to the statement that the shower producing radiation is a soft radiation. According to our theory, if the showers in lead are produced according to a law anything like that for the air secondaries, it is the *most energetic primary rays* which are the most efficient in the production of showers; but, in spite of this, they endow the shower production with a coefficient of increase with altitude which is large in proportion to the power of the energy which determines the shower production. It is true that, in the case of a photon hard component we could not predict the net increase of shower production with altitude without knowledge of the relative efficiency of the photons and the charged particles in producing showers (directly or through photon intermediaries); but, in the case of a hard component composed of particles which lose energy more or less continuously along their paths, so long as the shower production in lead by such particles depends upon a higher power of the energy than does the air secondary production by the hard component, shower production will increase with altitude more rapidly than does the cosmic-ray intensity. In the foregoing connections, it may be well to emphasize again, that the "softness" of the component, in the case of the p primaries, at any rate depends not merely upon the energy absorption but also upon the *energy distribution* of the incoming radiation.

East-west asymmetry. The view here taken removes a paradox which has existed between the variation of shower production with altitude, and the east-west asymmetry in shower production. According to the naive view that showers are produced by a soft radiation we might expect that they would show great asymmetry, since the east-west asymmetry is greater for the primary rays of smaller energy than for those of larger energy. Experimentally, however, very little asymmetry has been found in shower production. The reason on our present view, is very clear. It is the rays of high energy which produce the showers, so the showers show very little asymmetry. On the other hand, for the reasons stated, the intensity of shower production increases with altitude at a rate determined by a large coefficient.

Dependence of asymmetry upon altitude. The story of the dependence of asymmetry upon altitude is of interest. To fix our ideas let us imagine two similar cosmic-ray telescopes in a plane parallel to the equatorial plane and pointed at equal angles on the east and on the west side of the zenith. The asymmetry observed by these two instruments depends upon the rays which enter the atmosphere within certain energy limits, and which also succeed in penetrating

down to the instruments. If the apparatus be now taken to a higher altitude, the asymmetry will alter mainly through the effect of decreased absorption permitting rays at the lower energy limit to enter, which rays would not have penetrated to the apparatus at the lower depths.

Now, according to the form of theory we have developed the average entrance energy of the p primaries is approximately $3E_\varphi$ and is determined by the *lower* limit of the energy for entry, while even for the case of a charged particle hard component the average entrance energy of the q primaries is approximately $(n+1)E_{M_q}/(n+2)$ and is determined by the *upper* limit of the energy. Thus, it is the p primaries which are mainly concerned in the variations of asymmetry with altitude, which variations are determined by variations in the numbers of rays entering the instruments at the lower energy limit. *We should thus expect that variation of asymmetry with altitude would be determined by the soft component absorption coefficient*, rather than by the variations with altitude of the cosmic radiation as a whole. A further conclusion derivable from the theory, and one in harmony with the results of T. H. Johnson, is the conclusion to the effect that the latitude effect for shower production is smaller than for the total radiation. Since, according to the theory, shower production depends upon the higher energy rays, its latitude effect will be determined largely by the latitude effect for those rays; but, it is only the rays lying below the upper limit for equatorial entry that show any latitude effect at all.

The nature of the hard component primaries and the soft component primaries

While the present theory does not lead to any very specific conclusions as to the actual *nature* of the particles concerned, the fact that the east-west asymmetry is determined by the low energy rays, points to its becoming associated with the p primaries; and, the fact that asymmetry measurements require positively charged rays suggest that the p primaries may be protons, while the q primaries are electrons. An assumption of protons for the p primaries would not be inconsistent with our failure to find such protons at sea level,[2] since the p primaries and their secondaries are associated with the soft component, and so play but little role at sea level.

Addendum

(Made since delivery of the paper at the Harvard Tercentenary)

The chief weakness in the theory as given in the foregoing lies in its prediction of too low an altitude for the "secondary hump" in the intensity-altitude curve. This difficulty could be alleviated if we could permit for the p primaries a larger value of λ. If, in fact we could take $\lambda=0.5$ instead of 0.32, the modified curve corresponding to Fig. 1 would show an altitude corresponding to $x=5.3$ meters for latitude 55°, so that the secondary hump would come at $x=5.3$ for this latitude, and would be better in agreement with such experimental data as exist. A still larger value of λ would improve matters still further. The value $\lambda=0.5$, would result in $s=1$, so that the number of secondaries accompanying a primary would be proportional to the first power of the energy as assumed in the first form of the theory which I published in 1934.[10] With $s=1$, Eq. (35) requires $p=2$, so that $F(W_p)$ would be inversely proportional to W_n^2. With $s=1$, moreover, requirement (44) now reverts to $\epsilon/r=\lambda/\gamma$ so that γ can be as large as $\lambda\times10^{-8}$ *viz.* 0.5×10^{-8} ev without causing ϵ/r to be less than 10^8 ev per meter of water. With this value of γ, a 10^{10} ev electron would be accompanied by 50 secondaries and there is no value of W_p, no matter how large, which would give trouble as regards condition (44). However, with $\lambda=0.5$, and $\alpha=0.77\times10^8$, Eq. (4) gives for a 1.7×10^{10} ev electron a range of only 9.4 meters of water equivalent. Thus, there would be no *sea-level* critical latitude for the soft component. It would be necessary to leave the sea-level latitude variation entirely to the hard component. Eqs. (55) and (57) provide the story. For $n=0.5$ in (53), and with $\mu_h/\lambda_q=0.36$, which corresponds to $\mu_h=0.12$, and the value $\lambda_q=0.33$ appropriate to the sea-level critical latitude we find 1.13 for R, the ratio of the sea-level vertical intensity of the secondaries at 41° to the corresponding value at the equator. This value of R

is quite satisfactory. The q primaries have a larger latitude effect than the secondaries as shown by (55); but, with the value of k already taken in our former illustrations, the q primaries are entirely masked by their secondaries.

Under the foregoing conditions there would be no variation of latitude effect with altitude until the altitude corresponding to $x=9.4$ already cited, i.e., the altitude 0.6 meter of water, was attained. At this altitude, a critical latitude would appear for the soft component, and would gradually work its way towards increasing latitude with increasing altitude. Thus, for altitudes above 0.6 meter of water, the latitude effect would increase with further increase of altitude as the soft component assumed more and more of the dominant role.

If only one is justified in assuming for the soft component a critical latitude different from the known sea-level critical latitudes, but one which only makes its appearance at altitudes greater than 0.6 meter, then I favor the story just given in preference to that developed in the previous part of this paper, although the only difference is in the choice of the constants. The fundamental theory remains the same for both; and is exhibited better in the general form in which we have presented it in the body of this paper.

A recent development by George Pfotzer. Since the foregoing paper was presented at the Harvard Tercentenary Conference, a paper by George Pfotzer in the August, 1936 issue of the Zeitschrift für Physik has come to my attention.[16] In this paper, the author following the lines indicated by B. Gross, develops the consequences of my 1934 theory,[9, 10] which theory, as already stated, resulted in an exponential law of apparent absorption and is based upon the law of energy loss specified in Eq. (2), combined with the assumption that the number of secondaries accompanying a primary increases with the energy of the primary. It is convenient to take this opportunity to discuss some of the points in Pfotzer's paper for purposes of comparison. In the development which I formerly published, the law of the increase was one of proportionality between secondaries and the first power of the primary energy; and, this is the form used by Pfotzer. Incidentally Pfotzer also gives the form of energy distribution stated here in Eq. (19) which I have derived as a particular case of the more general form developed in (13).[17]

In the development of the present paper I had started with the hope of utilizng the law in which secondary production was proportional to the primary energy, but was driven from the simplicity of this assumption by the necessity of providing for a soft component absorption coefficient equal to 0.5 per meter of water both above and below the critical latitude as demanded by Millikan's observations.[11] As already demonstrated, the necessity for this provision demanded that $s\lambda=\mu_a$, where s is the exponent of the primary energy in the expression of the number of secondaries accompanying a primary. With the value $\lambda=0.25$ which was derived from the energy 6×10^9 ev for penetration at the sea-level critical latitude and from a value of α falling within the limits specified by C. Anderson,[6] s became equal to 2; and, in accordance with (39) p became equal to 3 which gave rise to a law of approximately the inversed cube of the energy for the energy distribution function. Such a law is used by Pfotzer, but purely on an empirical basis. In this form the theory gave considerable difficulty in providing for the proper value of the latitude effect without invoking a situation in which the calculated energy per unit range of the secondaries was too small. I felt the necessity of assuming a smaller value of s, but the value of α stood in the way, since it controlled the value of λ. The situation became eased when it was pointed out to me by Dr. C. G. Montgomery that the values quoted by Anderson for the equivalent of α should really be divided by the density of air. It was now possible to choose between the experimentally allowable limits a value of α which, with 6×10^9 ev for the energy of penetration of the atmosphere gave $s=1.5$. This gave a much more satisfactory story as regards the secondary production in relation to the latitude effect and, incidentally, it led to an energy distribution function inversely proportional, approximately to the power 2.5 of the energy (see Eq. 38). The

[16] G. Pfotzer, Zeits. f. Physik **102**, 41 (1936).

[17] The special form (19), but not the general form (13) quoted by Pfotzer from B. Gross, Physik Zeits. **37**, 12 (1936). In Gross' reference to my paper he quotes J. Frank. Inst. **219**, 97 (1935). A more complete account of the theory concerned is, however, given in Phys. Rev. **48**, 641 (1935).

more radical step involving a return to $s=1$ through the choice of a value of λ as high as 0.5 has been referred to above, and necessitates the assumption of two critical latitudes, one of which does not appear, however, at sea level.

Pfotzer, on the other hand, uses a very large value for μ_s, a value equal to 0.85 per meter of water, and he chooses a very large value, 3×10^8 for α, which value he obtains by empirical adjustment to fit the experimental data.

Pfotzer does not place upon his development the requirement of equality of a soft component absorption coefficient above and below the critical latitude. Had he done so, then, quite apart from the magnitude of all of the constants concerned, the logarithmic forms (36) and (37) would have resulted inevitably, and would have demanded the assumption of an upper limit to the primary energy.

Another point of difference between the present paper and that of Pfotzer lies in the fact that in the former we have provided for a variation of intensity with latitude and for a variation of the latitude effect with altitude, which phenomena placed very stringent requirements upon the theory. Pfotzer obtains the sea-level altitude effect from the hard component, but does not provide for an increase of latitude effect with altitude.

Pfotzer attributes the maximum in the intensity-altitude curve to a range phenomenon of the secondaries and determines from it the secondary range at these altitudes. In this, his conclusions are substantially similar to those which I have reported here and on various former occasions,[18] the calculated range being equivalent to about 82 centimeters of water.

In conclusion, I wish to express my appreciation of the services of Dr. and Mrs. C. G. Montgomery who have given me considerable assistance, necessitating careful discrimination, in the numerical calculations, and who have checked the mathematical calculations.

[18] W. F. G. Swann, "Cosmic-Ray Measurements." Presented at Washington, May 1, 1935, as part of a symposium on the 1935 National Geographic U. S. Army Air Corps Stratosphere Flight. See also W. F. G. Swann, G. L. Locher, W. E. Danforth, C. G. and D. D. Montgomery, National Geographic Society Contributed Technical Papers, Stratosphere Series, No. 2 (1936).

DECEMBER 15, 1936 PHYSICAL REVIEW VOLUME 50

Cosmic Rays as Electrical Particles*

ARTHUR H. COMPTON, *University of Chicago, Chicago, Illinois*

(Received October 12, 1936)

Positive evidence that the primary cosmic rays consist of electrical particles is drawn from three types of experiments:

1. Latitude and directional asymmetry effects. Clay finds 83 percent as intense ionization at the equatorial minimum as in high latitudes. Of the remainder, Rossi's directional experiments show that about 12 percent at least is due to positively charged particles. Corresponding to the 73 percent "nonfield sensitive" remainder at sea level, at high altitudes the remainder must be less than 20 percent, perhaps no more than 2 percent, of that observable in polar regions. An energy distribution analysis, following the method of Zanstra, but using new latitude effect data collected on the Pacific Ocean in collaboration with R. N. Turner, shows a continuous energy distribution of the primary cosmic-ray particles between 0.9 and 1.9×10^{10} ev, and indicates the electrical particle origin of a large part, very possibly the whole of the ionization.

2. Coincidence experiments. Auger, Street and their collaborators have proved that most of the multiple coincidences observed with counter tubes are caused by single high energy ionizing (hence electrical) particles. Experiments by Rossi and Hsiung show that these coincidence producing particles are not secondaries, but originate beyond the atmosphere. Likewise latitude effect experiments by Johnson and absorption experiments by Rossi indicate that the shower producing radiation is produced by electrical primaries. Cloud chamber studies show that almost all of the observed cosmic-ray ionization is due either to particles of the coincidence type or to showers, and is hence ascribable to electrical primaries.

3. Galactic rotation effect. A directional asymmetry of cosmic rays ascribable to the motion of the earth with the rotation of the galaxy, seems to be established by sidereal time variations very recently reported for the northern hemisphere by Illing and for the southern hemisphere by Schonland, Delatizky and Gaskell, and by a new provisional observation by Compton and Turner of a difference of 0.6 percent between the northern and southern

* Based upon a paper delivered at the Tercentenary Conference of Arts and Sciences at Harvard University, September 8, 1936.

hemispheres. These results are in quantitative agreement with the approximate predictions of Compton and Getting based upon electrically charged primaries; but the observed diurnal effect is only about ⅓th as great as is to be expected if the primary cosmic rays are photons. The data are thus difficult to reconcile with more than a few percent of primary photons.

Two lines of positive evidence for photon primaries have been put forward. 1. The flattening of the altitude *vs.* ionization curves at very high altitudes, once interpreted as indicating the gradual growth of secondary ionization as primary photons enter the atmosphere, has been shown by later balloon flights at different latitudes to be a geomagnetic phenomenon, indicating that the corresponding portion of the radiation is electrical in character. 2. Certain high energy nonionizing shower producing rays shown in cloud photographs by Anderson and his collaborators have been ascribed to primary photons. A more detailed examination of the photographs in question, however, seems to show that these shower producing rays are definitely of local and hence secondary origin. The arguments that have been raised by Bowen, Millikan and Neher against the explanation of cosmic-ray ionization as due to electrically charged primaries are all found to have a straightforward answer if we assume the correctness of current theories which make photon production the chief mechanism whereby a cosmic-ray electron loses its energy. The conclusion is drawn that primary photons are not responsible for any of the major features of the cosmic rays as we now know them. It seems necessary to assume the presence of both positive and negative electrons among the primaries. There is also some suggestion of the existence of protons.

IN several recent addresses[1] I have presented evidence which seemed to justify the conclusion that cosmic rays consist almost exclusively of electrically charged particles, and that electrically neutral primary rays, if present, are responsible for so small a fraction of the observed cosmic-ray effects as to be indistinguishable by our present experiments. A similar view has been expressed also by many others.[2] More recent data have seemed to me only to reinforce this position. There have however been put forward from time to time weighty arguments[3–6] for the contrary view that the major part of the cosmic rays is electrically neutral. As far as I am aware, no attempt has been made to answer these arguments in detail. It is my purpose in this paper to review the evidence in light of our present knowledge, and to attempt to reconcile the data that have been presented.

Permit me first to present the positive evidence that electrically charged particles constitute the major part of the primary cosmic rays:

1. Evidence from the Latitude Effect

It is well recognized that the geographical variations in cosmic rays follow the earth's magnetic field so closely that the effect must be a magnetic one. This means that a significant component of the cosmic rays observed near sea level is due to electrically charged primaries; for it has been shown[7–9] that the geographical effect is quantitatively explicable on this basis according to the theories of Störmer[10] and Lemaitre-Vallarta,[11] whereas it cannot be explained in terms of the effect of the earth's magnetic field on secondary electrical particles produced in the atmosphere.[7, 12, 13] The question remains as to what fraction of the observed cosmic-ray effects owes its origin to such electrically charged rays.

Three typical values of the magnitude of the sea-level latitude effect are Clay's datum[2d] of 17 percent reduction with an unshielded chamber between 45° and 0° magnetic latitude, my own figure of 14 percent with a 6 cm lead shield,[14] and Millikan and Neher's value[9] of 12.5 percent with

[1] a. Guthrie Lecture of the Physical Society, Feb. 1, 1935. Proc. Phys. Soc. London **47**, 747 (1935). b. American Philosophical Society Address, Apr. 20, 1935. Proc. Am. Phil. Soc. **75**, 251 (1935). c. Address before American Physical Society and Section B of AAAS, Jan. 1, 1936. Rev. Sci. Inst. **7**, 71 (1936).

[2] E.g., (a) W. Bothe and W. Kolhörster, Zeits. f. Physik **56**, 751 (1929); (b) B. Rossi, Zeits. f. Physik **82**, 151 (1933); Proc. London Conference on Nuclear Physics **1**, 233 (1935); (c) W. Kolhörster, Physik Zeits. **34**, 809 (1933); (d) J. Clay, Proc. Roy. Soc. **A151**, 202 (1935); (e) T. H. Johnson, Carnegie Inst. Supp. Pub. No. 13 (1935); (f) P. Auger, Comptes rendus **200**, 739 (1935); (g) P. M. S. Blackett, *La Radiation Cosmique* (Hermann & Cie., 1935).

[3] H. Kulenkampff, Physik Zeits. **30**, 561 (1929).

[4] Regener, Kramer and Lenz, Zeits. f. Physik **85**, 411 and 435 (1933).

[5] I. S. Bowen, R. A. Millikan and H. V. Neher, Address before London Conference on Physics, October, 1934. (London, 1935), p. 206. Also in Phys. Rev. **46**, 641 (1934).

[6] R. A. Millikan, paper before National Academy of Sciences, Apr. 28, 1936 (unpublished).

[7] A. H. Compton, Phys. Rev. **43**, 87 (1933).

[8] J. Clay, Physica **1**, 363 and 829 (1934).

[9] R. A. Millikan and H. V. Neher, Phys. Rev. **47**, 205 (1935).

[10] C. Störmer, Zeits. f. Astrophysik **1**, 237 (1930).

[11] G. Lemaitre and M. S. Vallarta, Phys. Rev. **43**, 87 (1933).

[12] I. S. Bowen, Phys. Rev. **45**, 349 (1934).

[13] P. M. S. Blackett, reference 2 (g), p. III–18.

[14] A. H. Compton, Trans. Am. Geophys. Union (1933), p. 154.

a 12 cm shield. Of these, Clay's value of 17 percent is to be preferred for our present purpose. This fraction is known to be due to electrically charged primaries, leaving 83 percent to be accounted for.

That a part of the remainder is electrical is established by directional experiments, made with coincidence counting tubes, which show that the rays reaching the earth at the equator come mostly from the west.[15] This, like the latitude effect, is due to the action of the earth's magnetic field, and shows an excess of positively charged particles. At a zenith angle of 45°, having filtered out the soft secondaries with 8 cm of lead, Rossi[15c] finds near the equator 0.76 as many rays from the east as from the west. For these equatorial rays, therefore, at least 24 percent of those incident at 45° west, or about 12 percent of those incident vertically, are due to positively charged primaries. Taking this 12 percent as a reasonable average, there thus remain $0.83\times0.88=73$ percent as an upper limit to be accounted for,[16] the remaining 27 percent having been proved electrical.

An energy distribution analysis based upon the latitude effect shows that these magnetically deflectable rays constitute a portion of what appears to be a continuous energy spectrum. Zanstra has pointed out[17] that, since there is a definite lower limit V_0 imposed by the earth's magnetic field upon the energy of the rays reaching the earth vertically at each latitude, a measurement of the latitude effect for such vertical rays should give their energy spectrum. If $\phi(V)dV$ is the ionization due to the vertical rays having energies between V and $V+dV$, Zanstra shows that

$$\phi(V)dV=-(d\psi/dV_0)dV, \qquad (1)$$

where ψ is the observed ionization due to the vertical rays, and V_0 is the lower limit to the energy of the transmitted electrons, which, expressed in electron volts, is*

$$V_0=1.92\times10^{10}\cos^4\lambda, \qquad (2)$$

λ being the geomagnetic latitude.

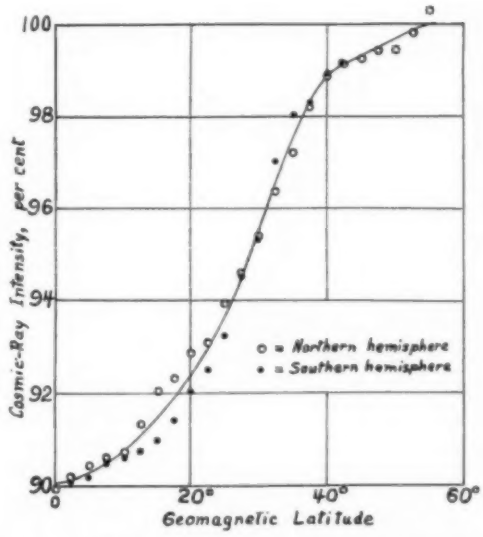

FIG. 1. Latitude effect between Vancouver and Sydney, expressed in percent. Mean of 4 voyages (Compton-Turner, 1936).

Though latitude effect measurements on the vertical rays have been made with coincidence counting tubes,[18] the observations have statistical errors which are too great to be suitable for such an analysis. Measurements of the distribution of cosmic rays with varying zenith angle show, however, that their angular distribution is within experimental error the same at different latitudes.[19] Accordingly, ionization measurements which average the intensity from all zenith angles should give very approximately

[15] E.g., (a) T. H. Johnson, Phys. Rev. **43**, 834; **44**, 856 (1933); (b) L. Alvarez and A. H. Compton, ibid. **43**, 835 (1933); (c) B. Rossi and S. de Benedetti, ibid. **45**, 214 (1934).

[16] Using the data from their own latitude effect and Korff's directional effect measurements in America, Bowen, Millikan and Neher, reference 5, calculate this remainder on a similar basis as 0.85.

[17] H. Zanstra, Naturwiss. **22**, 171 (1934).

* *Note added in proof:* The value of V_0 is given more exactly by the recent calculations of Lemaitre and Vallarta (Phys. Rev. **50**, 493 (1936), Fig. (10). The difference from Störmers formula (2) is however not sufficient to modify the conclusions here reached.

[18] a. P. Auger and L. Leprince-Ringuet, Nature **133**, 138 (1934); b. J. Clay, Physica **2**, 299 (1935).

[19] Among the best published results are those of Johnson, reference 20, in Peru (equator), and of Kolhörster and Janossy, reference 21, in Germany. They find, respectively, for the ratio of the intensity at zenith angle 45° to 0° the values 0.475 and 0.495, each with a probable error of about 1 percent. Auger and Leprince-Ringuet, comparing this ratio at latitudes 0° and 38° with somewhat lower precision, find a slight difference in the opposite sense.

[20] T. H. Johnson, Phys. Rev. **45**, 584 (1934).

[21] W. Kolhörster and L. Janossy, Zeits. f. Physik **93**, 111 (1934).

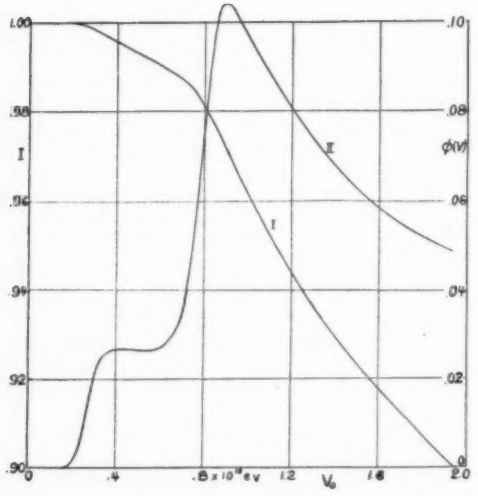

FIG. 2. Curve I represents data of Fig. 1 plotted against the geomagnetic energy minimum V_0. Curve II is the slope of curve I, and represents the energy spectrum of the rays (assumed to be electrons) transmitted by the atmosphere.

the relative values for the vertical component of the rays. We may thus use in place of Zanstra's Eq. (1),

$$\phi(V) = -dI/dV_0, \tag{3}$$

where I is the cosmic-ray intensity as observed with an ionization chamber.

Thanks to the courtesy of the Canadian Australasian Steamship Company, Captain Hill of the *R.M.S. Aorangi*, and especially the very skillful help of First Officer R. N. Turner, we have been able to obtain a series of repeated measurements of the latitude effect over the route from Vancouver, Canada, to Sydney, Australia, using one of the Carnegie Institution's model C meters[22] shielded with 12 cm of lead. The results of 4 trips are shown in Fig. 1, and represent the most suitable data for our modified Zanstra analysis which are now available. Recalling that each geomagnetic latitude corresponds to a given energy minimum V_0, these data may be averaged and plotted against V_0, as in curve I of Fig. 2. For energies lower than 0.2 the curve is drawn flat, in accord with Clay's result that north of $\lambda = 54°$ no change as great as 0.6 percent occurs.[23] When the slopes of this curve are taken, we obtain from Eq. (3) the values of $\phi(V)$ shown in curve II.

For values of V_0 below 0.9×10^{10} the effect of the earth's atmosphere becomes evident in limiting the rays that are received to a higher energy than the minimum admitted by the

[22] Cf. A. H. Compton, E. O. Wollan and R. D. Bennett, Rev. Sci. Inst. **5**, 415 (1934).

[23] J. Clay, C. G. t'Hooft and P. H. Clay, Physica **2**, 1033 (1935).

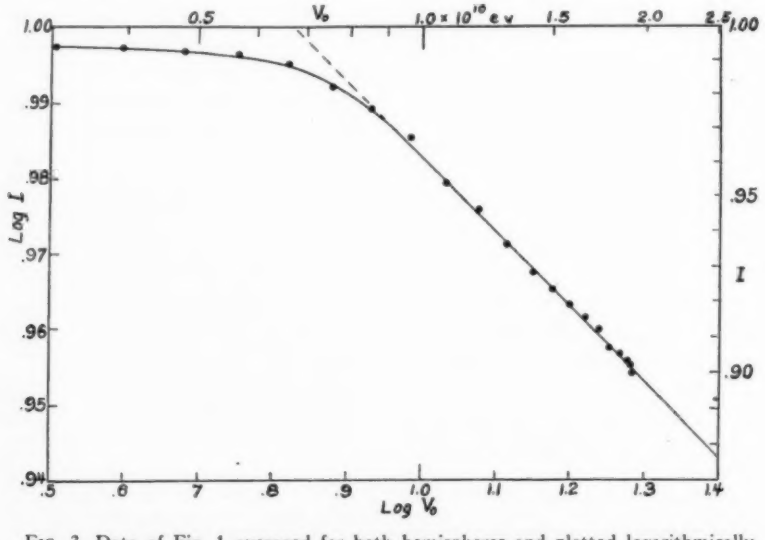

FIG. 3. Data of Fig. 1 averaged for both hemispheres and plotted logarithmically against V_0, showing that the magnetic latitude effect is limited only by the finite magnitude of the limiting energy V_0 corresponding to the earth's magnetic field.

magnetic barrier. The form of the curve for the lower energies strongly suggests two components, one with a limiting energy imposed by the atmosphere of about 8×10^9 ev ($\pm$electrons?) and the other of about 2.5×10^9 ev (protons?). There are several lines of evidence supporting this interpretation. It will, however, be preferable to postpone discussion of these interesting details until the further data now being collected are available.

For our present purpose the important point is that for energies over 0.9×10^{10} ev, where the atmospheric absorption is not a determining factor, there appears a continuous energy distribution as far as 1.92 ev, beyond which the method is no longer applicable.[24] The trend of the curve indicates, however, that electrical particles of much higher energies are present in considerable quantity.

In order to extrapolate to higher energies, a more suitable representation of the data is to plot log I against log V_0, as in Fig. 3, where the points represent the average measured intensities. For energies greater than 0.9×10^{10} ev it will be seen that the points fall within experimental error upon a straight line. If this line were to continue indefinitely, it would mean that for infinite limiting energy V_0 the percentage of transmitted cosmic rays I would be zero, i.e., all the cosmic rays would be proved electrical. In other words, this quantitative analysis indicates that the magnitude of the latitude effect is limited only by the strength of the earth's magnetic field, and if that field were very great, the cosmic rays might well be completely excluded near the equator.

The latitude effect at high altitudes has not been studied in sufficient detail to carry through a similar analysis. Its rapid increase with altitude is however well known. Fig. 4 shows typical results of recent high altitude measurements. Millikan and Neher have recently reported[6] that their airplane flights in the Philippines give results closely similar to those here shown for Peru, whereas Clay's values in Java are presented with reservations. These data indicate a ratio near the top of the atmosphere of at least 4 to 1 between 52° and the equator. There seems also little question but that near the poles the intensity at great altitudes should be considerably greater than at 52°.[25] Moreover, as in the case of the latitude effect at sea level, directional experiments show that much of the rays reaching the equator must be electrical. We may accordingly conclude that of the cosmic-ray ionization at very high altitudes, not more than a few percent can be due to neutral primaries.

2. Evidence from Coincidence Experiments

Perhaps the most striking proof that the coincidences observed with multiple counters in line are due to single high energy particles traversing them all is supplied by the recent experiment performed independently by Auger and Ehrenfest[26] and by Street, Woodward and

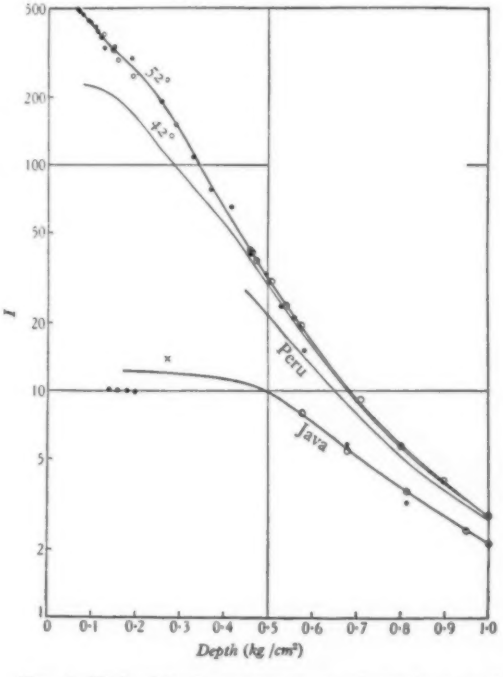

Fig. 4. High altitude measurements of cosmic rays at different latitudes. 52°, Compton-Stephenson-Millikan; 42°, Millikan-Bowen; Peru, Millikan-Neher; Java, Clay.

[24] This conclusion is similar to that reached by Clay, reference 18 (b), from his latitude effect experiments with counter tubes.

[25] Cf., however, *M.* Cosyns, Nature **137**, 616 (1936), whose balloon flights suggest that the latitude effect at high altitudes may end sharply at geomagnetic latitude 49° in Europe.

[26] P. Auger and Ehrenfest, Comptes rendus **199**, 1609 (1934).

Stevenson,[27] and illustrated in Figs. 5 and 6. Cloud photographs are taken when 3-fold coincidences are produced by rays traversing 45 cm of lead. With this arrangement, 90 percent of the photographs record single straight tracks. This is clear evidence that such coincidences are produced by highly penetrating particles. Experiments by Rossi[28] have shown that about half of these particles will penetrate a lead screen equivalent in mass to the atmosphere, which is about the same rate of absorption as is observed with the cosmic rays as measured by an ionization chamber. This strongly suggests that the penetrating particles are the primary cosmic rays, a confirmation of Bothe and Kolhörster's classical argument.[2a]

Rossi[2b] and Hsiung[29] have performed in different forms an experiment which shows that these penetrating particles are not secondaries producible at sea level, but must come from far above the apparatus. Thus in Fig. 7, if penetrating secondaries were excited in 20 cm of lead, the counts with arrangement *C* should be greater than in case *B*. After making allowance for the slight effect of the well-known soft secondary rays, both Rossi and Hsiung find the coincidence rate in cases *B* and *C* identical within experimental error. Thus all the coincidence producing particles originate above the apparatus.

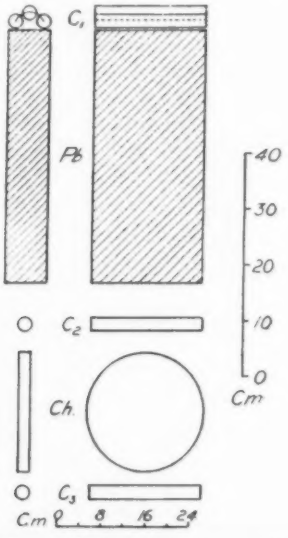

FIG. 5. Arrangement of coincidence counters, C_1, C_2, C_3 and expansion chamber *Ch* for photographing trails of penetrating cosmic rays (Street-Woodward-Stevenson).

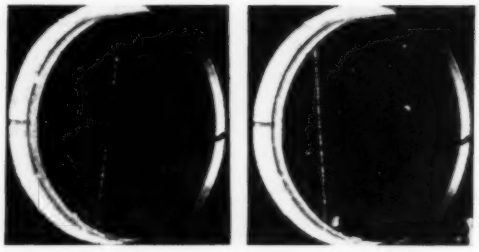

FIG. 6. Trails of two cosmic-ray particles after traversing 40 cm of lead (Street-Woodward-Stevenson).

It might be supposed that these penetrating particles are, however, secondaries excited high in the atmosphere by readily absorbable photons. This suggestion is ruled out by two facts. (1) The coincidence producing particles have been found to show the latitude effect in substantially the same way as does the total cosmic-ray ionization,[18] and also to exhibit directional asymmetry in the earth's magnetic field at the equator.[15] They are thus at least in large measure due to high energy primary electrical particles, and our knowledge of their high penetrating power can leave little doubt but that they are themselves these primary particles. (2) We shall see below that very high energy photons and electrons of the same energy should be absorbed at approximately the same rate. Thus if the high energy coincidence producing electrons are due to primary photons, some of these photons should penetrate the atmosphere, in intensity comparable with the secondary electrons, and excite more high energy electrons in the lead block of the Rossi-Hsiung apparatus. That this does not occur may be taken to mean that the fraction of the coincidence producing particles which are secondaries of high energy photons is zero, with a probable error of about 3 percent.[30]

In addition to these coincidence producing particles, a "shower producing radiation" is like-

[27] J. C. Street, R. H. Woodward and E. C. Stevenson, Phys. Rev. **47**, 891 (1935).
[28] B. Rossi, Naturwiss. **20**, 65 (1932); Zeits. f. Physik **82**, 151 (1933).
[29] D. S. Hsiung, Phys. Rev. **46**, 653 (1934).

[30] If, as Bowen, Millikan and Neher assume, the photons are much more penetrating than the electrons of the same energy, this argument becomes the more cogent; for the conditions for producing high energy electrons in the lead block are then ideal.

wise recognized.[31] This may be studied either with counting tubes out of line, or with a cloud chamber. The evidence strongly favors the view that this shower producing radiation consists of high energy photons. Johnson[31c] has shown, however, that this radiation also is subject to latitude effect, which means that the photons must themselves be produced by primary electrical particles.[32] It would appear that nearly all of the cosmic-ray tracks observed in cloud chambers are of either the high energy coincidence producing type or the shower type. Since both of these are ascribable to primary electrical particles, very little room is left for any ionization that may result from primary photons.

It should be added that cosmic rays in deep mines are measurable with multiple coincidence counters, which, as Kolhörster and Clay have pointed out,[2] means that the rays there observed are corpuscular in the same sense as are those at sea level.

3. Evidence from the Translational Effect

There is a third type of evidence regarding the nature of the primary cosmic rays which comes from the magnitude of the effect on the intensity of cosmic rays due to the earth's rapid motion with the rotation of the Milky Way. The experimental data are now adequate to state with considerable confidence that this effect exists, and is of the magnitude predicted upon the assumption of electrically charged rays. The observed effect is, however, much too small to fit the prediction based upon photons as the primary rays.

It will be recalled that according to the astronomers' recent findings the rotation of the galaxy carries the earth in the direction of the constellation Cygnus, about 45° north, at a speed of about 0.001 that of light. For rays such as cosmic rays going with approximately the speed of light, this produces a Doppler effect difference in frequency of 0.2 percent between the rays striking the front and the back of the earth, if the origin of these rays is assumed to be at rest outside of the galaxy. The corresponding Doppler effect in intensity at the surface of the atmosphere would be 4 times as great, or 0.8 percent. When account is taken of the absorption by the atmosphere, and the fact that the measurements, being made with an ionization chamber, include rays from all angles, Dr. Getting and I calculate about 1.0 percent difference between the front and the back of the earth.[33] This, of course, assumes that if the earth were not moving the intensity would be the same from all directions.

If the primary cosmic rays consist of photons or other neutral particles, this full effect should be observed. If they are electrically charged, according to Störmer's theory the particles will be so strongly deflected by the earth's magnetic field that the effect will be much reduced. A comparison of the predicted and the observed

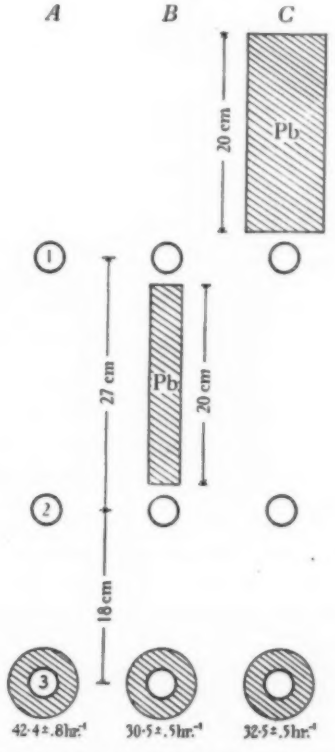

Fig. 7. Hsiung's coincidence experiment.

[31] (a) Cf. B. Rossi, reference 2 (b); (b) C. D. Anderson, R. A. Millikan, S. Neddermeyer and W. Pickering, Phys. Rev. **45**, 352 (1934); (c) T. H. Johnson, Phys. Rev. **47**, 318 (1935).

[32] Rossi (reference 2 (b)) reaches the same conclusion on the basis of absorption measurements.

[33] A. H. Compton and I. A. Getting, Phys. Rev. **47**, 817 (1935). The value there predicted is 1.2 percent difference between the front and the back of the earth. The slightly lower value here given involves a minor correction to our published calculation.

TABLE I. *Test of the translational effect.*
Percent variations.

	Theory		
	Photon Primaries	Positron Negatron Primaries	Experiment
Latitude 47°N			
Amplitude of diurnal variation	0.25	0.02–0.10	0.03+
Phase of diurnal variation	20h 40m	20h 40m	20h 50m
Latitude 34°S			
Amplitude of diurnal variation	0.28	0.03–0.12	0.04×
Phase of diurnal variation	20h 40m	20h 40m	21h 45m
N−S Difference	0.5	0.5	0.6=

+ Triennial mean, Illing.
× Triennial mean, Schonland, Delatizky and Gaskell.
= Provisional value, Compton and Turner.

values is shown in Table I for both the assumption of photon primaries and of positron-negatron primaries. This table shows the data that have been reported within the last few months. It may be noted that whereas the effect calculated for electrical particles is rather uncertain because of the unknown magnitude of the geomagnetic effect, if the cosmic rays are photons the only escape from an effect of about the predicted magnitude would seem to be the difficult assumption that there occurs a natural anisotropy in the source of the rays just sufficient to balance the translational effect.

A suggestive confirmation of the prediction was immediately possible using data obtained by Hess and Steinmaurer during the year 1932. Since that time Illing[34] has published, in June of this year, a reduction of Hess' measurements for the three years 1932, 1933 and 1934, corrected for barometer changes and plotted against sidereal time. The result, as indicated in the first row of Table I, shows a variation with precisely the predicted phase, and with an amplitude which lies within the range estimated for electron cosmic rays, though only 12 percent of that calculated for photon rays.

Illing left the existence of the effect open to some experimental doubt, because of possible seasonal variations. Just now, however, a similar summary of three years' measurements in the southern hemisphere has appeared, by Schonland and his collaborators at Capetown,[35] which shows an effect of the same order of magnitude and with almost exactly the same phase. This disposes of any possibility of a seasonal variation, since this should be opposite in phase in the two hemispheres. We may thus consider the galactic rotation effect to be real, and its magnitude to fit the rough estimates based upon the electron hypothesis of cosmic rays.

Our studies of the intensity of cosmic rays on the Pacific Ocean should eventually give us a good experimental value of the difference in intensity between the northern and southern hemispheres. As yet our results are only provisional, because the southern end of the journey is not far enough south to reach the polar plateau of cosmic-ray intensity. Basing our estimate, however, upon the observed intensity at the first knee in the northern and southern curves, we find a greater intensity in the north by about 0.6 percent—very close to the theoretical difference.

This tentative verification that the translational effect is of the full magnitude given by the theoretical calculation makes it very difficult indeed to reconcile the small diurnal variation with the assumption that photons constitute more than a few percent of the primary cosmic rays.

4. ARGUMENTS FOR PRIMARY PHOTONS

The most effective defense of the hypothesis of primary photons which has come to my attention is that of Bowen, Millikan and Neher,[5] presented before the London Congress of Nuclear Physics in 1934. They admit the electrical character of the primary rays responsible for about 15 percent of the ionization observed at sea level, as shown by latitude effect and directional experiments. They however consider practically the whole of the remaining "nonfield sensitive" portion, estimated as responsible for 85 percent of the sea-level ionization, to be due to primary photons. More recent statements by Professor Millikan[6] indicate that this view has remained essentially unaltered.

[34] W. Illing, Terr. Mag. and Elec. June (1936).

[35] B. F. J. Schonland, B. Delatizky and J. P. Gaskell, Nature **138**, 325 (1936).

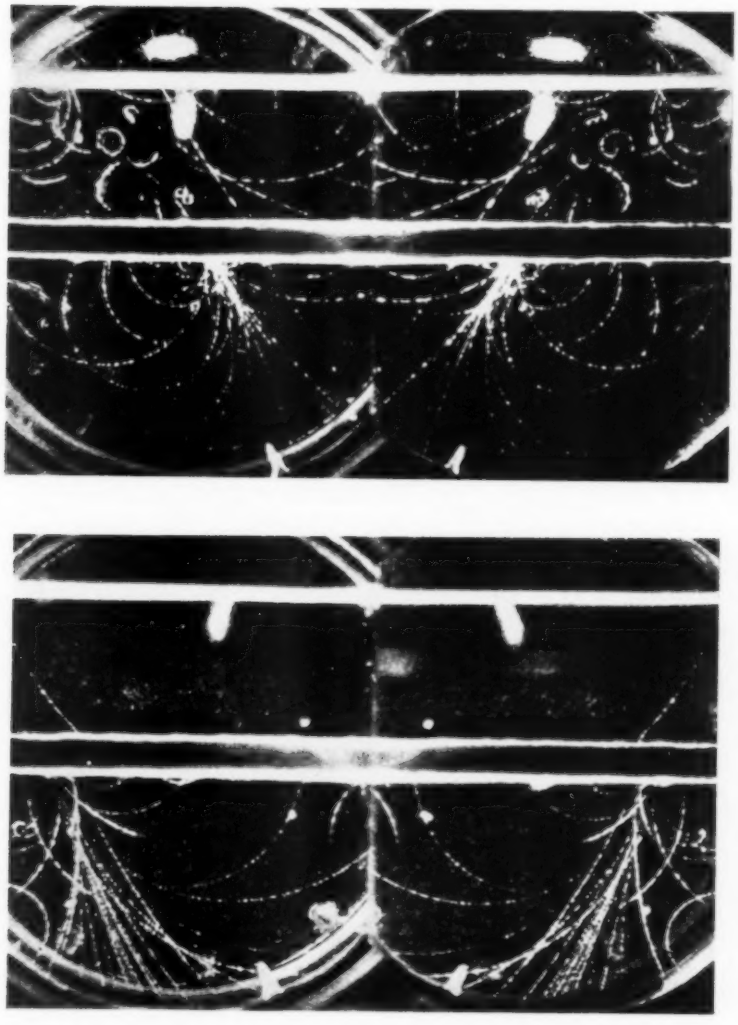

FIG. 8 AND FIG. 9. Cloud photographs of showers (Anderson, Millikan, Neddermeyer, Pickering) that have been used as evidence of incoming primary photons. The showers are interpreted in the text as due to secondary photons.

(1) The one positive argument put forward for primary cosmic-ray photons is the citation[5] of two of Anderson's cloud photographs, Figs. 8 and 9, which show showers of positrons and negatrons that must have been produced by photons having in some cases total energies exceeding 2.5×10^9 ev.[36] "There seems to be no escape," they comment, "from regarding these showers as resulting from incoming photons themselves."

[36] Cf. reference 31 (b), Figs. 9 and 11.

We would suggest the alternative interpretation that the photons which produce these showers are themselves secondaries from an event which occurred not far above the cloud chamber. In Fig. 8 we note that at least two of the showers, the high energy pair from the top of the chamber and the large shower from the central lead plate, have total energies of the same order of magnitude, $>5\times10^8$ ev. If it is assumed that these are caused by the same photon in

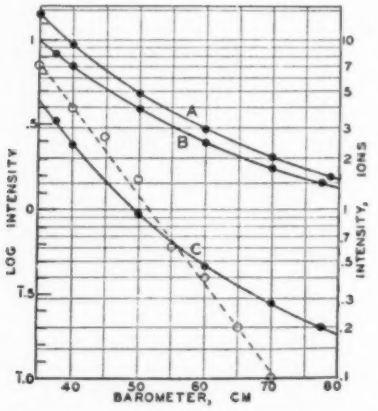

FIG. 10. Cosmic-ray intensity *vs.* latitude curves for, *A*, high magnetic latitudes, *B*, magnetic equator, *C*, difference between *A* and *B*, showing that equatorial rays *B* are absorbed in the same manner as are the magnetically deflectable rays *C* (Compton and Stephenson).

successive ionizing events, it indicates a rate of absorption much too great for a ray which can penetrate the atmosphere. If on the other hand they are due to different photons, their identity in time and direction and their small lateral separation shows that these photons must have originated in the same event not far above the chamber. In either case their secondary origin appears to be necessary. Similarly an examination of Fig. 9 shows at least 3 points of origin of the showers, close together in the central plate. Two of these showers are of the same large order of magnitude of energy. Their direction shows that no one can be considered as the parent of the others; it is clear that they are all due to a close bundle of nearly parallel, non-ionizing rays, presumably photons. Their close proximity indicates that their origin must have been only a short distance above the expansion chamber. Here also a secondary origin of the photons is therefore clearly indicated. The evidence presented for the occurrence of primary photons is thus unsatisfactory.

(2) All the remaining arguments are attempts to show that incoming electrical particles are incapable of producing the observed cosmic-ray effects. Thus Bowen, Millikan and Neher state that the absorption of the high energy electrons "cannot possibly yield an altitude ionization curve remotely resembling that found experimentally from sea level up to 4.5 m." This they emphasize as "the most general and the most cogent argument against the attempt to explain the nonfield sensitive portion of the cosmic-ray ionization as due primarily to incoming high energy electrons." They suppose rather that absorption of such high energy electrons should be of the "range" type instead of the "exponential" type. Such arguments are ineffective when it is recognized that the main part of the energy loss by high energy electrons is through the production of photons (as x-rays are produced by cathode rays), and that this type of energy loss leads necessarily to an approximately exponential diminution of ionization along the path of the electrons.

That high energy electrical rays are in fact absorbed exponentially was shown some years ago by our high altitude measurements of cosmic rays at different latitudes.[37] Thus in Fig. 10, curve *A* represents the absorption in the atmosphere of the rays received at high magnetic latitudes, and *B* that of the rays at the equator. Curve *C* is the difference between *A* and *B*, and thus shows the absorption of electrically charged rays of the type so affected by the earth's magnetic field that they cannot reach the earth at the equator. The close similarity of curve *C*, which includes only electrically charged rays, to curve *B*, which represents the rays transmitted by the earth's field at the equator, shows that electrically charged particles are absorbed in the manner characteristic of cosmic rays. As is well known, a curve of type *C*, being concave upwards, is expressible as a spectrum of exponentially absorbed components. In order to fit this curve the values of the absorption coefficients would need to extend at least from 0.035 to 0.12 per cm of mercury, corresponding to the electrical particles, perhaps of different natures, included in the energy range of from 2×10^9 to 2×10^{10} ev. This would seem to be an adequate answer to the argument against primary electrons quoted above.

According to Bethe and Heitler's theory of absorption,[38] for cosmic-ray energies there is a striking similarity in the dissipation of energy by photons and electrons. This is shown graphically

[37] A. H. Compton and R. J. Stephenson, Phys. Rev. **45**, 448 (1934).

[38] H. Bethe and W. Heitler, Proc. Roy. Soc. London **A146**, 83 (1934).

in Fig. 11, adapted from their paper. We may note that for electrons it is the electron collisions that result in "range" absorption. For energies greater than about 200 mc^2 or 10^8 ev the radiation process is the predominant factor, and the absorption should correspondingly be of the exponential type. This includes all of the important cosmic-ray energy range. Similarly, for energies greater than about 30 mc^2 pair production becomes the predominant method of energy dissipation for photons. It is especially to be noted as shown by the solid line, that while in the low energy range electrons are stopped much more quickly than photons, for energies greater than 1000 mc^2, or 5×10^8 ev, the predicted absorption rate for electrons is but little greater than for photons.

These major results are common also to the extension of Bethe and Heitler's theory proposed by Oppenheimer,[39] and to the alternative theory of Swann.[40] The rate of energy loss by electrons in lead as measured by Anderson has substantiated the predictions up to 800 mc^2, and shows at least no major departures up to 2000 mc^2. The theory is likewise consistent with what little is experimentally known regarding the absorption of high energy photons.

With this theory in mind, the remaining objections[5] to the primary electron hypothesis for cosmic rays are immediately answerable: (3) The photons which occur with energies up to 2.5×10^9 ev, as shown by photographs of cosmic-ray showers, may readily be interpreted as secondaries when we remember that primary electrons are found with energies more than 10 times as great, as proved by equatorial directional experiments. (4) The statement that the hypothesis of primary electrons would leave very few observable electrons at sea level in the intermediate energy range between 3×10^8 and 3×10^9 ev leaves out of account the tertiary electrons excited by the secondary photons, which would be expected to have energies within this range. (5) The claim that photons are 100 times as penetrating as electrons of the same energy is inconsistent with our present knowledge. (6) "Exponential" absorption for rays of cosmic-ray energy is not to be considered a unique characteristic of photons.

(7) The increase in penetrating power with depth at the equator, where the low energy primary electrons are absent, has been considered[5] to favor the primary photon hypothesis. It may be noted that Bethe and Heitler's theory, resulting as it does in a practically uniform absorption coefficient in air or water for all photons of energy greater than 10^7 ev, provides no means whereby *photon* radiation can be hardened as it traverses the atmosphere. Swann has suggested[40] a modification of the theory which would result in increased penetrating power of *electrons* on passing through matter. An alternative interpretation is the assumption that the electrical particles are of two or more types, such as electrons and protons. Protons should excite very little radiation, and should be much more penetrating. They should thus remain after the electrons are absorbed. There are some difficulties with this suggestion, though there are also several lines of supporting evidence. In any case the difficulty of accounting for the hardening of the rays on traversing matter is not removed by substituting photons for electrons as primary rays. On the other hand, direct coinci-

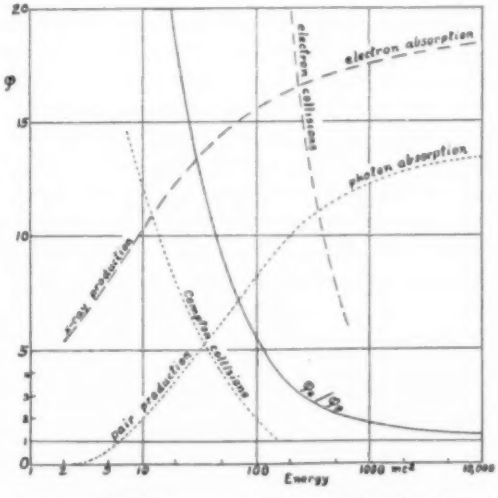

FIG. 11. Effective cross section (units $Z^2r^2/137$) of water molecules for the production of radiative and electron collisions by high energy electrons (broken lines), and pair production and Compton effect collisions by photons (dotted lines). The solid line gives the ratio of the total absorptional cross-sectional areas for electrons and photons (adapted from Bethe and Heitler).

[39] J. R. Oppenheimer, Phys. Rev. **47**, 44 (1935).
[40] W. F. G. Swann, Phys. Rev. **46**, 828 (1934); **47**, 250 (1935).

dence counter experiments by Rossi[28] and others, which record only electrical particles, show a continual hardening as the thickness of the absorption screen is increased to 100 cm. This constitutes direct evidence that electrical rays are hardened by filtering through matter.

(8) The observation by Anderson[41] of nearly equal numbers of positive and negative particles, at least for energies up to 10^9 ev, is taken[5] to imply that the electrons are secondaries resulting from pair production. This is undoubtedly the correct interpretation for most of the lower energy particles. Johnson[31c] has however given apparently conclusive evidence that the so-called "shower producing" cosmic rays are due to primaries consisting of approximately equal numbers of positive and negative rays. This evidence consists in showing that these rays are subject to the latitude effect and are hence electrical, but show very little directional asymmetry and must thus include equal numbers of positive and negative particles. It is thus unsafe to conclude from an equal distribution of positive and negative electrons that they are of local origin.

(9) In earlier discussions[3, 4] the flattening of the altitude *vs.* ionization curve at very high altitudes, as observed by Regener, was taken to indicate the photon character of the primaries, which should not ionize until they had produced secondary electrons, and should thus show feeble ionization near the top of the atmosphere. When, however, the Century of Progress balloon flight, made at a higher magnetic latitude, showed no such flattening, it became clear[1a] that this was a geomagnetic phenomenon, and indicated that the corresponding portion of the radiation is electrical in character.

Summary

These arguments accordingly fail to give any support to the photon hypothesis of the primary cosmic rays. They receive, however, a straightforward interpretation on the hypothesis of electrical primaries if we assume the correctness of the current theories which make photon production the chief mechanism by which an electron loses its energy.

On the other hand, near the top of the atmosphere latitude and directional experiments show that definitely more than 75 percent and probably more than 95 percent of the ionization near the poles is due to charged primaries.

At sea level, the latitude effect establishes the electrical origin of 17 percent of the ionization, and when analyzed in terms of energy distribution indicates a similar origin of a much larger part, very possibly the whole, of the ionization. Directional experiments also show that at least 12 percent of the remainder is electrical. The observed small magnitude of the diurnal changes of cosmic rays caused by the earth's motion with the rotation of the galaxy, seems irreconcilable with more than a few percent of primary photons. Coincidence counter experiments confirm this result, showing that all the coincidence producing rays, within a probable error of about 3 percent, are due to primary electrical particles.

At great depths, the fact that coincidence counting tubes give absorption values in good agreement with those from ionization measurements is evidence that the most penetrating cosmic rays also are electrically charged particles

It is rather surprising to note that there has not appeared positive evidence of a reliable character for any photons whatever among the primary cosmic rays It seems certain that they are not responsible for any of the major features of the rays as we now know them.

In order to describe adequately the properties to the cosmic rays, it seems necessary to assume the presence of both positive and negative electrons among the primaries. There is also some suggestion of the existence of protons. We cannot now discuss these interesting details. It seems however fair to consider the electrically charged nature of the primary cosmic rays as one of their important characteristics established by the last decade of cosmic-ray research.

[41] C. D. Anderson and S. H. Neddermeyer, Proc. Int. Conf. on Physics (London, 1935), Vol. I, p. 171.

On the Apparatus for the Multiple Acceleration of Light Ions to High Speeds

ERNEST O. LAWRENCE AND DONALD COOKSEY, *Radiation Laboratory, Department of Physics, University of California, Berkeley, California*

(Received October 1, 1936)

Significant improvements of the apparatus for the multiple acceleration of light ions, now called the "cyclotron," have recently been made. The apparatus produces many microamperes of deuterons having energies up to 6.3 Mev and a few tenths of a microampere of 11 Mev doubly charged helium ions. The means of deflecting the high speed ions from the accelerating system has also been improved, with the result that the ions can now be withdrawn completely from the apparatus into the air through a thin window in the chamber wall. The present paper is devoted to a detailed description of the cyclotron, including its adjustment and operation, with a discussion of the questions involved.

SINCE the first experiments[1] six years ago, work in our laboratory on the development of methods of accelerating charged particles has gone forward steadily with the endeavor of evolving methods and apparatus for nuclear physics that would find wide usefulness. Almost from the beginning, the method of multiple acceleration of light ions, wherein the ions circulate in a magnetic field in resonance with an oscillating electrical field, gave most promise, and accordingly has been given major attention in our laboratory. Four years ago, details of an apparatus that generates 1.2 Mev protons were described,[2] and two years ago an account[3] was given of a much larger apparatus of this type, capable of generating a fraction of a microampere of 5 Mev deuterons. In the meanwhile, significant improvements have been made not only in increasing the output of ions to many microamperes at higher voltages, and in the general convenience and reliability of the apparatus, but also in the means of withdrawing the ions from their spiral paths. It is the purpose of the present paper to describe these recent advances in design and also to discuss some of the questions involved, for some of the changes which we have made suggest the possibility of further improvements.

APPARATUS

A general view of the apparatus, which is now called[4] the magnetic resonance accelerator, or, more frequently, the "cyclotron," is shown in Fig. 1. The magnet which was described in the publication two years ago has not been changed in any respect. For some time we have intended to enlarge the pole faces beyond the original $27\frac{1}{2}$" diameter, but this change still remains for the future. All of our attention has been given to the improvement of the cyclotron at its present size. The drawing of Fig. 2 is a general view of the chamber with cover removed, showing the ion source, the accelerating electrodes, which are called duants, or dees, the electrode for deflecting the ions from their spiral paths, the rotatable beryllium and tungsten target, and the window in the chamber wall through which the ions emerge into the air. These component parts are discussed in the following paragraphs.

Ion source

As in the original arrangement, the ions are produced in the central region by a beam of electrons passing along the magnetic lines of force between the dees and ionizing the gas filling the chamber at a suitable pressure. Formerly, spiral filaments above and below the central region were mounted on glass tubes in copper pipes which extended from the chamber wall to the center, along a radius between the dees. These tubular shields extended to the center on one side only, thus introducing an undesirable asymmetry in the field between the dees. This has been corrected[5] in the present apparatus by bringing the filaments to the center across one dee, as shown in Fig. 3. Here may be

[1] E. O. Lawrence and N. E. Edlefson, Science **72**, 376–377 (1930).
[2] E. O. Lawrence and M. S. Livingston, Phys. Rev. **40**, 19–35 (1932).
[3] E. O. Lawrence and M. S. Livingston, Phys. Rev. **45**, 608–612 (1934).
[4] E. O. Lawrence, E. McMillan and R. L. Thornton, Phys. Rev. **48**, reference p. 495 (1935).
[5] In the Cornell cyclotron this correction has been achieved by the symmetrical placing of four filaments (M. S. Livingston, Rev. Sci. Inst. **7**, 55–68 (1936).

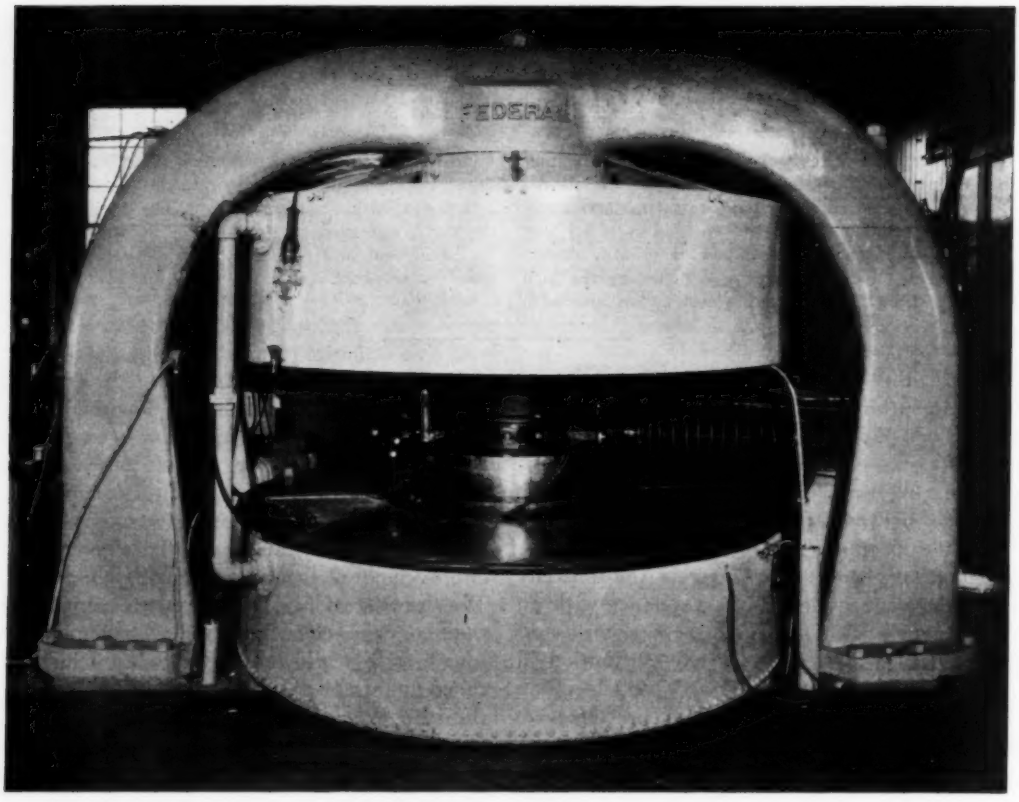

FIG. 1. General view of the cyclotron.

seen two filament supports, one above and one below one of the dees (which in this photograph has been removed). The flat spiral filaments, usually $5\frac{1}{2}$ turns of 30 mil tungsten with an over-all diameter of about $\frac{1}{2}''$, are mounted by clamping to water-cooled copper blocks. The filament support is enclosed in a copper shield

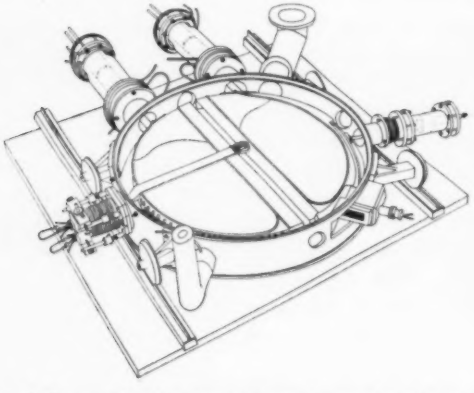

FIG. 2. Perspective drawing of the cyclotron chamber with iron cover plate removed.

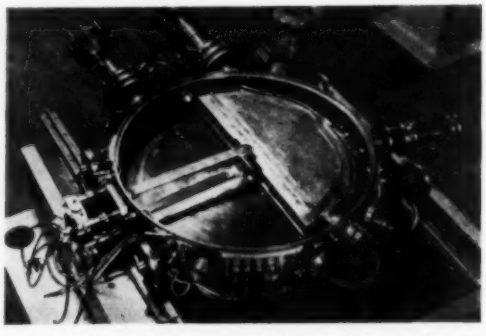

FIG. 3. Photograph of a cyclotron chamber with cover plate and one dee removed. In this apparatus the ions are not withdrawn completely but bombard targets within the chamber wall.

(because of the radio frequency potentials on the dees) and the whole assembly is made as thin as possible for maximum clearance between the dee and the filament structure. In practice, it has been our experience that $\frac{1}{4}''$ vertical or $\frac{1}{8}''$ horizontal clearance is enough to prevent trouble from breakdown discharges.

The filament support is mounted on a sylphon arrangement which permits moving the filament to various places in the central region. Theoretically, the ion source should be near the center of the cyclotron, inasmuch as the ions start their spirals on paths of small radii of curvature in the oscillating electric field between the accelerating electrodes. In practice, however, it is usually found that the optimum position of the filament is not at the center but off the center one way or another. This arises from the circumstance that in general the centers of the successive circular paths migrate from the geometrical center of the apparatus as a result of the lack of complete circular symmetry of the magnetic field. This migration of the paths of the ions can be changed by correcting the asymmetry of the field. This can be done by inserting suitable pieces of iron (which we call "shims") between the cover plates of the vacuum chamber and the magnetic pole faces, but oftentimes it is much simpler to make the correction by shifting the point at which the ions begin their spiral paths.

The whole filament assembly is bolted and waxed to a plate on the side of the chamber wall, and is made conveniently demountable for filament replacement. Water-cooling pipes pass around the filament shield and also are provided for the wax joints. The filament electrodes are insulated from the surrounding shield by glass tubes and emerge from the sylphon assembly through a rubber plug, the arrangement being made vacuum-tight by wax. The insulation is adequate for several thousand volts, but in general the filament is maintained at a negative potential not greater than 1000 volts with respect to the surrounding shield and the walls of the vacuum chamber.

Although there are two filaments (one above and one below) only one at a time is used, the other being moved to one side, to be available when the former burns out. The electron emission from the ion source passing down between the dees, strikes the iron (lid or base plate) and, inasmuch as no water cooling is provided at the point, large electron currents can give rise to excessive heating and evolution of gas. In the future when larger currents are used, it will be necessary to provide water cooling where the electrons strike, but for the currents used until now (less than 500 ma at 1000 volts) this has not been necessary.

From the magnitude of the current of high speed ions arriving at the periphery in comparison to the estimated amount of ionization at the ion source, it is clear that the focusing action of the electric and magnetic fields is such that a very considerable fraction of the ions starting at the center reach the target. Because space charge effects are negligible for such small currents at such high voltages, it is to be expected that the output of high speed ions would be proportional to the production of ions at the center, and therefore, it is of importance to consider means of increasing the source of ions.

The ion current will be proportional to the electron current and therefore it is necessary only to increase the filament emission in order to increase the ion output. Unfortunately, large electron currents are limited by space charge, and it is necessary to increase the accelerating electrical fields in order to increase emissions. In the present arrangement, it is not efficacious to increase the electron emission by increasing the electron accelerating voltage, because the probability of ionization of the gas—for example, the production of protons in hydrogen—falls off with increasing energy of the electrons, as has been shown by Bleakney.[6] The optimum energy of the electrons for the formation of protons or deuterons is in the neighborhood of 200 volts, and accordingly it is desirable to design the source of electrons to yield large currents at low voltage.

One way to accomplish this is to increase the size of the filament, since in practice it has been found that there is a relatively large central region that is suitable for the ion source. Over distances of as much as two inches the output of high speed ions in relation to the production at the ion source does not vary more than 50

[6] W. Bleakney, Phys. Rev. **35**, 1180–1186 (1930).

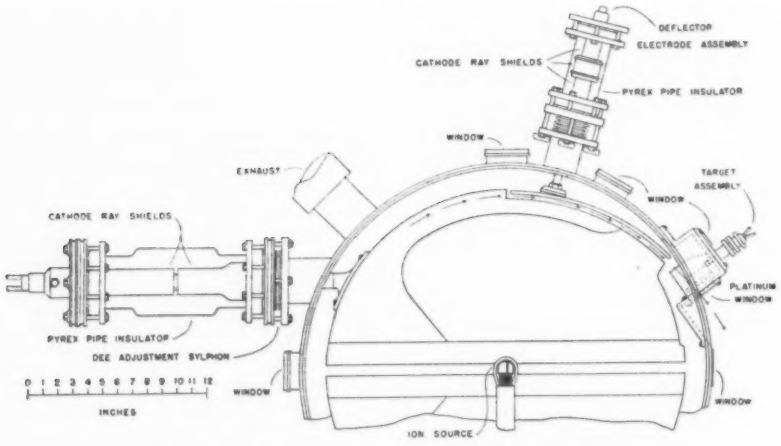

FIG. 4. Detail of accelerator electrodes and mountings.

percent. Space charge effects can be reduced also by the use of an accelerating electrode close to the filament. One suitable arrangement would be that of a heavy (perhaps 50 mil) straight tungsten wire several inches long, extending parallel to the diametrical edges of the dees, midway between them. With such a straight wire filament held accurately in position, it would be feasible to place, very close by, a water-cooled accelerating electrode having a narrow rectangular slot which would produce much higher fields at the filament surface than are obtained in the present arrangement.

Thus it appears that there should be no great difficulty in producing 5 or 10 times as much effective electron current as at present used, and accordingly that much greater output of high speed ions. At the present time, the maximum output current of high speed ions is about 25 microamperes and the usual steady-running currents are about 20 microamperes. With the ion source increased, the output of high speed ions should be more than one hundred microamperes.

The accelerator electrodes

The semi-circular hollow accelerator electrodes, or dees, are clearly shown in Fig. 2 and in more detail in Figs. 3 and 4. They are made entirely of copper, copper sheeting being soldered to a heavier copper frame, with water-cooling pipes to take care of the heating due to the high frequency charging currents and the bombardment by the circulating ions. The dees have an over-all diameter of $24\frac{1}{4}''$, while the exit slit, as may be seen in the drawing of Fig. 4, is such that the diameter of the final circular path of the ions is $23''$. The dees have a width at the center of $1\frac{3}{4}''$ which uniformly decreases to $1\frac{1}{4}''$ at the periphery. The widening of the dees at the center favors the production of ions there without unduly increasing the capacity of the system.

The dees are supported on the ends of $1''$ copper rods $22''$ long, which are in turn supported by means of Pyrex pipe insulators, the details of which are shown in the drawings of Figs. 2 and 4 and the photograph of Fig. 3. The insulators are standard $\frac{1}{4}''$ wall Pyrex glass flange pipes of $3''$ inside diameter which have been blown out in the central region to $4''$ diameter (the insulators shown in Fig. 3 are not blown out to $4''$), the glass being connected to the metal parts by fuse wire gaskets, according to the suggestions of D. L. Webster and P. A. Ross.

From a mechanical standpoint this arrangement for supporting the dees is very satisfactory, but there have been troubles with cathode-ray punctures of the insulators and high frequency hysteresis heating. These troublesome matters, however, have been practically eliminated by providing the cathode-ray shields shown in the drawings and also by providing air cooling of the glass. This geometry of the electrode arrangement not only practically eliminates cathode rays

but also distributes the high frequency electric fields in such a way as to minimize hysteresis heating effects; but nevertheless there remains enough heating of the glass to make it necessary to provide jets of air on the glass surfaces to keep them cool. With air flowing over the glass insulators, we have had no trouble with insulator breakdown for several months, and presumably the insulators will last indefinitely.

Of course, the endeavor always will be to produce larger numbers of high speed ions, at ever higher energies, and this will mean an ever-increasing applied high frequency voltage, so that doubtless the point will be reached where it will be difficult to prevent breakdown of the insulators. It will then be desirable to eliminate them practically altogether. This can be accomplished by mounting the dees on heavy and rigid inductance coils in vacuum. The high frequency power for such a circuit could be introduced through insulators at relatively low voltage and thereby it would be possible to increase the power input many fold without insulator difficulties. This arrangement, which makes use of vacuum insulation in the manner of the Sloan[7] radio frequency high voltage generator, will doubtless be used in our laboratory sometime in the future.

The question of the effect of dee width (i.e., height of opening) on the output of high speed ions is one of much interest and importance. The fact that many microamperes of high speed ions are obtainable indicates that the focusing action of the curved electrical fields between the dees is very good, but it is impossible to predict exactly the effect on the focusing action of the geometry of the accelerating electrodes. Of course, it can safely be argued that the number of ions produced at the center will be at least a linear function of the dee width at the center, but whether the peripheral width of the dees affects the ion output very much can only be determined by experiment.

To examine this question we have recently tried dees having a uniform internal width of 2″ and have found that steady output currents of 50μA are obtainable under approximately the same conditions that 20μA are obtainable from the narrower dees. Thus it seems that the output of ions increases somewhat faster with dee width than proportionally, and therefore a cyclotron designed for very large current output should not only have an ion source capable of giving large electron emissions, but also should have very wide dees.

[7] D. H. Sloan, Phys. Rev. **47**, 62–71 (1934).

Withdrawing the ions

The arrangement for withdrawing the ions is shown in Figs. 2 and 4. The ions emerging from one of the dees are deflected by a transverse electrostatic field and travel between the deflector plate and the dee on an approximately cricular path of radius 30 percent greater than the final circular path within the dee (of radius 11½″). Since the magnetic force acting on the circulating ions is equal to the centrifugal force, which is equal to twice the energy of the ions divided by the radius of curvature, it follows that the magnetic force on 5 Mev ions traveling on a radius of 30 centimeters would correspond to an electrical field of about 330,000 volts per centimeter. Thus, an applied electrostatic field of the order of magnitude of 100,000 volts per centimeter is used in the present arrangement. Since the pole face diameter is 27½″, the ions emerging from the interior of the dee are at a distance of 2¼″ from the wall of the vacuum chamber and with the deflecting fields used in the present experiments they are brought to the tank wall in a distance less than one-fourth of the circumference. As may be seen in Figs. 2 and 4, a water-cooled target mounted on a ground joint may be rotated in and out of the beam. Usually two targets make up the assembly, one of tungsten and one of berryllium, the former being used mainly for test purposes (to measure the beam intensity with a minimum of neutron background) while the latter is used as a source of neutrons. The arrangement of the inset in the chamber wall adjacent to the target makes it possible to place objects near to and directly in front of the source of the neutrons. Since the neutrons partake of the momenta of the bombarding deuterons, in general there is an enhancement of the intensity of the neutrons in the forward direction so that there is real advantage for investigations with neutrons to be able to place objects near and directly in front of the beryllium target.

It is frequently desirable to expose objects directly to the deuteron beam and for this purpose it is convenient to bring the beam out into the air. A thin platinum window is provided for this purpose. The platinum foil 0.0001" thick (stopping power, 1.5 centimeters of air) is soldered to a brass grid which is water cooled and able to dissipate the heat liberated by the deuteron beam striking and passing through the window into the air. The holes in the grid are such as to allow a little more than half of the beam to pass through. A beam of several microamperes of deuterons emerging into the air produces a luminosity of lavender color of considerable intensity and a photograph of a 5 microampere beam of 5.8 Mev deuterons passing out into the air from the window to a distance of 25 centimeters is shown in Fig. 5.

Although the arrangement here shown is quite convenient and useful in many investigations, for some purposes it would be desirable to withdraw a beam of ions through a vacuum tube to a point which is at a considerable distance from the accelerator system, in order to remove background radiations, produced by ions circulating between the dees that strike parts of the apparatus other than the intended target. This can be readily accomplished by attaching a vacuum tube of any desired length in place of the platinum window, and putting the platinum window on the other end of the tube. If no attention is given to refocusing, the ion beam will progressively diverge as it passes through such an extended vacuum tube, partly on account of the inhomogeneity of the magnetic fields external to the vacuum chamber. However, it is not a difficult matter to correct this inhomogeneity; in fact, pieces of iron can be placed around the tube in such a way as to refocus the beam of ions at the extended exit window. This has not actually been done as yet in our laboratory, but we intend to do so very soon for the purposes of certain experimental investigations in progress.

Oscillators

The source of high frequency power is a self-exciting (tuned grid—tuned plate circuit) oscillator which has the advantage of simplicity involving a minimum of equipment. Two oscillator tubes of our construction which have been recently described,[8] are used in a push-pull circuit. These tubes are rated at 30 kilowatts, although in practice much smaller powers are used. The anodes are supplied with three phase full wave rectified voltage up to a voltage of about 10,000 volts. The rectifier consists of three 220 volt to 6600 volt transformers connected for three phase full wave rectification with 872A rectifier tubes. In order to draw as large currents as might be desired, 12 of these rectifier tubes are actually used, parallel groups of two being connected with suitable stabilizing resistances in series. When the cyclotron is running, delivering 20 microamperes of 5.5 Mev deuterons, the anode voltage on the oscillators is about 8000 with an anode current of about three amperes. Of the total input power of about 25 kilowatts, it is found that about 12 kilowatts of high frequency power is delivered to the "tank circuit."

Although the simplicity of the self-exciting oscillator commends itself for many practical purposes, it has the disadvantage of inconstancy of frequency and a certain instability in operation; for variable frequency means variable output of high speed ions and for many purposes it is desired to have as great constancy as possible in the energy and intensity of the beam. We are at the present time engaged in the construction of a new oscillator system, using a master oscillator and successive stages of power amplifiers, an arrangement which should deliver to the accelerating system radio frequency power of constant frequency and great stability. With the present arrangement, it is possible to keep the beam steady within 10 percent by adjusting the magnetic field from time to time. The new oscillator should make it possible for the cyclotron to deliver a steady and homogeneous beam of high speed ions for considerable periods of time, perhaps hours, without requiring attention.

Adjustments

The dees

The sylphon arrangement in the dee supports makes it possible to change the position of the

[8] D. H. Sloan, R. L. Thornton and F. A. Jenkins, Rev. Sci. Inst. **6**, 675–82 (1935).

FIG. 5. Photograph of 5μA of 5.8 Mev deuterons (range 25 cm) emerging from platinum window of cyclotron.

dees during operation. As would be expected, it is often found that the optimum position is that in which the dees are accurately parallel to each other and symmetrically placed with respect to the magnetic field. Deviations from this symmetrical adjustment, of one millimeter for example, are sometimes detectable by as much as a 10 percent reduction in the output of ion current. This fact emphasizes the importance of constructing the dees so that they do not tend to wobble or sag out of position, and also the desirability of the sylphon arrangement for making adjustments. In this latter regard, it is found that a slight lack of parallelism of the dees can be partly compensated by adjustments of their relative position. The sylphons make it possible also to vary the separation of the dees, which when parallel are about $\frac{3}{4}''$ apart. No great variations are produced by varying the separation, but it does seem in general that the further the dees are apart the less the output of high speed ions. It is not known whether this is due to change in the production of ions at the center or to the focusing action of the fields out toward the periphery.

In the light of the above remarks, it would seem that with dees and supports of sufficient rigidity, the sylphon on the supports would not be needed, as the dees could be placed accurately in the optimum symmetrical positions at the time of assembly and would keep these positions during the course of operation. It is difficult to say whether in practice the simplification of the dee supports obtained by eliminating the sylphons would more than compensate the loss of the possibility of making dee adjustments.

The magnetic field

Neglecting relativity corrections, which are unimportant, the simple theory of operation of the cyclotron would suggest that the ideal magnetic field is uniform over the whole accelerating system. In practice, this ideal is not achieved, partly because of the imperfections of the geometry and the inhomogeneity of the iron of the magnetic circuit, and partly because the saturation of the iron pole pieces results in a decrease of the magnetic field toward the periphery of the dees; this latter, surprising as it may seem, is an inhomogeneity that is really desirable. The actual variation of the magnetic field from the center outward in the present cyclotron is shown in Fig. 6, where it is seen that from the center to the edge of the magnetic pole faces, the field falls off 25 percent, while even from the center to the point where the ions are withdrawn from the accelerating electrodes, radius $11\frac{1}{2}''$, the field actually diminishes by 7 percent. At first sight, one would think that such a marked radial inhomogeneity of the magnetic

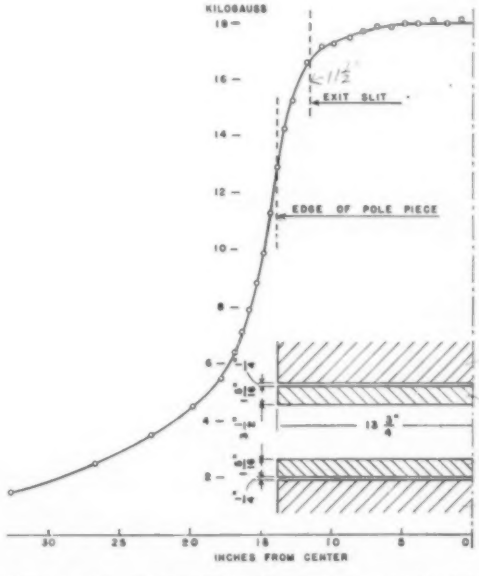

FIG. 6. The radial distribution of the magnetic field. The shaded areas indicate the magnet pole faces and the iron plates of the cyclotron chamber.

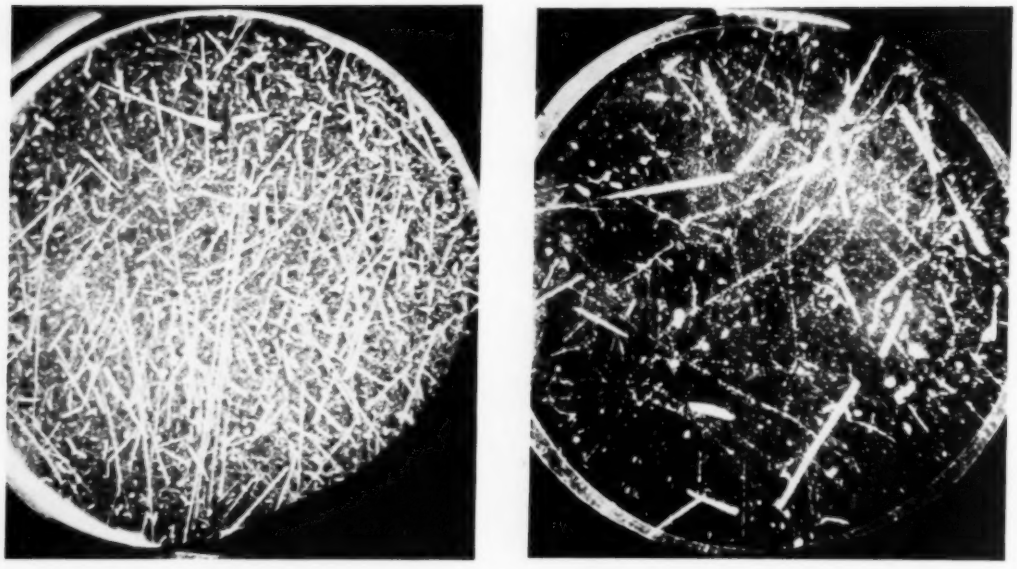

(a) (b)

FIG. 7. Photographs of recoil protons in Wilson cloud chamber filled with hydrogen at pressure of 100 cm Hg produced by neutrons from Be target bombarded with 7μA of 5.5 Mev deuterons. Distance of cloud chamber from Be target, (a) 6 ft., (b) 40 ft.

field would make it impossible to accelerate the ions to the periphery, but on second thought it is realized that if the high frequency accelerating voltage is of the order of magnitude of 100,000 volts in the production of 5 Mev deuterons, the ions circulate only about 25 complete revolutions and under these circumstances an inhomogeneity toward the periphery of only 7 percent would not seriously affect the synchronization of the circulating ions with the oscillating field. The high frequency voltage used in the present cylotron has not been measured reliably, but it is estimated to be somewhere between 50,000 and 100,000 volts.

This radial gradient of the magnetic field, which becomes quite large near the periphery, has the effect of opening up the spiral paths. Instead of traveling on circles within the dees, the decreasing field toward the edge causes the ions that do not have their path centers exactly at the center of the field, to spiral around on continuously increasing radii of curvature. The extent of this effect of the field gradient for the present cyclotron is illustrated by a simple approximate calculation of the path of an ion, on the assumption that the center of the spiral for the revolution, just before the ion is withdrawn from the dee, is $\frac{1}{8}''$ off center, and that the high frequency accelerating voltage is 50,000. The path of the ion, as approximately determined in this way, makes its exit from the dee at a distance of more than $\frac{1}{2}''$ from the previous spiral path. Thus it is seen that this outward field gradient produces a very considerable opening up of the spirals. This is obviously a desirable characteristic, inasmuch as it facilitates the withdrawal of the ions from the accelerating system.

But the fact that a shift of the center of the circuit of the spirals by $\frac{1}{8}''$ produces such a large effect on the spiral paths imposes a rigid requirement that the magnetic field be highly homogeneous in azimuth. If the average value of the magnetic field in one quadrant were appreciably different from that in the others, the effect would be to produce a migration of the centers of the spiral paths, and in turn, serious distortion of the paths, greatly magnified by the spiraling action of the radial field gradient. In adjusting the magnetic field of the cyclotron, therefore, it is necessary to insert

pieces of iron between the pole faces and the bottom and top of the cyclotron chamber (as indicated in Fig. 6, $\frac{1}{4}''$ gaps are provided for this purpose) in a purely empirical manner to correct the azimuthal inhomogeneity. In general, it may be said that increasing the magnetic field, let us say on the southern portion of the pole faces, has the result of causing the centers of the spiral paths to migrate toward the east, for clockwise rotation as seen from above. If it is found, therefore, that the ion beam emerging from the exit slit of the dee has an energy less than that to be expected, the presumption is that the centers of the spiral paths have migrated toward the exit slits so that the final radii of curvature are less than the distance from the exit slit to the center of the apparatus. Under such circumstances, the energy of the particles could be increased by inserting shims to increase the magnetic field in a particular region, which would cause the spiral paths to migrate back toward the center, and hence increase the radii of the final paths. Of course, it should be emphasized that in practice the adjustment of the magnetic field by the insertion of shims is largely an empirical matter. Although the effects of the shims cannot always be understood, the shim adjustment is fortunately not difficult to make; inasmuch as without any shims at all, a beam of ions is obtainable. Thus, the homogeneity, intensity and energy of the ion beam can be observed continuously as the magnetic field adjustment is carried out.

Performance

Hydrogen ions

The present cyclotron delivers several microamperes of 5 or 6 million volt deuterons without any adjustments after the vacuum chamber has been placed between the poles of the magnet. In the beginning of operation, the circulating ion beam liberates gas from the various metal parts of the apparatus, so that during the first few hours of operation, the output beam of ions steadily increases as the gas liberation decreases. It is found that for satisfastory operation, the pressure of foreign gases must be kept below 10^{-5} mm Hg, and that the largest currents are obtained when the hydrogen pressure is of the order of magnitude of 10^{-4} mm Hg. By making the various adjustments (i.e., the deflecting potential and the magnetic field distribution with shims and the position of the dees, the deflecting plate, and the ion source filament, which usually is at the center) the ion currents are usually built up to optimum values of 20 to 25 microamperes of 5.8 Mev deuterons, when using dees having an internal peripheral width of $1\frac{1}{4}''$, or about 50 microamperes of 4.3 Mev ions when using $2''$ width dees of smaller radius. It is found that the obtainable current is not appreciably dependent upon the output energy of the ions, as we have, when using the narrower dees, obtained just as large currents above 5 Mev as below 5 Mev. The maximum energy of deuterons that has been produced by the present cyclotron is 6.3 Mev.

The obtainable beams of high speed protons are usually equal in current to the deuterons, but less in energy on account of the required higher frequency of the electric oscillations.

Helium ions

The cyclotron, when adjusted for deuterons, is also in adjustment for doubly charged helium ions. The helium ions having twice the charge and mass relative to deuterons, receive twice the increments in energy each time they pass between the dees and arrive at the periphery with twice as much energy. Thus, apart from difficulties of producing doubly charged helium ions at the center, the cyclotron produces 10 Mev alpha-particles as readily as 5 Mev deuterons.

On one occasion, we replaced the deuterium with helium in the cyclotron chamber and obtained $1/10\mu$A of 11 Mev alpha-particles. (Several times larger currents doubtless could have been obtained by completing the adjustments.) That the beam of high speed ions was really made up of such high speed helium ions rather than deuterons of lower energy was definitely established in several ways. Thus, for example, it was observed that the alpha-particle beam attained its maximum intensity at a magnetic field slightly lower than that for the deuteron beam, had a range one-half that of the deuteron beam under similar circumstances, and produced a luminosity in the air in intensity equivalent to that of 4 times as large a deuteron current.

As yet we have not carried out experiments with these energetic alpha-particles, excepting to observe that they do not give rise to as large a neutron emission from a bombarded beryllium target as deuterons of half their energy.

Neutrons

Among the many elements that emit neutrons under deuteron bombardment, beryllium is particularly noteworthy. The neutron emission from a beryllium target bombarded by 7μA of 5 Mev deuterons is indicated by the cloud chamber photographs of Fig. 7. With the hydrogen-filled cloud chamber at a distance of 6 feet from the target, the number of recoil protons is too great for counting purposes, and a more suitable number is obtained at 40 feet. Although it is difficult to compare vastly different numbers of neutrons, estimates made in several ways indicate that the emission of neutrons from the beryllium target of the cyclotron is more than 10^5 times that from a mixture of one curie of radon and beryllium.

This great neutron intensity facilitates many nuclear studies, but on the other hand, hampers some investigations. Among the practical difficulties, there are the biological effects produced by the neutron rays, which make it necessary to provide considerable protection for the investigator. Some biological studies[9–11] have already been carried out which have shown that, in biological action, the usual neutron emission from the beryllium target of the present apparatus is equivalent to the gamma-radiation from 100 grams of radium. Accordingly, at the present time, for the protection of the operator, the cyclotron is controlled at a distance of 40 feet from the target with suitable intervening absorbing material. As the intensity of the neutron source is further increased, it will be necessary to provide additional absorbing screens.

Artificial radioactive substances

With 5 Mev deuterons, it has been found possible[12] to produce radioactive isotopes of many of the elements throughout the periodic table. In many cases, the yields of the radioactive substances are quite large; as for example, a day's bombardment of sodium metal with 20 microamperes of 5 Mev deuterons produces more than 200 milligrams—equivalent of radio sodium,[13] i.e., an amount of radio sodium having a gamma-ray activity equivalent to that of 200 milligrams of radium. That such large amounts of radioactive forms of many of the elements can be manufactured in the laboratory is of much importance in opening up new avenues of research both in the physical and the biological sciences.

We are greatly indebted to our laboratory colleagues, who have contributed so much to the work here reported. We acknowledge with thanks also the continued support of the Research Corporation, the Chemical Foundation, and the Josiah Macy, Jr., Foundation.

[9] J. H. Lawrence and E. O. Lawrence, Proc. Nat. Acad. **22** (2), 124–1933 (1936).
[10] R. E. Zirkle and P. A. Aebersold, Nat. Acad. Sci. **22** (2), 1934–138 (1936).
[11] J. H. Lawrence, P. A. Aebersold and E. O. Lawrence, Proc. Nat. Acad. **22**, 543–557 (1936).

[12] J. M. Cork and E. O. Lawrence, Phys. Rev. **49**, 788 (1936). J. J. Livingood, Phys. Rev. **50**, 425 (1936).
[13] E. O. Lawrence, Phys. Rev. **47**, 17 (1935).

Radioactivity Induced in Sulphur

R. SAGANE, *Radiation Laboratory, Department of Physics, University of California, Berkeley, California*

(Received October 5, 1936)

Under bombardment of 4–6 Mev deuterons, sulphur becomes radioactive with the emission of both positive and negative electrons with 3 periods 3 ± 0.1 *m*, 33 ± 1 *m* and 14 ± 0.3 *d*. These decay periods were found to have their origin in P^{30}, Cl^{34} (both positron emitters) and P^{32} (negative electron emitter). The energy distribution of positrons from Cl was studied by a cloud chamber. When bombarded by neutrons two radioactive substances were produced which emit negative electrons. The half-value periods were found to be 2.6 ± 0.2 *h* and 14 *d*, which are characteristic of Si^{31} and P^{32}.

INTRODUCTION

SINCE the discovery by Curie-Joliot of artificial radioactivity, many radioactive isotopes have been found produced by bombardment with protons, deuterons, α-particles and neutrons. Many light elements have been investigated in this laboratory by the use of the deuteron beam from the cyclotron. The work described in this paper is an investigation of radioactivity induced in sulphur by both deuteron and neutron bombardment.

APPARATUS

The source of deuterons was the large cyclotron[1] in the Radiation Laboratory. At the time of the bombardment it was adjusted to furnish deuterons of energy of 4–6 Mev.

The targets were, in all cases except the first two exposures, sulphur fused on Pb plates and covered with two sheets of Pt foils, 4 mm in air equivalence, to avoid contaminations. In the first two cases, sulphur was fused on Al plates and covered with Al foils. The bombardments were made in vacuum on a special target holder with a cooling device to prevent the sample from evaporating.

All the measurements of activity were carried out on a Lauritsen type quartz fiber electroscope with an Al window and absorption measurements were made by placing Al sheets between the source and the window. A Wilson chamber[2] was used to investigate the nature of the ionizing particles from the irradiated samples and also for the measurement of the energy distribution of the positrons from radiochlorine.

[1] E. O. Lawrence and M. S. Livingston, Phys. Rev. **45**, 608 (1934).

[2] I am indebted to Dr. Kurie for the use of the cloud chamber.

I. ACTIVATION BY DEUTERONS

Decay periods

A thick sulphur target on an Al plate was bombarded in vacuum at first for about 2 hours by an ion beam of 4 Mev in energy. At the end of the exposure the target was placed at the window of the electroscope. The measured activity as a function of time was plotted on a logarithmic scale and analysis of this curve shows the existence of two radioactive substances. The half-periods were observed to be 33 ± 1 *m* and 14 ± 0.3 *d*, and also there were traces of 2.6 *h* and 14 *h* activity. The ratio of the initial intensities of these substances was estimated roughly to be 360 : 1.6 : 0.3 : 0.2, respectively. Repeating the same exposure, the same type of decay curve was reproduced.

To find out whether there is a shorter period activity, a sulphur target on Pb covered with thin Pt foil, 0.0001″ in thickness, was bombarded for 10 minutes. After due allowance for the 33 *m* activity, a half-life of 3 ± 0.1 *m* was found. A short exposure of 5 *m* was made afterward and the same result was reproduced.

To investigate the nature of the ionizing particles, they were observed visually in a Wilson chamber which was placed in a magnetic field of a few hundred gauss. Both positrons and negative electrons were emitted from the target.

The active substances

Ordinary sulphur contains three isotopes, S^{32}, S^{33} and S^{34}, the relative abundance of which is reported to be 96 : 1 : 3. If sulphur combines

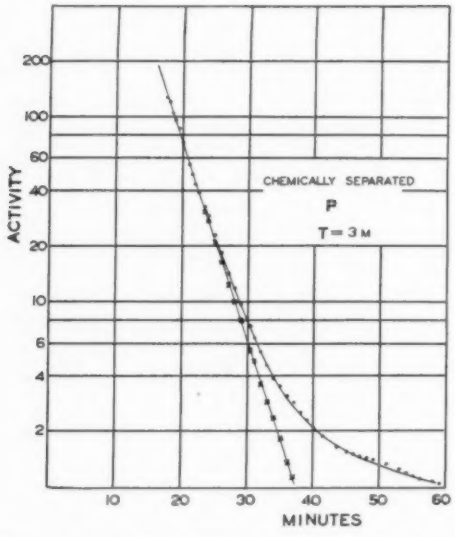

FIG. 1*A*. Logarithmic plot of the activity of the chemically separated P^{30}. Dots show the measured curve. *x*'s show the corrected curve for a small amount of contamination of Cl of about 1 percent in intensity.

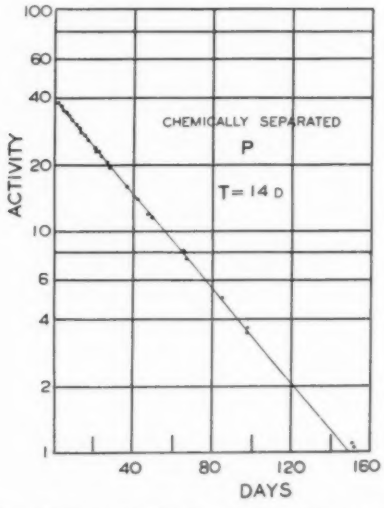

FIG. 1*B*. Logarithmic plot of the activity of the chemically separated P^{32}.

with deuterons, Cl^{34}, Cl^{35}, Cl^{36} are expected to result with the capture of deuterons (this is supposed to be very improbable); P^{30}, P^{31}, P^{32} with the emission of α-particles; Cl^{33}, Cl^{34}, Cl^{35} with the emission of neutrons; and S^{33}, S^{34}, S^{35} with the emission of protons.

The identity of P^{30} and P^{32} is apparent since the periods characteristic of these substances are known with good accuracy. As for Cl^{34}, Cl^{36} half-value periods of 40 ± 5 *m*[3] is given for Cl^{34} and 50[4] to 35 minutes for Cl^{36} (probably 37 *m*[5]). The accuracy of these measurements is not good enough to identify the 33 minutes activity.

Chemical tests were also made to check their identity. The sulphur sample was dissolved in CS_2, and mixed with dilute HNO_3, in which a small quantity of red phosphorus and a drop of dilute HCl was added. Then the solution was heated for a short time until the phosphorus was completely dissolved. After filtration of the water solution, Cl ions were precipitated with $AgNO_3$; then PO_4 ions were precipitated with magnesia mixture.

The logarithmic plot of the decay curves of these chemically separated samples evidenced excellent straight lines as shown in Fig. 1; consequently half-lives of P^{30} (by short exposure), P^{32} and Cl (by long exposure) were determined with sufficient accuracy. It is therefore obvious that the 3 *m* activity is due to P^{30}, 14 *d* to P^{32} and 33 *m* to Cl.

Examining the chemically separated Cl in the Wilson chamber it was found that the sample emitted chiefly positrons and a small number of negative electrons. The latter can be explained as Compton recoil electrons of annihilation radiation of positrons and also a small amount of contamination of P^{32}. A study of the periodic table reveals that 33 *m* activity is probably due to Cl^{34} or perhaps Cl^{33}, because the intensity of this Cl seems to be too strong to explain by the following process, if the fact is taken into account that the relative abundance of S^{33} is only 1 percent: $S^{33}+D^2=Cl^{34}+n$.

Thus the reactions are supposed to be

$$S^{32}+D^2=P^{30}+He^4 \qquad P^{30}\rightarrow Si^{30}+e^+$$
$$S^{33}+D^2=Cl^{34}+n \quad (S^{32}+D^2=Cl^{33}+n^1 \quad S^{32}+D^2=Cl^{34})$$
$$Cl^{34}\rightarrow S^{34}+e^+$$
$$S^{34}+D^2=P^{32}+He^4 \qquad P^{32}\rightarrow S^{34}+e^-.$$

[3] O. R. Frisch, Nature **22**, 434 (1934).
[4] A. T. Alichanow, A. J. Alichanian and B. S. Dzelepow, Nature **135**, 393 (1935); E. Fermi and others, Proc. Roy. Soc. **A146**, 483 (1934); F. N. D. Kurie, J. R. Richardson and H. C. Paxton, Phys. Rev. **47**, 796 (1935).
[5] A. R. Olson, W. F. Libby, F. A. Long, R. S. Halford, J. Am. Chem. Soc. **58**, 1313 (1936).

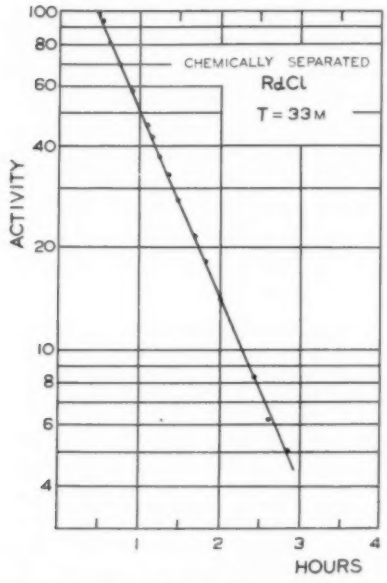

FIG. 1*C*. Logarithmic plot of the activity of the chemically separated radiochlorine.

P^{32} can also be expected to result from a neutron bombardment on sulphur and there is a probability that P^{32} might be created by neutrons from D+D. An experiment to test this point was made. Two similar samples of sulphur were put one upon another on the target holder, and the upper target was bombarded by deuterons. As these targets were rather thin, intensities on both targets of the neutrons created on the upper target by D+D were supposed to be the same order of magnitude. After bombardment the intensities of the activity of the lower target was found to be less than 1/200 of the upper target. This definitely demonstrated that P^{32} on the upper target was chiefly created by deuteron impacts.

The radioactive radiations

The beta- and gamma-rays from P^{30} and P^{32} have been studied in detail by many others and there is no need to reiterate it here. However, Frisch is the only person who has succeeded in making Cl^{34}. He created it by bombardment of P^{31} by α-particles, consequently the intensity must be very weak and the accuracy of the measurement is rather poor. In the present experiment radioactive chlorine was made by deuterons with strong intensity, the initial intensity of 2 hours' exposure being 300 divisions per second, that is 3×10^4 times the natural leak. Some detailed investigation of the radiations from radioactive chlorine was made.

Gamma-rays. Rather weak gamma-rays were found, the absorption coefficient of which was determined with lead sheets. A value of 5 mm of lead for the half-value thickness was obtained. Although the geometrical conditions were not satisfactory, this value probably corresponds to an energy of about 0.5 Mev. This is in agreement with the energy of the gamma-rays which is expected when positrons from Cl are annihilated.

Beta-rays. The energy distribution of β-rays from radioactive chlorine was studied by the use of the cloud chamber with a magnetic field of about 400 gauss. The source was chemically separated from the irradiated sulphur in half an hour after exposure and then mounted inside of the chamber, covered with a thin Al foil to protect the chamber from contamination. This source was rather thick owing to the addition of too much chlorine in the course of chemical separation and one could not get rid of some irregularity in absorption; still the result shows a typical positron distribution and the Konopinski-Uhlenbeck[6] plot gives a fairly good straight line as shown in Fig. 3.

The upper limit is estimated to be 3 Mev. The point corresponding to 3 Mev and 33 *m* placed on Sargent's[7] curves of beta-ray periods and energies lies right on the second group line.

II. Activation by Neutrons

A block of sulphur (20×15×3 mm) was put about 5 cm from the Be target of the cyclotron and irradiated for about 2 hours by neutrons. After irradiation the activity was measured as before. The decay curve was analyzed in two exponential curves showing the existence of two radioactive substances, the decay periods of which are 2.6 hours and 14 days.

These periods are characteristic of Si^{31} and P^{32} which are expected by the following reactions.

---

[6] E. J. Konopinski and G. E. Uhlenbeck, Phys. Rev. **48**, 107 (1935); F. N. D. Kurie, J. R. Richardson and H. C. Paxton, Phys. Rev. **49**, 368 (1936).

[7] B. W. Sargent, Proc. Roy. Soc. **139**, 659 (1933).

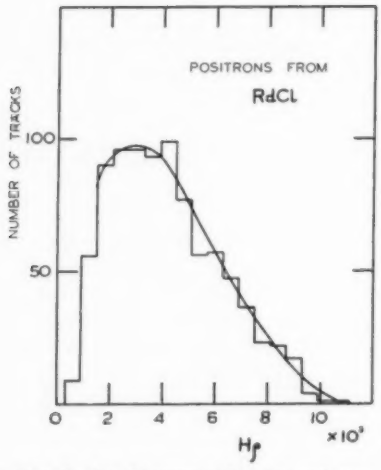

FIG. 2. Distribution histogram for the positrons emitted from chemically separated radiochlorine.

$$S^{34}+n=Si^{31}+He^{4},$$
$$S^{32}+n=P^{32}+H^{1}.$$

Rough chemical tests were made by dissolving activated samples with CS_2. A small quantity of Si powder and red phosphorus was added, as a mixture in dilute HNO_3. Then it was heated slightly till the powder of phosphorus was dissolved completely by HNO_3. After filtration of HNO_3 solution, phosphorus was precipitated by the magnesia mixture. The CS_2 solution was also filtered afterward and the Si powder was obtained as a residue.

By examining these samples it was found that the 14-day activity was due to a phosphorus isotope and the 2.6 hour activity to an Si isotope.

As for the CS_2 solution, it was dried to powder of sulphur. This was then oxidized by sodium chlorate and HNO_3 to H_2SO_4. The latter was precipitated with $BaCl_2$ as $BaSO_4$ in HCl solution. But this sample showed practically no activity.

A search for S^{35}

According to the consideration of reactions with S, a radioactive sulphur S^{35}, which is said to have a long half-life of about 80 days,[8] is expected to result from both deuteron and neutron bombardment.

A search for this isotope was made by making a careful chemical separation of sulphur as before. The first two or three chemically separated samples showed some small activity, but by repeating the process more carefully the activity was found to be much smaller than before and by measurement of the half-life, this activity was found to be due to the contamination of P^{32}.

The result shows that the deuteron bombardment for 3 hours with 13 microamperes beam on the target, cannot make S^{35} of intensity of more than 1/1000 of P^{32}.

As for neutron bombardment, the longest exposure was made on one sample which was put about 10 cm from the Be target of the cyclotron for about 20 days completely covered with paraffin. During these days the cyclotron ran very steadily with about 10–15 microamperes of 5.5 Mev deuterons and nearly every day neutron bombardment on mice and wheat seeds, etc., was continued. Yet the activity of the chemically separated sulphur from this sample was about the same order of magnitude of the natural leak and even this activity was also found afterward to be due chiefly to P^{32} contamination.

In case of this thick target, it is quite difficult to estimate the lower limit, but it seems the cross

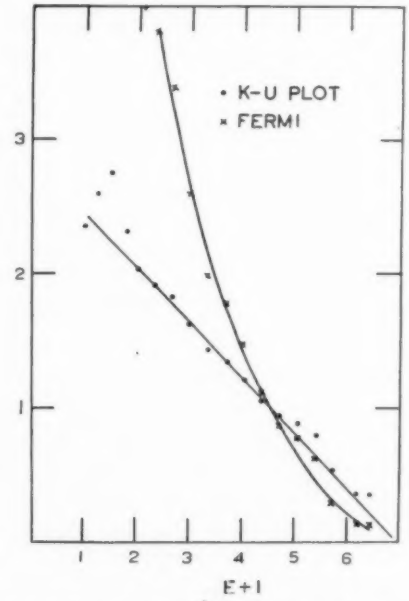

FIG. 3. $K-U$ plot for radiochlorine. This plot extrapolates to an upper limit at $E+I=6.9$, about 3 Mev.

[8] E. B. Andersen, Zeits. f. physik. Chemie **B32**, 237 (1936).

section for neutron capture by sulphur must be 1/100 of that for excitation of P^{32} although the samples was surrounded by paraffin.

ACKNOWLEDGMENT

The author is very greatly indebted to Professor E. O. Lawrence for the opportunity of using the cyclotron and for his helpful discussion and encouragement. He is also very grateful to members of the Radiation Laboratory for their valuable suggestions and discussions for this work. This work has been aided by grants from the Research Corporation, the Chemical Foundation and the Josiah Macy, Jr., Foundation.

DECEMBER 15, 1936 PHYSICAL REVIEW VOLUME 50

A Positive Energy Wave Packet Solution of the Dirac Equation

CARL ECKART AND B. L. GRIFFING, *Ryerson Laboratory, University of Chicago, Chicago, Illinois*

(Received October 3, 1936)

A wave packet solution of the Dirac equation is obtained by superposition of positive energy solutions only. The solution involves an arbitrary parameter, and it is shown that this can be chosen so that all three dimensions of the packet are less than $\hbar/mc$. The possibility of constructing such a packet had been doubted. It is also shown that in the limit $\Delta x=0$, $\Delta x\Delta p_x = 1.49\hbar$. It is not known whether this is the smallest value for the uncertainty product, subject to the condition that only positive energy solutions are used in the construction of the packet, or whether some other solution might yield a still smaller value.

A QUESTION of some technical interest is the following: can a wave packet be constructed by superposing only positive energy solutions of the Dirac equation for the free electron, such that all its dimensions are smaller than $\hbar/mc$? Apparently no conclusive answer to this question has been published.[1] In this note it will be shown that the omission of the negative energy solutions does not impose a lower limit on the size of the wave packet. This will be done by constructing a particular wave packet whose dimension at $t=0$ is arbitrary, and using only positive energy solutions in its construction.

Because of the relativistic invariance of the theory, it is sufficient to consider only packets whose centroids are at rest in the system of coordinates chosen. It is known that in general, that packet for which $\Delta x\Delta p_x$ is smallest is obtained by using a Maxwellian distribution of momenta. In a preliminary investigation, it was found very difficult to discover the analog of this theorem when the positive energy condition is imposed. It was therefore decided to use a distribution such that the Maxwellian is approached for large packets. A further consideration was that all necessary integrals should be calculable without dubious approximations.

In the following, $\hbar/mc$ will be used as unit of length, and $\hbar/mc^2$ as unit of time. Then the Dirac equation can be transformed to the Schrödinger-Gordon equation by the substitution

$$\psi = i[(\partial F/\partial t)+\boldsymbol{\alpha}\cdot\nabla F]-\alpha_m F. \tag{1}$$

In order that ψ satisfy the Dirac equation, the "spinor potential" F must satisfy

$$(\partial^2 F/\partial t^2)=\nabla^2 F - F. \tag{2}$$

Wave packet solutions of this equation are easily written down in the form

$$F_\sigma = \int G_\sigma(\mathbf{p}) \exp[i(\mathbf{p}\cdot\mathbf{x}\pm wt)]d\mathbf{p}, \tag{3}$$

where σ is the spin variable, and

$$w=(1+p^2)^{\frac{1}{2}}>0. \tag{4}$$

If the negative sign of w is chosen in Eq. (3), then ψ will involve only positive energy solutions.

For the present purpose, it is sufficient to take

$$G_1=A\exp(-\beta w), \qquad G_2=G_3=G_4=0, \tag{5}$$

[1] It is known that several investigators have arrived at conflicting conclusions regarding this question. The only definite expression of opinion that has been published seems to be that of L. de Broglie, *L'Électron Magnétique*, p. 286.

where β is an arbitrary constant determining the size of the packet, and A is the normalizing factor. Substituting into Eq. (3), transforming to polar coordinates in both configuration and momentum space, and using an obvious device to replace sin by exp:

$$F_1=(2\pi A/ir)\int_{-\infty}^{+\infty}\exp\left[ipr-w(\beta+it)\right]pdp. \quad (6)$$

In order to obtain ψ from Eq. (1), the following functions are also needed:

$$F_t=(2\pi A/r)\int\exp\left[\cdots\right]pwdp, \quad (6.1)$$

$$F_r=(2\pi A)\int\exp\left[\cdots\right]p^2dp. \quad (6.2)$$

In terms of these, the probability density is

$$D=\Sigma_\sigma|\psi_\sigma|^2 = |F_t-F_1|^2+|F_r-F_1|^2/r^2 \quad (7)$$

and is a function of r only.

The solution thus obtained will be discussed only for $t=0$, at which time the packet has its minimum extension. The integrals of Eqs. (6) can then be evaluated in terms of Hankel functions; setting

$$p=\sinh\alpha, \qquad \xi=(r^2+\beta^2)^{\frac{1}{2}}, \qquad \sin\theta=r/\xi,$$

it follows on substitution that

$$F_1=(\pi A/ir)\int_{-\infty}^{+\infty}\sinh(2\alpha)\times\exp\left[-\xi\cosh(\alpha-i\theta)\right]d\alpha. \quad (8)$$

The path of integration can be displaced from the real axis to the line $\mathrm{Imag}(\alpha)=\theta$; then setting $\lambda=\alpha-i\theta$,

$$F_1=(\pi A/ir)\int_{-\infty}^{+\infty}\sinh(2\lambda+2i\theta)\times\exp\left[-\xi\cosh\lambda\right]d\lambda$$

$$=(\pi A/r)\sin(2\theta)\int_{-\infty}^{+\infty}\cosh(2\lambda)\times\exp\left[-\xi\cosh\lambda\right]d\lambda.$$

Since[2]

$$\int_{-\infty}^{+\infty}\cosh(n\lambda)\exp\left[-\xi\cosh\lambda\right]d\lambda=(\pi i^{n+1})H_n^{(1)}(i\xi), \quad (9)$$

it follows that

$$F_1=(\pi A/r)(\pi i^2)H_2^{(1)}(i\xi)\sin 2\theta. \quad (10)$$

Similarly

$$F_t=(\pi A/2r)\{(\pi i^4)H_3^{(1)}(i\xi)\sin 3\theta+(\pi i^2)H_1^{(1)}(i\xi)\sin\theta\}, \quad (10.1)$$

$$F_r=(\pi A/2)\{(\pi i^4)H_3^{(1)}(i\xi)\cos 3\theta-(\pi i^2)H_1^{(1)}(i\xi)\cos\theta\}. \quad (10.2)$$

These formulae do not furnish a very clear picture of the solution, but on plotting the probability density as a function of r by the aid of tables,[3] its graph is found to be very similar to a Gauss error curve. The half-width is a monotonically increasing function of β and is zero for $\beta=0$.

As this is the principal point at issue, it was investigated in greater detail, using the known approximation formulae for the Hankel functions. When ξ is small (i.e., $r\ll 1$ and $\beta\ll 1$),[4]

$$(\pi i^{n+1})H_n^{(1)}(i\xi)=(n-1)!(2/\xi)^n\cdots, \quad (n\neq 0), \quad (11)$$

which leads to $F_1=8\pi A\beta/\xi^4\cdots, \quad (12)$

$$F_t=8\pi A(3\beta^2-r^2)/\xi^6\cdots, \quad (12.1)$$

$$F_r=8\pi A\beta(\beta^2-3r^2)/\xi^6\cdots, \quad (12.2)$$

whence

$$D=64\pi^2A^2\left[(1+\beta)^2\xi^2+8(1-\beta)\beta^2\right]/\xi^{10}\cdots. \quad (13)$$

It is easily seen that this function has a maximum for $r=0$; which becomes increasingly sharp as β approaches zero. The function diminishes monotonically with increasing r and has a single point of inflection, finally approaching zero as r^{-8}. While this cannot be the true asymptotic behavior of D, yet the error introduced by using Eq. (13) for all values of r will vanish with β. This can be seen in various ways: the correct asymptotic behavior of D can be obtained from[5]

$$(\pi i^{n+1})H_n^{(1)}(i\xi)=(2\pi/\xi)^{\frac{1}{2}}\exp(-\xi), \quad (\xi\gg 1). \quad (14)$$

[3] Jahnke-Emde, *Tables of Functions*, second edition, p. 218. The formula given there is for the Hankel function of the second kind, but it is readily transformed to the one above when n is an integer and ξ real.

[3] Reference 2, p. 286.
[4] Reference 2, p. 202.
[5] Reference 2, p. 204.

Thus the true curve will approach zero more rapidly than the approximate curve; because of the large negative exponent in Eq. (13), the resulting error will not be great, however. More precisely, when $r \ll \beta \ll 1$, then $D = D_0 = 64\pi^2 A^2 (9/\beta^8)$; if on the other hand, $\beta \ll r \ll 1$, then $D = 64\pi^2 A^2 / r^8 \ll D_0$. Thus most of the area under the D curve comes within the range of validity of Eq. (13). The validity of this argument can be checked, since the normalizing integral can be exactly evaluated by transforming to momentum space, and is given by a long, though finite, series of Hankel functions with the argument $2i\beta$. Using Eq. (11) to simplify this expression, we found that the normalizing integral is approximately

$$8\pi^4 A^2 [6\beta^{-5} - 3\beta^{-4} \cdots].$$

These first two terms of the series are identical with those of the series obtained by integrating Eq. (13). This result thus fixes the normalizing factor as $A^2 = \beta^5 / 48\pi^4 \cdots$.

The evaluation of the mean-square radius Δr was also attempted by transforming to momentum space, but the integrals encountered were not very tractable. It was therefore decided to use Eq. (13) in obtaining an approximate value of the integral

$$\Delta r^2 = 8\pi \int_0^\infty r^4 D dr.$$

It will be clear from the above discussion that the error involved in this procedure cannot be great provided that β is much less than unity. The result of an elementary integration is that

$$\Delta r^2 = 4\beta^2/3 \cdots.$$

This verifies the result previously obtained by graphical methods, that Δr approaches zero with β. Since $\Delta r^2 = 3\Delta x^2$ it follows that $\Delta x = 2\beta/3$ in the present units, or

$$\Delta x = (2/3)\beta\hbar/mc, \qquad \beta \ll 1. \tag{15}$$

While this would seem to be a conclusive answer to the question proposed above, it is of interest to note the value of the uncertainty product for this solution. The value of Δp_x is exactly calculable by transformation to momentum space, and is again a finite series of Hankel functions. For small values of β it is approximately given by

$$\Delta p_x = (5)^{\frac{1}{2}} mc/\beta. \tag{16}$$

Hence $\Delta x \Delta p_x = 1.49\hbar$ in this limit; as has been remarked above, it is not known whether this is the smallest value that the uncertainty product can have when the packet is constructed only of positive energy solutions and $\Delta x \ll \hbar/mc$. It seems very likely that this minimum is a complicated function of Δx.

It remains to discuss the case $\beta \gg 1$. This has not been as carefully studied as the other limit, but the following considerations are not apt to be seriously in error. It is easily seen that the momentum distribution function is

$$(2\pi)^3 A [(w-1)^2 + p^2] \exp(-2\beta w).$$

For large values of β, this may effectively be approximated by the Maxwellian distribution

$$A' \exp(-\beta p^2).$$

From this it may be concluded that when $\beta \gg 1$, $\Delta x \Delta p_x = \hbar$ and $\Delta x = \beta^{\frac{1}{2}} mc$.

Pressure Broadening of the Potassium Resonance Lines by Argon and Nitrogen*

GORDON F. HULL, JR., *Sloane Physics Laboratory, Yale University, New Haven, Connecticut*

(Received October 3, 1936)

Broadening of the potassium resonance lines in absorption by argon and nitrogen pressures from 1 to 40 atmospheres has been observed. Half-widths and shifts of the lines, when plotted against "relative density," yield curves that are straight lines up to about relative density 14, indicating that in this pressure region Lorentz type of broadening predominates. At about relative density 14, the curves depart from linearity. The results are in accord with theory, and partly in agreement with previous work. Theoretical contours for pressure broadened spectral lines have been fitted to those of experiment. Agreement is quite satisfactory, considering the approximations made in evaluating the theoretical curves. Three independent methods of calculation yield for the constant b (measure of van der Waals forces) the values $24(10)^{-32}$ and $18(10)^{-32}$ cm^4 sec.$^{-1}$ for argon and nitrogen, respectively.

INTRODUCTION

PRESSURE effects of nitrogen on the potassium resonance lines in absorption have already been investigated by Watson and Margenau.[1] However, they were able to obtain only three spectrograms between relative density 12 and 20. It is in this higher pressure region where departure of the linear relation between relative density and broadening occurs. In order to establish more definitely this point of departure, and to observe the broadening at higher relative densities, the present work was undertaken. Since the publication of the paper by Watson and Margenau, the latter[2] has extended further the theory of pressure broadening and given a theoretical contour for broadened spectral lines. Consequently in the present work it was possible to compare theoretical with experimental contours.

EXPERIMENTAL PROCEDURE

A detailed description of apparatus is given elsewhere.[3] It consisted of a steel absorption tube 87 cm long, fitted with 1 cm thick Pyrex glass windows. A three-section electric furnace served to vaporize the potassium in the absorption tube. Argon and nitrogen were used as perturbing gases up to relative density 28 (40 atmospheres). Above this the potassium doublet coalesces making measurements of half-width inaccurate. Pressures were reduced to relative densities by the law for perfect gases. The more exact van der Waals law was not used, since for even the highest pressures the correction term was found to be negligible. Correction was not made for thermal transpiration, as was done by Watson and Margenau.[1] Both experiment and theory have shown[4] that no correction for this phenomenon is necessary if the diameter of the outlet to the pressure gauge is many times greater than the molecular mean free path. In the apparatus used, the diameter of the outlet was several mm and the mean free paths of the order of $(10)^{-4}$ mm or less.

Spectrograms of the resonance lines (7665A and 7699A) were taken on Eastman type 144-N plates in the first order of a 21-foot concave grating in a stigmatic mounting. A Pointolite lamp was used as continuous light source, and second order Fe lines served for the comparison spectrum. The characteristic log I *vs.* D curve of the spectrograms was obtained from the blackening marks produced by a step filter. This consisted of a quartz disk on which were deposited five strips of platinum of different densities and had been previously calibrated for λ7650. The filter was placed directly in front of the plate and just to one side of the resonance lines. Both blackening marks and potassium lines were recorded simultaneously on the photographic plate, thus insuring the same continuous spectrum as well as the same exposure time for each. This method of obtaining the characteristic curve has the advantage of not relying on the reciprocity law. Microphotometer traces of the spectrograms were made on a Koch-Goos self-recording instrument, and those line contours which did not lie on

* Part of a dissertation to be presented to the Faculty of the Graduate School of Yale University in candidacy for the degree of Doctor of Philosophy.

[1] W. W. Watson and H. Margenau, Phys. Rev. **44**, 748 (1933).

[2] H. Margenau, Phys. Rev. **48**, 755 (1935).

[3] H. Margenau and W. W. Watson, Phys. Rev. **44**, 92 (1933).

[4] L. B. Loeb, *Kinetic Theory of Gases* (1927), p. 283.

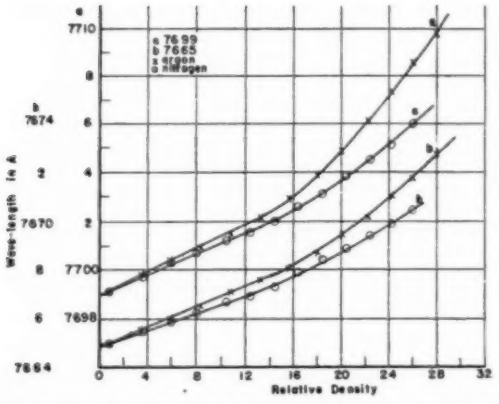

FIG. 1. Wave-lengths of the maxima of the potassium resonance lines *vs.* relative density of argon and nitrogen.

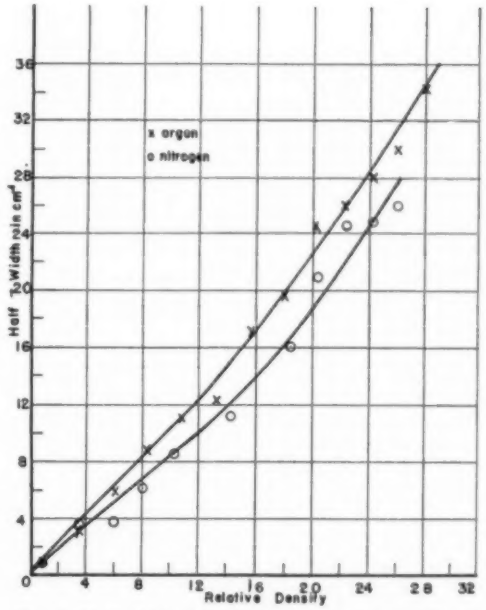

FIG. 2. Half-widths of the potassium resonance lines *vs.* relative density of argon and nitrogen. Points are averaged values for the two components of the doublet.

the straight line part of the characteristic curve were corrected to give true absorption contours. The wave-length of the maximum of each absorption curve as well as its half-width was calculated from the dispersion on the microphotometer trace as determined by interpolation between Fe lines.

RESULTS

The results are shown graphically in Figs. 1 and 2. In Fig. 1 the wave-lengths of the maxima of the potassium resonance lines are plotted against relative densities of argon and nitrogen, and in Fig. 2 the averaged half-widths of the doublet are plotted. (No significant difference between the half-widths of the doublet components was detected.) Curves have been drawn through the "mean" of the plotted points. The points in Fig. 1 lie more closely on the curves than do those in Fig. 2, which is to be expected, since wave-lengths of the maxima can be determined with greater accuracy than half-widths. The latter depend upon corrections for nonlinear plate characteristics, which do not affect the line maximum. Extrapolating the curves back to the axis of ordinates, the values 7664.84A and 7698.96A are obtained for the maxima of the potassium doublet at zero relative density, and 0.25 cm^{-1} for the half-widths. It is seen that argon produces a greater half-width and shift of the maximum than nitrogen, and the shift of λ7699 is slightly greater than λ7665. The curves up to relative density 14 are straight lines, indicating that in this pressure region "velocity" broadening[5] predominates. At about relative density 14, the curves depart from linearity, showing that "statistical" broadening[5] is becoming effective. This is in accordance with Margenau's theory.[2] and also with the previous work done by Watson and Margenau[1] using nitrogen as the perturbing gas. However, shifts and half-widths obtained for nitrogen in the present work are nearly twice as great as their values. Half this discrepancy can be accounted for by the fact that they made correction for thermal transpiration in reducing pressures to relative densities. In Table I are listed shifts and

TABLE I. *Summary of shifts and half-widths of the potassium resonance doublet.*

		Shift $\frac{\Delta\nu}{d}$	Half-Width $\frac{\Delta\nu_{\frac{1}{2}}}{d}$
Argon	7665A	0.360 cm^{-1}	1.01 cm^{-1}
	7699	0.420	
Nitrogen	7665	0.300	0.82
	7699	0.360	

[5] H. Margenau and W. W. Watson, Rev. Mod. Phys. **8**, 22 (1936).

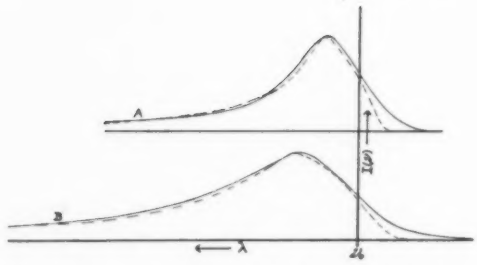

FIG. 3. Experimental (solid) and corresponding theoretical (dashed) contours of λ7699 perturbed by nitrogen (curves *A*), and by argon (curves *B*), relative densities 3.5 and 5.9, respectively.

half-widths per unit relative density as determined by the slope of the straight line part of the curves. According to theory, the half-width should be approximately twice as great as the shift when velocity broadening predominates. From Table I, we obtain $\Delta\nu_{\frac{1}{2}}/\Delta\nu = 2.6$ for argon and 2.5 for nitrogen.

To compare experimental with theoretical line contours, two microphotometer curves in the lower pressure range were chosen which did not need correction for the characteristic of the photographic plate. These were λ7699 contours for argon and nitrogen, relative density 5.9 and 3.5, respectively. In this pressure range, Margenau gives for an approximate theoretical contour:[2]

$$I(\nu') = \frac{1}{\Delta}\left[\phi\left(\frac{\pi\lambda^2}{\nu' - \Delta/2}\right)^{\frac{1}{2}} - \phi\left(\frac{\pi\lambda^2}{\nu' + \Delta/2}\right)^{\frac{1}{2}}\right], \quad (1)$$

where $$\phi(x) = (2/\pi^{\frac{1}{2}})\int_0^x e^{-y^2} dy.$$

Here, ν' is the frequency measured from the line origin ν_0, Δ the half-width, and $\lambda = \frac{2}{3}\pi |b|^{\frac{1}{3}} n$ where n is the number of perturbers per unit volume and b a constant, which is a measure of van der Waals forces. Eq. (1) was evaluated by numerical integration for various values of Δ and $\pi\lambda^2$. The best fit with the experimental contour for argon was obtained with $\pi\lambda^2 = 0.5\Delta$ where $\Delta = 4.28$ cm^{-1} and for nitrogen $\pi\lambda^2 = 0.4\Delta$, $\Delta = 2.50$ cm^{-1}. In Fig. 3 experimental (solid) and theoretical (dashed) contours are shown fitted together; curves *A* are for nitrogen, *B* for argon. Agreement is good on the long wave-length side of the maximum, but on the short wave-length side the theoretical curves fall off too rapidly. This is to be expected, however, because of the approximations made in deriving Eq. (1).

TABLE II. *Values of the van der Waals constant b calculated by three different methods.*

Calculation by Eq.	van der Waals Constant b Argon	Nitrogen
(1)	$24(10)^{-32}$	$18(10)^{-32}$ cm^6 sec.$^{-1}$
(2)	24	17
(3)	23	18

The relation between $\pi\lambda^2$ and Δ for the theoretical contours which best fit those of experiment, affords a means of calculating the van der Waals constant b. The values of b obtained in this manner are given in Table II. As a check on these values, two other methods of calculating b are available. The first is to apply Lorentz' formula as modified by Weisskopf:[6]

$$\Delta\nu_{\frac{1}{2}} = 2.2 b^{2/5} (V)^{3/5} n, \quad (2)$$

where V is the molecular root mean square velocity, and where we shall take for $\Delta\nu_{\frac{1}{2}}$ the half-widths of the theoretical curves. Secondly Margenau's theory states[2] that the curves of half-width and shift *versus* relative density depart from linearity when the velocity broadening half-width becomes approximately equal to the statistical half-width; i.e., when

$$\Delta\nu_{\frac{1}{2}} \leqq \pi\lambda^2. \quad (3)$$

Experimentally this point of departure is at about relative density 14, and the half-widths of the potassium doublet perturbed by argon and nitrogen at this relative density are 12.34 cm^{-1} and 11.29 cm^{-1}, respectively. Values of b calculated from (2) and (3) are also given in Table II. The results in Table II are in excellent agreement among themselves, but b for nitrogen does not agree with the value $[7(10)^{-32}$ cm^6 sec.$^{-1}]$ calculated by Margenau[2] from the previous work on the broadening of the potassium resonance lines.[1] The reason for this discrepancy has already been noted; the half-widths obtained by Watson and Margenau are about half as large as obtained in the present work.

The author wishes to thank Professor W. W. Watson for suggesting this problem and for his helpful criticism during the course of the work, and also Professor H. Margenau for his advice in the theoretical interpretation of the results.

[6] V. Weisskopf, Zeits. f. Physik **75**, 287 (1932).

The Infrared Absorption of Alcohol-Acetone Mixtures

WALTER GORDY,* *Department of Physics, University of North Carolina, Chapel Hill, North Carolina*

(Received October 12, 1936)

Several mixtures of methyl alcohol and acetone have been studied in the region 2.5μ to 8.5μ. The acetone was found to shift the OH vibrational band of alcohol to the shorter wave-lengths and to increase appreciably its intensity; the effects of the alcohol on acetone were to increase the intensity of the vibrational band of the CO group and to shift it to the longer wave-lengths. No other bands were measurably affected. The results indicate association of the alcohol and acetone through interaction of the OH and CO groups. The possibility of the formation of proton bonds is suggested.

INFRARED absorption studies[1] of aqueous and alcoholic solutions of inorganic acids, hydroxides and salts have revealed bands which indicate molecular association between the solvent and the solute molecules. More recently infrared studies[2] have been made of mixtures of water and some organic liquids. The present work on alcohol-acetone mixtures was undertaken to ascertain the influence of each liquid on the spectrum of the other in various mixtures of alcohol and acetone.

A Hilger infrared spectrometer with a fluorite prism was used as a resolving instrument throughout the investigation. Cell windows were of fluorite, and the absorbing layer was maintained at a constant thickness of 0.002 cm by mica washers. The chemicals were Baker's analyzed. The methyl alcohol was dried for several hours over CaO, and the acetone over $CaCl_2$ as an additional precaution against the presence of water in the samples.

A study was made of the 2.9μ alcohol band and of the acetone bands appearing at 5.73μ and at 8.17μ for several methyl alcohol-acetone mixtures. Fig. 1 shows the transmission curves for methyl alcohol and acetone and for four methyl alcohol-acetone mixtures in the region 2.5μ to 3.15μ. The broad band appearing in the region of 2.9μ in the methyl alcohol curve is characteristic of all alcohols, and arises from changes in the vibrational energy of the OH group. For alcohol concentration of 12 percent and below, this band appears at 2.75μ, having been shifted to the shorter wave-lengths by 0.15μ. In addition to the shift to higher frequencies, the intensity of the OH band is increased appreciably. That is, the intensity of the band does not decrease in proportion to the decrease in the number of absorbers. As the alcohol concentration is increased to 25 percent and to 50 percent, the band approaches that for pure alcohol. It may be that the bands for these concentrations are made up of two components with maximum of absorption at 2.75μ and 2.9μ. However, the bands are very broad, and it was not found possible to resolve them into two components. Fig. 2 shows the effects of alcohol on the vibrational band of the CO group of acetone. In contrast to the shift to the shorter wave-lengths of the OH alcohol band, the effect of the alcohol on the acetone is to shift the CO band to the longer wave-lengths. This shift is accompanied by an increase in intensity, as was the case of the OH alcohol band.

To show that the above mentioned variations of the OH and CO bands are not merely apparent effects due to the superposition of alcohol and acetone absorption, theoretical curves have been computed for mechanical mixtures in which no interaction occurs. In Figs. 3 and 4 these curves are shown in comparison with the experimental curves for the same mixtures. We have assumed that the transmission of the mixture for a given frequency is

$$T = e^{-f_1 m_1 - f_2 m_2},$$

where f_1 and f_2 are the fractional parts of alcohol

* Now at Mary Hardin-Baylor College.

[1] E. K. Plyler and W. Gordy, J. Chem. Phys. **2**, 470 (1934); E. K. Plyler and E. S. Barr, J. Chem. Phys. **2**, 306 (1934); E. K. Plyler and F. D. Williams, J. Chem. Phys. **2**, 565 (1934).

[2] D. Williams and E. K. Plyler, J. Chem. Phys. **4**, 154 (1936); D. Williams, R. D. Weatherford and E. K. Plyler, J. Opt. Soc. Am. **26**, 149 (1936).

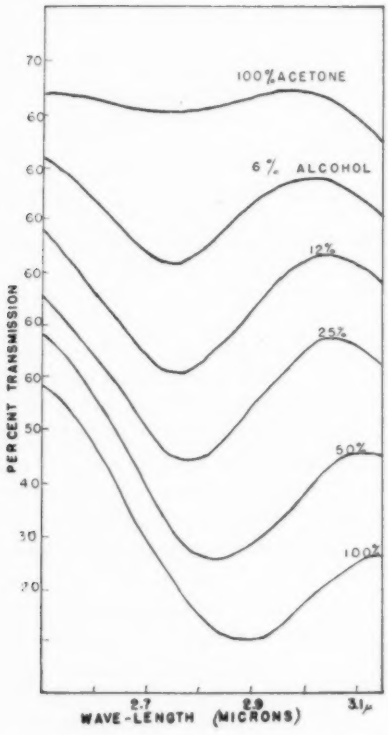

FIG. 1. The percent transmission of alcohol and acetone and alcohol-acetone mixtures in the region 2.5μ to 3.15μ.

and acetone, respectively, and where m_1 and m_2 are defined by

$$T_1 = e^{-m_1}, \quad T_2 = e^{-m_2},$$

T_1 and T_2 being the transmission of pure alcohol and pure acetone, respectively, for the given wave-lengths. It should be remembered that the cell thickness was the same in all cases.

From Fig. 5, which gives the absorption of several alcohol-acetone mixtures in the region 7.85μ to 8.45μ, it will be seen that the strong acetone band appearing at about 8.17μ, bottom curve, apparently is not shifted in position for any of the mixtures, nor is its intensity appreciably increased as was the case of the CO acetone band and the OH alcohol band. A curve was obtained for 6 percent acetone in alcohol which is not included in the figure. The intensity of the band was so low that the position of maximum absorption could not be ascertained.

An attempt was made to study other bands in the region 2.5μ to 9μ, but because of the overlapping of alcohol and acetone bands no definite results could be obtained. A study was made of the effects of benzene on the CO acetone band for concentrations of acetone in benzene varying from 50 percent to 6 percent. There appeared to be no shift in the CO band for any of the concentrations. A similar study was made of the effects of benzene on the OH band of alcohol. Likewise, no measurable shift was observed in the OH band, although there appeared for low alcohol concentrations a slight depression on the short wave-length side of the band, which may indicate the presence of vapor-like molecules of alcohol. Evidence for vapor-like molecules of alcohol in carbon tetrachloride solutions has been reported by Kinsey and Ellis.[3]

The pronounced changes in the electric moments of the CO and OH groups of acetone and alcohol indicate dipole interaction. It may be

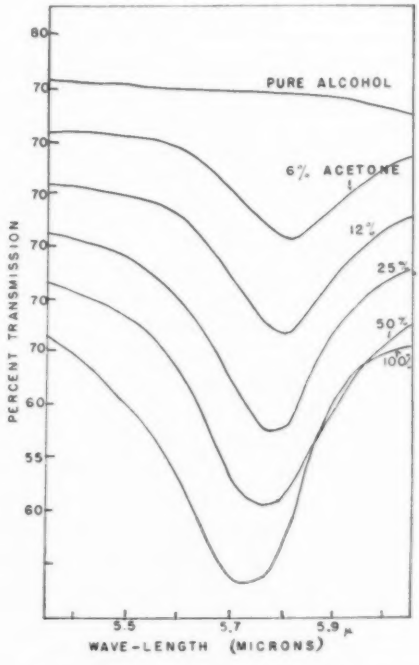

FIG. 2. The percent transmission of alcohol and acetone and alcohol-acetone mixtures in the region 5.35μ to 6.05μ.

[3] E. L. Kinsey and J. W. Ellis, Phys. Rev. **49**, 105 (1936).

that we have here the formation of proton bonds, the hydrogen of the OH group being shared between the oxygen of the two groups. This

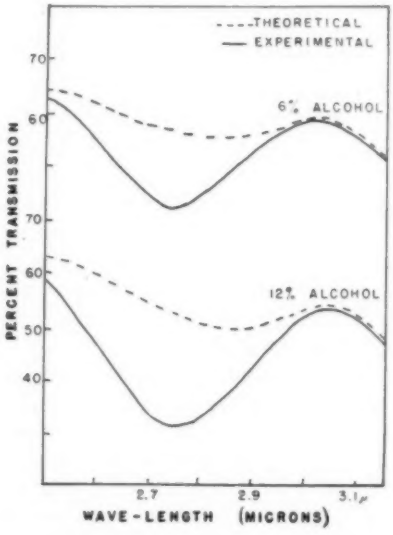

FIG. 3. Theoretical and experimental transmission of alcohol-acetone mixtures in the region 2.5μ to 3.15μ.

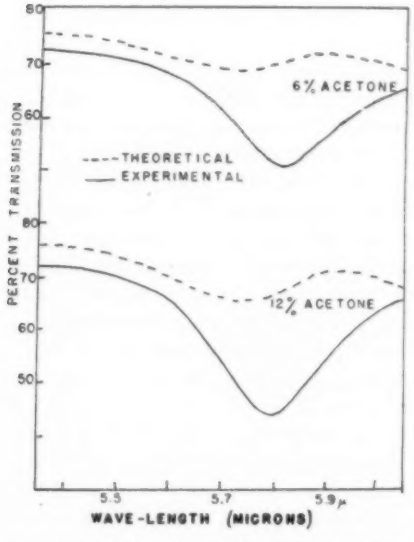

FIG. 4. Theoretical and experimental transmission of alcohol-acetone mixtures in the region 5.35μ to 6.05μ.

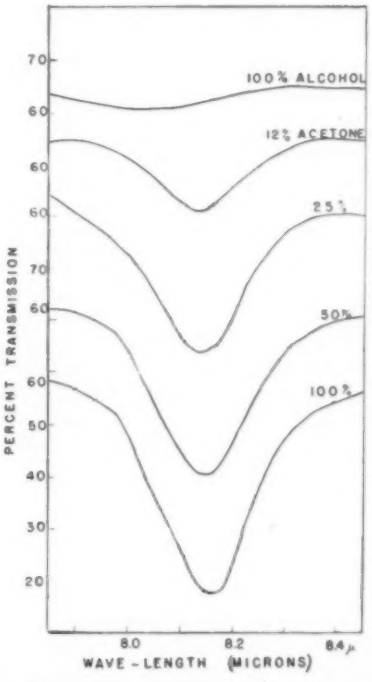

FIG. 5. The percent transmission of alcohol-acetone mixtures in the region 7.85μ to 8.45μ.

would account for the extreme changes in the polarization of these groups. Similar results[4] indicating dipole interaction in dioxane-water, methyl cyanide water, acetone-water mixtures and in mixtures of aniline with several other organic liquids may be explained by the proton bond theory. This theory has received other emphasis recently.[5] Abnormal results obtained in dielectric constant measurements of liquid mixtures are likely due to similar changes in the electric moments of certain groups which may be observable by infrared absorption measurements. The work is being continued.

The writer wishes to thank Dr. E. K. Plyler for the use of his instrument and Dr. J. A. Wheeler for suggesting a convenient method of making the theoretical computations.

[4] Unpublished data obtained by the author.

[5] L. Pauling, J. Amer. Chem. Soc. **57**, 2680 (1935); **58**, 94 (1936); L. Onsager, J. Am. Chem. Soc. **58**, 1486 (1936).

The Thermionic Emission of Platinum

L. V. WHITNEY, *University of Wisconsin, Madison, Wisconsin*
(Received October 7, 1936)

The thermionic emission from round filaments and flat strips of platinum was measured giving a value for the work function of 5.32 volts and 32 amperes/cm² deg² for the constant A. Highest possible vacuum conditions and heat treatment near 2000°K were found necessary for obtaining reliable results. The lack of such extreme heat treatment probably accounts for the abnormally high values of the constant A formerly found. Special theoretical explanations for platinum appear no longer necessary.

BECAUSE of the wide variation found experimentally for the constants in the thermionic equation, the study of the thermionic emission of platinum has been of special interest. Experimental values for the work function have ranged from 2.18 to 6.62 volts, and the values for the constant A from 10.7×10^{-4} to 10.7×10^{7}. Dushman and DuBridge have listed the results of various experimenters.[1, 2]

Since simple theory predicts A equal to 120 amperes/cm² deg² for all pure metals, many attempts have been made to explain differences actually found. Simple theory assumes a clean smooth metal surface, a negligible reflection coefficient for electrons, and a constant number density of electrons within the metal. If any of these conditions are not satisfied, one may expect variations in the values of A. Of course, most experimenters have attempted to have clean metal surfaces by using only the purest platinum obtainable, and subjecting it to long heat treatment under the best possible vacuum conditions.

If the surface of the metal is not perfectly smooth, the increased area due to the surface roughness would lead to an A larger than normal. Fowler[3] considered such a possibility as this in an effort to account for DuBridge's value of A, which was 1.7×10^{4}. This value would require a surface roughness factor of about 120, and a surface under such conditions would have to have a sort of sponge-like structure. Fowler pointed out that even if this were so, the accelerating field could have practically no effect for most of the assumed additional surface. At most, surface roughness could account for an increase in A of only about 50 percent.

A value of A smaller than 120 could be caused by a reflection coefficient for electrons greater than zero, but there is reason to believe that with a clean metal, such a coefficient could have but little effect, and probably could not be detected experimentally.

Bridgman[4] developed a theory to explain large departures of A from the universal value by connecting this departure with a temperature derivative of the photoelectric frequency and a nonvanishing of (S_p-S_m). This theory assumes that the surface of the metal has reached an equilibrium condition. DuBridge[5] points out that on the basis of this theory the thermionic equation can be written

$$I=A_0T^2\exp\,-(b-\alpha T)/T.$$

This equation is consistent with the observed linearity found for different values of $\log A$ and the work function as the specimen goes through succeeding stages of heat treatment.

Reimann[6] has also suggested a method of explaining departures of A from the universal value by allowing for the change in electron number density with temperature. On the basis of this theory the form of the thermionic equation remains the same, but an additional factor is introduced which, multiplied by the theoretical A of 120, gives a new effective A. For platinum the effective A turns out to be about 27. It should be added that this method is open to question from the theoretical point of view, since the expansion of the metal with temperature was allowed for in the final thermionic equation rather than earlier in the derivation.

[1] S. Dushman, Rev. Mod. Phys. **2**, 381 (1930).
[2] L. A. DuBridge, Phys. Rev. **31**, 236 (1928).
[3] R. H. Fowler, Proc. Roy. Soc. **122**, 36 (1929).
[4] P. W. Bridgman, Phys. Rev. **31**, 862 (1928).
[5] L. A. DuBridge, Proc. Nat. Acad. Sci. **14**, 788 (1928).
[6] A. L. Reimann, Nature **133**, 833 (1934).

DuBridge's and Van Velzer's Results

Most of the older thermionic work can be dismissed entirely because of poor vacuum technique. However, the results obtained recently by DuBridge and Van Velzer are of interest. In DuBridge's[7] latest work he reports a value of 6.27 ± 0.07 volts for φ and 1.7×10^4 for A. His tube was first baked for a short period, then the nickle cylinder heated with an induction furnace until no more gas was given off, then the tube rebaked for 24 hours, and finally the cylinder reheated with the induction furnace. During this time his platinum strip was at about 1573°K, occasionally being raised to 1773°K. His readings covered from about 1400°K to 1750°K.

Van Velzer[8] heat treated his specimens for longer periods and went to higher temperatures. He found abnormally high values of A and φ which persisted until he raised his filament to 1990°K. After a short heat treatment at this temperature, he obtained φ equal to 5.4 volts and A equal to 170 ± 20.

Apparatus for Present Work

For measuring thermionic emission, single platinum filaments were mounted in the center of a three-section guard ring type molybdenum cylinder. The diameter was 25 mm and the central section 25 mm long. Thermionic currents were measured with a shunted galvanometer having a sensitivity of 4.4×10^{-10} amperes/mm. Storage batteries were used for the plate potential and for the filament current.

Temperatures were measured with an optical pyrometer and readings were taken through a flat Pyrex window sealed to the experimental tube. To obtain a temperature scale, the emissivity of platinum was measured using rolled cylinders as described by the writer.[9] The temperature scale found agreed with that given by Worthing.[10]

Results

The thermionic emission from five specimens was measured. The first specimen was a round 12 mil wire, the purest platinum obtainable from the American Platinum Company. The experimental tube was baked for over 1000 hours at 450°C, and pressures while baking were finally better than 5×10^{-7} mm. Heat treatment of the filament was continued for over 1600 hours. After the first 500 hours steady heat treatment was maintained at about 1640°K; after 1000 hours the temperature of heat treatment was gradually increased to about 1730°K, where it was maintained for the last 400 hours. No readings from this specimen were included until after more than 1000 hours of heat treatment, and when readings were taken pressures as read by an ion gauge were better than 3×10^{-8} mm. The values of the thermionic constants showed no change during the last 700 hours of heat treatment. With readings taken up to 2000°K, A was found to be 35 and φ equal to 5.32 volts.

Air was then let into the system, and a side tube with an aluminum getter sealed on. Both DuBridge and Van Velzer had sealed off their experimental tubes with getters, and this procedure was used in the present work as a further check. Within experimental error, the results agreed with those found previously, φ and A being 5.31 volts and 32, respectively.

The filament was then removed, rolled flat to a thickness of about 0.05 mm, and remounted. Baking was continued for 200 hours and heat treatment for 350 hours. Readings were taken, but were given little weight since a temperature gradient, due to unevenness of the filament after rolling, was in evidence along the length of the filament. A simple theory was developed to take into account this gradient. Readings were sufficiently good to show that the thermionic constants were similar in magnitude to those found before. A measured 70 and φ 5.4 volts.

The second specimen was also flat, but it was rolled from an non-heat-treated round filament. This filament appeared perfectly uniform and there was no temperature gradient evident. Heat treatment was continued for only 270 hours, but the filament was flashed to high temperatures for short periods for forced aging. A was 33 and φ 5.28 volts.

The unrolled specimens, and specimens rolled before and after heat treatment, were measured to discover any differences that might result from preferred crystal orientation. The thermionic

[7] L. A. DuBridge, Phys. Rev. **32**, 961 (1928).
[8] H. L. Van Velzer, Phys. Rev. **44**, 831 (1933).
[9] L. V. Whitney, Phys. Rev. **48**, 458 (1935).
[10] A. G. Worthing, Phys. Rev. **28**, 174 (1926).

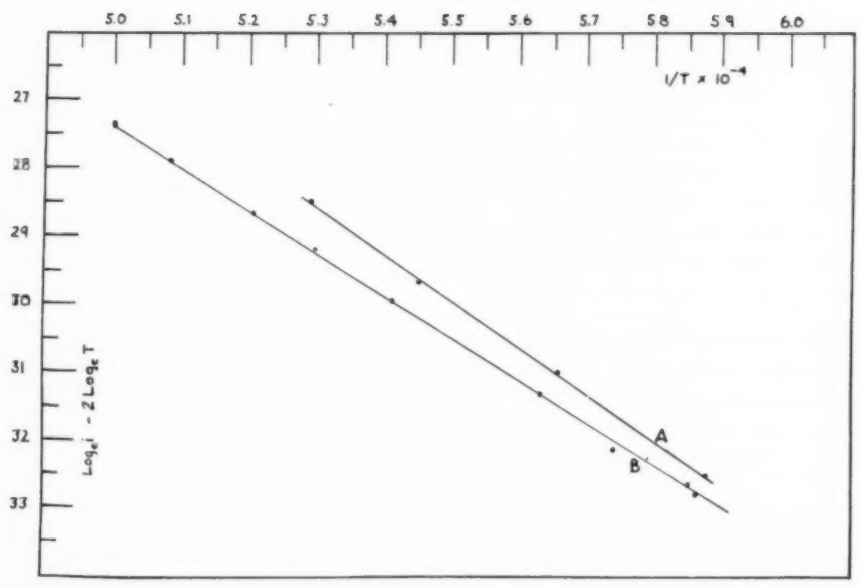

FIG. 1. Plot of $\log_e i - 2 \log_e T$ against $1/T$.

constants from one face of a crystal might differ from those of another face. Rolling might tend to orient the crystals and result in certain preferred crystal faces being exposed to the outside. However, no differences in thermionic constants could be detected.

The third specimen was a strip from the supply of platinum originally used by DuBridge at Wisconsin.[11, 12] Spectroscopic tests of this platinum showed traces of palladium which were not present in the other specimens used in this work. Due to the thinness of this third specimen, it did not stand the rigorous heat treatment given the others. The tube was baked for 120 hours and heat treatment of the filament continued for nearly 300 hours. Readings were made with pressures better than 3×10^{-8} mm. High values of A were found which dropped with heat treatment from more than 10^8 to 3×10^3. The final value of φ found for this specimen was 5.43 volts. These values are probably not characteristic of the clean metal as the specimen burned out before sufficiently high temperatures could be reached for steady and repeatable readings.

The fourth sample was a round filament from the same supply as the first and second, and was measured to find the effect of a shorter period of heat treatment but at higher temperatures. The temperature was raised to 1890°K and readings taken after the first 100 hours of heat treatment. Readings at this time were comparatively stable, φ measuring 5.8 volts and A 1.5×10^8. These results, which are consistent with those obtained by Van Velzer for similar heat treatment, are shown on curve A of the Richardson plot, Fig. 1. After this heat treatment, thermionic currents showed an almost imperceptible but definite decrease with time. However, after final heat treatment at 2000°K, thermionic currents appeared stable and values of A and φ dropped to 31 and 5.31 volts, respectively. Heat treatment was continued for over 100 hours after these lower values were found, but there was no noticeable further change.

The fifth specimen was a flat strip specially purified and kindly furnished by Dr. J. A. Becker of the Bell Laboratories. This burned out twice before readings above 1900°K could be obtained, but fortunately the failures were near the ends both times and the specimen could be remounted. After heat treatment at 1900°K, A measured 10^3 and φ 5.75 volts; heat treatment at 1930°K,

[11] L. A. DuBridge, Proc. Nat. Acad. Sci. **12**, 162 (1926).
[12] L. A. DuBridge, Phys. Rev. **29**, 451 (1927).

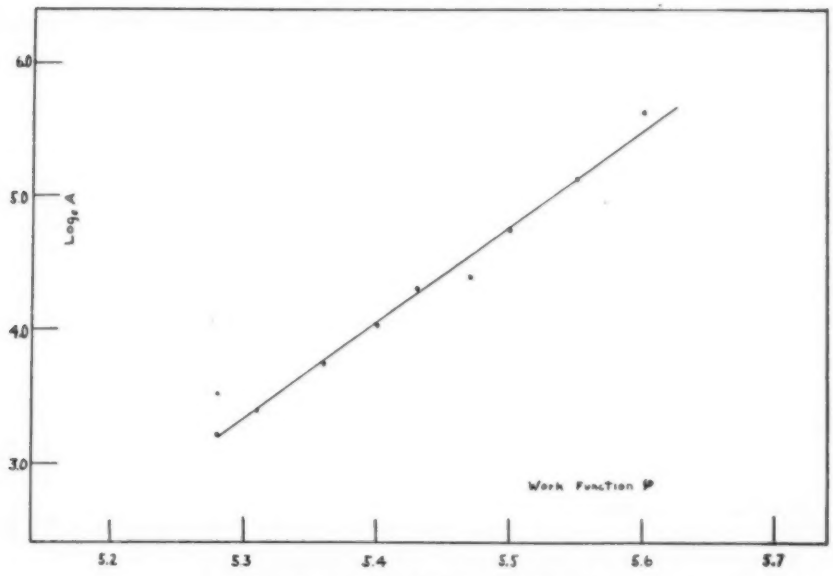

FIG. 2. Plot of work function against $\log_e A$.

A became 300 and φ 5.6 volts. Still lower values probably would have been found, but the filament failed when raised to higher temperatures.

Curve B, Fig. 1, of the Richardson plot is based on the data from the three specimens, No. 1, No. 2, and No. 4, which withstood the severe heat treatment. The average from these specimens give a value of 5.32 volts for φ and 32 for A uncorrected for any surface roughness. Results from the other specimens indicate that similar values were being approached. The linear relationship between log A and φ, which has been discussed at length by DuBridge,[5] is seen to hold as shown by Fig. 2.

The value of A found is seen to be well within the region predicted by theory. Special explanations to justify the exceptional behavior of platinum now seem unnecessary. The present work indicates the necessity of the best possible vacuum conditions, and verifies Van Velzer's conclusions as to the importance of high temperatures in the heat treating process. Apparently, heat treatment at nearly 2000°K for short periods is necessary for dependable results. The writer wishes to thank Professor H. B. Wahlin, under whose direction this work was done, for his suggestions and assistance.

The Variation of the Internal Friction and Elastic Constants with Magnetization in Iron. Part I

W. T. Cooke, *Columbia University, New York, New York*

(Received October 5, 1936)

A new and precise method is described for measuring the elastic constants and coefficients of internal friction of solid substances. The method is applied to investigate the variation of Young's modulus and the longitudinal coefficient of internal friction of annealed and unannealed Armco iron with magnetization at room temperature. Data are given which describe the behavior of the iron in three different magnetic states, *viz.*, at different points on the normal induction curve and on a hysteresis cycle, and in the anhysteretic state obtained when an alternating field, the amplitude of which is gradually reduced to zero, is superposed on a steady magnetizing field. The observed coefficients of internal friction of the unannealed specimen require correction, and this, together with the torsional data and theoretical interpretation of the results, are given in Part II of this paper.

THE amplitude of vibration at all points of a free body which is vibrating in one of its normal modes diminishes with the time in a manner described by the formula

$$u = u_0 \exp(-\Delta f t), \tag{1}$$

in which u denotes the amplitude, f the frequency of vibration, t the time, and Δ a quantity whose value depends, in the first instance, upon the substance and upon the nature of the stress associated with the particular mode of vibration. The name "internal friction" has been given to the property of solid substances of which this attenuation in amplitude is a measure. An alternative view of the phenomenon follows from a consideration of the rate of transfer of organized vibrational energy into heat.[1] Thus, if W denotes the energy dissipated per cm³ per cycle of vibration, then it can be shown that, in accordance with Eq. (1),

$$W = \xi S_0^2, \tag{2}$$

where S_0 is the stress amplitude, $\xi = \Delta/P$, and P is the appropriate elastic modulus.

The coefficients of internal friction, the ξ's, and the logarithmic decrements, the Δ's, of a substance resemble the elastic moduli in that their definition requires the specification of a stress. The types of stress here dealt with are the stretch and twist associated, respectively, with the longitudinal and torsional vibration of a slender bar. The corresponding decrements are hereafter denoted by the symbols Δ^E and Δ^G, and, conformably, the Young's and rigidity moduli by the symbols E and G.

The energy dissipated in a vibrating ferromagnetic body receives contributions from three distinct sources: first, internal friction of the sort present in nonferromagnetic materials; second, eddy currents induced in the medium by the change in magnetization produced by the varying stress; and third, internal friction of purely ferromagnetic origin. No theory of internal friction in nonferromagnetic solids has yet been written, nor has any attempt been made to lay an experimental basis for one. While it is hoped that the experimental method here described may encourage such an effort, the present research is concerned primarily with the two contributions to the internal friction which are associated with the magnetization. For, as will be shown in Part II of this paper, recent developments in ferromagnetic theory permit these to be correlated with other magneto-elastic properties of the material, and the success of such correlation lends added support to the theory.

Experimental Method

The experimental method utilizes the properties of a separately excited composite piezoelectric oscillator constructed by cementing a suitably cut right circular cylinder of crystalline quartz to one end of a cylinder of specimen material of identical cross section. The cement is hard shellac, softened by heating, and the join is made under pressure. The system is freely suspended, and a sinusoidally varying potential difference is applied between electrodes of gold leaf affixed in proper position to the quartz.[2]

[1] Kimball and Lovell, Phys. Rev. **30**, 948 (1927).

[2] Details of the method for preparing the quartz crystals are given in papers by Balamuth, Phys. Rev. **45**, 715 (1934), and Rose, Phys. Rev. **49**, 50 (1936).

In consequence of the piezoelectric stress which accompanies the electric field in the quartz, a stationary state of forced longitudinal or torsional vibration is established in the composite oscillator. A system of this sort offers two methods for measuring the elastic moduli and coefficients of internal friction of the specimen material.[3]

The first is that adopted by Zacharias,[4] who measured the variation of E and Δ^E with temperature in unmagnetized single and polycrystalline nickel over the temperature range 30°C to 400°C, and Siegel,[5] who measured the variation of E and Δ^E with magnetization and temperature in polycrystalline nickel over the same temperature range. In this method the amplitude of the applied potential difference is held constant, and means are provided for varying its frequency and for measuring the amplitude of the current which flows to the oscillator. The current amplitude varies critically with frequency in the neighborhood of certain "resonance frequencies" at which the amplitude of the forced vibration passes through a maximum. Values of the moduli and decrements are deduced from the observed nature of this variation. The method is generally applicable for the measurement of the moduli, but the precision of the decrement measurement is bad when the value of this quantity is less than about 10^{-3}. Accordingly it is not suitable for studying the internal friction of iron and most nonferromagnetic solids.

In the present method the composite oscillator forms one arm of an a.c. bridge which is excited by an alternating voltage of constant amplitude and variable frequency. Values of the moduli and decrements are deduced from the observed variation of the electrical impedance of the oscillator with frequency. The precision of the decrement measurement fails when this quantity is large of the order 10^{-3}, so that the two methods perfectly supplement each other.

The electro-mechanical theory of the single crystal oscillator,[6] and the mechanical theory of the two-part composite oscillator[7] have been set forth in detail by previous writers. The theoretical treatment of the present system follows so closely that of these others that it need here only briefly be outlined. The charge which must be placed on the gold leaf electrodes in order to establish a potential difference $\mathcal{E}$ between them can be separated into two parts: first, a part of the ordinary capacitative sort, equal to $C'\mathcal{E}$, where C' is the interelectrode capacity; and second, a part required to neutralize the piezoelectric charge produced by the vibrational strain in the quartz, and proportional to the space average value of this strain, taken along the cylinder. Accordingly, the current I, which flows to the oscillator, may be written in the form

$$I = C'd\mathcal{E}/dt - K'\epsilon dS_{av}/dt, \tag{3}$$

where K' is a geometrical constant, ϵ the appropriate piezoelectric coefficient, and S_{av} the average strain. Now S_{av} is proportional to $\mathcal{E}$, so that the ratio $Z = \mathcal{E}/I$ is independent of $\mathcal{E}$ and is the electrical impedance of the oscillator. The further development of the theory is concerned with the evaluation of S_{av}.

In order properly to estimate the effect of the layer of cement on the decrement measurements, the composite oscillator is initially regarded as composed of three coaxial cylinders of identical cross section and different lengths and materials. The actual piezoelectric stress in the quartz cylinder is represented by harmonically varying surface tractions over its end faces. The equation of motion of each medium is assumed to be of the form

$$\rho\partial^2 u/\partial t^2 = P(1 + T\partial/\partial t)\partial^2 u/\partial x^2, \tag{4}$$

where u is the particle displacement, ρ the density, P the appropriate elastic modulus, and T a dissipative coefficient which, in accordance with the theory of free vibrations in bars, is related to Δ by the formula

$$\Delta = 2\pi^2 fT. \tag{5}$$

The particle displacement in each medium is

[3] As a matter of fact, the composite piezoelectric oscillator has been used to measure the internal friction of solids by four different methods, of which the two here described are regarded as superior. For descriptions of the others see Quimby, Phys. Rev. **39**, 345 (1932), and reference 7.

[4] Zacharias, Phys. Rev. **44**, 116 (1933).

[5] Siegel and Quimby, Phys. Rev. **49**, 663 (1936).

[6] Dye, Proc. Lond. Phys. Soc. **38**, 399 and 457 (1926); Van Dyke, Proc. Inst. Radio Eng. **16**, 742 (1928).

[7] Quimby, Phys. Rev. **25**, 558 (1925); Balamuth, reference 2.

given by an expression of the form

$$u=\{A\exp(\alpha+i\beta)x+B\exp -(\alpha+i\beta)x\}\exp \text{int}, \quad (6)$$

where

$$n=2\pi f, \qquad \beta=n(\rho/P)^{\frac{1}{2}}, \qquad \alpha=\tfrac{1}{2}n\beta T,$$

and it is assumed that T is sufficiently small that $n^2T^2\ll 1$. The six amplitude coefficients (A and B for each medium) are evaluated by means of the six simultaneous equations which express, respectively, the continuity of stress and displacement at the two interfaces and of stress at the end faces of the oscillator. S_{av} is calculated from the resulting expression for u in the quartz, and the electrical impedance of the oscillator follows at once from Eq. (3).

The expression for Z can be arranged in the form $1/Z=inC'+1/Z_m$. Furthermore, in the neighborhood of a resonance frequency the form of the expression for Z_m is precisely the same as that for the electrical impedance of an inductance, capacity and resistance in series. It follows that, near resonance, a composite oscillator is electrically equivalent to a series resonant electrical circuit of impedance Z_m shunted by a capacity C'. If Z_m be written in the form $Z_m=R+iX$, then, for a three-part oscillator,

$$\begin{aligned}R=(Kn/D)\{&(M_1z_1/y_1)(\sec^2 y_1-p_1)\\&\times[1-(M_2y_2^2/M_3)p_2p_3]+(M_2z_2/y_2)\\&\times(\sec^2 y_2-p_2)[1-(M_1y_1^2/M_3)p_1p_3]\\&+(M_3z_3/y_3)(\sec^2 y_3-p_3)\\&\times[1-(M_1M_2y_3^2/M_3^2)p_1p_2]\},\end{aligned} \quad (7)$$

$$\begin{aligned}X=(Kn/D)\{&M_1p_1+M_2p_2+M_3p_3\\&-(M_1M_2y_3^2/M_3)p_1p_2p_3\},\end{aligned} \quad (8)$$

where

$$\begin{aligned}D=&2(1-\sec.\ y_2)[1-(M_1y_1^2/M_3)p_1p_3]\\&-(p_2y_2^2/M_2)(M_1p_1+M_3p_3),\\K=&\text{a constant,}^8\\M_i=&\text{mass of a cylinder, } (i=1,\ 2,\ 3)\\L_i=&\text{length of a cylinder,}\\z_i=&\alpha_iL_i,\\y_i=&\pi f/f_i,\\f_i=&(1/2L_i)(P_i/\rho_i)^{\frac{1}{2}},\\p_i=&(\tan y_i)/y_i,\end{aligned} \quad (9)$$

and the subscripts, 1, 2, 3, refer, respectively, to the specimen material, the quartz, and the cement. It will be noted that the quantities f_i are the fundamental frequencies of free vibration of the cylinders separately. The resonance frequencies of the oscillator are those at which $X=0$.

In practice the lengths of the quartz and specimen cylinders are so adjusted that f_2 is equal to an integral multiple of f_1 within ± 50 cycles at 50 kc. Furthermore, the thickness, L_3, of the layer of cement is small of the order 10^{-3} cm. A scrutiny of Eqs. (7) and (8) reveals that, under these circumstances and near a resonance frequency of the system, the presence of the cement is without appreciable effect upon the values of R and X. Accordingly, the resonance frequencies are the solutions for f of the equation

$$M_1p_1+M_2p_2=0. \quad (10)$$

Again, the variation of X with frequency near resonance is given by the formula

$$X=\tfrac{1}{2}\pi K(M_1+M_2)\delta f, \quad (11)$$

where δf is the departure from the resonance frequency, and the resistance of the oscillator at resonance by the formula

$$R=\tfrac{1}{4}K(M_1\Delta_1+M_2\Delta_2)f_0, \quad (12)$$

where f_0 is the resonance frequency.

The equivalent electrical inductance L, and capacity C, of the two-part oscillator are related to X by the formulae $L=1/n_0^2C=X/4\pi\delta f$, from which and Eq. (11),

$$L=\tfrac{1}{8}K(M_1+M_2), \quad (13)$$

and

$$C=8/Kn_0^2(M_1+M_2). \quad (14)$$

The experimental procedure for obtaining the elastic modulus and decrement of the specimen material is as follows: It will be noted that the behavior of the quartz crystal alone is described by Eqs. (10) to (14) with M_1 set equal to zero. Hence f_2 is the observed resonance frequency of the crystal vibrating alone, and Δ_2 is related to the observed resistance of the crystal by the equation $R=\frac{1}{4}KM_2\Delta_2f_2$. K is evaluated with Eq. (11) from the observed variation of the reactance of the composite oscillator with frequency. Finally, P_1 and Δ_1 are calculated with Eqs. (9), (10) and (12), from the observed resonance

[8] For longitudinal vibrations, $K=1/b^2\epsilon^2$, where b is the width of a gold leaf electrode.

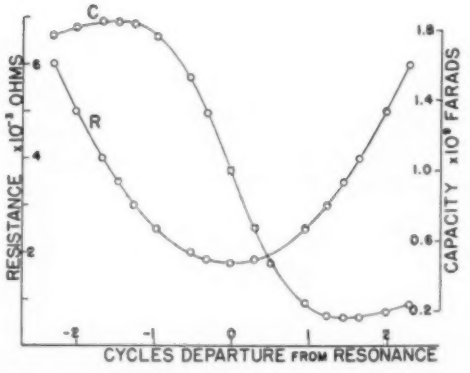

FIG. 1. Comparison of the observed and calculated values of the resistance and capacity required to balance an a.c. bridge in one arm of which is a composite piezoelectric oscillator.

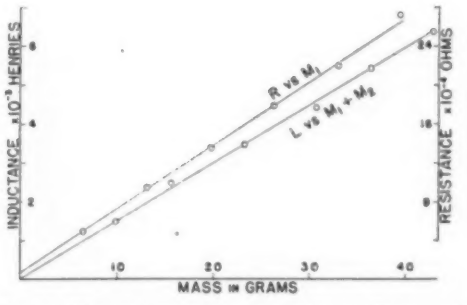

FIG. 2. The resistance of a composite oscillator varies linearly with the mass of the specimen cylinder, and its inductance with the sum of the masses of the quartz and specimen cylinders.

frequency and resistance of the oscillator at resonance.

The a.c. bridge employed is similar to that described by Stratton.[9] Essential features are adequate shielding and the use of a Wagner ground system. The ratio arms are those of a General Radio Co. type 210 unit, with an auxiliary variable condenser connected in parallel with the coil of lower resistance to compensate the distributed capacity of the other and the leakage resistance between the electrodes on the quartz. A condenser of about 30 cm capacity is connected in parallel with the oscillator in order that the reactance of this arm should be capacitative over the entire resonance range. The fourth arm of the bridge is a variable condenser connected in parallel with a Leeds and Northrup No. 4746 decade resistance box. Reliable measurements can be made of resistances as high as six megohms at 50 kc.

Power is supplied the bridge by a very stable vacuum tube oscillator[10] and amplifier. The frequency of the oscillator is controlled, in part, by a vernier condenser whose full scale represents a frequency change of 30 cycles at, roughly, 60 kc. Frequency differences can be measured with an accuracy of one-twentieth of a cycle. The vernier is frequency calibrated at intervals of 3 to 5 cycles by beating high harmonics of the oscillator against those of a piezoelectric clock.[11]

[9] Stratton, J. Opt. Soc. Am. **13**, 471 (1926).
[10] King, Bell Sys. Tech. J. **2**, No. 4, 31 (1923), Fig. 66.
[11] Dye, reference 6; Quimby, reference 3.

The apparatus functions remarkably well. The observations shown in Figs. 1 and 2 were made on a brass oscillator of square cross section 5 mm on edge. The brass cylinder was, initially, 18.64 cm long, and the resonance frequency 56,251 cycles. The points of Fig. 1 indicate the observed values of the resistance and capacity required to balance the bridge in the neighborhood of resonance. The curves, as drawn, represent the formulae of the theory. The agreement is noteworthy. The graphs of Fig. 2 show, in accordance with Eqs. (12) and (13), a linear variation of R with M_1 and L with (M_1+M_2). These data were secured with a succession of six oscillators, each obtained from its predecessor by sawing a half-wave of vibration from the brass cylinder, the resonance frequency thus remaining constant.

Fig. 3 is a cross section of the assembly for measuring the variation of the elastic moduli and internal friction of iron with magnetization. The oscillator is mounted in an evacuated glass tube on silk threads located at displacement nodes of vibration. The tube is surrounded, in turn, by a water jacket and by the magnetizing coils. The latter are designed to secure, as nearly as possible, a uniform magnetization over the length of the specimen. The end coils, B of Fig. 3, are each 190 turns of 5 mil copper strip 5 cm wide. The middle coil is six layers of No. 16 D.C.C. wire 21 cm long. Typical magnetic flux distribution curves are shown in Fig. 4.

Numerous experiments on iron oscillators of different lengths, oscillating at different harmonics of the fundamental mode, indicate that the experimental error in Δ_1 due to nonuniform

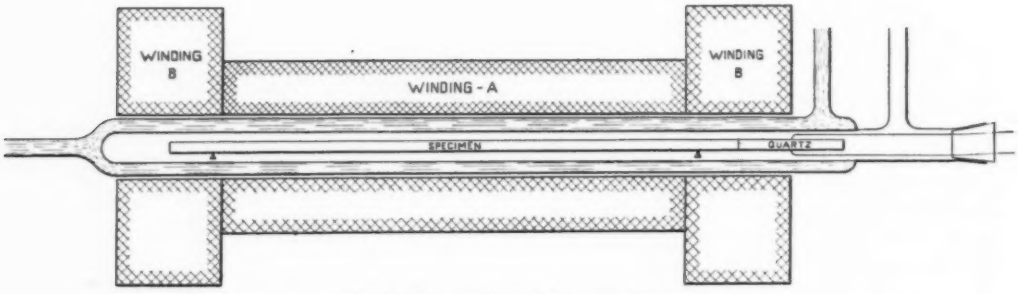

FIG. 3. Cross section of the assembly.

magnetization near the ends of the cylinder is never greater than 5 percent.[12] An error of about the same magnitude may occur in the measurement of the *percent change* of the elastic modulus with magnetization.

RESULTS

Specimen materials

The specimen materials upon which the observations here reported were made are cold-rolled Armco iron (hereafter designated "unannealed"), and the same substance after annealing at 930°C for 2 hours in hydrogen at atmospheric pressure and cooling to room temperature in 8 hours (hereafter designated "annealed"). The modulus, decrement and Wiedemann effect measurements were made on cylinders of circular cross section, 0.3 cm to 0.5 cm in diameter and about 30 cm long. The resonance frequencies at which the observations were taken lay in the neighborhood of 56 kc for the longitudinal vibrations and 39 kc for the torsional, so that there were seven half-waves of vibration in the specimen. The magnetic and magnetostriction measurements were made on an ellipsoid of revolution whose semi-axes are 0.197 cm and 15.24 cm.

Magnetic measurements

Modulus and decrement measurements were made subsequent to three different magnetic procedures: first, the iron was carried through many hysteresis cycles of magnetization at a chosen maximum value of the applied field, and left in the state corresponding to that maximum value (the data are hereafter designated "normal induction"); second, the iron was carried through a hysteresis cycle of magnetization and left at a chosen point on the cycle (the data are hereafter designated "hysteresis"); third, the iron was placed in a steady field of chosen value, and a 60-cycle alternating field was superposed thereon, the amplitude of which was gradually reduced to zero (the data are hereafter designated "anhysteresis").

The normal induction relations between magnetization J, and magnetizing field H, in the annealed and unannealed specimens are given in Table I. The hysteresis and anhysteresis data insofar as they differ from the normal induction, are given in Tables II and III. Values of J corresponding to values of H higher than those which appear in these two tables are in each case to be obtained from Table I.

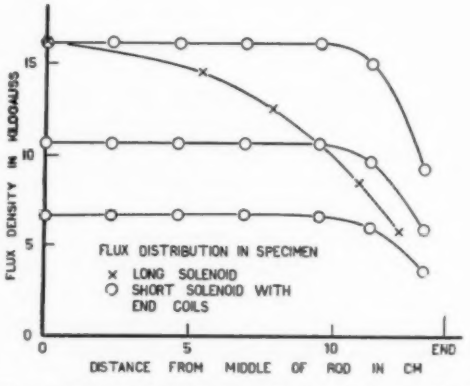

FIG. 4. Distribution of magnetic flux in the specimen. The curve with the crosses shows the distribution when the specimen is placed in a long solenoid.

[12] The same experiments reveal that, over the frequency range 36 kc to 72 kc, the coefficient of internal friction of unmagnetized, unannealed Armco iron is proportional to $f^{\frac{1}{2}}$. This is consistent with the data of Wegel and Walther (Physics **6**, 141 (1935)) who measured the frequency variation of the internal friction of many solids, and found values of the exponent of f ranging from $+0.54$ to -0.31.

TABLE I. *Normal magnetization data.*

Unannealed		Annealed	
H	*J*	*H*	*J*
1	19	0.2	20
2	117	.4	60
4	494	.6	470
6	797	.8	930
8	980	1	1070
10	1090	2	1144
12	1161	4	1188
15	1230	7	1219
20	1290	10	1238
30	1356	15	1254
40	1394	20	1267
60	1440	30	1292
80	1470	40	1313
100	1492	60	1349
150	1544	80	1380
200	1578	100	1406
250	1600	150	1462
300	1619	200	1506
350	1635	250	1539
400	1648	300	1567
450	1659	350	1590
500	1664	400	1609
550	1668	450	1626
		500	1641
		550	1656

TABLE II. *Hysteresis magnetization data.*

Unannealed			Annealed		
H	*J*		*H*	*J*	
0	570	570	0.0	1130	1130
5	1080	− 660	.2	1160	1000
10	1240	−1080	.5	1190	− 200
20	1340	−1290	1	1200	−1030
30	1380	−1350	2	1210	−1160
50	1430	−1420	5	1230	−1200
100	1500	−1500	10	1240	−1230
			15	1250	−1250

TABLE III. *Anhysteresis magnetization data.*

Unannealed		Annealed	
H	*J*	*H*	*J*
1	390	0.2	970
2	540	.4	1100
4	793	.6	1125
6	970	.8	1140
8	1085	1	1150
10	1160	2	1178
12	1206	4	1205
15	1249	7	1226
20	1301		

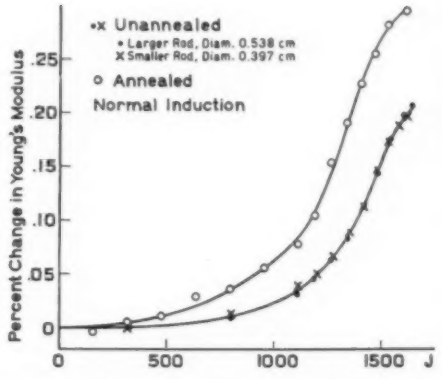

FIG. 5. The variation of Young's modulus with magnetization in unannealed and annealed Armco iron.

The coercive force, remanence, and initial susceptibility of the unannealed material are, respectively, 2.3, 570 and 7.4; and of the annealed material 0.46, 1130 and 28.7.

Young's modulus and longitudinal decrement

In order to test the validity of the theoretical expression for the contribution of the eddy currents to the internal friction, observations were made on two unannealed specimen bars of the same length and different diameters, *viz.*, 0.538 cm and 0.397 cm. Of these only the larger was subsequently annealed, since it was found that the internal friction in the annealed material is so large that the eddy current contribution is almost negligible.

The curves of Fig. 5 show the normal induction variation of Young's modulus E, with magnetization in unannealed and annealed Armco iron. The results obtained with the cylinders of different diameter are indistinguishable, as they should be, and supply a check on the method. The anhysteresis variation of E with J is the same as the normal induction. The value of Young's modulus is 18.6×10^{11} dynes/cm^2 for the unmagnetized unannealed material and 19.9×10^{11} dynes/cm^2 for the unmagnetized annealed material.

The points and circles of Fig. 6 show the observed variation of the longitudinal decrement Δ^E, with normal magnetization in the two unannealed specimens. The circles of which the right or left halves are blackened indicate the differences between the observed decrements of the two specimens and the contributions arising

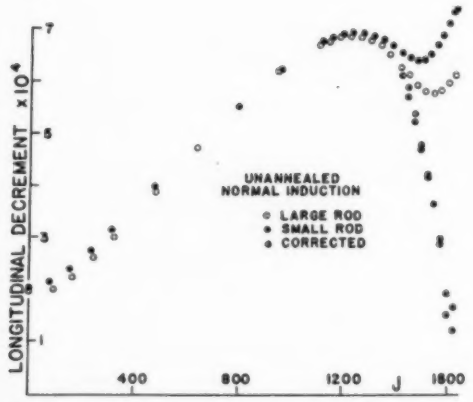

FIG. 6. The variation of the longitudinal internal friction with magnetization in unannealed Armco iron. The half-blackened circles indicate values of the decrement after the contribution arising from eddy currents has been subtracted.

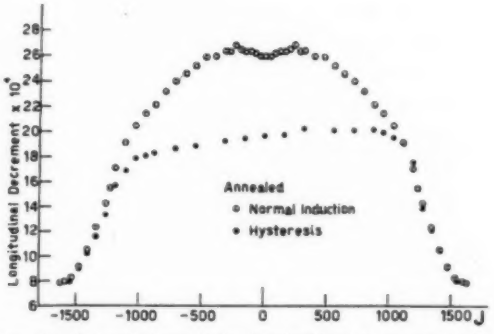

FIG. 7. The variation of the longitudinal decrement with magnetization in annealed Armco iron.

from eddy currents, when the latter are calculated in the manner described in Part II of this paper. It is clear that all effect of the form of the specimen is removed by this calculation, and that the course of the corrected curve in fact represents the variation with magnetization of that part of the internal friction which is of purely ferromagnetic origin.

The anhysteresis longitudinal decrement in the unannealed material differs inappreciably from the normal induction. The variation of the hysteresis decrement with magnetization is nearly the same at high magnetizations, but at low magnetizations the hysteresis values are all *larger* than the normal induction, and the variation does not show the marked asymmetry about the axis $J=0$ which characterizes the behavior of the torsional decrement (cf. Fig. 2 of Part II). The minimum value of the hysteresis decrement, which occurs at $J=0$, is about twice that of the normal induction.

The circles and points of Fig. 7 show, respectively, the normal induction and hysteresis variation of the longitudinal decrement in annealed Armco iron. It will be noted that here the effect of hysteresis is just the reverse of that in the unannealed material; the hysteresis values at low magnetizations are *smaller* than the normal induction. The eddy current contribution is responsible for most of the change in the slope of the curve at the highest magnetizations. Corrected values of Δ^E are given in Table I of Part II.

The Variation of the Internal Friction and Elastic Constants with Magnetization in Iron. Part II

WILLIAM FULLER BROWN, JR., *Columbia University, New York, New York*

(Received October 5, 1936)

The experimental method described in Part I of this paper is applied to measure the variation of the rigidity modulus and torsional decrement with magnetization in unannealed and annealed Armco iron. Formulae are derived which evaluate the contributions to the moduli and decrements arising from eddy currents induced in the vibrating specimen by the change in magnetization produced by the varying stress. These formulae contain the magnetostriction and Wiedemann effect coefficients, which, accordingly, have been measured. All effects of the eddy currents are thus eliminated from the final data, which are discussed in the light of recent ferromagnetic theory.

RIGIDITY MODULUS AND TORSIONAL DECREMENT

IN Part I of this paper[1] W. T. Cooke has described a precise experimental method for measuring the elastic moduli and coefficients of internal friction of solid substances, and has presented data which show the observed variation of Young's modulus E, and the longitudinal decrement Δ^E, with magnetization in specimens of unannealed and annealed Armco iron. The observed variation of the rigidity modulus G and the torsional decrement Δ^G with magnetization in the same specimens is shown in Figs. 1 to 3.

Both the longitudinal and torsional decrements are subject to correction, for, as was first pointed out by Kersten,[2] the energy dissipated in vibrating magnetized substances receives a contribution arising from eddy currents induced by the change in magnetization which accompanies the vibrational stress in the medium. It is evident that the magnitude of this contribution must depend on the shape of the specimen. In order, therefore, to arrive at a quantity characteristic of the material alone the observed values of Δ^E and Δ^G must be corrected by amounts which, it will be shown, depend in part on the longitudinal magnetostriction and on the Wiedemann effect, respectively. Accordingly these properties of the specimen material must be measured.

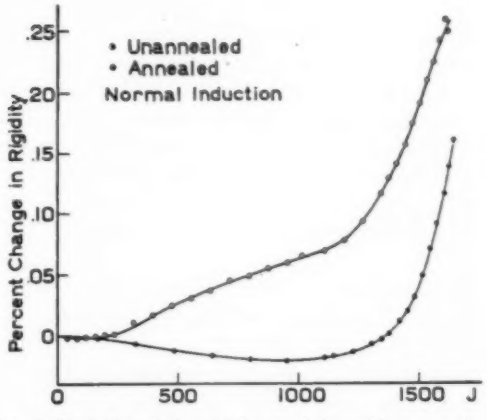

FIG. 1. Variation of the rigidity modulus with magnetization in unannealed and annealed Armco iron.

MAGNETOSTRICTION AND THE WIEDEMANN EFFECT

Magnetostriction

The magnetostriction measurements were made on the ellipsoid which yielded the magnetic data reported in Part I.[3] The "form effect" dis-

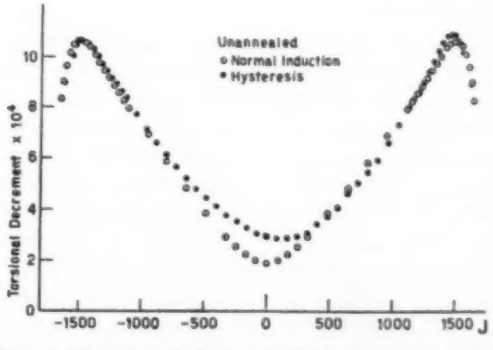

FIG. 2. Variation of the torsional decrement with magnetization in unannealed Armco iron.

[1] Cooke, Phys. Rev., preceding paper.
[2] Kersten, Zeits. f. tech. Physik **11**, 463 (1934).
[3] The experimental method is described in a forthcoming paper by D. Kirkham.

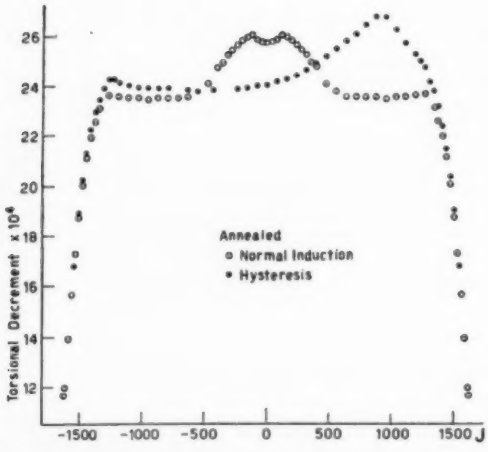

FIG. 3. Variation of the torsional decrement with magnetization in annealed Armco iron.

cussed by Becker[4] is negligible for such an ellipsoid. The results are shown in Fig. 4. The precision of the measurement of $\delta l/l$ is $\pm 0.10\times 10^{-6}$.

The unannealed specimen is evidently not isotropic, probably in consequence of a nonrandom distribution of internal stresses, or of microcrystalline axes. The anisotropy is manifest in an abnormally low value of Poisson's ratio, computed on the assumption of isotropy; in the value of the magnetization at high fields, which is larger before than after annealing; and in the fact that the Villari reversal does not appear in the unannealed material. The last named phenomenon has been discussed by Bitter.[5]

Wiedemann effect

It has been shown[6] that the Wiedemann effect is merely a complicated case of magnetostriction: the twist produced when a current is passed through a magnetized rod is a result of the rotation of the principal axes of strain in each volume element which occurs when a circular field, H_θ, is superposed on a longitudinal field, H_z. This twist may be regarded as due to a magnetostrictive shearing stress $-\eta' H_\theta$, where η' is a function of H_z alone provided $H_\theta^2 \ll H_z^2$. For a solid cylinder of radius R carrying a longitudinal current I e.m.u., the circular field at a distance r from the axis is $2Ir/R^2$. If the cylinder is twisted through an angle ϕ radians per cm length, the shearing strain is $r\phi$, and the resulting stress of elastic origin is therefore $Gr\phi$. The observed twist is determined by the condition $-\eta' 2Ir/R^2 + Gr\phi = 0$, whence $\eta' = GR^2\phi/2I$. It is this quantity η' that must be known in order to evaluate the contribution of the eddy currents to the torsional decrement. It can be determined by measurement of the Wiedemann effect at currents sufficiently low that $H_\theta^2 \ll H_z^2$; under this condition ϕ is proportional to I.

An accurate measurement of η' is possible only when the specimen is a long thin wire. Preliminary calculation indicated, however, that the cylinders used in the decrement measurements would yield data adequate for the present purpose. The experimental method is as follows: The magnetizing coil assembly described in Part I is mounted on a rigid frame with its axis vertical. The specimen is clamped at the upper end, and to the lower end is attached a brass rod which terminates in mercury. The twist of the uniformly magnetized portion of the specimen is measured by observing the deflection of a light beam successively reflected from two mirrors, lying in approximately perpendicular planes through the axis of the rod, and at the same height, but mechanically attached to opposite ends of the portion of the rod under test. The deflection of the beam is thus unaffected by rotation of the system as a whole, and depends only on the difference of rotation of the two mirrors. To measure the small deflections (a few tenths of a mm at 1 m distance) a slit illuminated by monochromatic light is used as a source, of which a lens between the source and the mirrors forms an image about 1 m from the mirrors. The

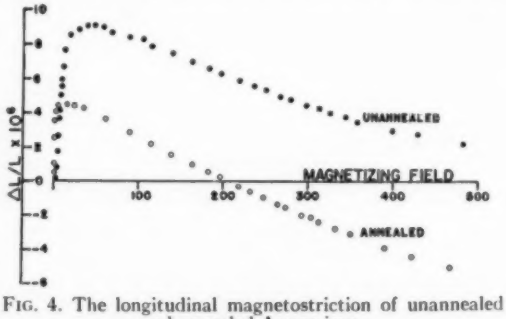

FIG. 4. The longitudinal magnetostriction of unannealed and annealed Armco iron.

[4] Becker, Zeits. f. Physik **87**, 547 (1933).
[5] Bitter, Phys. Rev. **42**, 705 (1932).
[6] Fromy, J. de phys. **7**, 13 (1926); Ann. d. physique **8**, 626 (1927).

image is viewed through a microscope equipped with a 32 mm objective and a filar micrometer eyepiece.

The deflection which accompanies a reversal of the current through the specimen is observed for different values of the current, the magnetization being held fixed. The initial slopes of the current deflection curves thus obtained are found by graphical extrapolation.

Because of the shortness and thickness of the cylinders used in the measurements, it is necessary to consider the effect of torques exerted on the ends of the specimen. It has been stated by Williams[7] that the end of the specimen, being a pole in a circular field, is subject to a torque of amount $2mI$, where m is the pole strength. This torque, if present, would introduce an error not greater than 1.5 percent of the maximum observed value of η'. Williams' formula, however, is obtained by attributing physical existence to the fictitious magnetic volume and surface distributions $\rho=-\nabla\cdot\mathbf{J}$ and $\sigma=\mathbf{n}\cdot\mathbf{J}$. Actually these distributions are obtained by a transformation of a volume integral, and lead to correct expressions for the total force and torque on a magnetized body, but not for the force and torque on a part of the body. Direct application of the formula $d\mathbf{F}=\mathbf{J}\cdot\nabla\mathbf{H}d\tau$ for the force $d\mathbf{F}$ on a volume element $d\tau$ shows at once that the only component of force exerting a torque about the cylinder axis is

$$dF_\theta=(J_z\partial H_\theta/\partial z+J_r\partial H_\theta/\partial r)d\tau.$$

Calculation of the resulting torque on the assumption of the worst possible conditions of nonuniformity of J and H at the ends of the specimen indicates that the error is less than 1 percent of the maximum value of η', and is therefore within the precision of the measurements, which is about 10 percent of this maximum value.

The variation of η' with intensity of magnetization in the annealed specimen is shown in Fig. 5. The relation between twist and current in the unannealed specimen is nonlinear, and shows much hysteresis. Hence it is possible only to set an upper limit of 0.5×10^5 on the value of η' in this material.

[7] Williams, Phys. Rev. **32**, 296 (1911).

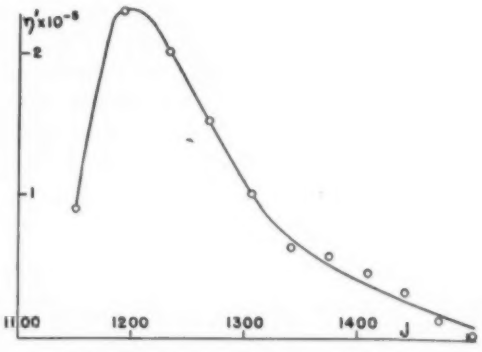

FIG. 5. The Wiedemann effect in annealed Armco iron.

THE DISSIPATION DUE TO EDDY CURRENTS

Kersten[2] has developed a theory which permits an evaluation of the contribution to Δ^E arising from eddy currents in a medium for which the simplifications of Becker's theory of ferromagnetism are valid, and which is in the remanent state of magnetization. For the present purpose a more complete theoretical analysis is necessary.

The specimen will be assumed to be an infinitely long, thin cylinder of radius R and resistivity ρ e.m.u., placed in a longitudinal magnetizing field H. Associated with the field are an induction B, and a longitudinal magnetostriction e. It will further be assumed that the changes resulting from a small variation of strain or of field are reversible. Under these assumptions, simple thermodynamic considerations[8] lead to relations between the alternating components of induction and stress, and those of field and strain.

Alternating longitudinal elongations, $\partial w/\partial z$, and associated lateral contractions (determined by the condition that the lateral tension shall vanish) produce an alternating induction B_z; the circular currents induced set up an alternating longitudinal field H_z, with consequent alternating longitudinal tension Z_z. The relations are

$$B_z=\mu H_z+4\pi\eta\partial w/\partial z, \tag{1}$$

and

$$Z_z=-\eta H_z+E\partial w/\partial z, \tag{2}$$

where μ is the incremental permeability, $\partial B/\partial H$,

[8] Cf. Houstoun, Phil Mag. **21**, 78 (1911); Becker, Zeits. f. Physik **87**, 547 (1933); Voigt, *Lehrbuch der Kristallphysik* (1928), pp. 223, 563, 939.

at constant strain,[9] E is Young's modulus at constant field, and $\eta = E(de/dH)$.

Alternating torsional strains, $\partial u_\theta/\partial z$, produce a circular induction B_θ; the longitudinal and radial currents induced set up an alternating circular field H_θ with consequent torsional stress θz.[10] The relations are

$$B_\theta = \mu' H_\theta + 4\pi\eta' \partial u_\theta/\partial z, \tag{3}$$

and

$$\theta z = -\eta' H_\theta + G\partial u_\theta/\partial z, \tag{4}$$

where μ' is the permeability, B/H (*not* $\partial B/\partial H$),[11] and G is the rigidity at constant field.

If the specimen is undergoing longitudinal displacements described by the formula

$$w = w_0 \exp i(\beta z + nt), \tag{5}$$

the components of magnetic field, magnetic induction, electric field and current density are determined by the electromagnetic field equations, in which the radiation terms may be neglected; by the auxiliary relations between magnetic field and induction, and between electric field and current density; and by the conditions of finiteness of the field vectors at $r=0$ and $r=\infty$, and of continuity of H_z and B_r at $r=R$. The usual relation, $B_z = \mu H_z$, is to be replaced by Eq. (1). Solution of these equations subject to these boundary conditions gives[12]

$$H_z = 4\pi i(n\beta w/\mu)[-1 + FI_0(hr)], \tag{6}$$

where

$$F = hK_1(\beta R)/[\mu\beta I_1(hR)K_0(\beta R) + hI_0(hR)K_1(\beta R)],$$
$$h^2 = \beta^2\mu/\mu' + 4\pi n\mu i/\rho,$$

and the I's and K's are Bessel functions as defined in reference 12. At the frequencies of vibration here considered the real part of h is negligibly small, so that the last equation reduces to $h = m\sqrt{i}$, where $m = (4\pi\mu n/\rho)^{\frac{1}{2}}$.

In accordance with Eq. (2) the field H_z produces a stress whose average value over the cross section of the rod is given by the expression

$$-\eta(H_z)_{\text{av}} = 4\pi(\eta^2/\mu) \times [1 - (2F/hR)I_1(hR)]\partial w/\partial z. \tag{7}$$

Like the stress of elastic origin, this contains $\partial w/\partial z$ as a factor, but the coefficient of $\partial w/\partial z$ is, in general, complex. The real part is equivalent to a change of Young's modulus, and measures the nondissipative reaction of the currents upon the mechanical vibration. The imaginary part is equivalent to a viscous coefficient, and measures the dissipation of energy by the currents. The changes in E and Δ^E thus produced by the currents are evaluated by comparing Eq. (2), in which the value of $-\eta H_z$ given by Eq. (7) has been substituted, with the usual stress-strain relation in a cylinder with elastic and viscous stresses. Thus

$$\frac{\Delta E}{E} = \frac{4\pi\eta^2}{E\mu}\left\{1 - \frac{2}{a}\frac{Q + (\mu b/a)(P^2+Q^2)}{(1+\mu bQ/a)^2 + (\mu bP/a)^2}\right\},$$

and

$$\Delta_c{}^E = \frac{4\pi^2\eta^2}{E\mu}\frac{2}{a}\frac{P}{(1+\mu bQ/a)^2 + (\mu bP/a)^2},$$

where

$$P = (\text{ber}\, a\, \text{ber}'a + \text{bei}\, a\, \text{bei}'a)/(\text{ber}^2 a + \text{bei}^2 a),$$
$$Q = (\text{ber}\, a\, \text{bei}'a - \text{bei}\, a\, \text{ber}'a)/(\text{ber}^2 a + \text{bei}^2 a),$$
$$a = (f/f_c)^{\frac{1}{2}}, \quad b = \beta R K_0(\beta R)/K_1(\beta R),$$

and $f_c = \rho/8\pi^2\mu R^2$.

At frequencies far below or above f_c the following simplifications are possible:

When $f \ll f_c$, $\dfrac{\Delta E}{E} = 0$ and $\Delta_c{}^E = \dfrac{1}{2}\dfrac{\pi^2\eta^2}{E\mu}\dfrac{f}{f_c}$.

When $f \gg f_c$,

$$\frac{\Delta E}{E} = \frac{4\pi\eta^2}{E\mu}\left\{1 - \sqrt{2}\left(\frac{f_c}{f}\right)^{\frac{1}{2}}\frac{1+c\sqrt{2}}{(1+c)^2+c^2}\right\}, \tag{8}$$

and

$$\Delta_c{}^E = \frac{4\pi^2\eta^2}{E\mu}\sqrt{2}\left(\frac{f_c}{f}\right)^{\frac{1}{2}}\frac{1}{(1+c)^2+c^2}, \tag{9}$$

where

$$c = \mu b/(a\sqrt{2}) = \mu(f_c/2f)^{\frac{1}{2}}\beta R K_0(\beta R)/K_1(\beta R).$$

[9] The μ obtained from the magnetization curve is the incremental permeability at zero stress, and exceeds the μ of Eq. (1) by $4\pi\eta^2/E$. This difference, as well as the differences between the adiabatic and isothermal values of μ, η, and E, is small enough to be neglected in this computation.

[10] The stress and strain notation is that of Love, *Treatise on the Mathematical Theory of Elasticity*, 4th edition, pp. 56, 90, 288.

[11] A small increment of H perpendicular to the original direction merely rotates the H and B vectors through the small angle $B_\theta/B = H_\theta/H$.

[12] See Gray, Mathews and Macrobert, *Bessel Functions*, 2nd edition, Chap. III; Russell, *Alternating Currents*, 2nd edition, Chap. VII.

Introduction of the values of η and μ at remanent magnetization, as given by Becker's theory,[13] and of a new reference frequency f_g, such that $f_c=(45\pi/512)f_g=0.2766f_g$, leads to formulae which agree with Kersten's[14] provided $c\ll 1$.[15]

If the specimen is undergoing torsional displacements described by the formula

$$u_\theta = r\phi = r\phi_0 \exp i(\beta' z + nt),$$

the quantities to be evaluated instead of H_z and $(Z_z)_{av}$ are H_θ and the total torque

$$2\pi \int_0^R \theta z r^3 dr$$

exerted across a surface normal to the cylinder axis. The analysis parallels that for longitudinal vibrations and leads to the following formulae:

$$\frac{\Delta G}{G} = \frac{4\pi\eta'^2}{G\mu'}\left\{1 - \frac{4}{a}P'\right\},$$

and

$$\Delta_e G = \frac{4\pi^2\eta'^2}{G\mu'}\frac{4}{a}\left(Q' - \frac{2}{a}\right),$$

where

$$P' = (\mathrm{ber}\, a\, \mathrm{ber}'a + \mathrm{bei}\, a\, \mathrm{bei}'a)/(\mathrm{ber}'^2 a + \mathrm{bei}'^2 a),$$

$$Q' = (\mathrm{ber}\, a\, \mathrm{bei}'a - \mathrm{bei}\, a\, \mathrm{ber}'a)/(\mathrm{ber}'^2 a + \mathrm{bei}'^2 a),$$

$$a = (f/f_c')^{\frac{1}{2}} \quad \text{and} \quad f_c' = \rho/8\pi^2\mu' R^2.$$

When $f \ll f_c'$, $\dfrac{\Delta G}{G} = 0$ and $\Delta_e G = -\dfrac{1}{6}\dfrac{\eta'^2}{G\mu'}\dfrac{f}{f_c'}$.

When $f \gg f_c'$,

$$\frac{\Delta G}{G} = \frac{4\pi\eta'^2}{G\mu'}\left\{1 - 2\sqrt{2}\left(\frac{f_c'}{f}\right)^{\frac{1}{2}}\right\}, \tag{10}$$

and

$$\Delta_e G = \frac{4\pi^2\eta'^2}{G\mu'} 2\sqrt{2}\left(\frac{f_c'}{f}\right)^{\frac{1}{2}}. \tag{11}$$

Application of the Theory

In all the measurements under discussion the formulae for $f \gg f_c$ are valid. Since the second terms in Eqs. (8) and (10) are small compared with the first, the measured values of the elastic moduli are very nearly those at constant B rather than at constant H. For it follows immediately, on setting B_z and B_θ equal to zero in Eqs. (1), (2) and (3), (4), that

$$[E]_B - [E]_H = 4\pi\eta^2/\mu$$

and

$$[G]_B - [G]_H = 4\pi\eta'^2/\mu',$$

and these are precisely the differences given by the first terms of Eqs. (8) and (10). As was pointed out by Kersten, this means that the alternations of magnetic flux occur only near the surface of the specimen.

The effect of the eddy currents on the torsional decrement is small, being nowhere more than one percent of the measured value for either of the specimen materials.

In the measurements of the longitudinal decrement for the unannealed material, two cylinders of different diameter were used (cf. Part I, Fig. 6). The agreement between the results obtained on these two specimens at low magnetization indicates that here the eddy current contribution is negligible, since, by Eq. (9), it should vary approximately in inverse proportion to the diameter. The second rise in the curves at high magnetization, however, is entirely due to eddy currents, and, together with the difference in behavior of the two specimens, disappears when the contribution of the eddy currents to the decrement is subtracted. Similarly, the eddy currents are responsible for the change of slope observable at the highest magnetizations in the curve of Δ^E *vs.* J for the annealed specimen (Part I, Fig. 7). The corrected values of Δ^E for this substance are given below in Table I.

It should be noticed that the formula, Eq. (9), involves two factors, η and μ, which must be evaluated by graphical differentiation of experimental curves, and which, moreover, are raised to powers higher than the first. It must be remembered also that the specimen is not actually infinitely long and not uniformly magnetized. Consequently the correction for eddy currents cannot be computed with great precision; but the success of the theory in explaining the second rise of the curves in Fig. 6, and in removing the discrepancies between the observations on different specimens at high magnetization, leaves

[13] Kersten, Zeits. f. Physik **71**, 553 (1931); **82**, 723 (1933).
[14] Kersten, reference 2, Eqs. (3) and (4).
[15] The terms involving c result from the finite wave-length prescribed by the mechanical oscillation. Kersten's analysis assumes this wave-length to be infinite.

TABLE I. *Variation of the decrements and elastic moduli at constant B with magnetization in annealed Armco iron. Corrected for the effect of eddy currents. Normal magnetization.*

J gauss	$\Delta^E \times 10^4$	$(\Delta E/E) \times 10^2$	$\Delta^G \times 10^4$	$(\Delta G/G) \times 10^2$
0	25.91	0	25.75	0
40	25.90		25.79	−0.0020
80	26.13		25.88	−0.0023
119	26.30		26.06	−0.0017
159	26.28	−0.0037	25.97	−0.0003
199	26.45		25.84	+0.0003
239	26.75		25.66	0.0005
279	26.30		25.44	0.0013
318	26.34	+0.0058	25.26	0.0103
358			24.94	
398	25.88		24.76	0.0187
477	25.83	0.0105	24.09	0.0244
557	25.19		23.78	0.0307
637	24.55	0.0289	23.55	0.0366
716	23.98		23.51	0.0446
796	23.19	0.0360	23.51	0.0481
875	22.11		23.51	0.0546
955	21.43	0.0556	23.46	0.0595
1034	20.43		23.51	0.0650
1113	19.13	0.0779	23.55	0.0700
1193	17.09	0.1041	23.60	0.0776
1233	15.48		23.64	
1269	14.27	0.1532	23.45	0.0938
1342	11.60	0.1926	22.94	0.1167
1376			22.34	0.1295
1410	8.81	0.2323	21.73	0.1412
1444			20.98	0.1571
1475	6.84	0.2625	20.01	0.1743
1506			18.75	0.1914
1537	5.30	0.2910	17.27	0.2106
1565			15.66	0.2257
1593	4.14		13.95	0.2421
1619			11.98	0.2582
1623	3.65	0.3077	11.66	

little doubt that it is adequate for the present purpose, and that the corrected values of the decrement are characteristic of the material itself.

Correction of the observed variations of E and G to obtain the values at constant B is easily accomplished, since the correction terms are the second in Eqs. (8) and (10) and these are small. The correction to constant H includes the first terms in these formulae and is less reliable. $[\Delta E/E]_H$ for the unannealed specimen follows the observed curve (Part I, Fig. 5) to $J=1400$; beyond this point the corrected curve flattens out, reaching a maximum of 0.12 percent at about 1490 gauss and decreasing to 0.11 percent at 1630 gauss. For the annealed specimen, the flattening out begins at $J=1250$, and the curve rises more slowly, reaching about 0.17 percent at 1630 gauss. The effect of eddy currents on the rigidity is negligible for the unannealed specimen; for the annealed specimen it is negligible except between $J=1100$ gauss and $J=1500$ gauss, where $[\Delta G/G]_H$ is lower than the observed value, differing therefrom by perhaps 0.025 percent at $J=1300$ gauss.

The corrected values of the decrements and of the changes in the elastic moduli at constant B, for the annealed material in normal magnetization are given in Table I.

THEORETICAL DISCUSSION

According to the domain theory of ferromagnetism,[16] a ferromagnetic crystal consists of a large number of "domains," each of which is permanently magnetized to saturation; the magnetization process for the crystal as a whole consists of a reorientation of the magnetization vectors in the domains. At high fields all the domains are magnetized in the field direction; in the demagnetized state their magnetization vectors are distributed at random among the various stable directions determined by crystalline forces and internal stresses. The transition from the demagnetized condition to technical saturation consists of two stages. In the steep part of the magnetization curve the random distribution changes to one in which most of the domains are magnetized along the stable direction nearest that of the field—this direction itself having meanwhile rotated toward the field. Above the knee of the magnetization curve the magnetization vectors are gradually rotated into the direction of the field. In the first stage, the redistribution occurs partly by a continuous and reversible growth of the more favorably oriented domains at the expense of the less favorably oriented, and partly by a sudden transition of the domain magnetization from a less stable to a more stable orientation, with dissipation of energy.

Stress plays a role similar to that of magnetic field in determining the possible directions of magnetization and the relative stability of these directions; and conversely, any change in the direction of magnetization of a domain (except a reversal) is accompanied by magnetostrictive changes in its dimensions. The application of a

[16] See especially Bozorth and Dillinger, Phys. Rev. **41**, 353 (1932); Becker, Physik. Zeits. **33**, 909 (1932).

tension or shearing stress to an unmagnetized ferromagnetic therefore produces redistributions and rotations similar to those produced by the field, and these give rise to a magnetostrictive component of strain in addition to the strain of purely elastic origin. At very high fields this is no longer true, because the direction of magnetization is that of the field and is unaffected by small stresses. There are two observable results of this magneto-mechanical process, both evident in the data on the elastic constants and decrements of *annealed* iron. First, the ratio of strain to corresponding stress is greater in the demagnetized state, and, in fact, throughout the steep part of the magnetization curve, than at high fields; and second, the energy dissipated per cycle of vibration is greater at low than at high magnetizations.[17]

It remains to explain why the internal stresses present in the *unannealed* material, which increase the magnetic hysteresis, nevertheless decrease the internal friction at zero magnetization. This is not difficult. For there is this important difference between the effect of field and stress: the former brings about a difference of stability between orientations 180 degrees apart and the latter does not. In relatively stress-free iron the stable directions are the six (positive and negative) crystal axes, and stress and field alike can reorient through 90 degrees, partly reversibly and partly irreversibly. In unannealed material, on the other hand, the stable directions are determined by the internal stresses, and are two in number, differing by 180 degrees. Transitions produced by the field are possible and are attended by considerable loss of energy, so that magnetic hysteresis is large. But transitions produced by stress cannot occur, and the only magneto-mechanical process which contributes to the ΔE and ΔG effects is a reversible rotation. As the field is increased, however, opposite orientations begin to differ in energy sufficiently that a small stress, acting on a domain magnetized in the less stable direction, can make this orientation unstable and produce an irreversible transition. Thus at fields sufficiently large to cause considerable difference in stability, yet not large enough to complete the transition process, a high mechanical decrement is observed.

A more detailed explanation of the variation of ferromagnetic internal friction with magnetization must await a more complete analysis of the magnetization process. In connection with the ΔE and ΔG effects, however, certain calculations are of interest.

Kersten's[18] theory of the ΔE effect for material under high internal stress is not applicable to iron, but Akulov's[19] theory for iron under low internal stress should be applicable to the annealed material. The theory contains formulae which describe the variation of E with magnetization at low magnetizations, and for the total change between demagnetization and saturation. The observed variation at low magnetizations is too small to yield any information, and even the highest fields used in this work are still considerably below that necessary for saturation. Nevertheless a comparison between the greatest observed change in E and G and the total change predicted by the theory should at least indicate whether the theory is correct as to order of magnitude.

The total changes in the elastic moduli between demagnetization and saturation in quasi-isotropic polycrystalline iron are given by the formulae

$$\Delta E/E = \tfrac{3}{5}\chi_0\lambda_{100}^2 E/J_\infty^2, \tag{12}$$

and

$$\Delta G/G = (9/5)\chi_0\lambda_{100}^2 G/J_\infty^2, \tag{13}$$

where J_∞ is the saturation magnetization, λ_{100} the longitudinal magnetostriction for a single crystal saturated in the (100) direction, and χ_0 the observed initial susceptibility of the material. The first of these formulae appears in Akulov's paper. The second can be derived therefrom in the following manner: It is assumed that the compressibility is independent of magnetization (since no magneto-mechanical process follows the application of a uniform pressure), and in both the demagnetized and saturated state the material is isotropic. If the compressibility of an isotropic substance is to remain constant then

[17] Cf. also the experiments of Becker and Kornetzki, on torsional stress cycles in annealed iron, Zeits. f. Physik **88**, 634 (1934).

[18] Kersten, Zeits. f. Physik **85**, 708 (1933).

[19] Akulov and Kondorsky, Zeits. f. Physik **78**, 801 (1932); **85**, 661 (1933).

variations in E and G must be related by the formula $\Delta G/G=(3G/E)\Delta E/E$.

Eq. (12) has proved only moderately successful in accounting for the ΔE effect in polycrystalline nickel.[20] In this connection it should be noted that it has never been possible to obtain entirely satisfactory agreement between the measured values of the elastic constants of a polycrystalline material and those calculated from the properties of the constituent crystals. This problem has been thoroughly discussed by Bruggeman.[21] In Akulov's theory, uniform stress is assumed throughout the aggregate of crystals and the strains are averaged. The alternative method, originally used by Voigt,[22] is to assume uniform strain and to average the stresses. If this method of averaging is used in Akulov's theory, the factor 1/5 in Eq. (12) is replaced by $(1/20)(c_{11}-c_{12})^2/G^2$,

TABLE II. *Comparison of theoretical and experimental values of the elastic moduli and of their variation with magnetization.*

		$E\times10^{-11}$	$G\times10^{-11}$	$k\times10^{-11}$	$\frac{\Delta E}{E}\times10^3$	$\frac{\Delta G}{G}\times10^3$
Theoretical	Uniform stress	19.45	7.42	17.3	0.309	0.393
	Uniform strain	22.80	8.90	17.3	0.101	0.128
Experimental		19.98	8.46	10.4	0.17	0.26

where the c's are the elastic constants of the crystals.

The experimental values of Young's modulus and the rigidity, and of their changes with magnetization up to the highest magnetizations attained, are compared with the values predicted by the theory on the alternative assumptions of uniform stress and uniform strain, in Table II. The following values of the constants were used in the calculation: $J_\infty=1710$; $\lambda_{100}=16.2\times10^{-6}$;[23] $\chi_0=28.7$;[24] $c_{11}=2.37\times10^{12}$, $c_{12}=1.41\times10^{12}$, $c_{44}=1.162\times10^{12}$.[25] The bulk modulus k is included to show the unreliability of the methods of averaging even when the question of uniform stress or uniform strain is not involved. The agreement between theory and experiment affords as good a confirmation of the theory as can be expected from measurements on polycrystalline materials. The desirability of measurements on single crystal specimens is obvious.

In conclusion the writers wish to acknowledge their indebtedness to Dr. S. L. Quimby, who suggested the research and followed its progress with helpful counsel and encouragement, and to those who at various times assisted them in the experimental work.

[20] Siegel and Quimby, Phys. Rev. **49**, 663 (1936).
[21] Bruggeman, Zeits. f. Physik **92**, 561 (1934).
[22] Voigt, *Lehrbuch der Kristallphysik*, p. 962.
[23] Average value from measurements of Honda and Mashiyama, Sci. Rep. Tohoku Imp. Univ. **15**, 755 (1926).
[24] Part I of this paper.
[25] From measurements of Goens and Schmid, Naturwiss. **19**, 520 (1931).

Ferromagnetic Anisotropy of Iron Crystals at Various Temperatures*

RAYMOND G. PIETY, *Sloane Physics Laboratory, Yale University, New Haven, Connecticut*

(Received August 14, 1936)

Magnetization curves in important crystallographic directions in small oblate spheroids cut from hydrogen-purified iron crystals show ferromagnetic anisotropy of the same sort as that previously reported for iron of less purity. At room temperature agreement with earlier work is good. At 296°C and at 500°C the principal (fourth-order) term in the anisotropy is larger, at 650°C and 696°C the same term is smaller than in earlier studies, anisotropy not being detected. The subsidiary (sixth-order) term is not accurately determined. The pendulum magnetometer method, which has certain advantages for such purposes over classical methods, was used and results for different spheroids agree well, especially at the higher temperatures.

INTRODUCTION

THE ferromagnetic anisotropy of iron crystals has been measured by Beck,[1] Webster,[2] Honda and Kaya,[3] Honda, Masumoto and Kaya.[4] The last of these studies covered the range in temperature from 5°C to 770°C, the others were confined to room temperature. Beck and Webster measured the torque on disks suspended in the air-gap of an electromagnet, Honda and Kaya measured the flux change through a search coil at the center of which an oblate spheroid was suddenly turned from one azimuth to another in the field of a magnetizing solenoid. Honda, Masumoto and Kaya used one of the same spheroids but changed the method of measurement by leaving the specimen in one azimuth during each cycle of heating and cooling, getting I–H curves at selected temperatures by reversing various currents in the solenoid.

All the data agree in fixing the tetragonal axes, of form <100>, as the directions for easiest magnetization, the trigonal axes, of form <111>, as the directions for most difficult magnetization. The digonal axes, of form <110>, are intermediate between these extremes. The quantitative differences between results from different laboratories are larger than the errors in measurement can easily explain, so that they must be ascribed in part to differences in chemical purity, in mechanical and thermal treatment. Under these conditions it seemed worth while to remeasure the anisotropy in very pure and nearly unstrained iron by a method capable of fair precision and relatively free from systematic errors. Such a method is that developed in this laboratory[5] and first applied here by J. W. Shih[6] to iron-cobalt alloys. It uses an accurately made oblate spheroid carried on a light pendulum at the common center of a magnetizing solenoid and a pair of coils producing a weak but spatially uniform magnetic field gradient. These various windings have a common horizontal axis so that the resultant force on the specimen is also horizontal and can be measured by the deflection of the pendulum. The computed value of I then depends, except for a factor constant for each specimen, only upon the measured deflection of the pendulum and the measured current in the gradient coils. The absolute value of H within the specimen depends upon the measured current in the magnetizing solenoid and upon the value of I, but the difference between values of H along different diameters of the spheroid for the same value of I does not depend upon I, and it is this difference which is most important in the analysis of the results. Points on I–H curves near I_{sat} are particularly important in anisotropy analyses. These points are determined with greatest precision by the new method, with least precision by the older methods.

Several improvements in technique, recently described[7] were devised and tested during the progress of the work reported herein.

* Based on part of a dissertation presented to the Faculty of the Graduate School of Yale University in candidacy for the degree of Doctor of Philosophy.

[1] K. Beck, *Dissertation* (Zürich, 1918); Vierteljahrsschrift der naturforschenden Gesellschaft in Zürich **63**, 116–186 (1918).

[2] W. L. Webster, Proc. Roy. Soc. **A107**, 496–509 (1925).

[3] K. Honda, S. Kaya, Sci. Rep. Tohoku Imp. Univ. [1] **15**, 755–770 (1926).

[4] K. Honda, H. Masumoto, S. Kaya, Sci. Rep. Tohoku Imp. Univ. [1] **17**, 111–130 (1928).

[5] L. W. McKeehan, Rev. Sci. Inst. **5**, 265–268 (1934).

[6] J. W. Shih, Phys. Rev. **46**, 139–142 (1934).

[7] L. W. McKeehan, R. G. Piety, J. D. Kleis, Rev. Sci. Inst. **7**, 494–497 (1936).

Specimens

Comparison of properties in different directions is safest when as many as possible of the important directions are accessible in one specimen. This condition is best met, as is well known, in an oblate spheroid with its equatorial plane of the crystallographic form {110}. If we choose to call this the $(01\bar{1})$ plane we have lying in it the following important axes: [100], [011], [111], $[1\bar{1}\bar{1}]$. Principal effort was therefore expended on spheroids of this sort, $(01\bar{1})$ spheroids. As a check a (001) spheroid was also cut, containing the important axes: [100], [010], [110], $[1\bar{1}0]$.

The iron was very kindly furnished by the Bell Telephone Laboratories in three flat pieces about 3 mm thick and several centimeters in diameter. These were parts of boxes in which P. P. Cioffi had purified small iron specimens by washing them with pure hydrogen at about 1450°C for 18 hours or more. His studies on this process,[8] which produces extreme magnetic and mechanical softness, lead to the expectation that the only nonmetallic impurities remaining in these boxes in measurable amounts are nitrogen, sulphur and phosphorus. The first three of these together should not exceed 0.01 weight percent. Silicon may be in excess of this limit, especially in those parts of the box which are in contact with the alundum support, but these parts were not used here. A provisional limit of 0.03 weight percent silicon is suggested. Manganese and copper may amount to about 0.02 weight percent each. It can be stated with confidence that this iron is more nearly pure Fe than any previously used in anisotropy studies.

The crystals present in the pieces as furnished were of ample size for the pendulum magnetometer. The surface was first etched rather deeply with a mixture of water solutions of HNO_3 and HCl, restrained with C_2H_5OH. By observing reflections from etch planes—here of form {100}—crystals of suitable size and orientation were selected. These were cut out by hand with a jeweler's saw and mounted on an optical goniometer of special design[9] for more accurate observation. The orientation of the <100> axes being thus determined with respect to the surface and edges of the fragment a rectangular iron bar was cut off at such an angle that when the fragment was cemented (with chaser's cement) on the cut in the proper azimuth, the axis of the spheroid to be cut was parallel to the axis of the bar. The blank was now faced off by extremely light slow cuts on a Brown and Sharpe surface grinder with a diamond-dressed wheel running at high speed. It was remounted on the squared end of a new holder and recut in the same way until the thickness was less than 0.5 mm but still somewhat greater than that of the proposed spheroid. It was now ready for an x-ray inspection of its orientation and freedom from distortion by the Laue method, using transmitted radiation so as to get a volume average. If the plane of the blank was found to be more than about 1° from the proposed crystallographic plane a new holder was cut and both sides were reground, otherwise only one side was reground. In either case the thickness was brought down to 0.006 cm over the proposed minor axis of the spheroid and the blank was filed, on its holder, to a circle a little larger than the proposed equatorial section. From this point on, the procedure has been described in the previous paper.[7]

The spheroids were finally given a second x-ray inspection by the Laue method to make sure that no serious distortion had resulted in the last stages of shaping. The criterion was that the Laue spots should be symmetrical ellipses without more than traces of radial asterism.

The applied field intensity, $H+NI$, is very much greater than the effective field intensity H in an oblate spheroid of practicable dimension-ratio (diameter/thickness). It therefore becomes very important to prove that the demagnetizing field, NI, is reasonably uniform in intensity throughout the volume, as the method of measurement supposes. Partly to test this and partly for other more obvious reasons two spheroids having the same orientation but differing in eccentricity were tested over the whole available range in temperature. The equatorial plane in each of these lay within the accuracy of the x-ray analysis (about 1°) parallel to the $(01\bar{1})$ plane. Their characteristics are given in Table I. Under N_{obs} is given the demagnetizing factor necessary to make the effective field sensibly zero up

[8] P. P. Cioffi, Phys. Rev. **39**, 363–367 (1932); **45**, 742 (1934).

[9] L. W. McKeehan, H. J. Hoge, Zeits. f. Krist. **92**, 476–478 (1935).

TABLE I. *Data on spheroids (01$\bar{1}$).*

Designation	Dimension Ratio	Major Axis (cm)	Minor Axis (cm)	Volume 10^{-3}cm^3	Mass (g)	N_{obs}	N_{calc}
P10	10/1	0.318	0.0318	1.768	0.0139	0.912	0.875
P12	12/1	0.307	0.0256	1.234	0.0097	0.710	0.743

to half-saturation in the actual measurements of I and H. This differs appreciably from N_{calc}, the demagnetizing factor for a perfect spheroid of the measured dimensions, but since N_{obs} was not dependent upon the direction along which H was applied it seems reasonable to suppose that the slight departures from ellipticity thus indicated are symmetrical with respect to the minor axis of each spheroid and that any resultant inhomogeneity in H and I throughout the volume is not so great as to make the measured averages misleading. It should be noticed that N_{obs} was greater than N_{calc} in one case, less in the other. A third spheroid cut with its equatorial plane parallel to (001) was tested less completely, but showed directional independence of N_{obs} and fair agreement between N_{obs} and N_{calc}.

Temperatures higher than 700°C could not, with available means, be kept constant enough to make I–H curves precise enough for anisotropy work. The difficulty is that temperature fluctuations change I_{sat} by relatively great amounts at temperatures near the Curie point so that it becomes very hard to take even one complete I–H curve under sufficiently constant conditions. So far as some unsatisfactory experiments indicated, however, there was no detectable anisotropy in magnetization above 700°C in this iron.

At 296°C and at 500°C the differences between I–H curves for the two (01$\bar{1}$) spheroids were so small that single curves were drawn to fit the combined data. At room temperature, 18°C, the data were treated separately.

Fig. 1 shows representative I–H curves and Table II gives areas included between such curves and the two lines $I=I_{sat}$ and $H=0$, together with derived quantities. All curves were carried to saturation, applied fields as high as 1800 oersted being used if necessary. Some of the areas differ slightly from those published in my dissertation. This occurs because all the areas have been redetermined by a more precise method.

TABLE II. *Work needed to magnetize.*

Specimens	°C	10^4 erg. cm^{-3} W_{111}	W_{110}	$W_{100}=K_0$	K_1	K_2
P10	18	16.10	13.16	2.48	+42.7	−17
P12	18	16.59	12.38	1.33	+44.2	+14
P10, 12	296	8.08	6.45	0.65	+23.2	− 8
P10, 12	500	2.56		0.21	+ 9.4	−21
P12	675	0.19			0	0
P12	696	0.31			0	0

ANALYSIS OF RESULTS

In the manner proposed by Gans [10] we suppose that the work needed for isothermal magnetization to saturation, measured by the area defined above, is for any arbitrary direction in an unconstrained cubic crystal given by

$$W_a=K_0+K_1(\alpha_2^2\alpha_3^2+\alpha_3^2\alpha_1^2+\alpha_1^2\alpha_2^2)+K_2(\alpha_1^2\alpha_2^2\alpha_3^2). \quad (1)$$

In this equation α_1, α_2, α_3 are the direction cosines of the chosen direction referred to the three <100> axes, K_0, K_1 and K_2 are not direction dependent and the only assumption made is that an equation of the sixth degree in the cosines is adequate.[11] The symmetry of the crystal annuls all other combinations of α_1, α_2, α_3. For the important directions of form <100>, <110> and <111> Eq. (1) reduces to

$$W_{100}=K_0;\ W_{110}=K_0+K_1/4;\ W_{111}=K_0+K_1/3+K_2/27. \quad (2)$$

These equations are not new. Some authors[12] use instead of K_1 a constant which in this notation is $2K_1$.

It is also possible, as Akulov[12] has shown, to compute I–H curves for particular values of K_1, assuming K_2 to be zero. As might be expected the computed curves agree best with experiment at room temperature and are not good approximations at high temperatures.

---

[10] R. Gans, Physik. Zeits. **33**, 924–928 (1932).

[11] The analysis which follows differs in one important respect from that presented in my dissertation. R. M. Bozorth has pointed out in private discussion that the sixth degree term in Eq. (1) is capable of explaining anisotropy hitherto regarded as completely anomalous. I have therefore used his method of computing the coefficient of this term, and have included it in Tables II and III. I am much indebted to him for the opportunity of using his method of analysis prior to its publication.

[12] Especially N. S. Akulov, Zeits. f. Physik **57**, 249–256 (1929); **67**, 794–807; **69**, 78–99 (1931).

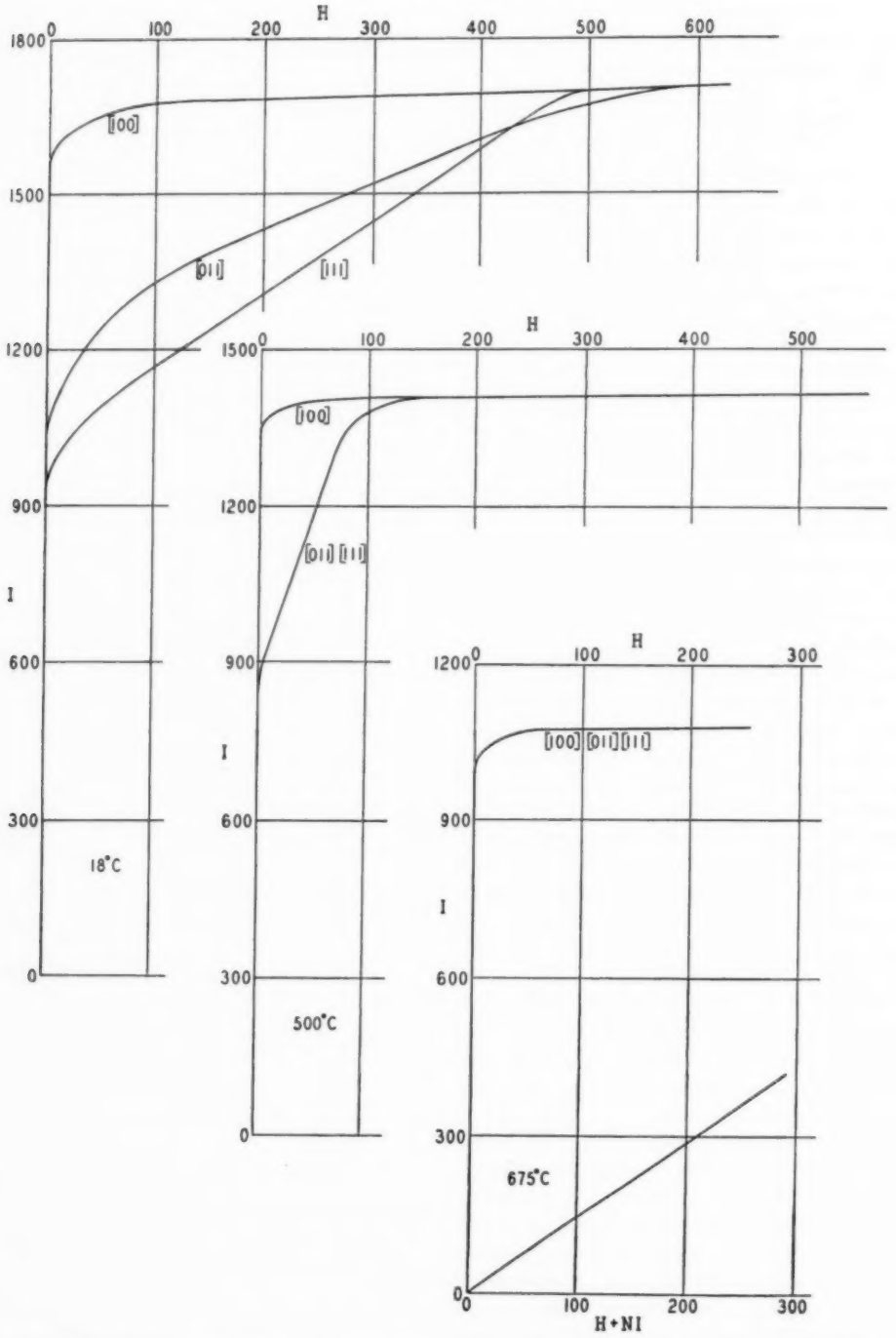

FIG. 1. Magnetization curves for specimen P12 at three temperatures, 18°C, 500°C and 675°C. In the last case the $I-(H+NI)$ curve is also shown (in part) to illustrate the importance of N.

It will be noticed that in Table II the constant K_2 varies widely in absolute value and even in sign. As far as these data go the necessity for the sixth degree correction is apparent only in the fact that W_{111} and W_{110} are indistinguishable at and above 500°. (Precise equality requires $K_2 = -9K_1/4$.) If the values of K_1 are plotted against temperature they fall on a straight line which intersects the line $K_1 = 0$ at 630°C. That K_1 does not actually become negative, however, is suggested by the tabulated values for 675° and 696°C. No permanent effect of heating and cooling the specimens during the measurement was detected at room temperature.

The agreement with the work of Honda, Masumoto and Kaya[4] is very good at room temperature, not so good at the higher temperatures. For comparison, values of K_0, K_1 and K_2 have been computed from their tables. In making this computation it has been assumed as in the present work that the correct demagnetizing factor to be used in getting H is that which makes the I–H curve rise vertically from the origin. This makes it necessary to decrease the areas derived from their tabulated H and I by an amount not exceeding 0.5×10^4 erg. cm^{-3} in any case, and usually much less. Where their maximum value of I does not occur at their maximum value of H it may be concluded that I has been over-corrected for flux through the air surrounding the specimen and the final drop in I has then been ignored in computing the area. Finally, small differences in I_{sat} have been corrected for by multiplying the computed areas by appropriate factors nearly equal to unity. The result of all this is to give a series of areas from which K_0, K_1 and K_2 may be computed as already explained. Table III presents the results. The values of K_1 and K_2, especially the latter, have been made to progress more smoothly up to 700°C by using faired curves for W_{100}, W_{110} and W_{111} to find the differences used in computation. Our values for

TABLE III. *Work needed to magnetize.* Derived from data of Honda, Masumoto and Kaya.

°C	K_0	10^4 erg. cm^{-3} K_1	K_2
5	0.60	+41.3	+14
100	0.27	+35.3	+20
200	0.26	+27.0	+22
300	0.38	+18.9	+19
400	0.015	+11.4	+11
500	0.014	+ 5.4	+ 9
600	0.065	+ 2.6	− 1
700	0.14	+ 1.0	− 2
750	0.21	+ 1.7	−12
770	0.33	+ 0.8	− 4

K_1 at 296°C and 500°C are considerably higher than those at 300°C and 500°C in Table III. It will be noticed that K_0 seems to rise a very little as the Curie point is approached in both sets of experiments. No one would be likely to suggest a linear drop in K_1 with increasing temperature from the values given in Table III. An exponential drop like that suggested for nickel by Akulov[13] in a very recent paper is a fair approximation above 200°, but not below.

In conclusion it can be stated that the purest iron we could procure is both qualitatively and quantitatively much like the iron used by Honda and his co-workers. It seems, however, to retain its anisotropy better at 300°C and 500°C and to lose it more suddenly in the neighborhood of 600°C. The sixth-order term in the anisotropy equation is relatively unimportant except at temperatures above 500°C where the fourth-order term falls to negligible values.

The author wishes to thank Professor L. W. McKeehan for suggesting the problem, for advice and encouragement during the progress of the work, and for analyzing the tables of Honda, Masumoto and Kaya. He also thanks J. D. Kleis for valuable assistance in manipulations and measurements.

[13] N. S. Akulov, Zeits. f. Physik **100**, 197–202 (1936).

Ferromagnetic Anisotropy of Nickel-Iron Crystals at Various Temperatures*

J. D. KLEIS, *Sloane Physics Laboratory, Yale University, New Haven, Connecticut*

(Received August 14, 1936)

Magnetization curves in important crystallographic directions at temperatures up to near the Curie points in small oblate spheroids cut from annealed face-centered cubic nickel-iron alloys with from 10 to 50 percent iron show a change in ferromagnetic anisotropy at about 24 percent iron. With less than this amount of iron the order of increasing difficulty for magnetization to saturation is, as in nickel at room temperature: <111>, <110>, <100>. With more than this amount of iron the order is <100>, <111>, <110>. A small decrease in the apparent demagnetizing factor of the spheroids with rising temperature was noted.

STUDIES of ferromagnetic anisotropy in solid solution alloys have already shown that the direction for easiest magnetization may change from one important crystallographic axis to another at room temperature as the composition changes. The first case of this sort to be reported occurs in the face-centered cubic alloys of nickel and iron. Lichtenberger[1] examined single crystal rods with their lengths parallel to a number of different directions in the crystal lattice. The number of specimens available in each composition was not large and the cross sections were not strictly uniform, so that the data scatter rather badly. He concluded that the directions for easiest magnetization changed from the form <111> to the form <100> as the iron content increased through 29 percent.

The second and third cases have been reported by Shih.[2] In body-centered iron-cobalt alloys, which he studied in this laboratory, he found the direction for easiest magnetization changed from the form <100> to the form <111> as the cobalt content increased through 42 percent. In face-centered nickel-cobalt alloys he found two transitions, from <111> to <100> at about 5 percent cobalt, from <100> to <111> at about 19.5 percent cobalt.

Lichtenberger's result has received partial confirmation from work by Burgers and Snoek,[3] who conclude from a change in the ferromagnetic anisotropy of rolled polycrystalline sheets that the critical composition in the nickel-iron series occurs at 34 percent iron. In view of the uncertainties already noted in Lichtenberger's work a more careful examination of a few alloys in the critical range was undertaken here before the notes by Burgers and Snoek appeared and was continued with even greater interest thereafter.

The ferromagnetic anisotropy of nickel has been studied over a wide range in temperature by Honda, Masumoto and Shirakawa.[4] Although they did not comment upon the fact, their tables and curves show that the direction for easiest magnetization changes in this face-centered cubic metal from <111> at room temperature to <100> at temperatures of 200°C and higher. The technique of measurement with the pendulum magnetometer, which has been described elsewhere,[5] made it relatively easy to extend the range of investigation on nickel-iron alloys from room temperature nearly to the Curie points, which in this series are not higher than 570°C.

SPECIMENS

Nickel-iron alloys of selected compositions were kindly furnished by the Bell Telephone Laboratories in the form of small rods. The original castings, rods about 2 cm in diameter, had been homogenized at high temperatures and rendered still more uniform in composition in the process of working. The pieces furnished were similar in quality to those used by Buckley,

* Based on part of a dissertation presented to the Faculty of the Graduate School of Yale University in candidacy for the degree of Doctor of Philosophy.

[1] F. Lichtenberger, Ann. d. Physik **15**, 45–71 (1932).

[2] J. W. Shih, Phys. Rev. **46**, 139–142 (1934); **50**, 376–379 (1936).

[3] W. G. Burgers and J. L. Snoek, Zeits. f. Metallkunde **27**, 158–160 (1935); J. L. Snoek, Nature **137**, 423 (1936).

[4] K. Honda, H. Masumoto and Y. Shirakawa, Sci. Rep. Tohoku Imp. Univ. [1] **24**, 391–410 (1935).

[5] L. W. McKeehan, Rev. Sci. Inst. **5**, 265–268 (1934); L. W. McKeehan, R. G. Piety, J. D. Kleis, Rev. Sci. Inst. **7**, 494–497 (1936).

TABLE I. *Data on spheroids (01$\bar{1}$). α is angle between rotation axis of spheroid and nearest axis of form <100>; β is angle between rotation axis and the plane (100); N is the demagnetizing factor necessary to make initial portion of I–H curves at room temperature coincide with the line H=0.*

Designation	Iron percent*	Nickel percent*	Diameter cm	Thickness cm	Volume cm³	$\alpha°$ $\beta°$	N
K10	10	90	0.3128	0.0284	0.001462	44 2	0.818
K30	30	70	0.3104	0.0259	0.001304	40 0	0.84
K35	35	65	0.3090	0.0256	0.001295	45 4	0.761
K50	50	50	0.3070	0.0276	0.001350	43 2	0.82

* By synthesis. Analysis for nickel and iron requires more material than could be spared. Castings made in the same way, however, always gave nickel and iron within one percent of the intended values.

McKeehan and Cioffi[6] in studies of magnetization and magnetostriction in the nickel-iron alloys in the permalloy range. Impurities, by analysis, are principally sulphur, silicon and cobalt, amounting to about 0.15 percent.

Crystals a few millimeters in diameter and a few centimeters long were grown in magnesium oxide crucibles by the slow solidification process using a furnace similar to one described by Quimby.[7] After breaking away the crucible as carefully as possible the castings were annealed in hydrogen at atmospheric pressure at about 1100°C for one hour and slowly cooled. Laue photographs show but a small amount of residual lattice distortion.

The method of selecting crystals for study was similar to that described by R. G. Piety[8] in connection with iron crystals. The only important difference lay in the occurrence of etch planes of forms {111} and {100} instead of {100} alone. Etching is more difficult, also, *aqua regia* being necessary for the more resistant compositions. After selection the process of forming an oblate spheroid in the desired orientation was that already described.[5] It was not generally feasible to cut the spheroid exactly as proposed, with the (01$\bar{1}$) plane equatorial, and a method of describing the actual orientation of the equatorial plane is therefore necessary. Let α be the angle between the rotation axis of the spheroid, which should be [01$\bar{1}$] and the nearest axis of form <100>, which must be either [010] or [00$\bar{1}$], and let β be the angle between the rotation axis and the plane (100). In a perfectly cut spheroid $\alpha=45°$ and $\beta=0$. It turns out that deviations of several degrees from the ideal values have a very small effect upon anisotropy in the equatorial plane because this passes through maxima and minima of the energy surface. The results can be corrected for such errors in cutting, as Shih[5] has pointed out in his latest paper, but this has not seemed necessary here.

Table I gives information about the spheroids used in the present work. The demagnetizing factor N is that observed to be necessary to make the initial portion of I–H curves at room temperature coincide with the line $H=0$.

TABLE II. *Work needed to magnetize.*

Specimen	°C	10^4 erg·cm^{-3} $W_{110}-W_{100}$	$W_{111}-W_{100}$	K_1	K_2
K10	14	−0.18	−0.33	−0.72	− 2.4
	150	−0.08	−0.15	−0.32	− 1.2
	300	0	−0.03	0	− 0.8
K30	14	0.17	0.17	0.68	− 1.5
	150	0.06	0.06	0.24	− 0.5
	300	0	0	0	0
	454	0	0	0	0
K35	14	0.36	0.22	1.44	− 7.0
	150	0.32	0.25	1.28	− 4.8
	298	0.24	0.20	0.96	− 3.2
	490	0.12	0.12	0.48	− 1.1
K50	14	0.83	0.43	3.32	−18.3
	150	0.69	0.52	2.76	−10.8
	300	0.46	0.36	1.84	− 6.8

RESULTS

The method of measurement and the reduction of observations to the form of I–H curves have already been described.[5] The results are presented in Figs. 1 to 4 and energy differences and energy coefficients are collected in Table II. For the method of computation and the meaning of symbols see the preceding paper by R. G. Piety.[8] The most unexpected result is that the direction for easiest magnetization changes not from <111> to <100> as iron increases beyond a critical amount, but from <11$\bar{1}$> to <110>. The transition occurs as nearly as these data can indicate at 24 percent iron, as is seen from Fig. 5. This is to be compared with Lichtenberger's 29 percent and Burger and Snoek's 34 percent. (All compositions herein are in weight percent.)

In the case of specimen K10, which is most nearly like nickel in its anisotropy, Akulov's

[6] O. E. Buckley and L. W. McKeehan, Phys. Rev. **26**, 261–273 (1925); L. W. McKeehan, P. P. Cioffi, Phys. Rev. **28**, 146–157 (1926).
[7] S. L. Quimby, Phys. Rev. **39**, 345–353 (1932).
[8] R. G. Piety, Phys. Rev. **50**, 1173–1177 (1936).

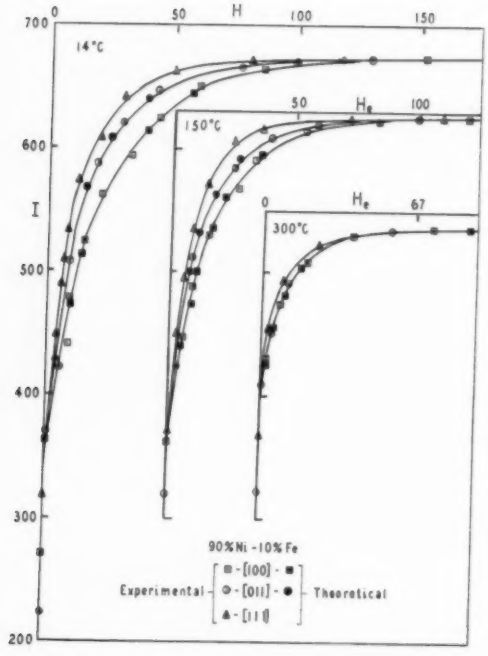

FIG. 1. *I–H* curves for specimen K10.

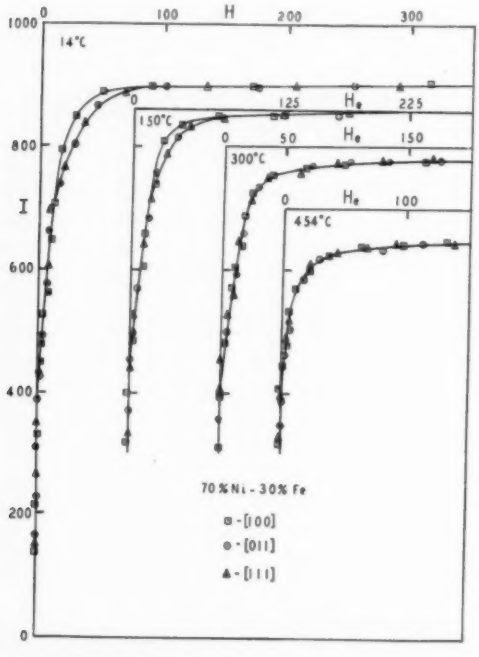

FIG. 2. *I–H* curves for specimen K30.

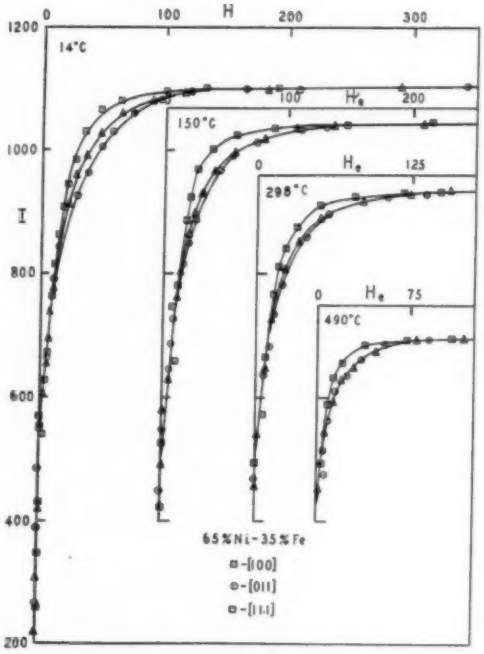

FIG. 3. *I–H* curves for specimen K35.

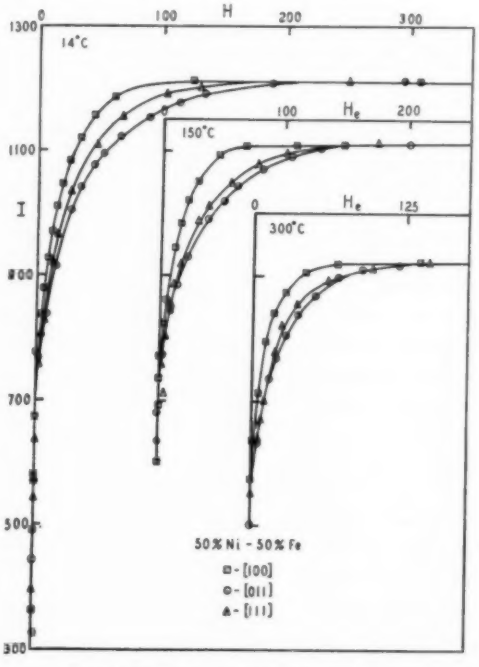

FIG. 4. *I–H* curves for specimen K50.

method[9] of computing I–H curves, which neglects K_2, is reasonably successful. Assuming I–H along [111] as a basis, several points have been computed for I–H along [011] and [100]. These are plotted on Fig. 1 and fall near the curves actually found.

One other peculiarity should be mentioned. As the temperature rises above room temperature the value of N which is apparently best at room temperature does not make the I–H curve rise vertically from the origin. A smaller value of N is called for. The variation of N with temperature for a typical case is as follows:

Specimen	Temperature	N
K35	14°C	0.761
	150	0.759
	298	0.754
	490	0.749

This variation makes W_0 uncertain, so that its values have not been presented in Table II. No satisfactory explanation for this behavior presents itself. It may be due to a variation in the thickness of a surface film magnetically very different from the interior. If so, the nature of this film and the factors upon which its thickness depends remain mysterious. A film of nonmagnetic material, everywhere of the same thickness, and thicker at higher temperatures, would change the apparent value of N in the observed manner.

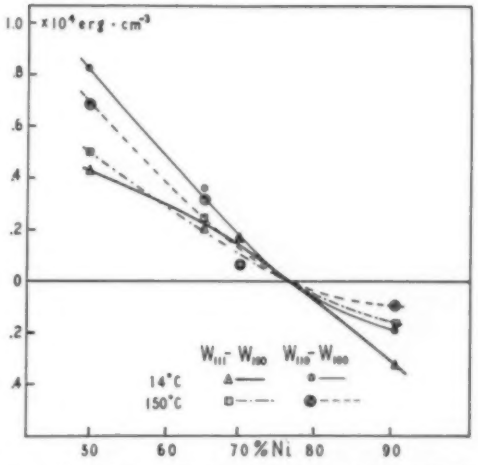

FIG. 5. Variation of energy differences with composition.

It is with great pleasure that the author takes this opportunity to thank Professor L. W. McKeehan, who suggested this problem, for his advice and aid throughout the entire investigation.

[9] N. S. Akulov, Zeits. f. Physik **67**, 794–807; **69**, 78–99 (1931).

DECEMBER 15, 1936 PHYSICAL REVIEW VOLUME 50

Electrical Resistivity of Single Crystals of Some Dilute Solid Solutions in Zinc

HAROLD E. WAY, *Physical Laboratory, University of Iowa, Iowa City, Iowa*

(Received September 15, 1936)

Sets of single crystals were grown of binary alloys consisting of dilute solid solutions of Cd, Cu, Ag, Au, Ni and Fe, each in zinc. Electrical resistivities at 20°C are expressed in terms of principal resistivities, ρ_0 and ρ_{90}, these values coming from the usual $\cos^2\theta$ (θ=orientation) plot of measured resistivities of a set of crystals. The resistance increases in a given series of alloys with increasing concentration, in a nonlinear fashion. The initial increase in resistivity (above that of pure zinc) in micro ohm-cm per atomic percent of solute is: Cd 0.94, Cu 0.4, Ag 1.1, Au 2.3, Ni 51.0, Fe 300.0. This is correlated with the nearness of the solute metal to zinc in the periodic table. The ratio of principal resistivities is slightly higher than that for the zinc crystal. Temperature coefficients decrease in such a way that Mathiessen's rule is satisfied (with a maximum deviation of 4 percent) for all the alloys.

INTRODUCTION

THE resistivity and temperature coefficient of resistivity of dilute solid solutions of one metal in another have been studied frequently and the type of result to be expected is known at least qualitatively. Such studies in the past are apparently lacking for metals crystallizing in the nonregular system, probably due to the difficulty of obtaining polycrystalline samples with grains oriented completely at random. It seemed worth while, therefore, to make a somewhat systematic study of single crystal samples, not only for the above reason, but because of the more fundamental nature of the approach using single crystals. Zinc was chosen as the solvent material. Binary alloys were made, each of zinc and some

TABLE I. *Designation of alloys and concentration of the solute material.*

Designation of alloys	Percent by weight			Atomic percent		
Cd[1]	0.125			0.0721		
Cu[1, 2, 3]	.125	0.250	0.500	.1285	0.2571	0.5142
Ag[1, 2, 3]	.125	.250	.500	.07575	.1515	.3030
Au[1, 2, 3]	.125	.250	.500	.04144	.08289	.1657
Fe[1, 2]	.005	.010		.00585	.01171	
Ni[1, 2]	.005	.010		.00557	.01114	
FeNi	.005 (Fe) +.005 (Ni)			.00585 (Fe) +.00557 (Ni)		

one other metal in various concentrations. The resistivity and the temperature coefficient of resistivity from 0° to 40°C were measured for sets of single crystals of the unalloyed zinc and the various alloys.

PREPARATION OF CRYSTALS

The zinc used was "Bunker Hill," a commercial zinc of exceedingly high purity, obtained from Platt Brothers and Company in the form of a single 50 lb. slab. By spectroscopic comparison with a test sample[1] of known purity it was estimated that the B. H. zinc contained: Cd, appreciably less than 0.0008 percent; Pb, slightly less than 0.0047 percent; Cu, slightly less than 0.002 percent; Ni, Au and Ag, none detected; Fe, appreciably more than 0.0004 percent (estimated by resistivity data, as shown later, to be about 0.002 percent), altogether certainly less than 0.01 percent impurity.

Binary alloys were made of zinc and certain selected concentrations of each of the following: Copper, silver, gold, iron, nickel and cadmium. See Table I. The method of preparation was usually to add to a known weight of the molten zinc the appropriate weight of the second constituent. Occasionally the most concentrated alloy (of a series) was first prepared and the lesser concentrations made by dilutions from it. Where both methods were used to prepare a certain concentration a good check on their equality was obtained in terms of the resistivity measurements. A single ternary alloy (Fe Ni in Table I) was prepared by mixing in equal proportions by weight the 0.01 percent Fe and 0.01 percent Ni alloys, thus giving an alloy of 0.005 percent by weight of each.

For the pure zinc and for each alloy a set of single crystals (from four to six) was grown with orientations evenly distributed within the possible range of orientation,[2] 0°–90°. The crystals were prepared as described by Cinnamon[3] and in the same furnace. They were about 10 centimeters long and with trapezoidal cross-sectional area of about 0.65 cm². For the pure zinc Cinnamon's "growth conditions" were substantiated, but for each alloy it was found necessary to determine appropriate growth conditions, which were toward higher gradients for about the same rates of growth used by Cinnamon. Keeping the ratio of gradient to rate of growth constant solely by decreasing the rate of growth did not produce single crystals. Moreover, it was found that for the alloys of lowest concentration single crystals were grown more easily than for pure zinc, both because the width of the range of successful growth was increased and also because "optical mosaics,"[4] were easily prevented. This was particularly noticeable with the smallest concentration (0.005 percent) of iron. With increasing concentrations growth conditions became more and more critical and it was not found possible to prepare a full set of crystals for greater concentrations than those given in Table I.[5] Also in most cases the highest concentrations were close to the probable limit of solid solubility.

MEASUREMENT OF RESISTIVITY AND TEMPERATURE COEFFICIENT

The resistance of a known length (about 8 cm) of the crystal was measured by comparison with a standard resistance using the customary potentiometer set-up. The crystal was placed in a wooden box and allowed to come to a constant temperature (room temperature, about 25°C) before resistivity measurements were made. The temperature was measured to 0.01 degree C by three thermocouples placed at each end and in the middle below the crystal. The distance between the potential contacts on the crystal was measured with a micrometer microscope and the cross-sectional area of the same part was meas-

[1] A. W. Hanson, Phys. Rev. **45**, 324 (1934), Table I.

[2] The angle between the length of the specimen and the vertical axis of the crystal.

[3] C. A. Cinnamon, Rev. Sci. Inst. **5**, 187 (1934).

[4] H. K. Schilling, Physics **5**, 1 (1934) and **6**, 111 (1935); W. J. Poppy, Phys. Rev. **46**, 815 (1934).

[5] With the exception of Cd, for which only one concentration was tried since a more thorough investigation would duplicate work known to be in progress elsewhere.

ured by the immersion method described by Hanson.[6] Resistivity at 20°C was computed from these measurements and the temperature coefficient.

The temperature coefficient was measured by placing the crystal in a large, sealed, brass tube which was immersed in water. The temperature was again measured by means of three spaced thermocouples, the leads being brought out through a small brass tube joined on the larger one and projecting above the surface of the bath. Resistivity measurements were made at three temperatures. For the first, ice was placed in the water surrounding the tube and stirred with a mechanical stirrer until the temperature of the crystal was constant as measured by the three thermocouples. Water at about 40°C was then substituted for the ice water and when equilibrium conditions were reached a second measurement was made. The third measurement was made after the crystal had come to, and remained for some time at, the temperature of the room. A resistance-temperature plot of these three points lay, within experimental error, along a straight line. The temperature coefficients of at least three crystals of each concentration were measured. The results for each concentration appeared constant within possible experimental error, there being indicated in particular no evident dependence on orientation.

Results and Discussion

The resistivities of the Bunker Hill zinc and the zinc-copper alloys are shown in Fig. 1, each plotted point representing one single-crystal specimen. Similar sets of curves were obtained for the other alloys. From these curves were read the values of the two principal resistivities, ρ_0 and ρ_{90}, parallel and perpendicular, respectively, to the vertical axis of the crystal. Table II includes these principals resistivities and other data for the B.H. zinc and the various alloys.

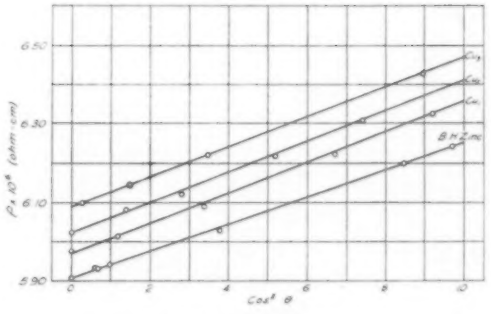

FIG. 1. Resistivity at 20°C as function of square of cosine of orientation θ for B.H. zinc and series of alloys containing copper. $Cu_1 = 0.129$, $Cu_2 = 0.257$, $Cu_4 = 0.514$ atomic percent.

It will be noted that the ratio ρ_0/ρ_{90} is appreciably increased (about 0.4 percent) by the smallest addition of any solute and is not changed very much by further additions. The behavior of the difference $\rho_0 - \rho_{90}$ is not so regular. The first addition causes an increase (3 percent to 8 percent) but there is a further increase in some cases as additional alloying material is added. The writer thinks it exceedingly probable that all the alloys are solid solutions with the solute atoms replacing zinc atoms in an entirely random fashion. The initial changes in ρ_0/ρ_{90} and $\rho_0 - \rho_{90}$ show that the crystal is slightly altered, supposedly in lattice dimensions, from the true zinc lattice by the addition of small amounts of solute atoms. The disturbance due to further additions is not so marked, as witness the constancy of ρ_0/ρ_{90}. The alloy designated Fe Ni was prepared to check the additiveness of the resistance change. Thus considering ρ_{90}, the addition of 0.005 percent Fe (Fe_1) and 0.005 percent Ni (Ni_1) cause an increase in resistance of 0.168 and 0.038, respectively, summing to 0.206. For the Fe Ni the resistance change is 0.209 or the total effect of two additions is equal to the sum of the individual effects within experimental error.

TABLE II. *Principal resistivities in micro ohm-cm, their ratio and their difference, all at 20°C.*

Material	ρ_0	ρ_{90}	ρ_0/ρ_{90}	$\rho_0 - \rho_{90}$
B.H. Zn	6.253	5.902	1.059	0.351
Cd_1	6.345	5.970	1.063	.375
Cu_1	6.352	5.966	1.065	.386
Cu_2	6.406	6.023	1.064	.383
Cu_4	6.466	6.086	1.062	.380
Ag_1	6.348	5.986	1.060	.362
Ag_2	6.425	6.062	1.060	.363
Ag_4	6.598	6.212	1.062	.386
Au_1	6.357	5.988	1.062	.369
Au_2	6.436	6.072	1.060	.364
Au_4	6.608	6.219	1.063	.389
Fe_1	6.450	6.070	1.063	.380
Fe_2	6.590	6.203	1.062	.387
Ni_1	6.301	5.940	1.061	.361
Ni_2	6.336	5.954	1.064	.382
Fe Ni	6.490	6.111	1.062	.379

[6] A. W. Hanson, Rev. Sci. Inst. **7**, 109 (1936).

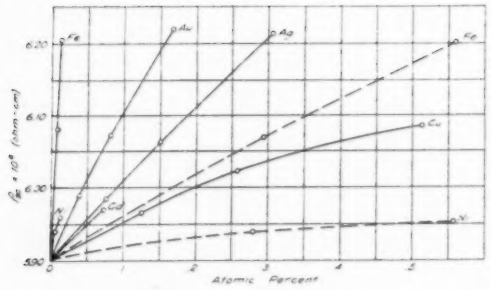

FIG. 2. Principal resistivity ρ_{90} at 20°C, as a function of atomic percent of solute. For dashed curves multiply abscissa scale by 2×10^{-2}.

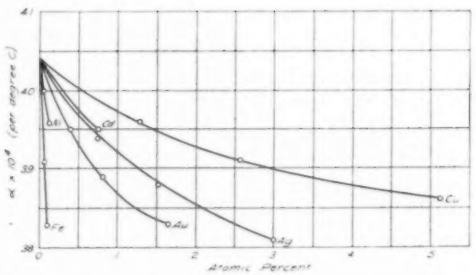

FIG. 3. Temperature coefficient of resistivity as function of atomic percent of solute.

Although it seemed unlikely that any type of "ordered alloy"[7] would be produced with these small concentrations of solute, this possibility was tested. Since the attainment of an ordered condition would depend on the rate at which the alloys were cooled after solidification it might be that the cooling during growth of the crystals was too fast.[8] A subsequent anneal and even slower cooling would test this point. Therefore, twenty-seven representative crystals had their resistivities remeasured several weeks after the first measurement.[9] Twenty-four of these not only checked the first measurement but also showed no change in resistivity after two anneals, one at 200°C for 72 hours and the other at 400°C for 36 hours. The cooling to room temperature after these anneals was extended over about 48 hours. To test the reverse point, i.e., whether an ordered condition had been attained during growth of the crystals, seven crystals were kept at 400°C for 24 hours and then quenched to 0°C by dropping them into iced water. No departure from the original resistivity occurred. It, therefore, seems likely that a simple random arrangement is stable both for slow and fast cooling.

TABLE III. *Relative effects of added elements.*

Material	Group	Initial $\Delta\rho$ per atomic percent	Reciprocal* effect
Cd	2	0.94	
Zn	2		
Cu	1	.4	0.29
Ag	1	1.1	.5
Au	1	2.3	.9
Ni	8C	51.0	
Fe	8A	300.0	

* The figures in the last column are taken from Norbury's work and show the reciprocal effect, i.e., one atomic percent of zinc in copper produces an increase in resistivity of 0.29×10^{-6} ohm-cm etc. Norbury's work was done with polycrystalline specimens.

In Fig. 2 the resistivities are shown as a function of atomic percent of the solute materials. Only one of the principal resistivities, ρ_{90}, is plotted but the other, ρ_0, would yield a similar plot. The relation between resistivity and concentration is definitely not linear, the effect becoming less for equal additions as the concentration increases. Nor do these curves fit a relation of the type proposed by Guertler:[10] $R=R_0+K(C-C^2)$ in which R_0 is the resistance of the pure solvent, K a constant, and C the concentration of the solute. The curves in fact bend towards the concentration axis more rapidly than the above relation predicts. The relative effects of the different added elements can be compared by computing (from the lowest concentration in each case) the increase in resistivity per atomic percent. This has been done and the results are arranged in Table III, the materials being listed in order of closeness to zinc in the periodic table, both horizontally and vertically. The data in the table could also be plotted to give a diagram similar to some given by Norbury[11] for various solutes in a single solvent metal.

The relation between temperature coefficient

[7] W. L. Bragg and E. J. Williams, Proc. Roy. Soc. **A151**, 540 (1935).

[8] Actually the crystals were left in the furnace for a period of fifteen hours while cooling from the melting point to room temperature.

[9] First measurements were made directly after the growth of the crystals. The remeasurement was made, first as a check that no change had occurred due to a very slow relaxation at room temperature, and second to guard against possible changes due to accidental strains.

[10] W. M. Guertler, J. Inst. Metals **6**, 135 (1911).

[11] A. L. Norbury, Trans. Faraday Soc. **16**, 570 (1921) and J. Inst. Metals **33**, 92 (1925).

and atomic percent of solute is given in Fig. 3. The decrease in temperature coefficient with increased concentration and with the nature of the solute is very similar to the increase of resistivity previously discussed. The relation between these two effects is, however, brought out much better in Table IV, in which a test is made of Mathiessen's rule. This rule states that $\alpha_m\rho_m=\alpha\rho$[12] in which α_m and ρ_m are temperature coefficient and resistivity, respectively, of an alloy, computed solely by "law of mixtures" and α and ρ are the actual measured quantities for the same alloy. For all the above described work, α_m and ρ_m are practically exactly the values for pure zinc, because of the use of such small concentrations. Therefore, for Mathiessen's rule to be obeyed the product $\alpha\rho$ for each alloy should be constant and equal to the value for the solvent material. The constancy of the last column in Table IV shows excellent agreement with this rule. The maximum variation from the value for the solvent (2206) is about 4 percent.

The resistivity of the B.H. zinc was appreciably higher than the resistivity determined by Poppy[4] for two samples of zinc of approximately the same grade of purity. Moreover, Poppy's two samples differed somewhat, which he attributed to a difference in the iron content. It seemed worth while therefore to check up on this point. A set of crystals was grown of the material of lower resistivity used by Poppy (designated E.W.B.) and their resistivities were determined. Spectrographic comparisons were made between this material, the B.H. zinc and the test sample[13] previously referred to.

TABLE IV. *Principal resistivity, ρ_{20}, at 0°C, temperature coefficient and their product.*

Material	ρ_{20} at 0°C	α	$\alpha\rho_{20}$
B.H. Zn	5.461	0.00404	2206
Cd_1	5.533	.00395	2185
Cu_1	5.514	.00397	2189
Cu_2	5.601	.00390	2184
Cu_3	5.648	.00386	2180
Ag_1	5.575	.00392	2185
Ag_2	5.674	.00385	2184
Ag_3	5.768	.00381	2198
Au_1	5.568	.00394	2194
Au_2	5.673	.00387	2195
Au_3	5.777	.00383	2213
Fe_1	5.630	.00391	2201
Fe_2	5.762	.00383	2207
Ni_1	5.500	.00400	2200
Ni_2	5.517	.00396	2185
Fe Ni	5.676	.00383	2174

[12] See Hume-Rothery, *The Metallic State*, p. 51, but note that his α's are temperature coefficients of conductivity. However, the similar relation for temperature coefficient of resistance is easily derived. It may also be shown that the relation $\alpha_m\rho_m=\alpha\rho$ follows by considering that the resistivity of the alloy is made up of two parts, one having the resistivity and temperature coefficient of pure zinc (for these small concentrations) and the other being an additional resistance unaffected by temperature.

TABLE V. *Comparison of various samples of zinc.*

	ρ_0	ρ_{90}	ρ_0/ρ_{90}	Fe lines detected
E.W.B. (Poppy)	6.161	5.842	1.055	none
E.W.B. (Way)	6.170	5.842	1.056	none
E.W.R. (Poppy)	6.218	5.882	1.057	18[13]
B.H. (Way)	6.253	5.902	1.058	37

The results are summarized in Table V. It will be noted that the resistivities are qualitatively consistent with the difference in iron content. Moreover, the E.W.B. is practically iron-free. In the light of the present work the other impurities[14] in any of the zincs are believed to have negligible effect on the resistivity. Also, the E.W.B. sample agrees very nicely in ρ_{90} with the determination of ρ_{90} for spectroscopically pure zinc,[15] ($\rho_{90}=5.847\times10^{-6}$ ohm-cm). Assuming thus that the values for E.W.B. are correct for 100 percent zinc, it is possible to extrapolate backwards from the iron resistivity-concentration curve (Fig. 2) and determine the actual iron content of the B.H. zinc. The result is that the B.H. zinc contained 0.0019 percent Fe.

Professor E. P. T. Tyndall's kind suggestions and cooperation in the development of this research problem are deeply appreciated by the author.

[13] None of Poppy's material of higher resistivity (designated E.W.R.) was available. The test sample was said by Hanson (reference 1) to contain about the same amount of iron as the E.W.R. and it was used therefore in the spectrographic comparison.

[14] Lead should perhaps be excepted since it is an impurity in all the samples of Table V. However, a second sample of B.H. zinc, obtained after the completion of this work and differing from the first only in the fact that it had less lead (2 lead lines, as against 8 in first sample), had precisely the same resistivity.

[15] E. P. T. Tyndall and A. G. Hoyem, Phys. Rev. **38**, 820 (1931). The value quoted above is corrected to a density of 7.13 g/cm³, the authors having computed cross section of crystals by weighing a measured length and using a density of 7.15 g/cm³.

LETTERS TO THE EDITOR

Prompt publication of brief reports of important discoveries in physics may be secured by addressing them to this department. Closing dates for this department are, for the first issue of the month, the eighteenth of the preceding month, for the second issue, the third of the month. The Board of Editors does not hold itself responsible for the opinions expressed by the correspondents.

Communications should not in general exceed 600 words in length.

Pressure Broadening of the HCN Band Lines and Intermolecular Forces

Some time ago, in an investigation of the fine structure of the photographic infrared HCN bands it was found by Herzberg and Spinks[1] that the strong line broadening observed is due to an exceptionally large pressure broadening. It was further concluded that it is connected with a strong interaction of the HCN molecules at rather large distances and not due to ordinary Lorentz collision broadening. Recently however Cornell and Watson[2] reinvestigated the HCN pressure broadening coming to rather different conclusions, namely that (1) the broadening is not particularly large but even slightly less than that found by Becker for the first harmonic band of HCl so that (2) dispersion forces are the predominating broadening influence and there is no evidence for molecular association. Also the dependence of the line width on the rotational quantum number found qualitatively by Herzberg and Spinks was not confirmed by the measurements of Cornell and Watson.

In order to investigate these differences one of us (W. W. W.) has photometered the spectrograms of Herzberg and Spinks. The photograms were then measured by both of us. Also, to shed further light on the causes of pressure broadening of the lines of infrared absorption bands of various molecules, we have photometered spectrograms taken by Herzberg and Spinks of the 10,370A band of C_2H_2,[3] the 11,977A band of HCl[4] and the 11,300A band of CH_4, all taken with atmospheric pressure of absorbing gas in a column 400 cm long. The slit width of the spectrograph was 0.05 mm for all the plates and the dispersion varied between 5.11A and 5.35A per mm. The photometer traces have been made with the 40:1 magnification of the registering Koch-Goos microphotometer.

Unfortunately, because these spectrograms were taken with the first Agfa plates sensitive to the 10,000A–12,000A region they have a rather heavy background fog, the lack of much contrast between absorption lines and continuous spectrum rendering the photometering difficult. Also there is no possibility of correcting the traces for any nonlinearity of the emulsion characteristic. Line widths for consecutive lines in a band do fluctuate considerably in an irregular manner, therefore, and in particular one cannot be too certain about the measured relative widths of weaker as compared to stronger lines. Nevertheless, in view of the fact that all apparatus conditions remained constant except for the pressure variation for the several HCN spectrograms, the comparison of these roughly quantitative half-widths is of some significance.

The average half-widths of all the *P*-branch lines measured in the 10,384A HCN band are approximately 0.57, 0.84, 0.94 and 1.37 cm^{-1} at vapor pressures of 130, 265, 360 and 650 mm, respectively. This is a somewhat more rapid rate of increase of line width with pressure than that found by Cornell and Watson. The explanation of this difference is undoubtedly the narrower apparatus line width in the case of Herzberg and Spinks' spectrograms. There is evidence here for the nonadditivity of apparatus line width and pressure broadening width in the range of low gas pressures (under 1 atmosphere). Because of this the linearity of the dependence of line width and pressure is not as certain as was believed by Cornell and Watson. For an accurate investigation of pressure broadening the apparatus width should be small compared to the width to be measured, a condition which is not always easy to fulfill.

The width of the HCN lines for atmospheric pressure, including apparatus width is about 1.5 cm^{-1} from Herzberg and Spinks' plates as compared to Cornell and Watson's 1.35 cm^{-1}.

From Herzberg and Spinks' plates we obtain a half-width of about 0.5–0.6 cm^{-1} for the absorption lines of CH_4, C_2H_2 and HCl at atmospheric pressure. Possibly the HCl line width is a trifle higher than that of the others. Considering that most of this line width is apparatus width, it is seen that the HCN line width is in fact very considerably larger than those of CH_4, C_2H_2 and HCl in agreement with Herzberg and Spinks' original qualitative estimates. Thus also Herzberg and Spinks' original conclusion is confirmed that there are particularly large van der Waals forces in the case of HCN which perturb the absorbing molecules.

As to the dependence of the broadening on the rotational quantum number the qualitative observation of Herzberg and Spinks of a decrease in line width for high J values could not definitely be confirmed by the quantitative measurements though they seem to indicate a slightly less broadening for both lines of high and low J value. Much more accurate measurements are necessary to decide this point.

G. HERZBERG
J. W. T. SPINKS
W. W. WATSON

Department of Physics,
University of Saskatchewan.
Sloane Physics Laboratory,
Yale University,
November 23, 1936.

[1] G. Herzberg and J. W. T. Spinks, Proc. Roy. Soc. **147**, 434 (1934).
[2] S. D. Cornell and W. W. Watson, Phys. Rev. **50**, 279 (1936).
[3] G. Herzberg and J. W. T. Spinks, Zeits. f. Physik **91**, 386 (1934).
[4] G. Herzberg and J. W. T. Spinks, Zeits. f. Physik **89**, 474 (1934).

The Electroresistive Effect and a Rectifying Property of Carborundum Crystals

The generalized Ohm's law

$$E_i = \sum_{k=1}^{3} R_{ik} I_k, \quad i = 1, 2, 3 \tag{1}$$

does not adequately predict the actual current-voltage equilibrium states, particularly in the group of crystals which rectify alternating currents. Experiments performed by the writer show that the electrical resistances of single, homogeneous crystals of carborundum and zincite vary rapidly with the applied voltage even under isothermal conditions and when the voltage gradients are uniform. The isothermal variation of the electrical resistance with the applied voltage will be called the "electroresistive effect."

When the effects of the applied magnetic fields can be neglected, the current-voltage equilibrium may be approximated by the power series

$$E_i = \sum_{k=1}^{3} R_{ik} I_k + \sum_{k=1}^{3}\sum_{l=1}^{3} R_{ikl} I_k E_l + \sum_{k=1}^{3}\sum_{l=1}^{3}\sum_{m=1}^{3} R_{iklm} I_k E_l E_m$$

$$+ \sum_{k=1}^{3}\sum_{l=1}^{3}\sum_{m=1}^{3}\sum_{n=1}^{3} R_{iklmn} I_k E_l E_m E_n + \cdots (i = 1, 2, 3), \tag{2}$$

where I_i and E_i $(i=1, 2, 3)$ are the cartesian components of the current and electric field intensity and R_{ik}, R_{ikl}, R_{iklm}, etc., are components of second, third, fourth, etc. order tensors. These tensor components are in general functions of temperature and pressure. The terms containing R_{ikl} and R_{iklm} are, respectively, linear and quadratic in the components of E. They describe, respectively, the linear and quadratic electroresistive effects. The term current-voltage equilibrium is here used since in many cases several hours are required for the current to approach a steady value following a change in the voltage.

The number of distinct or independent "electroresistive constants" R_{ikl}, R_{iklm}, etc., in any crystal class can be deduced from Neumann's hypothesis. Thus in the form of carborundum which belongs to the symmetry group C_{6v} (Wyckoff's notation) or $A_z{}^6E_x$ (Voigt's notation) the electroresistive constants for the linear and quadratic effects were found to be:

Linear case	*Quadratic case*
R_{333}; $R_{311}=R_{322}$;	R_{3333}; $R_{1111}=R_{2222}$; $R_{3113}=R_{3223}$;
$R_{131}=R_{232}$; $R_{113}=R_{223}$	$R_{3311}=R_{3322}$; $R_{3211}=-R_{3222}=R_{3112}$;
(4 constants) (3a)	$2R_{2112}=R_{1111}-R_{2211}$; $R_{1122}=R_{2211}$;
	$R_{1213}=R_{2113}$; $R_{1313}=R_{2323}$;
	$R_{1133}=R_{2233}$.
	(10 constants) (3b)

All other constants are zero. The integers 1, 2, 3 pertain, respectively, to the X, Y and Z axes. The Z axis is chosen as the axis of sixfold symmetry and the plane $x=0$ as one of the vertical planes of symmetry.

Assume that in (2) terms involving higher powers than the second of the components of E are negligible and suppose that a uniform voltage gradient E_3 is established in a rectangular carborundum crystal such that $E_1=E_2=0$. Since $R_{11}=R_{22}\neq R_{33}$ and $R_{ij}=0$ where $i\neq j$, the component of current along Z should obey the equation

$$E_3 = R_{33} I_3 + R_{333} I_3 E_3 + R_{3333} I_3 E_3{}^2. \tag{4}$$

The resistance of the specimen along the Z direction is given by

$$R_3 = E_3/I_3 = R_{33} + R_{333} E_3 + R_{3333} E_3{}^2. \tag{5}$$

If the sign of E_3 is reversed, the magnitude of R_3 changes by an amount depending upon $R_{333}E_3$, the term which originates from the linear electroresistive effect. Hence this theory affords an explanation of the rectifying property of carborundum crystals. The portion of rectification due to a point and plane is, of course, not taken into account by this phenomenological theory. Any term involving odd powers of E in (2) will affect the rectifying property.

Carborundum crystals were found, as predicted, to rectify currents caused to flow along Z by applying uniform voltage gradients $E_3 \sin \omega t$. Preliminary experiments indicate that in the case of voltage gradients which are greater than one volt/cm higher order tensors than the fourth are needed.

A later paper will contain a more complete account of the theory together with a list of the linear and quadratic constants for the various crystal classes and experimental data upon the intricate electroresistive phenomena in large, single crystals of carborundum and zincite.

HAROLD OSTERBERG

University of Wisconsin,
November 24, 1936.

Exchange Forces Between Elementary Particles

The Fermi theory of β-decay introduces an interaction term into the Hamiltonian of the elementary particles: proton, neutron, electron and neutrino. A consequence of this theory is the existence of an exchange force between protons and neutrons; this force is caused by the emission of light particles by one heavy particle and the absorption of these by the other particle, both processes occurring in one elementary act. It has been pointed out that only an interaction term containing the derivatives of the wave functions can give rise to a force of sufficient magnitude between heavy particles. The interaction term has the form

$$\Omega = g \cdot \alpha^{\rho\sigma\gamma\tau} \Psi^{\rho\alpha}(x) \Phi^{\sigma}(x) \cdot (\partial/\partial x)^m \psi^{\gamma\alpha}(x) \cdot (\partial/\partial x)^n \varphi^{\tau}(x) + \text{conj.} \tag{1}$$

Ψ, Φ, ψ, φ are the wave functions of the proton, neutron, electron, and neutrino, respectively; x stands for the four space-time coordinates; the Greek letters are the spin indices; $(\partial/\partial x)^m$ is a differential operator of degree m with respect to space and time; $\alpha^{\rho\sigma\gamma\tau}$ is a combination of Dirac matrices, making the term relativistically invariant; such a combination can be constructed in several ways.

It can be shown that the interaction energy (1) also gives rise to exchange forces between other elementary particles. Let us consider a neutron at a place I and an electron at a place II. Let the neutron decay into a proton, an electron,

and a neutrino. In a subsequent process the proton can be transmuted back into a neutron at place II by absorbing the neutrino emitted and the initial electron, leaving the electron emitted in the first process at place I. The net result is that the initial neutron and electron have changed places. The two processes occurring in one elementary act produce an exchange force analogous to that between heavy particles.

In general, exchange forces between two elementary particles A and B occur whenever B can be created by decay of A, or A by a decay of B. Such forces are possible between: proton and neutron; proton and positive electron; proton and neutrino; neutron and neutrino; neutron and negative electron; neutrino and electron (positive and negative).

To get the last two of these exchange forces we must assume the existence of a transmutation of an electron into a neutrino or *vice versa* with the simultaneous creation of a pair of heavy particles. It should be possible for a positive electron, for instance, to decay into a neutrino with emission of a proton and a neutron. It is easily shown that this kind of process is a consequence of the interaction term (1). Since we assume that the wave functions of all elementary particles follow the Dirac equation, we are forced to consider all negative energy states as occupied in the empty space. Then every interaction energy effecting a transmutation causes also a creation of two particles, since a transmutation of a particle in a negative state into another particle in a positive state must be considered as a creation of two particles.

A rough evaluation gives the following result: the potential of the exchange force between two elementary particles a and b in the distance r is of the following order of magnitude:

$$J^{ab}(r)\sim\epsilon g_0^2\left(\frac{\hbar c}{\epsilon}\Big/r\right)^{5+2(m+n-S_a-S_b)}\left(\frac{cp_a}{\epsilon}\right)^{2S_a}\left(\frac{cp_b}{\epsilon}\right)^{2S_b}.$$

Here ϵ is the mean energy of β-ray particles and g_0 is a dimensionless constant $g_0=g\cdot(\epsilon/\hbar c)^{2+m+n}\epsilon^{-1}\sim 5\times10^{-12}$ the order of magnitude of which is independent of the values assumed for m and n. S_a and S_b are the degrees of differentiation of the wave function of a and b in (1); p_a and p_b are the corresponding momenta. We assume as usual that this expression only holds for distances $r>d$, d being of nuclear dimensions, and that $J^{ab}(r)\sim J^{ab}(d)$ for $r<d$. Now $m=1$, $n=2$ is the only combination which can account for the observed proton-neutron force and for the asymmetrical position of the maximum in the intensity curve of β-ray spectra. We obtain for the exchange forces at zero distances (in volts) between

proton-neutron: $\sim10^8$ neutron-neg. electron: $\sim0.5\times10^4$
proton-electron: $\sim0.5\times10^4$ neutron-neutrino: $\sim2\times10^{-1}$
proton-neutrino: $\sim2\times10^{-1}$ electron-neutrino: $\sim10^{-5}$

(The energies of the light particles are taken as about 10^6 volts.) Thus the exchange forces, except in the case of two heavy particles, are too weak to be observed.

V. F. Weisskopf

Institute for Theoretical Physics,
Copenhagen, Denmark,
November 5, 1936.

On the Hard Component of Cosmic Rays

In a former paper[1] it was shown that the depth-ionization curve of cosmic rays measured 80–240 m below sea level can easily be represented by an exponential function. The newer measurements of Weischedel[2] confirm this in principle. Therefore it is of interest to examine what range distribution is obtained by extrapolation of this exponential behavior of the curve due to rays coming in from all directions. Then:

$$J=J_0\,e^{-\mu x}. \tag{1}$$

The intensity curve for rays descending vertically through the atmosphere is converted by the transformation[3] $\psi=J-xdJ/dx$ to

$$\psi=J_0\,e^{-\mu x}(1+\mu x) \tag{2}$$

and the range distribution $\rho=-d\psi/dx$ will be finally

$$\rho(x)dx=\mu^2x\,e^{-\mu x}dx. \tag{3}$$

For the average range one obtains

$$\bar{R}=2/\mu \tag{4}$$

and for the most frequent range

$$R_m=1/\mu. \tag{5}$$

Fig. 1 gives these relations with the value $\mu=1.889\times10^{-2}$ per meter of water, formerly obtained[1] for the hard component. A range phenomenon, curve II, is quite apparent after transformation to vertical incidence. The range distribution curve III is very like a Maxwellian one. A direct conclusion concerning the energy distribution is not yet available. In particular one cannot suppose a loss of energy exclusively produced by primary ionization, for this would require such small energy values of the incident rays that in the equatorial belt only a fraction could reach the earth's surface through the blocking effect of the earth's magnetic field. And then, contrary to all observations there should also result a strong latitude effect of this component.

It was pointed out by Lenz,[4] that the different "elementary functions" (exponential function, Gold's integral, Kulenkampff-function) on which the analysis formerly was

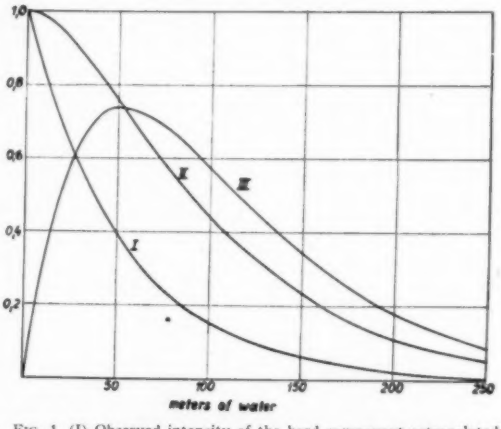

Fig. 1. (I) Observed intensity of the hard component extrapolated into low depths. (II) Intensity after transformation to vertical incidence. (III) Range distribution.

based, show a maximum after being multiplied with x. Thereupon he bases a method of analysis, forming the "deformed curve" $x \cdot J(x)$ by multiplying the measured values J by the absorbing depth. In the case of a band structure of the radiation this curve includes various maxima and so may be decomposed into deformed elementary functions. By the relations above mentioned a totally new significance is given to this proceeding. This is seen at once by writing Eq. (3) in the form

$$\rho(x) = \mu^2 x J(x)/J_0. \qquad (6)$$

This is exactly the deformed intensity curve. In the case of an exponential depth-ionization curve (or one representable by a sum of exponential functions) it is seen that the method of Lenz[4] signifies physically a decomposition into different range groups. In the depth-ionization curve—the part above 80 m—may be considered to be formed by two exponential functions. Thus the application of the Lenz-method means a decomposition into two range groups, the harder one we have treated above more rigorously.

With great pleasure I acknowledge my indebtedness to Professor Dr. E. L. da Fonseca Costa for his helpful advice.

B. GROSS

Instituto Nacional de Technologia
do Ministerio do Trabalho,
Rio de Janeiro,
October 28, 1936.

[1] B. Gross, Zeits. f. Physik **92**, 755 (1934).
[2] F. Weischedel, Zeits. f. Physik **101**, 732 (1936).
[3] B. Gross, Zeits. f. Physik **83**, 217 (1933).
[4] E. Lenz, Zeits. f. Physik **83**, 193 (1933).

Direct Effects of Particular Solar Eruptions on Terrestrial Phenomena

In this journal previously, I[1] called attention to the occurrence of widespread sudden fadeouts of high frequency radio transmission, and suggested that study be undertaken to determine possible relations of the effect to solar, earth-current, terrestrial magnetic, and other phenomena. This led to effective cooperation in such study, which has been rewarded by the observation of simultaneous happenings on numerous occasions in each of the four fields named. The work has corroborated the hypothesis advanced in the 1935 article that a radio fadeout is due to a sudden solar emanation lasting only a few minutes.

In the two years from July 1934 to June 1936 there were 94 reported radio fadeouts; 39 of these are known to have been accompanied by a simultaneous visible eruption on the sun; 15 of them are known to have been accompanied by simultaneous fluctuations of terrestrial magnetic elements; and for 4 of them simultaneous fluctuations of earth currents have been reported. The fluctuations in terrestrial magnetism and earth currents are abrupt pulses of about the same duration as the radio fadeouts, not similar to the fluctuations characteristic of magnetic storms. In none of these fields has there been an opportunity to make a comprehensive study of world-wide data, and there is good reason to suppose that the number of coincidences has been greater than is known at this time.

The occurrence of visible effects in the causative solar eruptions is probably more or less fortuitous. The cause of the terrestrial phenomena is a sudden outburst of highly penetrating solar radiation of ultraviolet (i.e., ultra-visible) frequencies. This produces sudden ionization of the atmosphere below (or possibly in) the E-layer of the ionosphere, where the air density is great enough to insure numerous collisions of moving ions and hence rapid absorption of the radio wave energy during the few minutes it lasts. The degree of absorption is less for the higher radiofrequencies than for lower ones. The ionization density of the F_2-layer is not affected. With the sudden ionization below (or in) the E-layer, sudden changes occur in the currents flowing there, currents which are the cause of a certain part of the earth's magnetism. The changes in these currents directly cause the special magnetic fluctuations which are observed, and also inductively produce changes in earth currents.

The absorbing ionization and the radio fadeouts are produced on the illuminated side of the earth and do not occur on the dark side. They are most intense where the sun's radiation is perpendicular (i.e., around noon and at low latitudes). This distribution is also true of the terrestrial magnetic variations, and probably of the earth current and other phenomena if any. The effect is thus quite distinct from ordinary magnetically disturbed periods, sometimes called magnetic storms, whose effects are much more marked at high than low latitudes. Ordinary magnetic disturbances and the special effect here reported have no necessary connection with each other, except for a general tendency to occur more frequently when sunspots are more numerous. Ordinary magnetic disturbances occur simultaneously with lowered ionization density in the F_2-layer, as shown by my colleagues.[2] Thus magnetic storms and the special magnetic effects simultaneous with radio fadeouts are associated with different levels in the atmosphere. It is believed that certain rare observations reported in the past by astronomers, of magnetic pulses simultaneous with visible solar effects, such as the coincidence reported by Professor C. A. Young as occurring on August 3 and 5, 1872, were the special type of magnetic effect now found to be associated with radio fadeouts.

The radio fadeouts reached an extraordinary climax in May and June, 1936. In the three months, April to June, there were 54 reported fadeouts, more than the total number reported previously (in the two years the phenomenon has been known). Then in the following three months, July to September, there were only 16 fadeouts. Of the 54 fadeouts in April to June, 21 were accompanied by solar eruptions, and 10 were accompanied by the special magnetic effect. As there is reason to suppose that radio fadeouts (and the associated magnetic and other phenomena) are caused by one type of ultraviolet (i.e., ultra-visible) solar radiation, and that ordinary magnetic disturbances, auroras, etc., are caused by a solar emanation of different character, these phenomena present powerful means of keeping track of two different and very interesting types of events on and in the sun. They deal with emanations which are not only invisible but probably do not reach the earth's surface at all.

J. H. DELLINGER

National Bureau of Standards,
November 24, 1936.

[1] Dellinger, Phys. Rev. **48**, 705 (1935).
[2] Kirby, Gilliland, Judson, Smith, Reymer, Phys. Rev. **48**, 849 (1935) and **50**, 258 (1936).

Investigations of the Deuteron-Deuteron Reaction

Last year we reported some results on the yield of neutrons produced by bombarding different targets containing deuterium, beryllium or lithium with ion beams of deuterium, which were accelerated by a 400 kv transformer rectifier outfit.[1]

In continuation of these investigations we have studied in more detail the neutrons and the protons produced by bombarding different deuterium targets with fast deuterons ("D-D" reaction). This case is especially interesting on account of the apparently very high yield[2] (about 10^{-6}) and because these neutrons have all the same energy[2, 3] (about 2×10^6 volts).

The accelerating voltage is measured both with an improved generating voltmeter and with a high resistance and microammeter.[4] The current carried by the magnetically analyzed ions is recorded by a current integrator. In some experiments the molecular ions (mass 4) from a low voltage arc are used. Voltages applied between the Faraday cage containing the target and adjacent diaphragms and an auxiliary small magnetic field prevent any effects from secondary electrons. The protons produced in the D-D reaction penetrate thin aluminum windows and are counted by means of an ionization chamber, linear amplifier and a scale-of-eight thyratron counter.[5] The neutrons are recorded with the same apparatus, by the use of a paraffin-lined chamber for the fast neutrons, a boron-lined chamber for slow neutrons, or a simple air chamber (for calculating absolute values). The yield of the neutrons was compared with that of neutrons from a 15 mg radium-beryllium source replacing the target. A comparison of the radium source with a radon beryllium source of the same gamma-ray activity showed the neutron activity to be the same within 10 percent.[6]

As solid targets of D-compounds did not last long under bombardment, we used liquid D_3PO_4 for longer series of measurements, which proved to be very satisfactory.

The results obtained so far are the following:

1. The excitation function of the "thick" targets between 40 and 100 kv is the same for protons and neutrons as found before by Alexopoulos[2] and agrees approximately with that given by Oliphant, Harteck and Rutherford. The relative yield is 1 : 4.4 : 8 for 100, 200 and 300 kv. No resonance has been found between 40 and 100 kv although measurements were made every 5 kv.

2. The increase of slow neutrons absorbable by 0.6 mm of cadmium with increasing thicknesses of paraffin cylinders surrounding the source and the ionization chamber has been measured, both for the D-D neutrons and the Ra-Be neutrons. The two such curves coincide above 5 cm of paraffin. For smaller thicknesses relatively more slow neutrons are observed from the Ra-Be. This effect is probably due to the large number of relatively slow neutrons originating from the Ra-Be source.

3. The yield of Cd neutrons produced in 7.5 cm of paraffin from a D_3PO_4 target bombarded by 1μA D-ions at 100 kv is the same as that of our 15 mC Ra-Be source; but a slight change of the geometry of the neutron source inside the paraffin has an appreciable effect. The yield of fast neutrons for 1μA D-ions at 100 kv is the same as that of 44 mC Ra-Be. The main reason for this difference is the higher initial proportion of relatively slow neutrons from Ra-Be which give no measurable recoil protons in the paraffin-lined chamber.

4. The total number of protons produced in D_3PO_4, measured at 90° from the direction of the ion beam, is 7.10^4/sec. at 100 kv and 1μA on the assumption of isotropic emission in all directions. Actually appreciably more neutrons were found *in* the direction of the beam than at 90°, in accordance with recent reports from the Cavendish laboratory.[9] Multiplying the yield by 50/3, the ratio of the number of electrons in D_3PO_4 and the number of D-atoms, one gets as yield for the D-D reaction 1 proton for 6.10^6 impinging deuterons. Solid targets—$(ND_4)_2SO_4$, ND_4Cl, KOD—give within 20 percent the same yield after correcting for the stopping power in the same way as for the D_3PO_4 target. Oliphant, Harteck and Rutherford estimate the yield to be of the order of magnitude of 1 in 10 at 100 kv.

5. When using the simple air chamber for counting fast neutrons and taking the cross section of 1.8×10^{-24} cm^2 given by Dunning[7] for the scattering of neutrons from Rn-Be, we find about half as many neutrons as we found protons before,—under the assumption that every recoil O or N atom from scattered neutrons produces a count in our ionization chamber.[8] So it is safe to say that the two reactions produced by the D-D collision give approximately the same yield.

We wish to express our appreciation to the Rockefeller Foundation for a special grant and to Messrs. Y. Beers, J. Giarratana and M. H. Kanner for valuable help in some of the experiments.

R. LADENBURG
R. B. ROBERTS

Palmer Physical Laboratory,
Princeton, New Jersey,
November 12, 1936.

[1] Ladenburg, Roberts and Sampson, Phys. Rev. **48**, 467 (1935).
[2] See Oliphant, Harteck and Lord Rutherford, Proc. Roy. Soc. **144**, 612 (1934); Alexopoulos, Helv. Acta **8**, 513 and 601 (1935).
[3] Dee, Proc. Roy. Soc. **A148**, 623 (1935); Bonner and Brubaker, Phys. Rev. **49**, 19 (1936).
[4] Hafstad, Heydenburg and Tuve, Phys. Rev. **50**, 504 (1936).
[5] This device was constructed for these experiments by J. Giarratana who developed a special Wynn-Williams circuit, adapted for RCA thyratrons.
[6] Our method for mixing Ra and Be is described by Erbacher and Philipp, Zeits. f. physik. Chemie **A176**, 175 (1936) who used a similar method.
[7] Dunning, Phys. Rev. **45**, 586 (1934).
[8] Alexopoulos estimates (reference 2, p. 513) the number of neutrons produced by 1μA and 100 kv to be 4.10^6 per second, i.e., about 50 times as big as we find, and without correcting for the stopping power of his target he gives as yield 1 neutron per 1.6×10^6 deuterons of 100 kv. The yield given by Kikuchi, Aoki and Husimi (Proc. Phys. Math. Soc. Japan **18**, 122, 299 (1936)) does approximately agree with our value, but the percentage of D-ions in their beam is only estimated and not measured by magnetic analysis.
[9] Kempton, Brown and Maasdorp, Proc. Roy. Soc. **157**, 372 (1936).

Erratum: On the Binding of Neutrons and Protons

J. B. FISK, *Society of Fellows, Harvard University,*
L. I. SCHIFF, *Massachusetts Institute of Technology,*
W. SHOCKLEY, *Bell Telephone Laboratories*

(Phys. Rev. **50**, 1090 (1936))

In the preparation of the manuscript for the above Letter to the Editor the wrong drawing was used in making

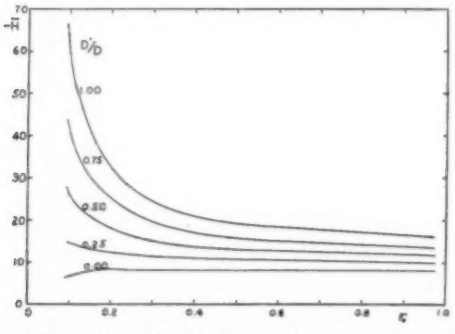

FIG. 1. The variational binding energy of H_3 *vs.* the "effective radius of interaction," r_0, for several values of D'/D, the ratio of depths of neutron-neutron to neutron-proton holes.

the cut for Fig. 1. The authors are not responsible for this error and the correct cut for their figure is shown here.

AMERICAN INSTITUTE OF PHYSICS
Publications Department

Erratum: Precision Cosmic-Ray Measurements up to Within a Percent or Two of the Top of the Atmosphere

R. A. MILLIKAN, H. V. NEHER AND S. K. HAYNES, *Norman Bridge Laboratory of Physics, Pasadena, California*

(Phys. Rev. **50**, 992 (1936))

To correct an error in the checking of proofs in this office the word **"proton,"** last line page 995 and line 23 second column, page 998 should read **"photon."**

AMERICAN INSTITUTE OF PHYSICS
Publications Department

The β-Ray Spectrum of Li^8

According to a recent communication of Rumbaugh and Hafstad[1] there is a discrepancy between the mass of Li^8 as obtained from the reaction $Li^7+H^2 \rightarrow Li^8+H^1$ and the reaction $Li^8 \rightarrow Be^8+e^-$. From the former they conclude that $Li^8 > 8.022(8)$ and from the latter[2] $Li^8 = 8.019(3) \pm 0.001$. This discrepancy can be explained by supposing that the β-ray spectrum of Li^8 gives rise to an excited Be^8 nucleus so that the reaction reads $Li^8 \rightarrow (Be^8)' + e^-$ with the understanding that $(Be^8)'$, Be^8 stand, respectively, for excited and normal nuclei, having an energy difference $(Be^8)' - Be^8 > 0.0035 \pm 0.001$ mass units. In order that this explanation should work it is necessary to suppose that the disintegration of Li^8 into Be^8+e^- is ruled out by a selection rule and that there is available an excited level of Be^8 at least 0.002 mass units above the normal which is not ruled out. According to the calculations of Feenberg and Wigner[3] there exists a ^1D level of Be^8 at approximately 0.003 mass units above the normal ^1S level. The $(Be^8)'$ nucleus is in the ^1D level according to this explanation. On the other hand their calculations for Li^8 give a P level which is built on doublets in neutrons and on doublets in protons. The observed effect can, therefore, be explained by supposing that the normal level of Li^8 is a $^3P_2$ because then[4] the selection rule $\Delta i = 0, \pm 1$ for total angular momentum will make the transition to $(Be^8)'$ possible and will rule out that to Be^8.

An explanation could be attempted by supposing that Li^8 is left in an excited state $(Li^8)'$ after the ejection of the proton. It could then emit a γ-ray, become a normal Li^8 and finally emit a β-ray. The energy of $(Li^8)'$ would have to be about 4 or 3 Mev above that of Li^8. It should be more probable that the protons will be emitted with the full available energy and that the Li^8 nucleus will be left in its normal state. One could suppose that Li^8 cannot be formed on account of a selection rule. The likely selection rules are those of the orbital, spin and total angular momenta as well as of parity.[5] The normal state of Li^7 is[3] an odd $^2P_{3/2}$ state, that of H^2 an even $^3S_1$ and that of Li^8 an even ^2P. It is possible to have conservation of parity[5] and of the total orbital and spin angular momenta as well as of their resultant by assuming the angular momentum of relative motion to be (a) zero initially and one finally or else (b) one initially and zero finally. Case (a) is more probable than (b) because the incident deuterons have a lower energy than the protons which could be emitted with the formation of Li^8. The fact that the final angular momentum of the proton is one and not zero does not decrease the probability of the reaction by a large factor because the addition of $\hbar^2/Mr^2$ to the potential barrier amounts to about 5 Mev at a distance of 4×10^{-13} cm. There is, thus, no special reason why the formation of Li^8 in its normal state should not occur. It appears, therefore, that the formation of an excited Be^8 is a more natural explanation. Gamma-rays of about 3 Mev energy should accompany the reaction on the present view.

E. WIGNER
Princeton University,
G. BREIT
University of Wisconsin,
November 22, 1936.

[1] L. H. Rumbaugh and L. R. Hafstad, Phys. Rev. **50**, 681 (1936).
[2] H. R. Crane, L. A. Delsasso, W. A. Fowler, C. C. Lauritsen, Phys. Rev. **47**, 971 (1935).
[3] E. Feenberg and E. Wigner, Phys. Rev. in press.
[4] G. Gamow and E. Teller, Phys. Rev. **49**, 895 (1936).
[5] E. Wigner, *Gruppentheorie* (Vieweg & Son, 1931). See p. 287.

Author Index to Volume 50

References with (A) are to abstracts of papers presented at meetings of the Physical Society. References with (L) are to Letters to the Editor.

Abramson, Harold A. (see Moyer, Laurence S.)—398(A)

Adams, Norman I., Jr. (see Kovarik, Alois F.)—99(L)

Ahearn, A. J. Effect of temperature, degree of thoriation and breakdown on field currents from tungsten and thoriated tungsten—238

——— Field currents and thermionic currents from thoriated tungsten and pure tungsten—398(A)

Aiya, S. V. Chandrashekhar. Continuous spectrum observed in Raman scattering—260(L)

Amaldi, E. and E. Fermi. On the absorption and the diffusion of slow neutrons—899

——— **and E. Segrè.** Behavior of slow neutrons at different temperatures—571(L)

Anderson, Carl D. and Seth H. Neddermeyer. Cloud chamber observations of cosmic rays at 4300 meters elevation and near sea-level—263

Anderson, Paul A. Continuous measurement of changes in the electronic work function during the fusion of tin—386(A)

——— (see Sampson, Milo B.)—385(A)

Anslow, Gladys A. and Madeleine DeBlois Watson. Total ionization of nitrogen by electron collisions—162

Anthony, R. L. Collisions of alpha-particles with sulphur nuclei—395(A)

——— Collisions of alpha-particles with sulphur nuclei—726

Aten, A. H. W., Jr. (see Urey, H. C.)—575(L)

Atkinson, R. d'E. (see Menzel, D. H.)—872(A)

Bacher, R. F. and D. H. Tomboulian. In^{115}, hyperfine structure deviations and electric quadrupole moment—1096(A)

Bachman, C. H. (see Fox, G. W.)—939

Bainbridge, Kenneth T. (see Jordan, Edward B.)—98(L)

——— **and Edward B. Jordan.** Mass spectrum analysis. 1. The mass spectrograph. 2. The existence of isobars of adjacent elements—282

Baker, Richard F. (see Plesset, Milton S.)—399(A)

Ballantine, R. J. (see Emeleus, K. G.)—672(L)

Barker, E. F. (see Migeotte, M. V.)—418

Bardeen, John. Electron exchange in the theory of metals—1098(A)

Barnett, S. J. New determination of gyromagnetic ratios for ferromagnetic substances—390(A)

——— Two gyromagnetic models (with demonstrations)—390(A)

Bartlett, J. H., Jr., J. J. Gibbons, Jr. and R. E. Watson. Magnetic moment of the Li^7 nucleus. II—315

Bayley, D. S., B. R. Curtis, E. R. Gaerttner and S. Goudsmit. Diffusion of slow neutrons—461

Beams, J. W. (see Snoddy, L. B.)—469, 1094(A)

——— **and F. B. Haynes.** Separation of isotopes by centrifuging—491(L)

Bearden, J. A. (see Kanne, W. R.)—935

——— (see Roseberry, H. H.)—204

Beeck, Otto. Accommodation coefficient and molar heat of various hydrocarbon molecules—387(A)

Bennett, Ralph D. (see Heyworth, D.)—400(A), 589

Beth, Richard A. Mechanical detection and measurement of the angular momentum of light—115

Bethe, H. A. Attempt to calculate the number of energy levels of a heavy nucleus—332

——— Nuclear radius and many-body problem—977, 1100(A)

——— **and E. J. Konopinski.** Transmutation functions and the many-body model of the nucleus—1100(A)

——— **and M. E. Rose.** On magnetic moments of light nuclei in the individual particle model—1100(A)

Bilinsky, S. (see Zener, Clarence)—101, 489(L)

Blanchet, Louis A. G. Polarity changes of elements when in various combinations of couples to form a cell—391(A)

Bleakney, Walker (see Sampson, Milo B.)—382(L), 456, 732

———, **John P. Blewett, Rubby Sherr and Roman Smoluchowski.** Mass-spectrograph analysis of beryllium—545

Blewett, John P. (see Bleakney, Walker)—545

——— **and Ernest J. Jones.** Filament sources of positive ions—464

Bloch, F. On the continuous γ-radiation accompanying the β-decay—272

——— On the magnetic scattering of neutrons—259(L)

——— **and G. Gamow.** On the probability of γ-ray emission—260(L)

Bollman, V. L. (see DuMond, Jesse W. M.)—97(L), 383(L), 524

Bonner, T. W. and W. M. Brubaker. Disintegration of nitrogen by fast neutrons—781(L)

——— **and W. M. Brubaker.** Disintegration of beryllium, boron and carbon by deuterons—308

Bothe, W. and H. Maier-Leibnitz. Photon theory and Compton effect—187(L)

Bouckaert, L. P., R. Smoluchowski and E. Wigner. Theory of Brillouin zones and symmetry properties of wave functions in crystals—58

Bourgin, D. G. New relativity—864

——— One-dimensional problem in the new relativity—400(A)

——— Sound absorption and velocity in mixtures—355

Bowen, I. S., R. A. Millikan, S. A. Korff and H. V. Neher. Latitude effect in cosmic rays at altitudes up to 29,000 feet—579

Boyce, J. C. (see Menzel, D. H.)—872(A)

Bozorth, R. M. Determination of ferromagnetic anisotropy in single crystals and in polycrystalline sheets—1076

Brady, James J. and Joseph H. Rochel, S.J. Photoelectric sensitization of potassium by means of hydrogen—870(L)

Brandt, W. H. Quartet states in diatomic molecules intermediate between cases *a* and *b*—778
Brasefield, Charles J. (see Pollard, Ernest)—890, 1095(A)
——— **and Ernest Pollard.** Transmutation of sulphur by Th C′ alpha-particles—296
Breit, G. (see Wigner, E.)—1191(L)
———, **E. U. Condon and R. D. Present.** Theory of scattering of protons by protons—825
——— **and E. Feenberg.** Possibility of the same form of specific interaction for all nuclear particles—850
Brode, R. B., H. G. MacPherson and M. A. Starr. Heavy particle component of the cosmic radiation—383(L)
———, **H. G. MacPherson and M. A. Starr.** Heavy particle component of the cosmic radiation—581
———, **H. G. MacPherson and M. A. Starr.** Wilson cloud chamber for the study of showers—389(A)
Brown, Joseph G. Effect of wind upon the electric potential gradient at the earth's surface—388(A)
Brown, M. V. and Allan C. G. Mitchell. Beta-ray spectra of radioactive manganese, arsenic and indium—593
Brown, William Fuller, Jr. Variation of the internal friction and elastic constants with magnetization in iron. Part II—1165
Brubaker, W. M. (see Bonner, T. W.)—308, 781(L)
Bruce, W. A. (see Jauncey, G. E. M.)—408, 413

Campbell, J. S. (see Hunt, M. H. M.)—397(A)
Cartmel, W. B. The integral proof of Lorentz and the Michelson-Morley experiment—1097(A)
——— The triangle proof of Lorentz—1100(A)
Cashman, R. J. (see Jamison, N. C.)—624
——— **and Noel C. Jamison.** Note on the analysis of photoelectric data—568
Cassen, B. and E. U. Condon. On nuclear forces—846
Chao, Siu-Hung. Photographic infrared absorption spectrum of gaseous ammonia—27
Chodorow, Marvin (see Manning, Millard F.)—399(A)
Ch'u, Sheng-Lin. Positive ray analysis of ions from a high frequency spark—212
Cleeton, C. E. and N. H. Williams. The shortest continuous radio waves—1091(L)
Cole, Kenneth S. and H. J. Curtis. Electric impedance of nerve—1097(A)
Cole, W. C. (see Varney, R. N.)—261(L)
Colwell, R. C. and A. W. Friend. Lower ionosphere—632
———, **A. W. Friend, N. I. Hall and L. R. Hill.** Velocity of radio waves—381(L)
Compton, Arthur H. Cosmic rays as electrical particles—1119
——— Scattering of x-rays by a spinning electron—878
Condon, E. U. (see Breit, G.)—825
——— (see Cassen, B.)—846
Cooke, W. T. Variation of the internal friction and elastic constants with magnetization in iron. Part I—1158
Cooksey, Donald (see Lawrence, E. O.)—1131
Cornell, S. D. and William W. Watson. Pressure effect in the HCN bands in the near infrared—279
——— **and William W. Watson.** Pressure effect in the HCN bands in the near infrared—397(A)
Cowie, D. B. Temperature dependence of Geiger-Müller counter characteristics—385(A)
Crane, H. R., E. R. Gaerttner and J. J. Turin. Cloud chamber study of the Compton effect—302
Curtis, B. R. (see Bayley, D. S.)—461
Curtis, Howard J. (see Cole, Kenneth S.)—1097(A)
Cuykendall, Trevor R. Absorption of x-rays of wave-length $50 \leq \lambda < 150$ X.U. by elements of low atomic number—105

Dancoff, Sidney and D. R. Inglis. On the Thomas precession of accelerated axes—784(L)
Darrow, Karl K. Concept of spin—873(A)
Delsasso, L. A., W. A. Fowler and C. C. Lauritsen. Production of pairs and Compton electrons by gamma-radiation from the bombardment of lithium by protons—389(A)
Dellinger, J. H. Direct effects of particular solar eruptions on terrestrial phenomena—1189(L)
Dempster, A. J. Isotopic constitution of iron and nickel—98(L)
——— Isotopic constitution of strontium and tellurium—186(L)
Dennison, D. M. (see Randall, H. M.)—397(A)
DeVoe, Charles F. Photoelectric properties of zinc—481
Dickinson, Roscoe G. (see Yost, Don M.)—128
Dieke, G. H. $2s^1\Sigma \rightarrow 2p^1\Sigma$ bands of the hydrogen molecule—797
Dietrich, J. R. (see Snoddy, L. B.)—469, 1094(A)
Doan, Richard L. Apparatus for transmitting cosmic-ray data from the stratosphere—1100(A)
Dodd, L. E. Further simultaneous measurements of density and surface tension—387(A)
Donley, H. L. Atomic wave functions for two stages of ionization of silicon—1012
DuBridge, Lee A. (see Mann, Marvin M.)—398(A)
DuMond, Jesse W. M. and V. L. Bollmann. New and unexplained effects in Laue x-ray reflection in calcites—97(L)
——— **and V. L. Bollman.** Tests of the validity of x-ray crystal methods of determining *e*—383(L), 524
Duncan, A. B. F. Ultraviolet absorption spectrum of ammonia. III. The absorption spectra of the deutero-ammonias. A note on Rydberg series in ammonia—709
Durand, Milo A. Temperature variation of the elastic moduli of NaCl, KCl and MgO—449

Eaton, V. E. Surface tension of water from the velocity of capillary waves—399(A)
Eckart, Carl and B. L. Griffing. Positive energy wave packet solution of the Dirac equation—1145
Edwards, Hiram W. and Robert P. Petersen. Reflectivity of evaporated silver films—871(L)
Ellis, Cecil B. Energy levels in crystals of samarium salts—675(L)
Emberson, Richard Maury. Polarimetric determination of optical properties—396(A)
Emeleus, K. G. and R. J. Ballantine. Electron velocity distribution in gases—672(L)

Evans, Robley D. (see Schiff, L. I.)—873(A)
——— **and M. H. Kanner.** Proportional counter for studying neutron intensities and neutron stimulated nuclear disintegrations—394(A)
Ewing, Douglas H. and Frederick Seitz. On the electronic constitution of crystals; LiF and LiH—760
——— On the electronic structure of LiF and LiH—400(A)

Failla, G. An ionization chamber for neutron measurements in biological experiments—1098(A)
Fano, Ugo. Some theoretical considerations on anomalous diffraction gratings—573(L)
Farwell, H. W. Christiansen filters as polarizers—486(L)
Fay, Charles H. Scattering of fast neutrons by heavy nuclei—560
Feenberg, Eugene. On relativity corrections in the theory of the deuteron—674(L)
——— (see Breit, G.)—850
——— **and Simon S. Share.** Approximate solution of nuclear three and four particle eigenvalue problems—253
Fermi, E. (see Amaldi, E.)—899
Finck, J. L. An apparatus for measuring the thermal conductivity of refractories at high temperatures—1098(A)
Fink, George A. Production and absorption of thermal energy neutrons—738
——— (see Mitchell, D. P.)—189(L), 401(A)
Fisk, J. B. The absorption of slow electrons in Cl_2—1096(A)
——— (see Morse, Philip M.)—748
———, **L. I. Schiff and W. Shockley.** On the binding of neutrons and protons—1090(L); Erratum—1191(L)
Fitzsimmons, K. E. Magazine plate camera for photography in vacuum—386(A)
Focke, Alfred B. and John R. Hill. Electrical resistivity of bismuth single crystals—179
———, **R. B. Lindsay and C. R. Wilks.** Young's modulus in bismuth crystals—872(A)
Folsom, T. R. Effective method for using low-melting metals for x-ray tube targets—396(A)
Foster, E. S., Jr. (see Miller, R. D.)—417
Fowler, W. A. (see Delsasso, L. A.)—389(A)
Fox, G. W. and C. H. Bachman. Line intensity variations in the hydrogen high frequency glow discharge—939
Fox, M. (see Millman, S.)—220
Fraser, R. G. J. and T. N. Jewitt. Ionization potentials of free radicals—1091(L)
Fredrickson, W. R. (see Humphreys, R. F.)—542
Friend, A. W. (see Colwell, R. C.)—381(L), 632
Froman, Darol K. and J. C. Stearns. Absorption of cosmic-ray secondaries and showers—787
Furry, W. H. Action of nonelectric forces on electrons and positrons—1099(A)
——— On the introduction of nonelectric forces into Dirac's equations—784(L)
——— On the theory of neutron absorption in aqueous solutions—381(L)

Gaerttner, E. R. (see Bayley, D. S.)—461
——— (see Crane, H. R.)—302
Gamow, G. (see Bloch, F.)—260(L)
Gans, David M. (see Harkins, William D.)—980
Germer, L. H. Electron diffraction experiments upon crystals of galena—659
——— (see Storks, K. H.)—676(L)
Gibbons, J. J., Jr. (see Bartlett, J. H., Jr.)—315
Gibson, G. E. and O. K. Rice. Correction to note on "The electric moment of $^1\Sigma_+$ to O^+ transition in the continuum of Cl_2"—871(L)
——— **and O. K. Rice.** Electric moment of the $^1\Sigma_+$ to O^+ transition in the continuum of Cl_2—380(L)
Gilliland, T. R. (see Kirby, S. S.)—258(L)
Ginsburg, N. (see Randall, H. M.)—397(A)
Goeppert-Mayer, M. and Albert May. Some lattice sums involved in the calculation of elastic constants—99(L)
Goldsmith, H. H. and F. Rasetti. On the resonance capture of slow neutrons—328
Gordy, Walter. Infrared absorption of alcohol-acetone mixtures—1151
Goudsmit, S. (see Bayley, D. S.)—461
——— (see Zahn, C. T.)—570(L)
Green, J. B. Paschen-Back effect of hyperfine structure. III. Separation of Hg_{199}—126
——— **and R. A. Loring.** Paschen-Back effect—$^2S^2P$ multiplets in strong fields—975(L)
Griffing, B. L. (see Eckart, Carl—1145)
Gropper, Leon. Quantum theory of the equation of state at low temperatures—963
Gross, B. On the hard component of cosmic rays—1188(L)

Hafstad, L. R. (see Tuve, M. A.)—806, 490(L)
——— (see Rumbaugh, L. H.)—681
———, **N. P. Heydenburg and M. A. Tuve.** Excitation-curves for fluorine and lithium—504
Hall, N. I. (see Colwell, R. C.)—381(L)
Hanson, Elmo E. (see Nier, Alfred O.)—722
Hardy, T. C. Reversible change of thermal energy accompanying adiabatic change of magnetization in nickel—395(A)
Harkins, William D., M. D. Kamen, H. W. Newson and D. M. Gans. Neutron-proton interaction: The scattering of neutrons by protons—980
Harrington, E. L. (see Zahn, C. T.)—570(L)
Haworth, L. J. Energy distribution of secondary electrons from columbium—216
Haynes, F. B. (see Beams, J. W.)—491(L)
Haynes, S. K. (see Millikan, R. A.)—992, 1191
Headrick, L. B. and E. A. Lederer. Films formed on electrodes during activation of oxide coated cathodes—1094(A)
Heaps, C. W. Magnetization of nickel under compressive stresses and the production of magnetic discontinuities—176
Hemmendinger, H. (see Menzel, D. H.)—872(A)
Henderson, Joseph E. Two-stage oil diffusion pump of metal for use on large volumes—388(A)
——— (see Libby, Tyng M.)—387(A)
Hendricks, Sterling B. (see Maxwell, Louis R.)—41
Henshaw, C. L. Normal energy distribution of photoelectrons from potassium films as a function of temperature—398(A)

Herzberg, G., F. Patat and H. Verleger. Photographic infrared absorption spectrum of heavy acetylene (C_2HD) and internuclear distances in the acetylene molecule—386(A)
——— **and H. Verleger.** Infrared absorption spectra and molecular structure of HNCO (cyanic acid), HCOOH (formic acid) and CH_3OH (methyl alcohol)—390(A)
———, **J. W. Spinks and W. W. Watson.** Pressure broadening of the HCN band lines and intermolecular forces—1186(L)
Heydenburg, N. P. (see Hafstad, L. R.)—504
——— (see Tuve, M. A.)—806
Heyworth, D. and Ralph D. Bennett. Measurements of the effect of paraffin and lead on the rate of production of very large cosmic-ray bursts—400(A)
——— **and Ralph D. Bennett.** Measurements of the effect of paraffin and lead on the rate of production of very large cosmic-ray bursts—589
Hickman, R. W. (see Hunt, F. V.)—1094(A)
Higgs, Paul M. and F. A. Osborn. Elimination of the effect of stray sound upon the measurement of acoustic absorption by the parallel beam method—384(A)
Hill, John R. (see Focke, Alfred B.)—179
Hill, L. R. (see Colwell, R. C.)—381(L)
Hirsh, F. R., Jr. Enhancement of certain L- and M-series x-ray satellite lines by the auger effect—191
Hoffman, Banesh, A. G. Shenstone, and L. A. Turner. Coincidences in time in Compton scattering—1092(L)
Hoffman, J. G. (see Livingston, M. Stanley)—401(A)
Holmes, F. T. Angular momentum in certain optical problems—396(A)
Horvay, Gabriel. On the slowing down of neutrons in water—897
Houston, William V. Analysis of interferometer patterns of Hα—392(A)
Hughes, A. L. and S. S. West. Scattering of fast electrons by helium—320
Hulburt, E. O. (see Young, L. C.)—45
Hull, G. F., N. C. Little and H. Margenau. Colloquium on the teaching of intermediate physics—873(A)
Hull, Gordon F., Jr. Pressure broadening of the potassium resonance lines by argon and nitrogen—1097(A), 1148
Humphreys, R. F. and W. R. Fredrickson. Pressure effect on the C band of strontium hydride—542
Hunt, F. V., and R. W. Hickman. Electronic voltage stabilizers—1094(A)
Hunt, M. H. M. and J. S. Campbell. Hyperfine structure and wave-length of the infrared Hgl 6^1P-7^1S line—397(A)

Inglis, D. R. Nuclear calculation—399(A)
——— Spin-orbit coupling in nuclei—783(L)
——— (see Dancoff, Sidney)—784(L)

Jacquinot, P. Paschen-Back effect—$^3S^3P$ multiplets in strong fields—573(L)
Jamison, Noel C. (see Cashman, Robert J.)—568
——— **and R. J. Cashman.** Photoelectric properties of barium and calcium—624
Jaques, A. T. (see Jauncey, G. E. M.)—672(L)
Jauncey, G. E. M. Velocity distribution of atomic electrons by the method of electron impact—326
——— **and W. A. Bruce.** Anisotropy in the atomic vibrations of zinc crystals. I. Evidence from x-ray scattering—408
——— **and W. A. Bruce.** Anisotropy in the atomic vibrations of zinc crystals. II. Diffuse scattering of x-rays from single crystals—413
——— **and A. T. Jaques.** Intensity of the central spot produced by x-rays penetrating piezoelectrically oscillating quartz—672(L)
Jenkins, F. A. (see Nolan, Philip)—943
Jeppesen, Myron A. $^1\Sigma^*-^1\Sigma$ band system of copper deuteride—445, 386(A)
Jewitt, T. N. (see Fraser, R. G. J.)—1091(L)
Johnson, A. G. (see Johnson, E. A.)—170
Johnson, E. A. and A. G. Johnson. Theoretical analysis of the operation of ionization chambers and pulse amplifiers—170
Jones, Ernest J. (see Blewett, J. P.)—464
Jones, Matthew T. Absorption of ultra-short x-rays by elements of high atomic number—110
Jordan, Edward B. (see Bainbridge, Kenneth T.)—282
——— **and Kenneth T. Bainbridge.** Mass-spectrographic determination of the mass difference $N^{14}+H^1-N^{15}$ and the nitrogen disintegration reactions—98(L)

Kamen, Martin D. (see Harkins, William D.)—980
Kanne, W. R. and J. A. Bearden. Columnar ionization—935
Kanner, M. H. (see Evans, Robley D.)—394(A)
Kaplan, Joseph. High pressure afterglow in nitrogen—384(A)
——— Two afterglow phenomena in nitrogen—390(A)
Kellogg, J. M. B., I. I. Rabi and J. R. Zacharias. Gyromagnetic properties of the hydrogens—472
———, **I. I. Rabi and J. R. Zacharias.** Magnetic moment of the proton—396(A)
Kellström, Gunnar. Viscosity of air and the electronic charge—190(L)
Kiang, A. T., S. T. Ma and Ta-You Wu. Attempt to observe the spectrum of doubly excited helium—673(L)
Killian, T. J. Improved manometer and pressure control—390(A)
——— **and R. S. Prescott.** Cathode drop in low pressure discharge tube—399(A)
——— **and R. S. Prescott.** Characteristics and energy balance in gaseous discharge lamps containing carbon dioxide—389(A)
King, Allen and W. M. Rayton. Extrapolated ranges from number-disturbance curves—394(A)
Kingdon, K. H. and H. E. Tanis, Jr. Measurements of the diffusion of ions in mercury vapor—1095(A)
——— (see Lawton, E. J.)—1095(A)
Kinsey, Bernard B. Attempts at disintegration using lithium ions—386(A)
Kip, Arthur F. and Leonard B. Loeb. Nature of the effect of the sign of charge on ions in the C. T. R. Wilson cloud condensation experiments—392(A)
Kirby, S. S., T. R. Gilliland, N. Smith and S. E. Reymer. Ionosphere, solar eclipse and magnetic storm—258(L)

Kirkpatrick, Paul, P. A. Ross and H. O. Ritland. Characteristics of the Compton modified band—928
Kleis, J. D. Ferromagnetic anisotropy of nickel-iron crystals at various temperatures—1178
——— (see McKeehan, L. W.)—1093(A)
Konopinski, E. J. (see Bethe, H. A.)—1100(A)
Korff, S. A. (see Bowen, I. S.)—579
Kovarik, Alois F. and Norman I. Adams, Jr. Disintegration constant of thorium and branching ratio of thorium C—99(L)
Kovner, M. Band spectrum of OH^+—188(L)
Krishnan, K. S. and Asutosh Mookherji. Magnetic anisotropy of copper sulphate pentahydrate $CuSO_4 \cdot 5H_2O$, in relation to its crystal structure. Part I.—860
Kurie, Franz N. D. (see Richardson, J. Reginald)—999

Ladenberg, R. and R. B. Roberts. Investigations of the deuteron-deuteron reaction—1190(L)
Lamb, W. E., Jr. Unobservable decay of Na^{22}—388(A)
Lane, C. T. Magnetic analysis of evaporated bismuth films—1094(A)
Lang, R. J. On the spectrum of Ce IV—397(A)
Langer, R. M. Energy liberation in stellar interiors—388(A)
Langmuir, Irving and John Bradshaw Taylor. Heat conductivity of tungsten and the cooling effects of leads upon filaments at low temperatures—68
——— **and John Bradshaw Taylor.** Erratum: Heat conductivity of tungsten and the cooling effects of leads upon filaments at low temperatures—190
Laporte, Otto. Connection between the Kepler problem and the four-dimensional rotation group—400(A)
Laslette, L. Jackson. Long period positron activity—388(A)
——— Stopping power of foils for high speed deuterons—391(A)
Lauritsen, C. C. (see Delsasso, L. A.)—389(A)
Lawrence, Ernest O. and D. Cooksey. On the apparatus for the multiple acceleration of light ions to high speeds—1131
Lawton, E. J. and K. H. Kingdon. Some factors influencing the sparking potential in Hg vapor—1095(A)
Lawton, W. E. (see Plimpton, S. J.)—1066
Lederer, E. A. (see Headrick, L. B.)—1094(A)
Lemaitre, G. and M. S. Vallarta. On the allowed cone of cosmic radiations—493
Lewis, Gilbert N. Theory of orbital neutrons—857
Libby, Tyng M., Joseph E. Henderson and Donald H. Loughridge. Controlled mercury-pool device for high voltage and current rectification and switching—387(A)
Libby, W. F. and Earl A. Long. Effect of hydrocarbons at low temperatures on slow neutrons—575(L)
——— **and Earl A. Long.** Bond effect in the action of protons on neutrons—577(L)
Lindsay, R. B. (see Focke, A. B.)—872(A)
Little, N. C. (see Hull, G. F.)—873(A)
Livingood, J. J. Deuteron induced radioactivities—425
——— Deuteron induced radioactivities of antimony and tin—385(A)
——— Deuteron induced radioactivities in ruthenium and copper—391(A)
——— **and Glenn Seaborg.** Deuteron induced radioactivity in tin—435
Livingston, M. Stanley and J. G. Hoffman. Slow neutron disintegration of Li^6 and the disintegration mass scale—401(A)
Locher, Gordon L. Cosmic-ray disintegrations in light elements—394(A)
——— Geiger-Müller counters for special purposes—1099(A)
Loeb, Leonard B. (see Kip, Arthur F.)—392(A)
Long, Earl A. (see Libby, W. F.)—575(L), 577(L)
Longacre, Andrew. Energy distribution of cosmic rays—674(L)
Loring, R. A. (see Green, J. B.)—975(L)
Loughridge, Donald H. (see Skramstad, Harold K.)—677
——— (see Libby, Tyng M.)—387(A)
——— **and N. Kermit Olsen.** Effect of a magnetic field upon the photoelectric properties of iron—389(A)
Lowen, Irving S. Effect of nuclear motion in the Dirac equation—1098(A)
Luhr, Overton and F. J. Studer. A spectroscopic study of the magnetron discharge—1095(A)
Lyman, Ernest M. Shape of the β-ray spectrum of P^{32}—385(A)

Ma, S. T. (see Kiang, A. T.)—673(L)
Mac Adam, David L. Use of the reflection echelon for interferometric wave-length comparisons extending into the Schumann region—185(L)
MacPherson, H. G. (see Brode, R. B.)—581, 383(L), 389(A)
Maier-Leibnitz, H. (see Bothe, W.)—187(L)
Malter, Louis. Thin film field emission—48
Manley, J. H. and S. Millman. Nuclear spin and magnetic moment of Li^6—380(L)
Mann, Marvin M. and Lee A. DuBridge. Absolute photoelectric yield of beryllium, magnesium and sodium—398(A)
Manning, Millard F. and Marvin Chodorow. Energy bands in metallic tungsten—399(A)
Margenau, H. Relativity and nuclear forces—342
——— (see Hull, G. F.)—873(A)
Mattauch, Josef. Double-focusing mass spectrograph and the masses of N^{15} and O^{18}—617; Erratum—1089
Maxwell, Louis R., V. M. Mosley and Sterling B. Hendricks. Nuclear separation of the S_2 molecule by electron diffraction—41
May, Albert (see Goeppert-Mayer, M.)—99(L)
McDonald, John C. Effects of chemical combination on the K beta lines of 26 Fe-30 Zn—694
——— Effects of chemical combination on x-ray emission spectra—782(L)
McKeehan, L. W., R. G. Piety and J. D. Kleis. Ferromagnetic anisotropy in alpha iron and in gamma nickel-iron and nickel-cobalt-iron at and above room temperature—1093(A)
Menzel, D. H., H. Hemmendinger, R. d'E. Atkinson and J. C. Boyce. Automatic spectrographs of the Harvard-M.I.T. eclipse expedition—872(A)

Migeotte, M. V. and E. F. Barker. Fundamental absorption bands of the deuteroammonias—418
Miller, R. D. and E. S. Foster, Jr. Anisotropy in the atomic vibrations of zinc crystals. III. The (0002) and (1010) reflection of the Mo $K\alpha$ x-rays from powdered zinc—417
Millikan, R. A. (see Bowen, I. S.)—579
——— **and H. Victor Neher.** Precision world survey of sea-level cosmic-ray intensities—15
———, **H. V. Neher and S. K. Haynes.** Precision cosmic-ray measurements up to within a percent or two of the top of the atmosphere—992; Erratum—1191
Millman, S. (see Manley, J. H.)—380(L)
——— **and M. Fox.** Nuclear spins and magnetic moments of Rb^{85} and Rb^{87}—220
Mitchell, Allan C. G. (see Brown, M. V.)—593
———, **Edgar J. Murphy and Martin D. Whitaker.** Scattering of slow neutrons. II—133
Mitchell, Dana P. and Philip N. Powers. Bragg reflection of slow neutrons—486(L)
———, **F. Rasetti, G. A. Fink and G. B. Pegram.** Experiments with photo-neutrons—401(A)
———, **F. Rasetti, G. A. Fink and G. B. Pegram.** Some experiments with photo-neutrons—189(L)
Mohler, F. L. (see O'Brien, Brian)—1099(A)
Montgomery, C. G. and D. D. Montgomery. Dependence of burst production upon atomic number—490(L)
——— **and D. D. Montgomery.** Heavy particle component of the cosmic radiation—975(L)
——— **and D. D. Montgomery.** Production of bursts of cosmic-ray ionization from various materials—395(A)
———, **D. D. Montgomery, W. E. Ramsey and W. F. G. Swann.** Search for protons in the primary cosmic-ray beam—403
Montgomery, D. D. (see Montgomery, C. G.)—975(L), 403, 490(L), 395(A)
More, Kenneth R. and C. A. Rieke. Wave-length standards in the extreme ultraviolet—1054, 1096(A)
Morgan, J. E. and W. M. Nielsen. Cosmic-ray shower production and absorption in various materials—882
Mookherji, Asutosh (see Krishnan, K. S.)—860
Moore, Dan H. Relation between electron field emission and contact electromotive force for liquid mercury—344
Morgan, Frank. Band spectra of MgCl, MgBr and MgI in absorption—603
Morse, Philip M., J. B. Fisk and L. I. Schiff. Collision of neutron and proton—748
Mosley, V. M. (see Maxwell, Louis R.)—41
Motz, Lloyd and M. E. Rose. On space quantization in time varying magnetic fields—348
Moyer, Laurence S. and Harold A. Abramson. Electrical charge of mammalian red blood cells under normal conditions and in the anemias—398(A)
Mueller, Hans. Optical properties of nonpolar liquids—547
Mulliken, Robert S. The low electronic states of simple heteropolar diatomic molecules I. General survey—1017 II. Alkali metal hydrides—1028
Murphy, Edgar J. (see Mitchell, Allan C. G.)—133
Mutch, W. W. Fine structure in the K x-ray absorption edge of gallium—197
Neddermeyer, Seth H. (see Anderson, Carl D.)—263
Neher, H. V. (see Bowen, I. S.)—579
——— (see Millikan, Robert A.)—15, 992, 1191
Newson, Henry W. (see Harkins, William D.)—980
Nielsen, Russell A. Absolute values of the electron drift velocity in nitrogen, helium, neon and argon—950
——— Absolute values of the electron drift velocity in the rare gases—386(A)
Nielsen, W. M. (see Morgan, J. E.)—882
Nier, Alfred O. Mass-spectrographic study of the isotopes of argon, potassium, rubidium, zinc and cadmium—873(A), 1041
——— **and Elmo E. Hanson.** Mass-spectrographic analysis of the ions produced in HCl under electron impact—722
Nolan, Philip and F. A. Jenkins. Intensities in the $^3\Pi$, $^3\Sigma$ band of PH—943
Norgorden, Oscar. Piezoelectric properties of Rochelle salt—782(L)
Nottingham, W. B. Influence of crystal structure on electron emission from "218" tungsten wire—398(A)

O Brien, Brian. High speed running film camera for photographic photometry—400(A)
———, **F. L. Mohler and H. S. Stewart.** Vertical distribution of ozone in the upper atmosphere—1099(A)
O'Bryan, H. M. and E. G. Schneider. Absorption of some metallic halides in the Schumann region—1096(A)
Olsen, N. Kermit (see Loughridge, Donald H.)—389(A)
Oppenheimer, J. R. On the elementary interpretation of showers and bursts—389(A)
——— **and R. Serber.** Density of nuclear levels—391(A)
Osborn, F. A. (see Higgs, Paul M.)—384(A)
Osterberg, H. (see Taschek, R.)—572(L)
——— Electroresistive effect and a rectifying property of carborundum crystals—1187(L)

Parratt, Lyman G. On x-ray satellites, relative intensities and line widths—598
——— $K\alpha$ satellite lines—1
——— (see Shaw, Charles H.)—1006, 1096(A)
Patat, F. (see Herzberg, G.)—386(A)
Peczalski, Thaddeus. Mutual reactions of metals and salts—785(L)
Pegram, G. B. (see Mitchell, D. P.)—401(A), 189(L)
Petersen, Robert P. (see Edwards, Hiram W.)—871(L)
Piety, Raymond G. Ferromagnetic anisotropy of iron crystals at various temperatures—1173
——— (see McKeehan, L. W.)—1093(A)
Plesset, Milton S. and Richard F. Baker. On the elastic constants of an anisotropic solid—399(A)
Plimpton, S. J. and W. E. Lawton. A very accurate test of Coulomb's law of force between charges—1066
Plyler, E. K. and D. Williams. The infrared absorption of heavy acid solutions—1097(A)
Pollard, Ernest and Charles J. Brasefield. Transmutation of potassium, chlorine and phosphorus by Th C′ alpha-particles—890
——— (see Brasefield, Charles J.)—296
——— **and C. J. Brasefield.** Alpha-particle bombardment of neon, argon and calcium—1095(A)

Posin, Daniel Q. Townsend coefficients and spark discharge—650
Powers, Philip N. (see Mitchell, Dana P.)—486(L)
Prescott, R. S. (see Killian, T. J.)—399(A), 389(A)
Present, R. D. (see Breit, G.)—825
——— Second-order spin effects in H^3—870(L)
——— Must neutron-neutron forces exist in the H^3 nucleus?—635

Rabi, I. I. (see Kellogg, J. M. B.)—472, 396(A)
Ramsey, W. E. (see Montgomery, C. G.)—403
Randall, H. M., N. Ginsburg, D. M. Dennison and R. L. Webber. Pure rotation spectrum of water vapor—397(A)
Rasetti, F. (see Goldsmith, H. H.)—328
——— (see Mitchell, D. P.)—401(A), 189(L)
Rayton, W. M. (see King, Allen)—394(A)
——— **and T. R. Wilkins.** Alpha-ray ranges of uranium isotopes—394(A)
Reymer, S. E. (see Kirby, S. S.)—258(L)
Rice, O. K. (see Gibson, G. E.)—871(L), 380(L)
Richardson, J. Reginald and F. N. D. Kurie. The radiations emitted from artificially produced radioactive substances II. The gamma-rays from several elements—999
Ridenour, Louis N. (see Sampson, Milo B.)—382(L)
Rieke, Carol A. (see More, Kenneth R.)—1054, 1096(A)
Ritland, H. O. (see Kirkpatrick, Paul)—928
Roberts, R. B. (see Ladenberg, R.)—1190(L)
Robertson, H. P. Conservation of photons in general relativity—385(A)
Robinson, Howard A. Spectra Be III and Be IV—99(L)
Rochel, Joseph H., S.J. (see Brady, James J.)—870(L)
Rodgers, Eric. Polarization of hard x-rays—875
Roebuck, J. R. Kelvin temperature of the ice point—370
Rogers, F. T., Jr. Precise measurement of three radium B beta-particle energies—515
Rose, John L. and R. K. Stranathan. Geologic time and isotopic constitution of radiogenic lead—792
Rose, M. E. (see Motz, Lloyd)—348
——— (see Bethe, H. A.)—1100(A)
Roseberry, H. H. and J. A. Bearden. Effects of chemical composition on x-ray lines—204
Ross, P. A. (see Kirkpatrick, Paul)—928
Rudberg, Erik. Inelastic scattering of electrons from solids—138
——— **and J. C. Slater.** Theory of inelastic scattering of electrons from solids—150
Rumbaugh, L. H. and L. R. Hafstad. Disintegration experiments on the separated isotopes of lithium—681

Sabine, G. B. Reflecting power of evaporated metal films in the near and far ultraviolet—396(A)
Sagane, R. Radioactivity induced in sulphur—1141
Sampson, Milo B. and Paul A. Anderson. Transition phenomena in the condensation of silver vapor on clean and gas-covered tungsten—385(A)
——— **and Walker Bleakney.** Relative abundance of the isotopes in Mn, Cb, Pd, Pt, Ir, Rh and Co—732
——— **and Walker Bleakney.** Mass spectrograph study of Ba, Sr, In, Ga, Li and Na—456
———, **Louis N. Ridenour and Walker Bleakney.** Isotope of cobalt and their radioactivity—382(L)
Sanderson, J. A. Infrared absorption of CS_2 at 4.57μ—209
Sawyer, J. H. Absorption of shower-producing cosmic rays—25
Saxl, Irving J. Physics in textile research—1098(A)
Schiff, L. I. (see Morse, Philip M.)—748
——— (see Fisk, J. B.)—1090(L)
——— Counter statistics for chain disintegrations—394(A)
——— Statistical analysis of counter data—88
——— **and Robley D. Evans.** Statistical analysis of the counting rate meter—873(A)
Schneider, E. G. (see O'Bryan, H. M.)—1096(A)
Schoepfle, G. K. Deep terms in the spectra of Pb V and Bi VI—538
Seaborg, Glenn (see Livingood, J. J.)—435
Seeley, Samuel (see Zinn, W. H.)—1101(A)
Seitz, Frederick (see Ewing, Douglas H.)—400(A), 760
Segrè, E. (see Amaldi, E.)—571(L)
——— **and C. T. Zahn.** Resonance energy of cadmium for neutron capture—577(L)
Serber, R. (see Oppenheimer, J. R.)—391(A)
——— Proton-proton forces and the mass defect curve—389(A)
Shambon, Arthur (see Watson, William W.)—607
Shankland, Robert S. Scattering of gamma-rays—571(L)
Share, Simon S. Coulomb energy of He^3—488(L)
——— (see Feenberg, Eugene)—253
Shaw, Charles H. and L. G. Parratt. $K\alpha$ satellite lines for elements Zn(30) to Pd(46)—1006, 1096(A)
Shenstone, A. G. (see Hoffmann, Banesh)—1092(L)
Sherr, Rubby (see Bleakney, Walker)—545
Shih, J. W. Magnetic anisotropy of nickel-cobalt single crystals—376
Shockley, W. Electronic energy bands in sodium chloride—754
——— (see Slater, J. C.)—705
——— (see Fisk, J. B.)—1090(L)
Shortley, George H. Note on Fock equations for complex configurations—1072
Sinclair, David and Harold W. Webb. Lifetime of potassium doublets λ4047–4 and λ3447–6—440
——— Mean lives of potassium doublets λ4047–4 and λ3447–6—397(A)
Sixtus, K. J. Coercive force in single crystals of silicon ferrite—395(A)
Skramstad, Harold K. and Donald H. Loughridge. Primary ionization of high energy electrons in nitrogen and neon—677
Slater, J. C. (see Rudberg, E.)—150
——— **and W. Shockley.** Optical absorption by the alkali halides—705
Smith, N. (see Kirby, S. S.)—258(L)
Smoluchowski, Roman (see Bleakney, Walker)—545
——— (see Bouckaert, L. P.)—58
——— Theoretical investigation of the fine structure of x-ray absorption edge of gallium—201
Smythe, W. R. (see Wooldridge, Dean E.)—233
Snoddy, L. B., J. W. Beams and J. R. Dietrich. Propagation of potential in discharge tubes—469, 1094(A)

Sommerfeld, A. Concerning the shape of the Compton lines (from a letter to A. H. Compton)—38
Spedding, Frank H. Nature of energy states in solids—574(L)
Speh, Karl C. Gamma-rays of lithium and fluorine under alpha-particle bombardment—395(A), 689
Spinks, J. W. (see Herzberg, G.)—1186(L)
Starr, M. A. (see MacPherson, H. G.)—581
——— (see Brode, R. B.)—389(A), 383(L)
Stearns, J. C. (see Froman, Darol K.)—787
Stephenson, S. T. *K* x-ray absorption spectra of some compounds of bromine, rubidium and strontium—790
——— *K* x-ray absorption spectrum of bromine—387(A)
Storks, K. H. Orientation in thin layers of stearic acid by electron diffraction—396(A)
——— **and L. H. Germer.** Electron diffraction by films built from many monomolecular layers—676(L)
Stewart, H. S. (see O'Brien, Brian)—1099(A)
Stranathan, R. K. (see Rose, John L.)—792
Studer, Frank J. (see Luhr, Overton)—1095(A)
Swann, W. F. G. Numerically consistent corpuscular theory of cosmic rays—1103.
——— A possible critical latitude phenomenon limited to altitudes above sea level—1099(A)
——— (see Montgomery, C. G.)—403

Tanis, H. E., Jr. (see Kingdon, K. H.)—1095(A)
Taschek, R. and H. Osterberg. Crystalline symmetry and shear constants of Rochelle salt—572(L)
Taylor, John Bradshaw (see Langmuir, Irving)—68, 190
Thomas, Charles D. The scattering of light by light according to the Born-Infield theory—1046
Tomboulian, D. H. (see Bacher, R. F.)—1096(A)
Thompson, Julian L. Note on diurnal variation of cosmic-ray intensity—869(L)
Tonks, Lewi. Complete equation of state of one, two and three-dimensional gases of hard elastic spheres—955
——— Force at an anchored cathode spot—226
Tousey, Richard. Optical constants of fluorite in the extreme ultraviolet—1057
Townsend, Agnes. Illumination meter for photographic laboratory work—396(A)
Turner, Louis A. (see Hoffman, Banesh)—1092(L)
Turin, J. J. (see Crane, H. R.)—302
Tuve, M. A. (see Hafstad, L. R.)—504
——— Nuclear forces—869(L)
——— **and L. R. Hafstad.** Scattering of neutrons by protons—490(L)
———, **N. P. Heydenburg and L. R. Hafstad.** Scattering of protons by protons—806

Uehling, Edwin A. Positron theoretic deviations from the Klein-Nishina formula—387(A)
Urey, H. C. and A. H. W. Aten, Jr. On the chemical differences between nitrogen isotopes—575(L)

Vallarta, M. S. (see Lemaitre, G.)—493
Van Voorhis, S. N. Artificial radioactivity of copper, a branch reaction—895
Varney, Robert N. Ionization of gases by collisions of their own accelerated atoms—159
——— Ionization of mercury vapor by positive sodium ions—1095(A)
——— **and W. C. Cole.** Ionization of mercury vapor by positive sodium ions—261(L)
Verleger, H. (see Herzberg, G.)—386(A), 390(A)
Vonnegut, B. and B. Warren. Structure of crystalline bromine—872(A)

Wahlin, H. B. and L. V. Whitney. Positive and negative thermionic emission from tungsten—735
Warren, B. (see Vonnegut, B.)—872(A)
Watson, Madeleine DeBlois (see Anslow, Gladys A.)—162
Watson, R. E. (see Bartlett, J. H., Jr.)—315
Watson, William W. (see Cornell, S. D.)—279, 397(A)
——— (see Herzberg, G.)—1186(L)
——— **and Arthur Shambon.** Spectrum of indium oxide—607
Way, Harold F. Electrical resistivity of single crystals of some dilute solid solutions in zinc—1181
Way, K. and John A. Wheeler. Comparison of Majorana-Heisenberg and velocity-dependent forces—675(L)
Webb, Harold W. (see Sinclair, David)—397(A), 440
Webber, R. L. (see Randall, H. M.)—397(A)
Weisskopf, V. F. Exchange forces between elementary particles—1187(L)
Wells, William H. (see Williams, John H.)—186(L)
West, S. S. (see Hughes, A. L.)—320
Wheeler, John A. (see Way, K.)—675(L)
——— Dependence of nuclear forces on velocity—643
Whitaker, Martin D. (see Mitchell, Allan C. G.)—133
Whitney, L. V. Thermionic emission of platinum—1154
——— (see Wahlin, H. B.)—735
Wigner, E. (see Bouckaert, L. P.)—58
——— **and G. Breit.** β-ray spectrum of Li^8—1191(L)
Wilkins, T. R. Further observations of cosmic-ray tracks in photographic emulsions—1099(A)
——— (see Rayton, W. M.)—394(A)
Wilks, C. R. (see Focke, A. B.)—872(A)
Williams, Dudley. Infrared absorption of hydrogen chloride in nonionizing solvents—719, 1097(A)
——— (see Plyler, E. K.)—1097(A)
Williams, John H. and William H. Wells. Evidence from efficiency curves for the nature of the disintegration process for boron—186(L)
Williams, N. H. (see Cleeton, C. E.)—1091(L)
Wilson, Robert R. Very short time lag of sparking—1082
Witmer, Enos E. The magnetic susceptibility of molecular hydrogen—1094(A)
Wooldridge, Dean E. and W. R. Smythe. Separation of gaseous isotopes by diffusion—233
Wu, Ta-You (see Kiang, A. T.)—673(L)

Yerzley, Felix L. Investigation of irregularities in thermionic emission from tungsten—610
Yost, Don M. and Roscoe G. Dickinson. Diffusion and absorption of neutrons in paraffin spheres—128
Young, L. C. and E. O. Hulburt. Radio and the sunspot cycle—45

Zacharias, J. R. (see Kellogg, J. M. B.)—396(A), 472
Zahn, C. T. (see Segrè, E.)—577(L)
——— **E. L. Harrington and S. Goudsmit.** Method for the determination of absorption cross sections for thermal neutrons—570(L)
Zener, Clarence and S. Bilinsky. On the intensity of x-rays reflected from zinc—489(L)
——— Theory of the effect of temperature on the reflection of x-rays by crystals. III. High temperatures. Allotropic crystals—101
Zenor, Hughes M. The cooling of a surface by photoelectric emission—1050
Zinn, W. H. and S. Seeley. Production of neutrons with low voltage—1101(A)
Zinszer, R. H. The effect of pressure on the absorption and optical activity of water—1097(A)

Analytic Subject Index to Volume 50

References with (A) are to abstracts of papers presented at meetings of the Physical Society. References with (L) are to Letters to the Editor.

Absorption phenomena
- Effect of pressure on absorption of water, R. H. Zinszer—1097(A)
- Of hydrogen chloride in non-ionizing solvents, D. Williams—719, 1097(A)
- Of metallic halides in Schumann region, H. M. O'Bryan, E. G. Schneider—1096(A)
- Optical absorption by alkali halides, J. C. Slater, W. Shockley—705

Accommodation coefficient
- And molar heat of hydrocarbon molecules, O. Beeck—387(A)

Acoustics
- Absorption and sound velocity in mixtures, D. G. Bourgin—355
- Stray sound and measurement of acoustic absorption, P. M. Higgs, F. A. Osborn—384(A)

Afterglow
- In N_2, J. Kaplan—384(A), 390(A)

Arcs (see also **Discharge of electricity in gases**)
- Force at cathode spot, Hg arc, L. Tonks—226

Astrophysics
- Energy liberation in stellar interiors, R. M. Langer—388(A)
- Spectrographs of eclipse expedition, D. H. Menzel, H. Hemmendinger, R. d'E. Atkinson, J. C. Boyce—872(A)
- Sunspot cycle and radio, L. C. Young, E. O. Hulburt—45

Atmosphere (see **Meteorology**)

Atmospheric electricity (see **Meteorology**)

Biophysics
- Electric impedance of nerve, K. S. Cole, H. J. Curtis—1097(A)
- Electrical charge of mammalian red blood cells, L. S. Moyer, H. A. Abramson—398(A)
- Neutron measurements in biological experiments, G. Failla—1098(A)

Chemical reactions
- Reactions of metals and salts, T. Peczalski—785(L)

Collision diameter (see **Molecular radii**)
- Cross sections of Cl_2 and N_2 for slow electrons, J. B. Fisk—1096(A)
- Of neutrons and protons, P. M. Morse, J. B. Fisk, L. I. Schiff—748; J. B. Fisk, L. I. Schiff, W. Shockley—1090(L)

Compton effect (see **X-rays, diffraction, scattering**)

Constants, physical, standards
- Kelvin temperature of ice point, J. R. Roebuck—370
- Validity of x-ray crystal determination of e, J. W. M. DuMond, V. L. Bollman—383(L), 524
- Viscosity of air and electronic charge, G. Kellström—190(L)
- Wave-length standards in extreme ultraviolet, K. R. More, C. A. Rieke—1054, 1096(A)

Cosmic radiation
- Absorption of secondaries and showers, D. K. Froman, J. C. Stearns—787
- Absorption of shower-producing rays, J. H. Sawyer—25
- Allowed cone of radiation, G. Lemaitre, M. S. Vallarta—493
- Burst production and atomic number, C. G. Montgomery, D. D. Montgomery—490(L)
- Bursts from various materials, C. G. Montgomery, D. D. Montgomery—395(A)
- Bursts in light elements, G. L. Locher—394(A)
- Cloud chamber observations on Pike's Peak and near sea-level, C. D. Anderson, S. H. Neddermeyer—263
- Consistent corpuscular theory, W. F. G. Swann—1103
- Critical latitude phenomena, W. F. G. Swann—1099(A)
- Diurnal variation, J. L. Thompson—869(L)
- Energy distribution, A. Longacre—674(L)
- Evidence for electrical particles, A. H. Compton—1119
- Hard component, range phenomena, B. Gross—1188(L)
- Heavy particle component, R. B. Brode, H. G. MacPherson, M. A. Starr—383(L), 581; C. G. Montgomery, D. D. Montgomery—975(L); C. G. Montgomery, D. D. Montgomery, W. E. Ramsey, W. F. G. Swann—403
- Interpretation of showers and bursts, J. R. Oppenheimer—389(A)
- Large bursts; effect of paraffin and lead, D. Heyworth, R. D. Bennett—400(A), 589
- Latitude effect up to 29,000 ft., I. S. Bowen, R. A. Millikan, S. A. Korff, H. V. Neher—579
- Measurements near top of atmosphere, R. A. Millikan, H. V. Neher, S. K. Haynes—992; erratum—1191
- Sea-level survey, R. A. Millikan, H. V. Neher—15
- Shower production and absorption in various materials, J. E. Morgan, W. M. Nielsen—882
- Tracks in photographic emulsions, T. R. Wilkins—1099(A)
- Transmitting data from stratosphere, R. L. Doan—1100(A)
- Wilson cloud chamber for showers, R. B. Brode, H. G. MacPherson, M. A. Starr—389(A)

Crystal structure
- Of bromine, B. Vonnegut, B. Warren—872(A)
- Of $CuSO_4 \cdot 5H_2O$, K. S. Krishnan, A. Mookherji—860
- Symmetry of Rochelle salts, R. Taschek, H. Osterberg—572(L)

Crystalline state
- Analysis of evaporated Bi films, C. T. Lane—1094(A)
- Anisotropy in atomic vibrations of Zn crystals, G. E. M. Jauncey, W. A. Bruce—408, 413; R. D. Miller, E. S. Foster, Jr.—417; C. Zener, S. Bilinsky—489(L)
- Calculation of elastic constants, M. Goeppert-Mayer, A. May—99(L)

Coercive force in crystals of silicon ferrite, K. J. Sixtus—395(A)
Condensation of metal on metal, M. B. Sampson, P. A. Anderson—385(A)
Electron diffraction by films built of monomolecular layers, K. H. Storks, L. H. Germer—676(L)
Electron diffraction by galena crystals, L. H. Germer—659
Electron exchange in metals, J. Bardeen—1098(A)
Electronic constitution of LiF and LiH, D. H. Ewing, F. Seitz—400(A), 760
Electronic energy bands in NaCl, W. Shockley—754
Energy bands in metallic tungsten, M. F. Manning, M. Chodorow—399(A)
Energy levels in Sm salts, C. B. Ellis—675(L)
Energy states in solids, F. H. Spedding—574(L)
Ferromagnetic anisotropy of iron crystals, R. G. Piety—1173
Ferromagnetic anisotropy of Ni-Fe crystals, J. D. Kleis—1178
Ferromagnetic anisotropy in single crystals and polycrystalline sheets, R. M. Bozorth—1076
Intensity of x-rays penetrating oscillating crystals, G. E. M. Jauncey, A. T. Jaques—672(L)
Internal friction, elastic constants, magnetization in Fe, Part I, W. T. Cooke—1158; W. F. Brown, Part II—1165
Orientation in stearic acid by electron diffraction, K. H. Storks—396(A)
Reactions of metals and salts, T. Peczalski—785(L)
Rectifying properties of crystals, H. Osterberg—1187(L)
Resistivity of Bi crystals, A. B. Focke, J. R. Hill—179
Resistivity of single crystals of solid solutions in Zn, H. E. Way—1184
Shear constants of Rochelle salt, R. Taschek, H. Osterberg—572(L)
Theory of Brillouin, L. P. Bouckaert, R. Smoluchowski, E. Wigner—58
Young's modulus of Bi crystals, A. B. Focke, R. B. Lindsay, C. R. Wilks—872(A)

Diffraction of electrons (see **Electron diffraction**)
Discharge of electricity in gases (see also **Arcs**)
Cathode drop in low pressure discharge tubes, T. J. Killian, R. S. Prescott—399(A)
Columnar ionization by α-particles, W. R. Kanne, J. A. Bearden—935
Cross sections of Cl_2 and N_2 for slow electrons, J. B. Fisk—1096(A)
Diffusion of ions in Hg vapor, K. H. Kingdon, H. E. Tanis, Jr.—1095(A)
Discharge lamps containing CO_2, T. J. Killian, R. S. Prescott—389(A)
Electron velocity in gases, K. G. Emeleus, R. J. Ballantine—672(L)
Propagation of potential in tubes, L. B. Snoddy, J. W. Beams, J. R. Dietrich—469, 1094(A)
Sparking potential in Hg vapor, E. J. Lawton, K. H. Kingdon—1095(A)
Time lag of sparking, R. R. Wilson—1082
Townsend coefficients and spark discharge, D. Q. Posin—650
Discharge of electricity in high vacuum (see also **Thermionic emission; High voltage tubes and machines**)
Field emission and contact electromotive force for Hg, D. H. Moore—344
Disintegration of nucleus
Of Be, B and C by H^2, T. W. Bonner, W. M. Brubaker—308
Collisions of α-particles with S, R. L. Anthony—395(A), 726
Deuteron-deuteron reaction, R. Ladenburg, R. B. Roberts—1190(L)
Efficiency curves for the disintegration of B, J. H. Williams, W. H. Wells—186(L)
Excitation-curves for F and Li, L. R. Hafstad, N. P. Heydenburg, M. A. Tuve—504
Gamma-rays of Li and F under alpha-particle bombardment, K. C. Speh—395(A), 689
Of Li^6 by neutrons, M. S. Livingston, J. G. Hoffman—401(A)
Of Li^6 and Li^7, L. H. Rumbaugh, L. R. Hafstad—681
Of Li^8, β-ray spectrum, E. Wigner, G. Breit—1191(L)
Of N, A and Ca by α-particles, E. Pollard, C. J. Brasefield—1095(A)
Nitrogen disintegration reactions, E. B. Jordan, K. T. Bainbridge—98(L)
Of N by fast neutrons, T. W. Bonner, W. M. Brubaker—781(L)
Pairs and Compton electrons by γ-radiation from Li, L. A. Delsasso, W. A. Fowler, C. C. Lauritsen—389(A)
Of K, Cl and P by Th C′ α-particles, E. Pollard, C. J. Brasefield—890
Of S by Th C′ alpha-particles, C. J. Brasefield, E. Pollard—296
By use of Li ions, B. B. Kinsey—386(A)
Without capture, T. R. Wilkins—1099(A)

Elasticity
Constants of anisotropic solid, Cauchy's relations, M. S. Plesset, R. F. Baker—399(A)
Internal friction, elastic constants, magnetization in Fe, Part I, W. T. Cooke—1158; W. F. Brown, Part II—1165
Shear constants of Rochelle salt, R. Taschek, H. Osterberg—572(L)
Temperature variation of the moduli of NaCl, KCl and MgO, M. A. Durand—449
Young's modulus of Bi crystals, A. B. Focke, R. B. Lindsay, C. R. Wilks—872(A)
Electrical conductivity and resistance (see **Resistance, electrical**)
Electrical oscillations and waves
Short continuous waves, C. E. Cleeton, N. H. Williams—1091(L)
Electrolytic cells
Polarity changes of elements, L. A. G. Blanchet—391(A)

Electron diffraction (see also **Electrons, scattering of**)
By films built of monomolecular layers, K. H. Storks, L. H. Germer—676(L)
By galena crystals, L. H. Germer—659
Nuclear separation of S_2 by electron diffraction, L. R. Maxwell, V. M. Mosley, S. B. Hendricks—41
Orientation in stearic acid by electron diffraction, K. H. Storks—396(A)
Electrons (see also **Positive electron**)
Viscosity of air and electronic charge, G. Kellström—190(L)
X-ray determination of e, J. W. M. DuMond, V. L. Bollman—383(L), 524
Electrons, positive (see **Positive electrons**)
Electrons, scattering of
Inelastic scattering from solids, E. Rudberg—138
Inelastic scattering from solids, theory of, E. Rudberg, J. C. Slater—150
Of 2–4000 volt electrons by He, A. L. Hughes, S. S. West—320
Velocity distribution of atomic electrons by scattering of electrons, G. E. M. Jauncey—326
Electrons, secondary
From Cb, energy distribution, L. J. Haworth—216
Thin film emission, L. Malter—48
Electrostatics
Accurate test of Coulomb's law, S. J. Plimpton, W. E. Lawton—1066
Equations of state
Of one, two and three-dimensional gases, L. Tonks—955
Quantum theory at low temperatures, L. Gropper—963
Errata
A double-focusing mass spectrograph and the masses of N^{15} and O^{18}, J. Mattauch—1089
The electric moment of $^1\Sigma_+$ to O^+ transition in the continuum of Cl_2, G. E. Gibson, O. K. Rice—871(L)
Heat conductivity of tungsten and the cooling effects of leads upon filaments at low temperatures, I. Langmuir, J. B. Taylor—190
Measurements near top of atmosphere, R. A. Millikan, H. V. Neher, S. K. Haynes—1191
On binding of neutrons and protons, J. B. Fisk, L. I. Schiff, W. Shockley—1191

Field currents
And contact electromotive force for Hg, D. H. Moore—344
Thin film emission, L. Malter—48
From tungsten and thoriated tungsten, A. J. Ahearn—238, 398(A)

Gases (see **Kinetic theory**)
Geophysics
Geologic time and radiogenic lead, J. L. Rose, R. K. Stranathan—792
Gyromagnetization (see **Magnetic properties**)

Heat conduction (see **Thermal conductivity**)
High voltage tubes and machines
Cyclotron improvements, E. O. Lawrence, D. Cooksey—1131
Hyperfine structure (see also **Nuclear spin**)
Of In II, deviations and quadrupole moment, R. F. Bacher, D. H. Tomboulian—1096(A)
Of Hg I, 6^1P-7^1S line, M. H. M. Hunt, J. S. Campbell—397(A)

Instruments (see **Methods and instruments**)
Ionization by particles (see also **Ionization potentials**)
Columnar ionization by α-particles, W. R. Kanne, J. A. Bearden—935
Of gases by neutral atoms, R. N. Varney—159
Ions produced in HCl under electron impact, A. O. Nier, E. E. Hanson—722
Of Hg by Na^+ ions, R. N. Varney, W. C. Cole—261(L); R. N. Varney—1095(A)
Of N_2 by electrons, G. A. Anslow, M. DeB. Watson—162
In N_2 and Ne by β-rays, H. K. Skramstad, D. L. Loughridge—677
Ionization potentials
Of free radicals CH_3 and C_2H_5, R. G. J. Fraser, T. N. Jewitt—1091(L)
Ionization by radiation
Ions, mobility
Electron drift velocity in N_2, He, Ne and A, R. A. Nielsen—386(A), 950
Isotopes
Of A, K, Ru, Zn and Cd, A. O. Nier—873(A), 1041
Of Be, W. Bleakney, J. P. Blewett, R. Sherr, R. Smoluchowski—545
Of Ba, Sr, In, Ga, Li and Na, M. B. Sampson, W. Bleakney—456
Chemical differences between N isotopes, H. C. Urey, A. H. W. Aten, Jr.—575(L)
Of Co and their radioactivity, M. B. Sampson, L. N. Ridenour, W. Bleakney—382(L)
Geologic time and radiogenic lead, J. L. Rose, R. K. Stranathan—792
Ions from high frequency spark, S. L. Ch'u—212
Of Fe and Ni, A. J. Dempster—98(L)
Isobars of adjacent elements, K. T. Bainbridge, E. B. Jordan—282
Of Mn, Cb, Pd, Pt, Ir, Rh and Co, M. B. Sampson, W. Bleakney—732
Mass difference $N^{14}+H^1-N^{15}$, E. B. Jordan, K. T. Bainbridge—98(L)
Of N and O; masses, J. Mattauch—617; Erratum—1089
Separation by centrifuging, J. W. Beams, F. B. Haynes—491(L)
Separation by diffusion, D. E. Wooldridge, W. R. Smythe—233
Of Sr and Te, A. J. Dempster—186(L)

Joule-Thomson effect
Kelvin temperature of ice point, J. R. Roebuck—370

Kinetic theory of gases
Complete equation of state of one, two and three-dimensional gases, L. Tonks—955

Magnetic properties
Analysis of evaporated Bi films, C. T. Lane—1094(A)
Anisotropy in alpha iron and in alloys, L. W. McKeehan, R. G. Piety, J. D. Kleis—1093(A)
Anisotropy of copper sulphate pentahydrate, K. S. Krishnan, A. Mookherji—860
Anisotropy of iron crystals, R. G. Piety—1173
Anisotropy of Ni-Co crystals, J. W. Shih—376
Anisotropy of Ni-Fe crystals, J. D. Kleis—1178
Anisotropy in single crystals and in polycrystalline sheets, R. M. Bozorth—1076
Coercive force in crystals of silicon ferrite, K. J. Sixtus—395(A)
Gyromagnetic models, S. J. Barnett—390(A)
Gyromagnetic properties of the hydrogens, J. M. B. Kellogg, I. I. Rabi, J. R. Zacharias—472
Gyromagnetic ratios for ferromagnetic substances, S. J. Barnett—390(A)
Of Ni under stress, C. W. Heaps—176
Susceptibility of molecular hydrogen, E. E. Witmer—1094(A)
Thermal energy; magnetization in Ni, T. C. Hardy—395(A)
Mass defects (see **Isotopes**)
Mass ratios (see **Isotopes**)
Mechanics, quantum—atomic structure and spectra
Hydrogen problem and the four-dimensional rotation group, O. LaPorte—400(A)
Wave functions for ionization of Si, H. L. Donley—1012
Mechanics, quantum—general
Equation of state at low temperatures, L. Gropper—963
Nuclear motion in Dirac equation, I. S. Lowen—1098(A)
Scattering of electrons from solids, E. Rudberg, J. C. Slater—150
Scattering of light by light, Born-Infeld theory, C. D. Thomas—1046
Space quantization in varying magnetic fields, L. Motz, M. E. Rose—348
Wave-packet solution of Dirac equation, C. Eckart, B. L. Griffing—1145
Mechanics, quantum—of solid bodies
Electron exchange in metals, J. Bardeen—1098(A)
Electronic constitution of LiF and LiH, D. H. Ewing, F. Seitz—400(A), 760
Electronic energy bands in NaCl, W. Shockley—754
Energy bands in metallic tungsten, M. F. Manning, M. Chodorow—399(A)
Energy states in solids, F. H. Spedding—574(L)
Theory of Brillouin in crystals, L. P. Bouckaert, R. Smoluchowski, E. Wigner—58
Metals (see **Crystalline state**)
Meteorology
Electric potential gradient, effect of wind, J. G. Brown—388(A)
Lower ionosphere, R. C. Colwell, A. W. Friend—632
Solar eclipse and magnetic storm, S. S. Kirby, T. R. Gilliland, N. Smith, S. E. Reymer—258(L)
Solar eruptions and terrestrial phenomena, J. H. Dellinger—1189(L)
Vertical distribution of ozone, B. O'Brien, F. L. Mohler, H. S. Stewart—1099(A)
Methods and instruments
Analysis of counter data, L. I. Schiff—88
Analysis of ionization chambers and pulse amplifiers, E. A. Johnson, A. G. Johnson—170
Angular momentum of light, measurement of, R. A. Beth—115
Calculation of elastic constants, M. Goeppert-Mayer, A. May—99(L)
Christiansen filters as polarizers, H. W. Farwell—486(L)
Counter for neutron nuclear disintegrations, R. D. Evans, M. H. Kanner—394(A)
Counter statistics for chain disintegrations, L. I. Schiff—394(A)
Counting rate meter, L. I. Schiff, R. D. Evans—873(A)
Cyclotron improvements, E. O. Lawrence, D. Cooksey—1131
Discharge lamps containing CO_2, T. J. Killian, R. S. Prescott—389(A)
Double-focusing mass spectrograph, J. Mattauch—617; erratum—1089
Electronic voltage stabilizers, F. V. Hunt, R. W. Hickman—1094(A)
γ-ray measurements, J. R. Richardson, F. N. D. Kurie—999
G-M counter characteristics, D. B. Cowie—385(A)
G-M counters for special purposes, G. L. Locher—1099(A)
Gyromagnetic models, S. J. Barnett—390(A)
High speed running film camera, B. O'Brien—400(A)
Illumination meter for photographic work, A. Townsend—396(A)
Interferometric wave-length comparisons, Schumann region, D. L. Mac Adam—185(L)
Ions from high frequency spark, S. L. Ch'u—212
Low-melting metals for x-ray tube targets, T. R. Folsom—396(A)
Magazine plate camera for vacuum, K. E. Fitzsimmons—386(A)
Magnetron discharge, spectroscopic study, O. Luhr, F. J. Studer—1095(A)
Manometer and pressure control, T. J. Killian—390(A)
Mass spectrograph, K. T. Bainbridge, E. B. Jordan—282
Mass-spectrograph with permanent magnets, M. B. Sampson, W. Bleakney—456
Mercury pool rectifier, T. M. Libby, J. E. Henderson, D. H. Loughridge—387(A)
Neutron measurements in biological experiments, G. Failla—1098(A)
Oil diffusion pump of metal, J. E. Henderson—388(A)
Physics in textile research, I. J. Saxl—1098(A)
Positive ion source, J. P. Blewett, E. J. Jones—464
Propagation of potential in tubes, L. B. Snoddy, J. W. Beams, J. R. Dietrich—469, 1094(A)
Ranges from number-distance curves, A. King, W. M. Rayton—394(A)
Separation of isotopes by centrifuging, J. W. Beams, F. B. Haynes—491(L)
Sign of charge on ions in Wilson cloud experiments, A. F. Kip, L. B. Loeb—392(A)

Stopping power of foils for deuterons, L. J. Laslett—391(A)
Thermal conductivity of refractories, J. L. Finck—1098(A)
Transmitting data from stratosphere, R. L. Doan—1100(A)
Velocity of radio waves, R. C. Colwell, A. W. Friend, N. I. Hall, L. R. Hill—381(L)
Wilson cloud chamber for showers, R. B. Brode, H. G. MacPherson, M. A. Starr—389(A)
Mobility of ions (see **Ions, mobility**)
Molecular radii (see **Collision diameter**)
Molecular structure and constants (see also **Spectra, molecular and Raman spectra**)
Of S_2 by electron diffraction, L. R. Maxwell, V. M. Mosley, S. B. Hendricks—41

Neutrons
Absorption and the diffusion of slow neutrons, E. Amaldi, E. Fermi—899; D. S. Bayley, B. R. Curtis, E. R. Gaerttner, S. Goudsmit—461; A. C. G. Mitchell, E. J. Murphy, M. D. Whitaker—133
Absorption in aqueous solutions, theory of, W. H. Furry—381(L)
Absorption cross-sections, C. T. Zahn, E. L. Harrington, S. Goudsmit—570(L)
Behavior at different temperatures, E. Amaldi, E. Segrè—571(L)
In biological experiments, G. Failla—1098(A)
Bond effect in hydrogen and hydrocarbons, W. F. Libby, E. A. Long—577(L)
Bragg reflection of slow neutrons, D. P. Mitchell, P. N. Powers—486(L)
Diffusion and absorption in paraffin, D. M. Yost, R. G. Dickinson—128
Hydrocarbons at low temperatures, effect of, W. F. Libby, E. A. Long—575(L)
Magnetic scattering of, F. Bloch—259(L)
Orbital neutrons, theory of, G. N. Lewis—857
Photo-neutrons, D. P. Mitchell, F. Rasetti, G. A. Fink, G. B. Pegram—189(L), 401(A)
Production and absorption, G. A. Fink—738
Production at low-voltage, W. H. Zinn, S. Seeley—1101(A)
Resonance capture of slow neutrons, H. H. Goldsmith, F. Rasetti—328
Resonance energy of Cd for capture, E. Segrè, C. T. Zahn—577(L)
Scattering by heavy nuclei, C. H. Fay—569
Scattering by protons, M. A. Tuve, L. R. Hafstad—490(L); W. D. Harkins, M. D. Kamen, H. W. Newson, D. M. Gans—980
Slowing down in water, G. Horvay—897
Nuclear moments and spin (see also **Hyperfine structure**)
Of the hydrogens, J. M. B. Kellogg, I. I. Rabi, J. R. Zacharias—472
Of light nuclei, individual particle model—H. A. Bethe, M. E. Rose—1100(A)
Of Li^6, J. H. Manley, S. Millman—380(L)
Of Li^7, computed, J. H. Bartlett, Jr., J. J. Gibbons, Jr., R. E. Watson—315
Magnetic moment of proton, J. M. B. Kellogg, I. I. Rabi, J. R. Zacharias—396(A)
Of Rb^{85} and Rb^{87}, S. Millman, M. Fox—220
Nucleus (see also **Disintegration of nucleus; Neutrons**)
Collision of neutron and proton, J. B. Fisk, L. I. Schiff, W. Shockley—1090(L), erratum—1191; P. M. Morse, J. B. Fisk, L. I. Schiff—748; W. D. Harkins, M. D. Kamen, H. W. Newson, D. M. Gans—980
Coulomb energy of He^3, S. S. Share—488(L)
Density of nuclear levels, H. A. Bethe—332; J. R. Oppenheimer, R. Serber—391(A)
Excitation-curves for F and Li, L. R. Hafstad, N. P. Heydenburg, M. A. Tuve—504
Forces between particles, V. Weisskopf—1187(L)
γ-ray emission, probability of, F. Bloch, G. Gamow—260(L)
Interaction between nuclear particles, G. Breit, E. Feenberg—850
Li and F under α-particle bombardment; γ-rays, K. C. Speh—395(A), 689
Majorana-Heisenberg and velocity-dependent forces, K. Way, J. A. Wheeler—675(L)
Many-body model, transmutation function, H. A. Bethe, E. J. Konopinski—1100(A)
Neutron-neutron forces in $_1H^3$, R. D. Present—635
Nonelectric forces and Dirac's equations, W. H. Furry—784(L)
Nonelectric forces on electrons and positrons, W. H. Furry—1099(A)
Nuclear calculation, D. R. Inglis—399(A)
Nuclear forces, B. Cassen, E. U. Condon—846; M. A. Tuve—869(L)
Nuclear forces and velocity, J. A. Wheeler—643
Nuclear motion in Dirac equation, I. S. Lowen—1098(A)
Nuclear three and four particle eigenvalue problems, E. Feenberg, S. S. Share—253
Orbital neutrons, theory of, G. N. Lewis—857
Proton-proton forces and mass defect curve, R. Serber—389(A)
Radius and many-body problem, H. A. Bethe—1100(A)
Relativity and nuclear forces, theory of deuteron, E. Feenberg—674(L); H. Margenau—342
Scattering of protons by protons, M. A. Tuve, N. P. Heydenburg, L. R. Hafstad—806
Scattering of protons by protons, theory of, G. Breit, E. U. Condon, R. D. Present—825
Second-order spin effects in H^3, R. D. Present—870(L)
Spin-orbit coupling, D. R. Inglis—783(L)

Optical constants and properties
Anomalous diffraction gratings; theoretical, U. Fano—573(L)
Christiansen filters as polarizers, H. W. Farwell—486(L)
Of fluorite in extreme ultraviolet, R. Tousey—1057
Of metal films in near and far ultraviolet, G. B. Sabine—396(A)
Of metallic films, R. M. Emberson—396(A)

Of nonpolar liquids, H. Mueller—547
Reflectivity of evaporated Ag-films, H. W. Edwards, R. P. Petersen—871(L)
Optical theory
Angular momentum of light, measurement of, R. A. Beth—115
Angular momentum in optical problems, F. T. Holmes—396(A)
Michelson-Morley experiment, W. B. Cartmel—1097(A)
Scattering of light by light, Born-Infeld theory, C. D. Thomas—1046
Triangle proof of Lorentz; interferometer, W. B. Cartmel—1100(A)

Paschen-Back effect
Of hyperfine structure, separation of Hg_{199}, J. B. Green—126
$^2S^2P$ multiplets in strong fields, J. B. Green, R. A. Loring—975(L); P. Jacquinot—573(L)
Photoelectric effect and properties; cells
Absolute yields of Mg, Be, and Na, M. M. Mann, Jr., L. A. DuBridge—398(A)
Analysis of data, R. J. Cashman, N. C. Jamison—568
Of Ba and Ca, N. C. Jamison, R. J. Cashman—624
Cooling of a surface by emission, H. M. Zenor—1050
Crystal structure and electron emission from W wire, W. B. Nottingham—398(A)
Energy distribution of photoelectrons from K films as function of temperature, C. L. Henshaw—398(A)
Of Fe, effect of magnetic field, D. H. Loughridge, N. K. Olsen—389(A)
Sensitization of K by H, J. J. Brady, J. H. Rochel—870(L)
Of zinc, C. F. DeVoe—481
Piezoelectric effect
Properties of Rochelle salt, O. Norgorden—782(L)
Positive electron
Nonelectric forces on electrons and positrons, W. H. Furry—1099(A)

Radio
Ionosphere, solar eclipse and magnetic storm, S. S. Kirby, T. R. Gilliland, N. Smith, S. E. Reymer—258(L)
Lower ionosphere, R. C. Colwell, A. W. Friend—632
Short continuous waves, C. E. Cleeton, N. H. Williams—1091(L)
Solar eruptions and terrestrial phenomena, J. H. Dellinger—1189(L)
Sunspot cycle and reception, L. C. Young, E. O. Hulburt—45
Velocity of waves, R. C. Colwell, A. W. Friend, N. I. Hall, L. R. Hill—381(L)
Radioactivity (see also **Disintegration of nucleus**)
α-decay as many-body problem, H. A. Bethe—977
Alpha-ray ranges of U isotopes, W. M. Rayton, T. R. Wilkins—394(A)
Of Sb and Sn induced by $_1H^2$, J. J. Livingood—385(A)
β-ray spectra of RaE and P^{32}, E. M. Lyman—385(A)
β-rays from Mn, As, and In, M. V. Brown, A. C. G. Mitchell—593
Of Co isotopes, M. B. Sampson, L. N. Ridenour, W. Bleakney—382(L)
Collisions of alpha-particles with S nuclei, R. L. Anthony—395(A)
Of Cu, a branch reaction, S. N. Van Voorhis—895
Compton scattering of gamma-rays, R. S. Shankland—571(L)
Continuous γ-radiation accompanying the β-decay, F. Bloch—272
Decay of Na^{22}, W. E. Lamb, Jr.—388(A)
Deuteron-induced Cu, Zn, Sb, Ru, and Bi, J. J. Livingood—391(A), 425
Deuteron-induced Sn, J. J. Livingood, G. Seaborg—435
γ-rays from several elements, J. R. Richardson, F. N. D. Kurie—999
Half-value period of Th; branching ratio of Th C, A. F. Kovarik, N. I. Adams, Jr.—99(L)
Long period positron activity, L. J. Laslett—388(A)
RaB beta-particle energies, F. T. Rogers, Jr.—515
Ranges from number-distance curves, A. King, W. M. Rayton—394(A)
Of Ru and K, A. O. Nier—873(A), 1041
Of S, R. Sagane—1141
Raman spectra
Continuous spectrum, S. V. C. Aiya—260(L)
Relativity
Conservation of photons, H. P. Robertson—385(A)
Michelson-Morley experiment, W. B. Cartmel—1097(A)
New relativity, D. G. Bourgin—864
And nuclear forces, H. Margenau—342
One-dimensional problem, D. G. Bourgin—400(A)
Thomas precession of accelerated axes, S. Dancoff, D. R. Inglis—784(L)
Resistance, electrical (see **Electrical conductivity and resistance**)
Of Bi crystals, A. B. Focke, J. R. Hill—179
Resistivity of single crystals of solid solutions in Zn, H. E. Way—1181

Scattering of electrons, neutrons, and ions (see also **Electrons, scattering of; Electron diffraction**) (see **Neutrons** for scattering of neutrons)
Of protons by protons, M. A. Tuve, N. P. Heydenburg, L. R. Hafstad—806
Of protons by protons, theory of, G. Breit, E. U. Condon, R. D. Present—825
Of single crystals, H. Osterberg—1187(L)
Of slow electrons in Cl_2, J. B. Fisk—1096(A)
Secondary electrons (see **Electrons, secondary**)
Spark discharge (see **Discharge of electricity, etc.**)
Spectra, absorption (see also **Absorption of light**)
Of alcohol-acetone mixtures, W. Gordy—1151
Of NH_3; infrared, S. H. Chao—27
Of CS_2 at 4.57μ, J. A. Sanderson—209
Of HNCO, HCOOH, and CH_3OH, G. Herzberg, H. Verleger—390(A)
Of the deuteroammonias, A. B. F. Duncan—700; M. V. Migeotte, E. F. Barker—418

Energy levels in Sm salts, C. B. Ellis—675(L)
Of heavy acid solutions, E. K. Plyler, D. Williams—1097(A)
Of HCl in nonionizing solvents, D. Williams—719, 1097(A)
Of MgCl, MgBr, and MgI, F. Morgan—603
Of metallic halides in Schumann region, H. M. O'Bryan, E. G. Schneider—1096(A)
Optical absorption by alkali halides, J. C. Slater, W. Shockley—705
Pressure effect in HCN bands, S. D. Cornell, W. W. Watson—279, 397(A)

Spectra, atomic
Balmer lines in high frequency discharge, G. W. Fox, C. H. Bachman—939
Of Be III and Be IV, H. A. Robinson—99(L)
Of Ce IV, R. J. Lang—397(A)
Fock equations for complex configurations, G. H. Shortley—1072
Of He, doubly excited, A. T. Kiang, S. T. Ma, T. Y. Wu—673(L)
Interferometer patterns of Hα, W. V. Houston—392(A)
Of Pb V and Bi VI, G. K. Schoepfle—538
Mean lives of K doublets, D. Sinclair, H. W. Webb—397(A), 440
Of Hg I, 6^1P-7^1S line, M. H. M. Hunt, J. S. Campbell—397(A)
Wave functions for ionization of Si, H. L. Donley—1012

Spectra, general
Pressure broadening of K lines, G. F. Hull, Jr.—1097(A), 1148
Spectrographs of eclipse expedition, D. H. Menzel, H. Hemmendinger, R. d'E. Atkinson, J. C. Boyce—872(A)
Wave-length standards in extreme ultraviolet, K. R. More, C. A. Rieke—1096(A), 1054

Spectra, molecular (see also **Molecular structure and constants**)
Of C_2HD, G. Herzberg, F. Patat, H. Verleger—386(A)
Of Cl_2, electric moment, G. E. Gibson, O. K. Rice—380(L), 871(L)
Of CuD, M. A. Jeppesen—386(A), 445
HCN bands in infrared, pressure effect, S. D. Cornell, W. W. Watson—279, 397(A)
HCN bands, pressure broadening, intermolecular forces, G. Hertzberg, J. W. T. Spinks, W. W. Watson—1186(L)
Of H_2, G. H. Dieke—797
Of OH^+, calculation of constants, M. Kovner—188(L)
Of InO, W. W. Watson, A. Shambon—607
Low electronic states of heteropolar diatomic molecules, I. General survey, R. S. Mulliken—1017; II. Alkali metal hydrides—1028
Of PH, P. Nolan, F. A. Jenkins—943
Quartet states in diatomic molecules, W. H. Brandt—778
Of SrH, pressure effect on C band, R. F. Humphreys, W. R. Fredrickson—542
Of water vapor, H. M. Randall, N. Ginsburg, D. M. Dennison, R. L. Webber—397(A)

Spectroscopy, technique
Magnetron discharge; spectroscopic study, O. Luhr, F. J. Studer—1095(A)

Stark effect

Surface tension
Density and surface tension measurements, L. E. Dodd—387(A)
From velocity of capillary waves, V. E. Eaton—399(A)

Thermal conductivity
Of refractories at high temperatures, J. L. Finck—1098(A)
Of tungsten at low temperatures, I. Langmuir, J. B. Taylor—68, 190

Thermionic emission of electrons; emitting surfaces
Changes in work function during fusion of Sn, P. A. Anderson—386(A)
Films formed on electrodes, L. B. Headrick, E. A. Lederer—1094(A)
Irregularities in emission from W, F. L. Yerzley—610
Of Pt; constants, L. V. Whitney—1154
Of W; constants, H. B. Wahlin, L. V. Whitney—735

Thermionic emission of positive ions
Of W; constants, H. B. Wahlin, L. V. Whitney—735

Viscosity
Of air and electronic charge, G. Kellström—190(L)

Work function (see also **Thermionic emission of electrons; Photoelectric effect**)
Photoelectric of Mg, Be, and Na, M. M. Mann, Jr., L. A. DuBridge—398(A)

X-rays, absorption
Of compounds of Br, Ru, and Sr, S. T. Stephenson—387(A), 790
By elements of high atomic number, M. T. Jones—110
By elements of low atomic number, T. R. Cuykendall—105
Of Ga, fine structure in K edge, W. W. Mutch—197
Of Ga, theoretical investigation, R. Smoluchowski—201

X-rays, diffraction, scattering, reflection, refraction, and polarization
Anisotropy in atomic vibrations of Zn crystals, G. E. M. Jauncey, W. A. Bruce—408, 413; R. D. Miller, E. S. Foster, Jr.—417; C. Zener, S. Bilinsky—489(L)
Cloud chamber study of Compton effect, H. R. Crane, E. R. Gaerttner, J. J. Turin—302
Coincidences in Compton scattering, B. Hoffmann, A. G. Shenstone, L. A. Turner—1092(L); R. S. Shankland—571(L)
Compton band, characteristics of, P. Kirkpatrick, P. A. Ross, H. O. Ritland—928
Deviations from Klein-Nishina formula, E. A. Uehling—387(A)
Intensity of x-rays penetrating oscillating crystals, G. E. M. Jauncey, A. T. Jaques—672(L)
New effects in Laue reflection in calcite, J. W. M. DuMond, V. L. Bollman—97(L)

Photon theory and Compton effect, W. Bothe, H. Maier-Leibnitz—187(L)
Polarization of hard x-rays, E. Rodgers—875
Reflection by crystals; high temperatures, allotropic crystals, C. Zener, S. Bilinsky—101
Scattering by spinning electron, A. H. Compton—878
Shape of Compton lines, A. Sommerfeld—38
Validity of x-ray-crystal determination of e, J. W. M. DuMond, V. L. Bollman—383(L), 524

X-rays, emission
Chemical composition, effects of, J. C. McDonald—694, 782(L); H. H. Roseberry, J. A. Bearden—204
$K\alpha$ satellite lines, S(16) to Ge(32), L. G. Parratt—1
$K\alpha$ satellites for Zn(30) to Pd(46), C. H. Shaw, L. G. Parratt—1096(A), 1006
Low-melting metals for x-ray tube targets, T. R. Folsom—396(A)
Satellite lines Auger effect, F. R. Hirsh, Jr.—191
Satellites, line widths, and intensities, L. G. Parratt—598

53

THE JOHN CRERAR
DEC 2 1936
LIBRARY

THE PHYSICAL REVIEW

VOLUME 50 *Second Series* NUMBER 12

DECEMBER 15, 1936

Published for the

AMERICAN PHYSICAL SOCIETY

by the

AMERICAN INSTITUTE OF PHYSICS
Incorporated

LANCASTER, PA., AND NEW YORK, N. Y.

CONTENTS

PHYS. REV. 50 (1936) DECEMBER 15

Numerically Consistent Corpuscular Theory of Cosmic Rays . . . . . W. F. G. SWANN 1103

Cosmic Rays as Electrical Particles . . . . . ARTHUR H. COMPTON 1119

On the Apparatus for the Multiple Acceleration of Light Ions to High Speeds . . . . . ERNEST O. LAWRENCE AND DONALD COOKSEY 1131

Radioactivity Induced in Sulphur . . . . . R. SAGANE 1141

Positive Energy Wave Packet Solution of the Dirac Equation . . . . . CARL ECKART AND B. L. GRIFFING 1145

Pressure Broadening of the Potassium Resonance Lines by Argon and Nitrogen . . . . . GORDON F. HULL, JR. 1148

Infrared Absorption of Alcohol-Acetone Mixtures . . . . . WALTER GORDY 1151

Thermionic Emission of Platinum . . . . . L. V. WHITNEY 1154

Variation of the Internal Friction and Elastic Constants with Magnetization in Iron. Part I. . . . . W. T. COOKE 1158

Variation of the Internal Friction and Elastic Constants with Magnetization in Iron. Part II . . . . . WILLIAM FULLER BROWN, JR. 1165

Ferromagnetic Anisotropy of Iron Crystals at Various Temperatures . . RAYMOND G. PIETY 1173

Ferromagnetic Anisotropy of Nickel-Iron Crystals at Various Temperatures . . J. D. KLEIS 1178

Electrical Resistivity of Single Crystals of Some Dilute Solid Solutions in Zinc . . . . . HAROLD E. WAY 1181

Letters to the Editor:

Pressure Broadening of the HCN Band Lines and Intermolecular Forces . . . . . G. HERZBERG, J. W. T. SPINKS AND W. W. WATSON 1186

Electroresistive Effect and a Rectifying Property of Carborundum Crystals . HAROLD OSTERBERG 1187

Exchange Forces Between Elementary Particles . . . . . V. F. WEISSKOPF 1187

On the Hard Component of Cosmic Rays . . . . . B. GROSS 1188

Direct Effects of Particular Solar Eruptions on Terrestrial Phenomena . . . J. H. DELLINGER 1189

Investigations of the Deuteron-Deuteron Reaction . . . . R. LADENBURG AND R. B. ROBERTS 1190

Erratum: On the Binding of Neutrons and Protons . . J. B. FISK, L. I. SCHIFF AND W. SHOCKLEY 1191

Erratum: Precision Cosmic-Ray Measurements up to Within a Percent or Two of the Top of the Atmosphere . . . . . R. A. MILLIKAN, H. V. NEHER AND S. K. HAYNES 1191

β-Ray Spectrum of Li^8 . . . . . E. WIGNER AND G. BREIT 1191

Author Index to Volume 50 1192

Analytic Subject Index to Volume 50 1201

LANCASTER PRESS, INC., LANCASTER, PA.